

AD-A063 612

BEN-GURION UNIV OF THE NEGEV BEERSHEBA (ISRAEL)  
THE DYNAMICS OF LONGITUDINAL DUNES.(U)  
JUL 78 H TSOAR

DEPT--ETC F/G 8/6

DA-ERO-76-G-072

NL

UNCLASSIFIED

1 OF 2

AD  
A063612



LEVEL

12

AD

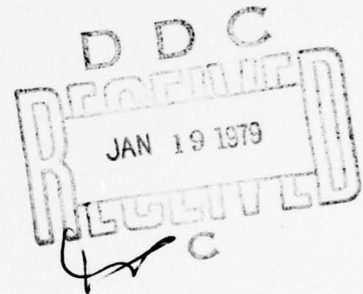
# The Dynamics of Longitudinal Dunes

Final Technical Report

by

HAIM TSOAR

July 1978



AD A063612

DDC FILE COPY.

EUROPEAN RESEARCH OFFICE

United States Army

London England

GRANT NUMBER DA-ERO-76-G-072.

Department of Geography ✓  
Ben-Gurion University of the Negev

Approved for Public Release; distribution unlimited

79 01 17 052



UNCLASSIFIED

SECURITY CLASSIFICATION OF THIS PAGE (When Data Entered)

REPORT DOCUMENTATION PAGE		READ INSTRUCTIONS BEFORE COMPLETING FORM
1. REPORT NUMBER	2. GOVT ACCESSION NO.	3. RECIPIENT'S CATALOG NUMBER
4. TITLE (and Subtitle) The Dynamics of Longitudinal Dunes		5. TYPE OF REPORT & PERIOD COVERED Final Technical Report Sept 76 - Jul 78
7. AUTHOR(s) Haim/Tsoar		6. PERFORMING ORG. REPORT NUMBER
9. PERFORMING ORGANIZATION NAME AND ADDRESS Ben-Gurion University of the Negev Ber-Sheva, Israel		8. CONTRACT OR GRANT NUMBER(s) DAERO-76-G-072
11. CONTROLLING OFFICE NAME AND ADDRESS US Army R&S Gp (Eur) Box 65, FPO NY 09510		10. PROGRAM ELEMENT, PROJECT, TASK AREA & WORK UNIT NUMBERS 6.11.02A-1T61102BH57-01-00- 593
14. MONITORING AGENCY NAME & ADDRESS (if different from Controlling Office) 172p		12. REPORT DATE Jul 78
		13. NUMBER OF PAGES 140
		15. SECURITY CLASS. (of this report) UNCLASSIFIED
16. DISTRIBUTION STATEMENT (of this Report) Approved for Public Release; Distribution Unlimited		15a. DECLASSIFICATION/DOWNGRADING SCHEDULE
17. DISTRIBUTION STATEMENT (of the abstract entered in Block 20, if different from Report)		
18. SUPPLEMENTARY NOTES		
19. KEY WORDS (Continue on reverse side if necessary and identify by block number) Sand Dunes; Longitudinal dunes; Barchans; Geomorphology; Sediment; Zibar; aeolian processes.		
20. ABSTRACT (Continue on reverse side if necessary and identify by block number) Longitudinal sand dunes, which are the most widespread type of dunes in the desert, are characterized by a symmetrical cross profile, a sharp edged crest and continuous elongation in one direction. Several theories have been put forward to explain some of their typical characteristics elongation for many tens of miles, equal distances between the dunes, and sinuosity of their crest lines.		

PTO

DD FORM 1 JAN 73 1473 EDITION OF 1 NOV 65 IS OBSOLETE

UNCLASSIFIED

SECURITY CLASSIFICATION OF THIS PAGE (When Data Entered)

UNCLASSIFIED

SECURITY CLASSIFICATION OF THIS PAGE (When Data Entered)

Cont  
> The present research concentrated on a field study of the mechanism of movement and advance of the longitudinal dune and on the mutual relationship between their morphology and dynamics.

Research methods included field measurements like macro and micro wind direction and velocity, grain size analysis, tracing and the movement of sand grains by marking them with a fluorescent dye, analysis of the internal structure, measurement of the rate of advance and of profile changes during several seasons.

Results of the measurement show that when wind encounters the dune body obliquely, the wind direction on the lee flank is deflected and blows along that flank parallel to the crest line. The magnitude of the deflected wind depends on the angle between the wind and the crest line. When the wind meets the crest line at an acute angle of  $30^{\circ}$  or less (which is the common case), the velocity of the deflected wind on the lee side is higher than on the crest line or the windward flank. This fact brings about erosion on both flanks of the dune. When the angle between the wind direction and the crest line becomes less acute ( $50^{\circ}$  to  $90^{\circ}$ ) the velocity of the deflected wind drops on the lee flank. This occurs when the dune meanders, and as a consequence, the angle becomes less acute. Further on, the dune returns to its former position and the angle once more becomes acute with erosion taking place again along the lee flank of the dune, and so on, resulting in the sinuous outline of the crest line.

ACCESSION for	
NTIS	<input checked="" type="checkbox"/>
DDC	<input type="checkbox"/>
UNANNOUNCED	<input type="checkbox"/>
JUSTIFICATION	<input type="checkbox"/>
BY	
DISTRIBUTION ANALYST'S NOTES	
Dist	<input type="checkbox"/>
<input checked="" type="checkbox"/>	<input type="checkbox"/>

## CONTENTS

	Page
I INTRODUCTION	15
1.1 Outline of Subject Matter	15
1.2 Previous Theories and Approaches in the Study of Longitudinal Sand Dunes	16
1.3 Aim of Present Work and Its Application	19
1.4 Research Method and Approach	20
1.5 Selection and Description of Research Area	21
1.6 Description of the Dune Selected for Investigation	21
II WIND REGIME IN THE RESEARCH AREA	27
2.1 Instrumentation	27
2.2 Processing of the Data	27
2.3 Threshold Velocity of the Dune Sand	28
2.4 Effective Wind	31
2.5 Results and Discussion	31
III MICROMETEOROLOGICAL WIND MEASUREMENTS	37
3.1 Introduction	37
3.2 Instrumentation	37
3.3 Results of Anemometer Measurements	37
3.4 Tracing Eddies by Smoke Candles	49
3.5 Summary	58
3.6 Interpretation and Discussion	60
IV GRAIN SIZE CHARACTERISTICS	66
4.1 Introduction	66
4.2 Sampling and Sieving Methods	66
4.3 Results and Conclusions	68
V TRACING SAND MOVEMENT BY FLUORESCENT DYE	80
5.1 Introduction	80
5.2 Techniques Used	80
5.3 Releasing the Fluorescent Dyed Sand	83
5.4 Graphical Representation of Dyed Sand Movement	84
5.5 Results and Discussion	85
5.6 Summary	97
5.7 A Model of Grain Movement on a Longitudinal Dune	98
VI DEPOSITIONAL SURFACES AND INTERNAL STRUCTURE OF THE DUNE	101
6.1 Introduction	101
6.2 Previous Work on the Internal Structure of Longitudinal Dunes	101
6.3 Research Method	102
6.4 Results and Discussion	103
6.5 A Model for the Internal Structure of a Longitudinal Dune	111

## CONTENTS

	Page
VII MEASUREMENT OF ELONGATION AND MOVEMENT OF THE DUNE	114
7.1 Introduction	114
7.2 Results	114
7.3 Discussion and Summary	116
VIII LATERAL MOVEMENT AND CROSS SECTION DECLINATIONS	118
8.1 Methods	118
8.2 Results	119
8.3 Declination of the Flanks	121
8.4 Summary	129
IX SUMMARY	130
9.1 Genesis of Longitudinal Dunes	130
9.2 The Zibar as a Source for Longitudinal Dunes	131
9.3 The Morphodynamic Model of a Longitudinal Dune	133
9.4 Spacing Between the Dunes	141
9.5 Dynamic Implications of the Distribution of Longitudinal Dunes in Deserts	142
LITERATURE CITED	144
APPENDIX	
1 Frequency table of wind direction and velocity (percentage) for the period: 1973, 1974.	150
2 Frequency table of wind direction and velocity (percentage) for the period: Winter 1972/73; 1973/74.	152
3 Frequency table of wind direction and velocity (percentage) for the period: Summer 1973, 1974, 1975.	154
4 Frequency table of wind direction and velocity (percentage) for the period: Fall 1973, 1974.	156
5 Frequency table of wind direction and velocity (percentage) for the period: Spring 1973, 1974, 1975.	158
6 Table of wind velocity (in meters/sec) and direction measured at point no. 18 (Fig. 3.3).	160
7 Table of wind velocity (in meters/sec) and direction measured at point no. 5 (Fig. 3.4).	160



# CONTENTS

	Page
8 Table of wind velocity (in meters/sec) and direction measured at point no. 5 (Fig. 3.5).	161
9 Table of wind velocity (in meters/sec) and direction measured at point no. 5 (Fig. 3.6).	162
10 Table of wind velocity (in meters/sec) and direction measured at point no. 9 (Fig. 3.7).	162
11 Table of wind velocity (in meters/sec) and direction measured at point no. 4 (Fig. 3.10).	162
12 Table of wind velocity (in meters/sec) and direction measured at point no. 4 (Fig. 3.11).	163
13 Table of wind velocity (in meters/sec) and direction measured at point no. 6 (Fig. 3.12).	163
14 Cross section of point no. 18 (for Fig. 3.3).	164
15 Cross section of point no. 5 (for Figs. 3.4, 3.5, 3.6).	164
16 Cross section of point no. 9 (for Fig. 3.7).	164
17 Cross section of point no. 9 (for Figs. 3.8, 3.9).	164
18 Results of moment statistics computed for the sand sampled from the ripples trough and crest separately.	165
19 Results of moment statistics computed for the sand samples from the ripple trough and its crest together.	166
20 Results of moment statistics computed for sand samples of the three top layers of the ripple.	167
21 Cross section of point no. 3 (vertical exaggeration x3).	168
22 Cross section of point no. 5 (vertical exaggeration x3).	168
23 Cross section of point no. 6 (vertical exaggeration x3).	168
24 Cross section of point no. 7 (vertical exaggeration x3).	169



## CONTENTS

		Page
25	Cross section of point no. 9 (vertical exaggeration x3)	169
26	Cross section of point no. 9 (vertical exaggeration x3).	169
27	Frequency tables of distribution of declinations across the dune flanks.	170

## FIGURES

1.1	An aerial photograph of the dune as of Nov. 27, 1970.	22
1.2	Grain size distribution for the seif dune crest, zibar crest and zibar flank.	23
1.3	Aerial photograph of zibar and longitudinal dunes in the Tenere desert (Niger).	24
1.4	The "tear drop" from the longitudinal dune.	24
1.5	Sketch of longitudinal dune drawn from an oblique and side view.	26
2.1	The wind recorder.	30
2.2	Values of threshold velocities ( $V_t$ ) of different grain sizes (in $\phi$ units) on different heights (Z) of a dune that is 10 meters high.	30
2.3	Circular diagram of the effective summer wind directions (percentage). Dashed line indicates the dune axis.	33
2.4	Circular diagram of the effective winter wind directions (percentage). Dashed line indicates the dune axis.	33
2.5	Circular diagram of the effective fall wind directions (percentage). Dashed line indicates the dune axis.	33
2.6	Circular diagram of the effective spring wind directions (percentage). Dashed line indicates the dune axis.	35
2.7	Circular diagram of the effective annual wind directions (percentage). Dashed line indicates the dune axis.	35

# CONTENTS

	Page
3.1 The RIMCO Miniature-Cup Anemometers across the dune flank.	38
3.2 Close view of an anemometer.	38
3.3 Results of wind measurements taken across the dune flank at point no. 18.	40
3.4 Results of wind measurements taken across the dune flank at point no. 5.	40
3.5 Results of wind measurements taken across the dune lee flank at point no. 5.	42
3.6 Results of wind measurements taken across the dune lee flank at point no. 5.	42
3.7 Results of wind measurements taken across the dune lee flank at point no. 9.	43
3.8 Results of wind measurements taken across the dune flanks at point no. 9.	47
3.9 Results of wind measurements taken across the dune flanks at point no. 9.	47
3.10 Results of wind measurements taken along the dune lee flank at point no. 4.	48
3.11 Results of wind measurements taken along the dune lee flank at point no. 4.	50
3.12 Results of wind measurements taken along the dune lee flank at point no. 6.	51
3.13 Plan of average wind directions on both dune flanks for measurements presented by Figs. 3.3-3.9.	52
3.14 Plan of the dune at point no. 9. The location of the anemometers and the flags as in Figs. 3.8 & 3.9.	52
3.15 Separation of flow above a profile of a longitudinal dune.	54

## CONTENTS

	Page
3.16 Separation of flow above a profile of a longitudinal dune (with wind profiles).	54
3.17 A separation flow above a slip face of a barchan demonstrated by smoke.	56
3.18 A helix vortex on the lee flank of a longitudinal dune demonstrated by smoke. Dashed line designates the smoke movement.	56
3.19 The wind deflection on the lee side of the longitudinal dune demonstrated by smoke.	56
3.20 Smoke movement on the windward flank of the dune.	56
3.21 Wind movement along the lee flank in the deflection area demonstrated by smoke.	57
3.22 Wind movement along the lee flank in the deflection area demonstrated by smoke.	57
3.23 Wind movement along the lee flank in the deflection area demonstrated by smoke.	57
3.24 Wind movement along the lee flank in the deflection area demonstrated by smoke.	57
3.25 Angle between the wind direction and the crest line versus velocity measured on the lee flank.	59
3.26 Angle between the wind direction and the crest line versus distance of the measuring point in the lee flank from the crest line.	59
3.27 Plan of the changes in the horizontal wind component that is perpendicular to the crest line.	61
3.28 The lee flank of the longitudinal dune covered with ripples indicating flow parallel to the crest line up to a distance of half a meter from the crest.	65
3.29 Different rates of slip face development on various sections of the lee flank.	65

# CONTENTS

	Page
4.1 Location of sampling points on a cross section of the dune.	69
4.2 Mean ( $\bar{X}_\phi$ ) versus ripple wavelength.	69
4.3 Difference in mean grain size between the ripple crest and the trough versus the ripple wavelength.	71
4.4 Difference in mean grain size between the ripple crest and the trough versus the mean grain size of both together.	71
4.5 Standard deviation (sorting) versus mean ( $\bar{X}_\phi$ ).	76
4.6 Grain size distribution curve, sample no. 45.	76
4.7 Grain distribution curve, sample no. 46.	76
4.8 Kurtosis ( $Kg_\phi$ ) versus mean ( $\bar{X}_\phi$ ).	77
4.9 Grain size distribution curve, sample no. 45 + 46.	77
4.10 Grain size distribution curve, sample no. 23 + 24.	77
4.11 Grain size distribution curve, sample no. 23.	77
4.12 Grain size distribution curve, sample no. 24.	78
4.13 Grain size distribution curve, sample no. 1 + 2.	78
4.14 Grain size distribution curve, sample no. 3 + 4.	78
4.15 Grain size distribution curve, sample no. 5 + 6.	78
5.1 Distribution of grain size in the dune before and after dyeing.	82
5.2 Sampling card (after taking a sample) attached to post by rubber bands.	82
5.3 Sampling post to which sampling card is attached.	82
5.4 Board holding the sampling card system.	82

## CONTENTS

	Page
5.5      Sampling map of released fluorescent dyed sand on both flanks of the dune at point no. 5.	86
5.6      Sampling map of released fluorescent dyed sand on both flanks of the dune between points no. 5 and 6.	87
5.7      Sampling map of released fluorescent dyed sand on both flanks of the dune at point no. 11.	89
5.8      Sampling map of released fluorescent dyed sand on both flanks of the dune between points no. 9 and 10.	91
5.9      Sampling map of released fluorescent dyed sand on both flanks of the dune at point no. 10.	92
5.10     Sampling map of released fluorescent dyed sand on both flanks of the dune at point no. 18.	94
5.11     Sampling map of released fluorescent dyed sand on both flanks of the zibar at point no. 1.	96
5.12     Model of sand direction movement on a longitudinal dune.	99
6.1      Cross section showing the ideal internal structure of a longitudinal dune.	102
6.2      Contact lines on the laminae with the surface (on the southern flank of point no. 5), as exposed after a severe rainstorm accompanied by strong winds from the S and W.	104
6.3      Contact lines of the laminae with the surface (on the southern flank of point no. 5) according to Fig. 6.2.	104
6.4      Contact lines of the laminae with the surface (on the southern flank of point no. 7), as exposed after a severe rainstorm accompanied by strong winds from S and W.	105
6.5      Contact lines of the laminae with the surface (on the southern flank of point no. 7), according to Fig. 6.4.	105



# CONTENTS

	Page
6.6 Contact between the main laminae and the laminae parallel to the crest line (point no. 7).	107
6.7 Model of Fig. 6.5 in three dimensions.	107
6.8 Slip face development next to the crest line which represent the secondary deposition which creates the laminae parallel to the crest line (point no. 5).	109
6.9 Contact between the main laminae and the laminae parallel to the crest line, in a 1-meter pit on the upper part of the flank.	109
6.10 Distribution of the condition of the dip and the azimuth of the investigated laminae.	112
6.11 Model of the internal structure of a longitudinal dune.	112
7.1 Elongation at the far end of the dune.	115
8.1 2 cross sections at different periods at point no. 4.	120
8.2 9 cross sections at different periods at point no. 1 (zibar).	120
8.3 11 cross sections at different periods at point no. 3.	120
8.4 6 cross sections at different periods at point no. 4.	122
8.5 4 cross sections at different periods at point no. 5.	122
8.6 2 cross sections at the beginning and end of the summer season at point no. 3.	122
8.7 2 cross sections at the beginning and end of the summer season at point no. 5.	123
8.8 2 cross sections at the beginning and end of the summer season at point no. 7.	123
8.9 2 cross sections at the beginning and end of the summer season at point no. 9.	123

# CONTENTS

	Page
8.10 2 cross sections at the beginning of the summer season at point no. 6.	124
8.11 2 cross sections at the beginning and end of the winter season at point no. 3.	124
8.12 2 cross sections at the beginning and end of the winter season at point no. 5.	124
8.13 Frequency distribution of declination of the flanks at point no. 1 (zibar); Nov. 8, 1974.	126
8.14 Frequency distribution of declinations of the southern flank at point no. 1 (zibar); Nov. 8, 1974.	126
8.15 Frequency distribution of declinations of the northern flank at point no. 1, Nov. 8, 1974.	126
8.16 Frequency distribution of declinations of the flanks at point no. 3, Sept. 30, 1974.	127
8.17 Frequency distribution of declinations of the southern flank at point no. 3, Sept. 30, 1974.	127
8.18 Frequency distribution of declinations of the northern flank at point no. 3, Sept. 30, 1974.	127
8.19 Frequency distribution of declinations of the flanks at point no. 3, April 27, 1973.	128
8.20 Frequency distribution of declinations of the southern flank at point no. 3, April 27, 1973.	128
8.21 Frequency distribution of declinations of the northern flank at point no. 3, April 27, 1973.	128
9.1 Plan of the longitudinal dune showing the depositional areas in two seasons. All other areas are subjected to erosion.	135
9.2 Erosion along the lee flank by wind blowing at acute angle to the crest line. The erosion is demonstrated by means of laminae exposures.	135

## CONTENTS

	Page
9.3      Concentration of light chips (dark color) on the deflection point (point no. 5).	136
9.4      Close-up of the symmetrical ripples and the chips appearing in Fig. 9.3.	136
9.5      Model of the formation of a meander in an initial linear longitudinal dune.	138
9.6      Model showing the formation of peaks and saddles along the dune.	138

## TABLES

2.1      Summary of wind data	32
2.2      Percentage of effective wind from various sectors.	34
3.1      Wind direction data on the crest and on the lee flank.	41
3.2      Results of wind velocity and direction measurements on the crest and on both flanks.	45
4.1      The mean moments at the 5 sampling points on the dune.	68
4.2      Distribution of wavelengths of ripples in various sampling sites, mean values and size range including 90% of the sampling.	70
4.3      Results of F and t tests of different groups of sampling sites.	73
6.1      Summary of data on measured dips and their azimuth.	110
7.1      Dune elongation.	115
7.2      Longitudinal displacement of the peaks and saddles.	116

ACKNOWLEDGEMENT

I want to express my gratitude to  
Professors Dan H. Yaalon and  
David Sharon of the Hebrew University  
of Jerusalem for supervising this  
work.

# THE DYNAMICS OF LONGITUDINAL DUNES

by  
*Haim Tsoar*

## I. INTRODUCTION

### 1.1 Outline of Subject Matter

A glance at the sand deserts of the world reveals a large morphological variation of sand dunes which we are accustomed to see as two main types: transverse and longitudinal, according to the orientation of the dunes in relation to the wind. It is surprising that this classification of the dunes in the desert is made without any available data about the wind, and that it is based more on intuition than on simple scientific facts.

There is an extensive terminology for longitudinal dunes relating to changes in the form of the dune and to its geographic location, for example: sand ridge, parallel ridge, uruq, arq, irq, draa, seif chain, linear dune, oblique ridge, silk, sigmoidal dune, etc. Cooke and Warren<sup>(1)</sup> write that now in dune literature it is usual to think of a longitudinal dune as one which is generally straight and very elongated with a sharp crest line. From this description comes the term 'seif' (a sword in Arabic), which is common in North Africa. Accordingly, it is suggested that transverse and longitudinal dunes are differentiated according to their profile - longitudinal dunes have a symmetrical and sharp profile, and transverse dunes have an asymmetrical profile and a flat crest line<sup>(2)</sup>. In addition, observations carried out in the Sahara, Arabian and Australian Deserts indicate that longitudinal dunes, which are not disturbed by vegetation, reveal a few additional morphological characteristics in common.

- a) The dune meanders and does not continue in a straight line.
- b) The crest-line rises and falls; i.e. there are peaks and saddles along the dune.
- c) The distances between one dune and another are nearly equal.

The dimensions of longitudinal dunes change from one place to another, their length varying from a few hundred meters to a few hundred kilometers. Their height varies from 5 to 50 meters and their width, in relation to their height, from tens of meters to more than a hundred meters.

Longitudinal dunes are the most widespread dunes in the large sand deserts of the world<sup>(3)</sup>: Saharan Desert<sup>(4)</sup>, Arabian Desert<sup>(5)</sup> and Australian Desert<sup>(6)</sup> (In the United States, where the extent of sand desert is small, longitudinal dunes are not common). It seems that the meteorological conditions of these major deserts are more favorable to the creation



of longitudinal than transverse dunes. The dynamics of the latter is rather simple and clear, that of the former more complicated and less clear.

## 1.2 Previous Theories and Approaches in the Study of Longitudinal Sand Dunes

While the relatively simple mechanism of movement of the transverse dunes has been researched and studied even quantitatively<sup>(7)(8)</sup>, the understanding of the dynamics and morphology of longitudinal dunes is still controversial and enveloped in obscurity. A researcher of longitudinal dunes is faced with several difficulties, the main one being the inaccessibility of those sand deserts in which longitudinal dunes are found in their full development. Fully-developed transverse dunes, on the other hand, are to be found even along the sandy coastal plains of humid climates<sup>(9)</sup>.

Those researchers who have dealt with longitudinal dunes had to explain certain facts related to the morphology and to the distribution of these dunes. For example:

- 1) the nearly equal distances between one dune and another,
  - 2) the lengths of the dune to distances of up to tens or even hundreds of kilometers,
  - 3) the meandering of the dunes,
  - 4) the relationship between the wind and the movement of the dune.
- None of the researchers tried to explain all of the above phenomena.

The fact that the longitudinal dunes stretch out in straight lines for great distances in the Sahara, Arabian and Australian deserts caused several researchers to believe that the dunes are erosional and not depositional forms in origin. Aufrère<sup>(10)</sup> was the first to claim that longitudinal dunes are residual relief features created as a result of a longitudinal erosion that created the depressions, the "gassi" between the dunes. This approach, developed by King<sup>(11)</sup> in Australia, who assumed that during the Pleistocene, before the present erosional era, there were fluvial conditions which caused flood plains and lakes to receive a great amount of detritus sediment. In the following dry period, the wind shaped the detritus covering to form sand ridges; thus it is not necessary, according to this theory, to explain the shifting sands in order to explain the longitudinal ridges which continue for hundreds of kilometers. Melton<sup>(12)</sup> called this type of dune a "wind drift dune," and they were created, according to his opinion, by strong winds which blew in a permanent direction. Verstappen<sup>(13)</sup>, who observed fixed dunes in Pakistan, came to the conclusion that in a former humid period, parabolic dunes were formed, which created the linear lines of the longitudinal dunes. Connection between two lines of dunes, known as "tuning fork", he sees as a parabolic dune. Folk<sup>(14)</sup> believes that

longitudinal dunes are essentially erosional and therefore do not pile up to great thickness; barchans and transverse dunes are according to him depositional forms and are able to build to great thicknesses by climbing one on top of the other.

In contrast to the view that favors the "wind drift" dune we can claim that a thick, sandy plain cannot remain flat for a great length of time, and that such plains are not found today in arid or semi-arid areas. Mabbutt and Sullivan<sup>(15)</sup> did not find any relationship between the dunes and the sub-aeolian surface in the Simpson Desert, and also did not find any sign of a fluvial core. Wopfner and Twidale<sup>(16)</sup> also doubted King's findings<sup>(11)</sup> about the Australian Desert. The fact that we find longitudinal dunes with an internal aeolian structure<sup>(17)</sup> proves beyond all doubt that the dune has an aeolian origin.

Among the researchers who agree that the longitudinal dunes are depositional forms differences of opinion arise as to the nature of the prevailing winds that cause them. Bagnold<sup>(7)</sup> believes that in order for a longitudinal dune to develop a diagonally blowing storm wind is necessary in addition to a prevailing wind, that the longitudinal dune will form from the horn of a barchan, and will continue parallel to the resultant of both winds. A similar conclusion was reached by Cooper<sup>(9)</sup> about coastal longitudinal dunes in Oregon, by McKee and Tibbitts<sup>(17)</sup> and Smith<sup>(18)</sup> about the 'seif' dunes in Libya, and by Wopfner and Twidale<sup>(16)</sup> of dunes in the Simpson Desert in Australia.

In contradiction to this view, most researchers believe that longitudinal dunes form parallel to storm winds. Hanna<sup>(19)</sup> presents proof of this from various sources and from all the sandy areas of the world. Folk<sup>(14)</sup> is of the opinion that the orientation of the dunes is parallel to one dominant wind and that occasional crosswinds only cause the summit to be asymmetrical.

Wilson<sup>(20)</sup> claims that a uni-directional wind creates both longitudinal and transverse dunes. In his opinion the type of dune is determined by the secondary wind currents<sup>(21)</sup>. Warren<sup>(22)</sup> does not agree with the explanation that sees the dune orientation determined by the direction of the resultant yearly wind. He found in the 'erg' of Algeria and Libya two clear arrangements of 'seifs' that were crossed by sharp angles.

Most of the supporters of the opinion that the longitudinal dunes are caused by a uni-directional wind believe that the wind develops through a helicoidal flow movements which is the cause of many of their aforementioned characteristics. This opinion was first developed by Bagnold<sup>(23)</sup>, who suggested that helicoidal flow was caused by differential heating of the surface of the sandy areas. As proof of this he presents the parallelism between the resultant summer wind and the directions of the

longitudinal dunes in Egypt. Hanna<sup>(19)</sup>, who tried to give a better-based meteorological explanation to the phenomenon of helicoidal flow, based his conclusions on the research done on the formation of cloud streaks in the atmosphere at an altitude of several kilometers. He assumes that the conditions of the formation of flows are the most common in the latitudes of the trade winds and concludes that proof of the validity of this hypothesis will come once experiments will be conducted to follow the movements of weather balloons above the Sahara or any other great desert. Experiments with weather balloons that were conducted in Idaho<sup>(24)</sup> showed helicoidal flow at an average altitude of 2000 meters above the ground. The balloons indicated the existence of helicoidal flows which did not move in a constant direction, as would be expected of flows which are allegedly the cause of a stable dune alignment.

Glennie<sup>(25)</sup> believes that the helicoidal flow is formed by the pressure gradient caused by the resistance of the dune to the wind. Folk<sup>(14)</sup> believes that this flow is the cause of the "tuning-fork" form common in the longitudinal dunes of Australia. Mabbutt et al.<sup>(26)</sup> explained, with the help of this flow, the asymmetry of the longitudinal dunes in Australia. Folk<sup>(27)</sup> created a pattern similar to longitudinal dunes with the aid of grease spread on a layer of glass upon which a cylinder was rolled.

All these opinions which claim that longitudinal dunes are a product of helicoidal circulation in the atmosphere are based mainly on the intuition of the researchers, and not on a sound theoretical basis or on actual measurements in the field<sup>(28)</sup>.

Wilson<sup>(21)</sup> developed the view that sees secondary flows as the morphological shaping factor of the dune types. He sees longitudinal dunes as the creations of double longitudinal helicoidal flows. The creation of transverse flows causes transverse dunes, in his opinion. A combination of transverse and longitudinal flows will lead to diagonal or meandering forms. Wilson did not observe these currents in the desert and he assumes their existence on the basis of experiments with ripples in water done by Allen<sup>(29)</sup>. Wilson<sup>(30)</sup> is not certain if the secondary currents existed before the development of the dunes or if they came into being after the dunes developed. Cooke and Warren<sup>(1)</sup> believe, basing themselves on Wilson, that the oblique dune shapes are universal. They see the lengthening of the barchan arm as an oblique growth caused by helicoidal flow on the lee flank.

Twidale<sup>(31)</sup> claims a different development of the longitudinal dunes in Australia, which start from the lee flank of the lunettes or foredunes on the borders of the playas. The wind that blows from the playas outwards changes direction after hitting the foredune, and as a result of this the blown sand concentrates in elongated lines, and a longitudinal dune is formed which lengthens along the direction of the wind.



It seems that the effort on the part of most researchers to explain the longitudinal dune as an extension parallel to the storm wind is derived from the fact that the dune extends in one direction and that it is difficult to explain its elongation by winds not blowing in their direction of movement.

In summation, we see that there are many theories about the phenomenon of longitudinal dunes. The lack of unity in these opinions of their origin, dynamics and morphology derives from the fact that these opinions were frequently formed after only a simple trip to one of the sandy seas<sup>(32)(33)(20)</sup>, or were based only on aerial photographs<sup>(19)</sup>. The conclusions were reached by intuition according to the impression that the longitudinal dunes made on the researcher. In other studies, tests were made of only one aspect of the longitudinal dunes, for example, their internal structure<sup>(17)</sup> or an analysis of their grain size<sup>(14)</sup>. We suggest that a research, in which a comprehensive examination and analysis is made of all aspects, including dynamics, morphology, sedimentology and meteorology, it is more likely to reach well founded conclusions on the formation, morphology and dynamics of the longitudinal dunes.

### 1.3 Aim of the Present Work and Its Application

The aim of this project is to study all the dynamic processes at work on longitudinal dunes. Research of this sort demands understanding both of the morphology of the longitudinal dunes and of the mutual relations between the dune morphology and their dynamics. Study of the mechanism of movement and advance of the longitudinal dunes, and interpretation of the processes which build them, will validate or disprove one of the existing theories on this subject (especially the theory of helicoidal flow) or it will suggest a completely different mechanism.

The results of this study may be important for the understanding of the dynamics of sand fields as a background to sand stabilization and reclamation work, as well as to the understanding of other dune types, especially mega-dunes (draa), which are built from segments with profiles identical to those of longitudinal dunes, and upon which the same processes are working as on longitudinal dunes.

With the aid of the data and the results of this work it will be possible to define better fossilized aeolian deposits which originated from longitudinal dunes, and to understand more fully the paleogeography of the era when they were deposited.

The results of this work are important also to the understanding of aeolian and meteorological processes that take place on Mars. From the pictures taken by Mariner 9<sup>(34)(35)</sup> and Viking 1<sup>(36)</sup> it was shown that large portions of the Martian surface are covered with sand dunes very

similar to the dunes found upon earth. Before we come to any conclusions about the aeolian processes which take place on the surface of Mars we should know more about these same processes in the deserts of the earth.

The subject of this paper is composed of two parts. The first part is concerned with the question: - how is the first shape of the longitudinal dune formed? The second part is concerned with the development and preservation of longitudinal dunes after its formation. The answer to the first question will have to be speculative, since there is no possibility, in a short period in the field, of observing the formation of a longitudinal one. Therefore, the results of this research will be concerned with the mechanism of movement and advance of the longitudinal dune after the typical elongated shape has formed. In any case, with the results of this research, it will be possible to understand and study the factors that created the first longitudinal form.

This research project does not intend to solve all the problems relating to sand dunes in general or to longitudinal dunes in particular. The subject is too complicated and too wide to be solved by one research project. However, the results and conclusions of this work can give partial answers, or can solve some of the central problems, and can be used as a background and springboard for further work in the field.

#### 1.4 Research Method and Approach

The method used in this research project is to study one longitudinal dune using a combination of meteorological, micrometeorological, dynamic, geomorphological and sedimentological measurements. Each particular aspect will be summarized independently, and finally on integration of all the results will provide an overall picture that will make it possible to build a model of the advancing mechanism valid for the longitudinal dune.

The research methods are the following, to be described in detail in each chapter.

a) Wind measurement. Both macro and micro-measurements were used; the former to study the prevailing wind regime in the research area, the latter to record changes in wind direction and magnitude of eddies that are formed as the result of the encounter of wind with the body of the dune.

b) Grain size measurements. Characteristic parameters were determined on samples of sand from different parts of the dunes, and their dynamic significance was checked.

c) Tracers. The sand movement was traced with the aid of sand marked with fluorescent dye, and the results were analysed with the help of the general wind data.



- d) Internal structure. The make-up of the internal structure was determined by digging of sections and samplings of 'peels' with the aid of cementing polymers. The results indicate locations where sand is deposited or eroded.
- e) Rate of advance. Measurements were carried out in the field with the help of pegs positioned at the beginning of the research project and also by aerial photographs.
- f) Cross section. A study of changes in the profile of the dune in different seasons and of the declinations of the flanks was carried out with the aid of a level and a staff.

#### 1.5 Selection and Description of Research Area

The research was carried out on a typical longitudinal dune in the south of Israel in the Negev. This particular dune was chosen for several reasons:

- a) This is a typical longitudinal dune (see Fig. 1.1) which we find in abundance in the large sand seas of the world. The proof of the universality of this type of dune can be seen in its appearance in many places in the world, such as: the 'Chech' erg in Algeria<sup>(37)</sup>; the Simpson Desert in Australia<sup>(38)(39)</sup>; the Arabian Desert<sup>(40)</sup>; the libyan Desert<sup>(17)(21)</sup>; the Tenéré Desert in Niger<sup>(41)(42)</sup>. A similar type of dune is also found on the planet Mars<sup>(36)(43)</sup>.
- b) The dune is situated on an alluvial plain and the interdune area is bare of sand so that the aeolian action takes place on a longitudinal strip of sand, and therefore complications are avoided which could otherwise be caused by the formation of other structures in the interdune area.
- c) The dune is short, its length is 1½ kilometers. This facilitates the continuing investigation of various sections of the dune from the beginning to the end.
- d) There is easy access to the dune for the vehicle carrying the research equipment.

The amount of rain in the area averages about 60-70 millimeters a year, with about ten days of rain yearly in general.

The meagre flora in the area, mostly of perennial shrubs, is limited to the base of the dune and to the interdune areas, in which there are thin sand strips lying on an alluvial plain.

#### 1.6 Description of the Dune Selected for Investigation

The dune (Fig. 1.1) continues for 1500 meters and starts from a low, flat, sandy strip, without any slip-faces. This strip, which is 3 kilometers long, is built of bi-modal sand with a coarse mode that is not



Fig. 1.1 An aerial photograph of the dune as of Nov. 27, 1970. Numbers indicate the reference point along the dune. (By courtesy of Survey of Israel, Tel Aviv).

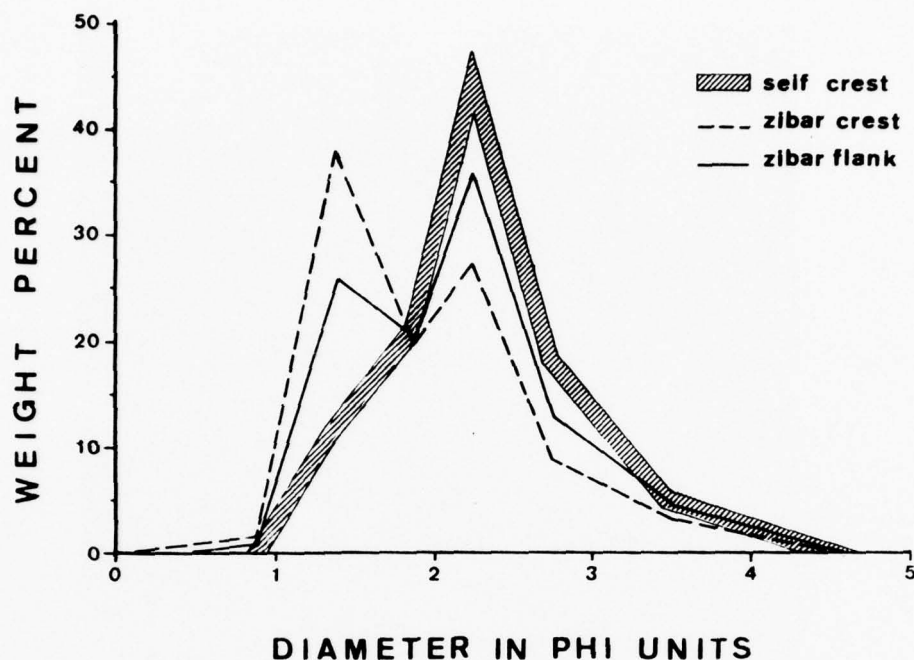


Fig. 1.2 Grain size distribution for the self dune crest, zibar crest and zibar flank.

found in dune sand (Fig. 1.2). Similar sand strips are common on extensive plains in the sandy deserts of the world. Holm<sup>(40)</sup> described such sand strips in Rub Al Khali in Arabia and he called them by their native name "zibar". He points out that the "zibars" create hard sandy surfaces which permit the passage of vehicles. The term "zibar" appears again in Warren<sup>(41)</sup> and in Wilson<sup>(44)</sup> in a similar description of coarse bi-modal sand strips. It can be assumed that the various descriptions of coarse bi-modal sand by McKee and Tibbits<sup>(17)</sup> and Folk<sup>(45)</sup> refer to the "zibar". Also, the undulating sand plain in Australia<sup>(6)</sup>, and the 'Whaleback' in the Libyan Desert<sup>(32)</sup> are similar to the descriptions of the "zibar". Fig. 1.3 of the Tenéré Desert in Niger shows a longitudinal dune that begins from "zibar" strips, similar to the dune under investigation (Fig. 1.1). Therefore it is possible to conclude that the "zibar" is frequently a source of origin of the longitudinal dune.

The dune begins from the "zibar" developing a sharp profile typical of a longitudinal dune. It meanders at nearly equal intervals, and peaks and saddles are found along its span; the peaks are always found on its

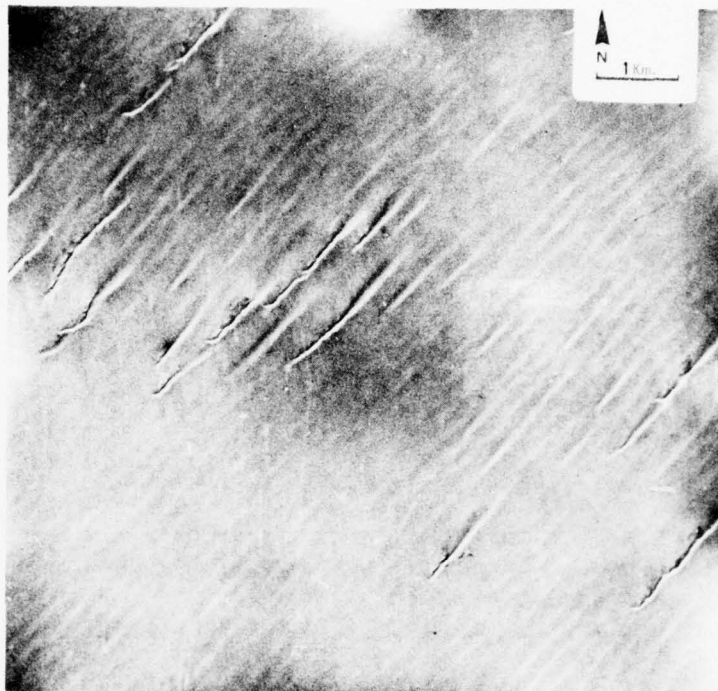


Fig. 1.3 Aerial photograph of zibar and longitudinal dunes in the Tenéré desert (Niger).



Fig. 1.4 The "tear drop" from of the longitudinal dune.



convex section facing south, and the saddles on the concave section facing south (see Figs. 1.1 & 1.5). The dune is divided into asymmetrical sections, where each section stretches from one saddle to another. The peak is found at the end of each section and there the deflection begins at the crest line and continues in the direction of the nearest saddle. The length of each section of the dune is 175 meters. This typical appearance of the longitudinal dune, as seen from a side view (Fig. 1.4), is called by Bagnold<sup>(7)</sup> (plate 12b) 'tear drop' and was also observed by Madigan<sup>(39)</sup> in the Australian longitudinal dunes.

The "zibar" can reach a height of 4-5 meters above the interdune plain. The dune peaks reach to 12-14 meters and the saddles to 5-8 meters. Fig. 1.5 shows the dune in schematic form from an oblique view from above and from the side. The "zibar", the crest line, the peaks and saddles and all the deflection points, which exist where the crest line meanders, can be distinguished. The deflection points are identified with the peaks and saddles. Between the deflection point situated at the peak, and the deflection point situated at the saddle, we find the meandering area of the dune which is characterized by a slope whose height decreases toward the saddle.

At the beginning of the research project reference points were fixed along the dunes and were marked by pegs. The reference points were placed at the peaks and saddles of the dune sections as they existed at that time. Each point was marked by 4 pegs placed in the interdune area, on both sides of the dune and perpendicular to it. The dune is situated along a line whose direction is  $110^{\circ}$ - $290^{\circ}$  and the pegs at a line whose direction is  $20^{\circ}$ - $200^{\circ}$ . All in all, 19 points fixed (Fig. 1.1); point No. 1 is situated in the "zibar" area and point No. 19 at the point where the dune ended at that time. The pegs permit cross-sectioning of the dune profile along well-defined lines, study of various sections along the dune, and a follow-up of the rate of advance in various sections of the dune.

25



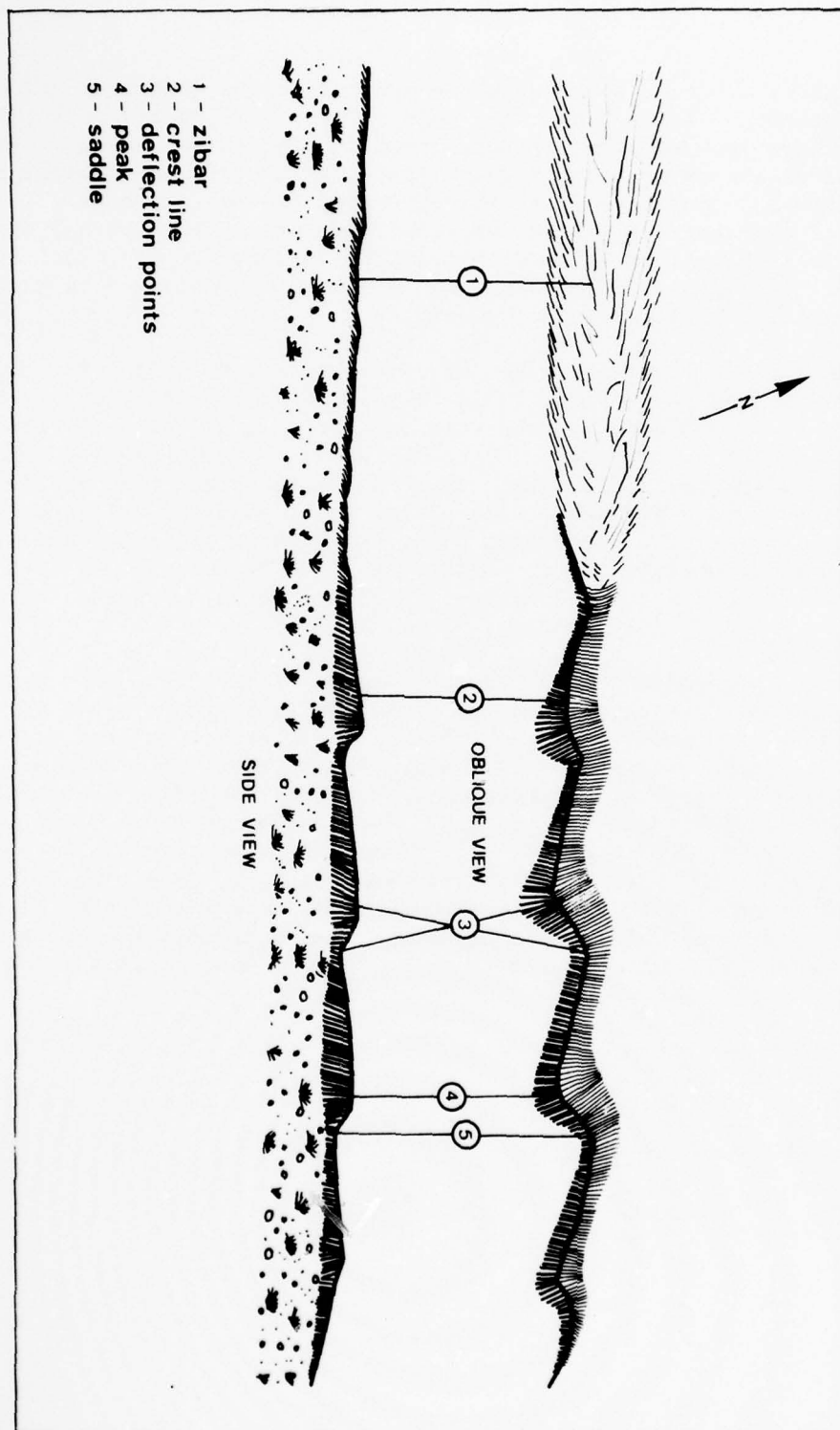


Fig. 1.5 Sketch of longitudinal dune drawn from an oblique and side view.

## II. WIND REGIME IN THE RESEARCH AREA

### 2.1 Instrumentation

The wind regime in the research area was studied with the aid of an automatic wind recorder of the Woelfle type, which registers the wind-run per hour and its direction. The instrument is operated with cups and a vane (see Fig. 2.1) and a chart strip (moved by a clock mechanism) for a period of 31 consecutive days. The instrument is capable of recording wind velocity at magnitudes from 0.5 to 60 meters/second. It cannot be used for micrometeorological measurements. The data which it furnishes gives an accurate picture only of the general wind regime. Therefore the data was used as background material and as an aid in the analysis of the results of the dynamic measurements, such as micrometeorological wind measurements and tracing of sand shifts on the dune with fluorescent markings.

The instrument is fixed on a pole at a height of  $3\frac{1}{2}$  meters above the crest of the dune at point No. 2, situated on the transition from the zibar to the dune (Fig. 1.1). The instrument is at a height of about 11 meters above the interdune plane. It was assumed that at this height the influence of the dune structure on the wind is at a minimum.

### 2.2 Processing of the Data

The wind chart recorder is interpreted with the aid of the digitizer, which transfers the data on the chart directly to punch cards. A further processing, through a computer, gives average values of the wind velocity reading and direction for every hour. The accuracy of the average wind velocity reading per hour is up to 1/10 meter/second and the direction is within  $10^\circ$ . The results appear on tables that represent the percentage of wind frequency at an interval of  $10^\circ$  in direction and of 2 meters/second in velocity, which starts from 6 meters/second (which is the threshold velocity - see the following) and up to 16 meters/second (a velocity that is very rare in the research area). The tables are arranged in the following manner for a two year period (Appendix 1) and for different seasons (Appendices 2, 3, 4, 5). A definition of the seasons follows: Fall - the period between September 16th and November 30th; Winter, from December 1st to March 15th; Spring, from March 16th to June 15th; Summer, from June 16th to September 15th.

Calculations were made for each table for the following parameters: (1) hourly vector mean wind velocity and direction; (2) degree of wind constancy. The calculations are according to Brooks and Carruthers<sup>(46)</sup>.

$$V_R = \frac{1}{N} \sqrt{[(\Sigma V_N)^2 + (\Sigma V_E)^2]}$$

where:

$V_R$  = hourly vector mean wind velocity;

$N$  = number of vectors;

$V_E$  ;  $V_N$  = north and east vector components of the wind.

These components are calculated:

$$V_N = V \cos \alpha$$

$$V_E = V \sin \alpha$$

where:

$V$  = wind velocity

$\alpha$  = the direction (in degrees) from which the wind blows.

The hourly vector mean wind direction is calculated according to the following formula:

$$\tan \theta = \Sigma V_E / \Sigma V_N$$

$$\theta = \arctan \Sigma V_E / \Sigma V_N$$

where:

$\theta$  = the hourly vector mean wind direction.

The degree of wind constancy is calculated according to the following formula:

$$q = 100 V_R / V_S$$

where:

$q$  = degree of constancy in percentage;

$V_S$  = scalar mean wind velocity. It is calculated:  $V_S = \frac{1}{N} \Sigma V$ .

$V_S > V_R$  except when the wind blows all the time from the same direction. The level of constancy is zero when the wind blows at an equal frequency and speed from all directions, and is 100% when the wind blows all the time, from only one direction.

### 2.3 Threshold Velocity of the Dune Sand

The threshold velocity of the dune sand is important in the analysis of the general wind regime. Wind velocities below the threshold must be ignored and attention paid only to those velocities above the threshold. The threshold velocity estimation cannot be unequivocal since each grain

size has its own threshold velocity and the threshold velocity changes with the height of the dune. Another problem arises because of the fact that we find a range of sand grains on the dune, so that a small grain, which is moved directly by the wind, manages, by its movement, to move a larger grain of sand, its threshold velocity not yet being reached by the wind<sup>(47)</sup>.

The threshold velocity of the sand can be determined by two methods:

(a) A theoretical calculation according to Bagnold's<sup>(7)</sup> formula:

$$V_t = 5.75A \sqrt{\frac{\sigma - \rho}{\rho}} g d \log \frac{z}{k}$$

where:

$V_t$  = threshold velocity measured at height  $z$

$A$  = coefficient ( $\approx 0.1$ )

$\sigma$  = density of sand grains ( $\approx 2.65$ )

$\rho$  = density of the air ( $\approx 1.22 \times 10^{-3}$ )

$d$  = diameter of the grains

$k$  = degree of surface irregularity ( $\approx d/30$ )

The two unknown factors in the above formula, the diameter of the grains and the height at which the wind is measured, are the two determining factors that have already been mentioned. Fig. 2.2 presents the threshold velocity for the various grains and levels of the dune, as they were calculated for the wind recorder. The common size group of the sand of the dune is  $1\frac{1}{2} - 3 \phi$  so we can determine that the sand movement starts at a velocity of 6 meters/second, especially at the crests, and absolute movement of the sands will be at a velocity of 9 meters/second.

(b) Another possibility to determine the threshold velocity is based on field observations during the beginning of sand storms. Sixteen observations that were carried out during the research period showed that sand movement, on the highest crests of the dune, begins at a wind velocity of 6 meters/second. At wind velocity of 7 meters/second movement was noticed also at lower levels of the dune, and at a velocity of 9 meters/second there was general movement at all levels of the dune.

From this aspect there is a complete correlation between the calculated and the observed data. Fig. 2.2 shows that coarse grains have relatively significant differences in the value of the threshold velocity between low elevations close to the ground and above 6 meters in height. This phenomenon is caused by the quick rise with height of the velocity of the high wind necessary to move large sand particles. We can understand, according to the above, why sand dune made up of large sand grains such as the zibar are always low and flat.



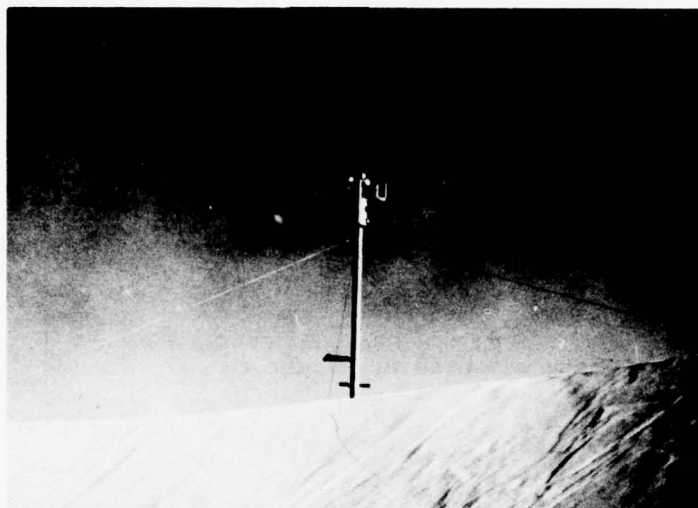


Fig. 2.1 The wind recorder.

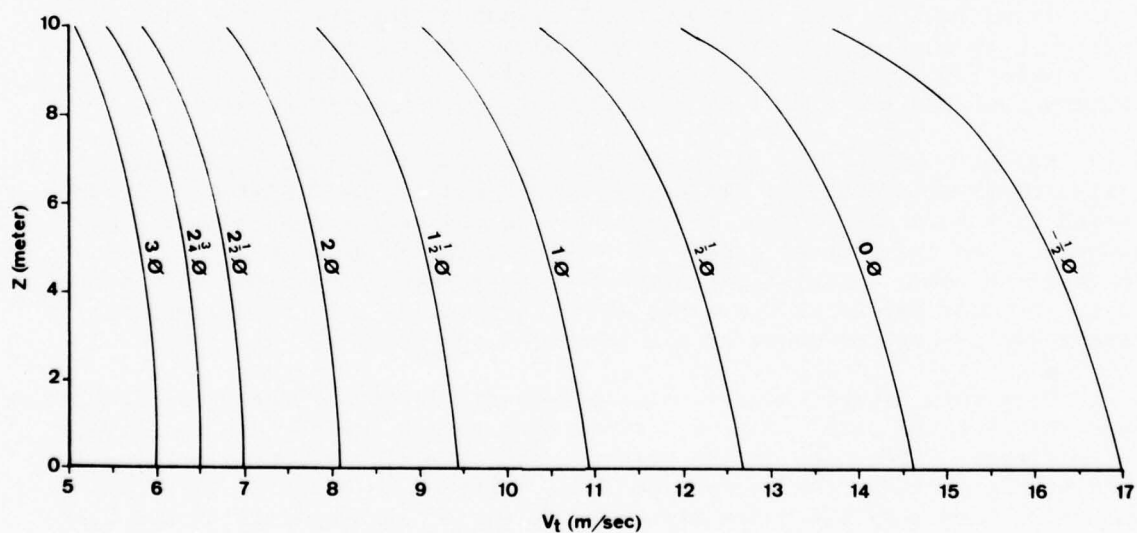


Fig. 2.2 Values of threshold velocities ( $V_t$ ) of different grain sizes (in  $\phi$  units) on different heights ( $Z$ ) of a dune that is 10 meters high.

In summation, the value of 6 meters/second can be considered the lower limit of the threshold velocity of the wind which influences dune sand. Therefore, consideration of the wind regime which influence dune sand will be for velocities above 6 meters/second.

#### 2.4 Effective Wind

The aim of the study of the wind in the present research is to get a clear picture of the amount of energy exerted by winds from various directions on both sides of the dune. This can be expressed according to the sand flow. Hsu<sup>(48)</sup> claims that the flow of aeolian sand increases according to third power of wind velocity. Therefore we can learn the total effect of the wind in its various velocities by calculating for each hourly wind velocity the number of hours at a velocity of 6 meters/second that would do the same amount of work.

For each wind direction, the calculation has been done according to the equation:

$$T_{(6)} = \sum \left( \frac{V}{6} \right)^3$$

where:

- $T_{(6)}$  = The hours of the effective wind (equivalent to 6 meters/second) in a certain direction.  
 $V$  = Hourly mean wind velocity.

This calculation gives us the hypothetic wind regime at a magnitude of 6 meters/second only that would do the same amount of work as the real wind regime. The effective wind regime enables us to discern the wind directions responsible for most of the work on the dune (Appendixes 1-5; Tables 2.1, 2.2; Figs. 2.3-2.7).

#### 2.5 Results and Discussion

All results are contained in appendixes 1-5, Tables 2.1, 2.2, and Figs. 2.3-2.7. The wind was above the threshold velocity only one quarter of the time in all seasons and periods.

In the summer 85% of the effective winds come from sectors between 320° to 360°, where the most modal sector was 340°-350° (Appendix 3, Fig. 2.3). These were sea breezes which blow regularly every day during the early afternoon to the evening. Since the synoptic situation is the summer is uniform the degree of constancy of the summer winds is highest and reaches 94%. The intensity of the winds in the summer is relatively lower and only rarely rises above the velocity of 10 meters/second.

Table 2.1 Summary of wind data.

Period	Definition of period	Percent of hours above threshold velocity	Wind vector		Degree of wind constancy	Effective wind	
			Direction in degrees	Velocity in meter/second		Modal direction in degrees	Frequency in percent
12.1.72-3.15.73 12.1.73-3.15.74 12.1.74-3.15.75	Winter	26.2	226	4.8	56.7	190-200	21.3
6.16.73-9.15.73 6.16.74-9.15.74 6.16.75-8.28.75	Summer	25.9	342	7.0	93.8	340-350	36.1
9.16.73-11.30.73 9.16.74-11.30.74	Fall	23.4	329	3.8	50.5	340-350	22.9
3.16.73-6.15.73 3.16.74-6.15.74 3.16.75-6.15.75	Spring	27.6	337	5.7	72.2	340-350	21.2
1.1.73-12.31.74	Two years	26.4	314	3.6	45.3	340-350	17.8

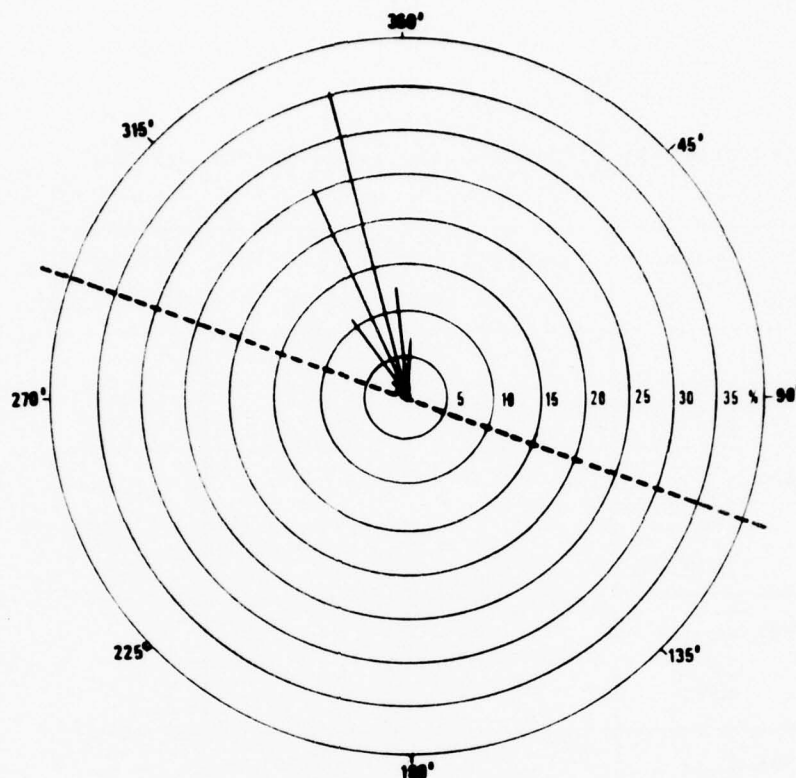


Fig. 2.3 Circular diagram of the effective summer wind directions (percentage). Dashed line indicates the dune axis.

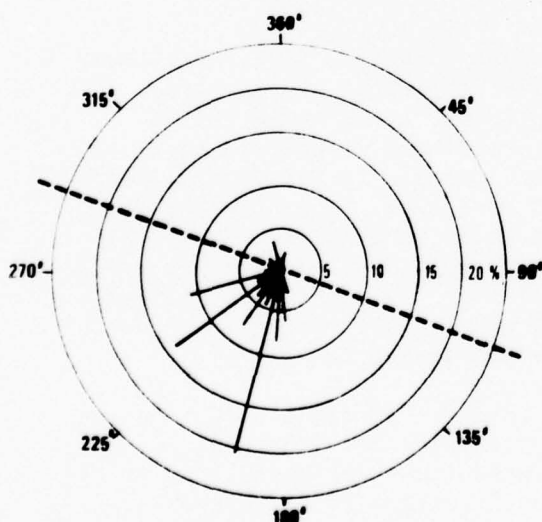


Fig. 2.4 Circular diagram of the effective winter wind directions (percentage). Dashed line indicates the dune axis.

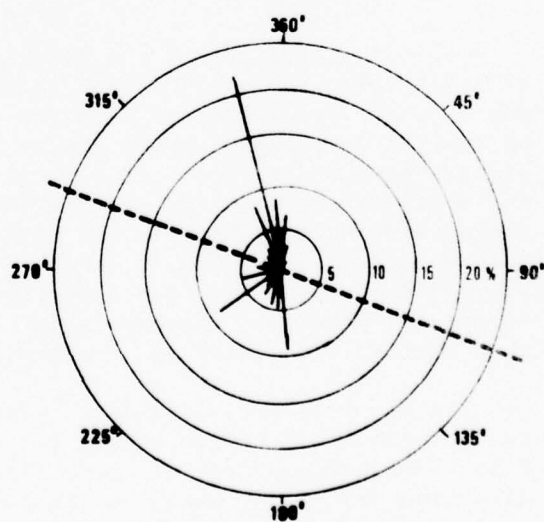


Fig. 2.5 Circular diagram of the effective fall wind directions (percentage). Dashed line indicates the dune axis.



Table 2.2 Percentage of effective wind from various sectors

Period \ Sector	(Southerly) 180° to 290°	(Northerly) 290° to 40°	(Easterly) 40° to 180°
Two years 1973 1974	44.1	49.4	6.5
Winter 1972/73 1973/74 1974/75	77.9	12.1	9.9
Summer 1973 1974 1975	2.0	97.9	0.1
Spring 1973 1974 1975	24.7	72.4	2.9
Fall 1973 1974	31.4	56.8	11.7

In the winter 80% of the effective winds come from the sector between 170°-260° when the modal sector is 190°-200° (Appendix 2, Fig. 2.4). Winter winds are connected with the synoptic situation which brings barometric depression to the Middle East. Southern Israel, in this period, gets winds from S to W directions. Changes in the depressions and their movement brings changes in wind direction. Therefore, the degree of wind constancy in the winter is lower than in the summer and reaches 57% (compare Fig. 2.3 with Fig. 2.4). 7% of the effective winds in the winter come from the directions 320°-360°, which is the direction of the sea breezes. The magnitude of the wind in the winter is higher than that in the summer and reaches 16 meters/second and more.

In the transitional seasons (Fall & Spring) the winds come from the two sectors which typify summer and winter (Appendixes 4,5; Figs. 2.5, 2.6). The modal sector of the effective winds in these seasons is in the direction 340°-350°, which is the dominant direction of sea breezes.

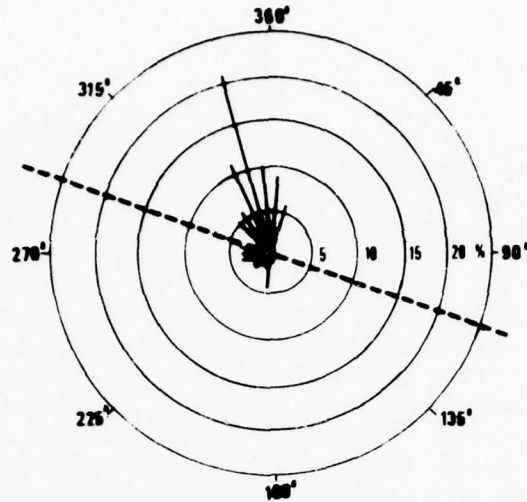


Fig. 2.6 Circular diagram of the effective spring wind directions (percentage). Dashed line indicates the dune axis.

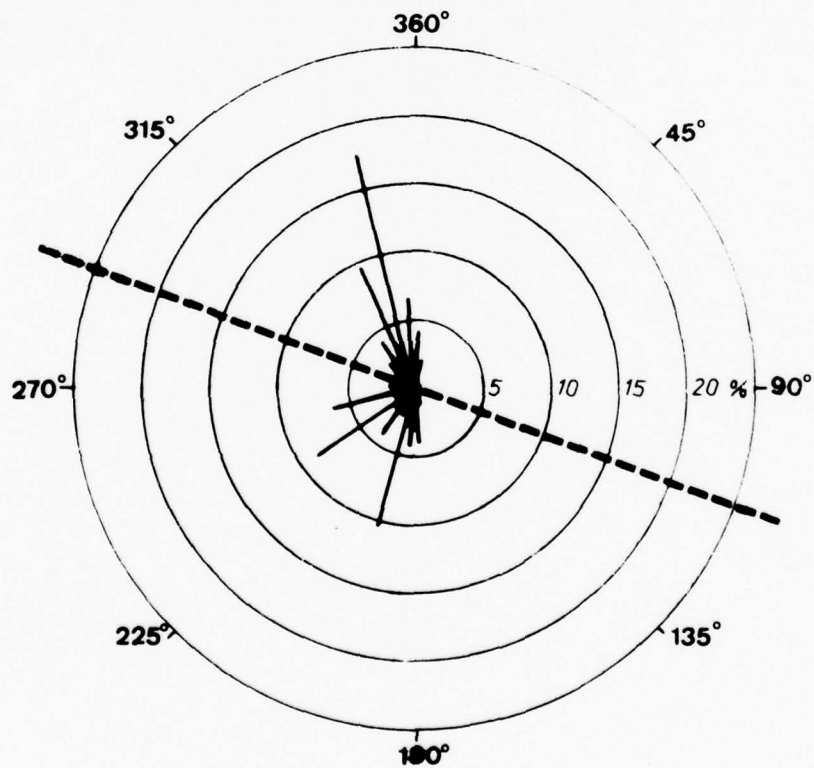


Fig. 2.7 Circular diagram of the effective annual wind directions (percentage). Dashed line indicates the dune axis.

A summary of the effective winds for the years 1973 and 1974 shows that the longitudinal dune is under a bi-directional wind regime (Appendix 1; Fig. 2.7). The dune stretches between the two dominant wind directions, where there is a deviation of  $24^\circ$  between the spread of the dune ( $290^\circ$ ) and the hourly vector mean wind direction (Table 2.1). The effective winds, which come from the northern sector of the dune ( $290^\circ$ - $40^\circ$ ) are of a 5% higher frequency than those which come from the southern sector ( $180^\circ$ - $290^\circ$ ) (Table 2.2). The winds from the northern sector come from a narrow range of directions (Fig. 2.7) relative to those from the southern sector. This is expressed even in the high degree of constancy in the summer. In addition the mode of the summer winds ( $340^\circ$ - $350^\circ$ ) is at an angle of  $50^\circ$ - $60^\circ$  to the axis of the dune, and on the other hand the mode of the winter winds ( $200^\circ$ - $190^\circ$ ) is at an angle of  $90^\circ$ - $100^\circ$  to the dune axis.

From the above data and facts one can come to the conclusion that the winds which blow from the northern sector influence the dune more than those from the southern sector. It is worth mentioning that the percentage of the effective winds which blow in the direction of the spread of the dune ( $290^\circ$ - $110^\circ$ ) is almost zero. Therefore it is clear that the longitudinal dune is not a product of a uni-directional wind.

### III. MICROMETEOROLOGICAL WIND MEASUREMENTS

#### 3.1 Introduction

The dune, as a structure situated in the path of wind advancement, causes disturbances in the flow of the wind and the formation of eddies; the eddies are important in the formation and shaping of sedimentary structures<sup>(49)</sup>.

Measurements of changes in the magnitude and direction of the wind in the leeward flank were done mostly on transverse dunes<sup>(9)(50)</sup>. No work has been done on longitudinal dunes. The wind recorder (Fig. 2.1) furnished data on the general wind regime. In order to obtain data on the changes in direction and magnitude of the wind near the dune ground level, where the actual sand movement occurs, micrometeorological instrumentation is necessary.

#### 3.2 Instrumentation

The micrometeorological measurements of wind magnitude were done with the aid of cup anemometers. The instrument used was the RIMCO Miniature Cup Anemometer (product of Rauchfuss, Australia). This instrument contains 6 cups which are capable of measuring the wind run simultaneously. Fig. 3.1 represents the anemometers on one of the dune flanks. The five anemometers in Fig. 3.1 are attached to a pole 8 centimeters above the ground (the cups themselves are at a height of 16 centimeters above the ground) and they are connected by cables (Fig. 3.2) to a junction box from which a multi-cord cable leads to the control box where the recording meters are situated (Fig. 3.1).

The instrument is operated on the Reed Switch Principle<sup>(51)</sup> and it has properties which fulfill the requirements of micrometeorological measurements. The instrument was developed by E.F. Bradley of C.S.I.R.O. in Canberra, Australia, as an anemometer system for use near the ground, mostly for Agricultural meteorology. Bradley<sup>(2)</sup> gives technical details and lists the advantages of this instrument.

An estimation of the wind direction, simultaneously with the measurements of wind magnitude, was made by means of little flags that were set on the measured area at the anemometer height. Observations of the changes in wind direction and localization of the eddies were done with smoke candles with a burning time of one to two minutes.

#### 3.3 Results of Anemometer Measurements

##### 3.3.1 Introduction

There are two types of measurements: those done across the dune,



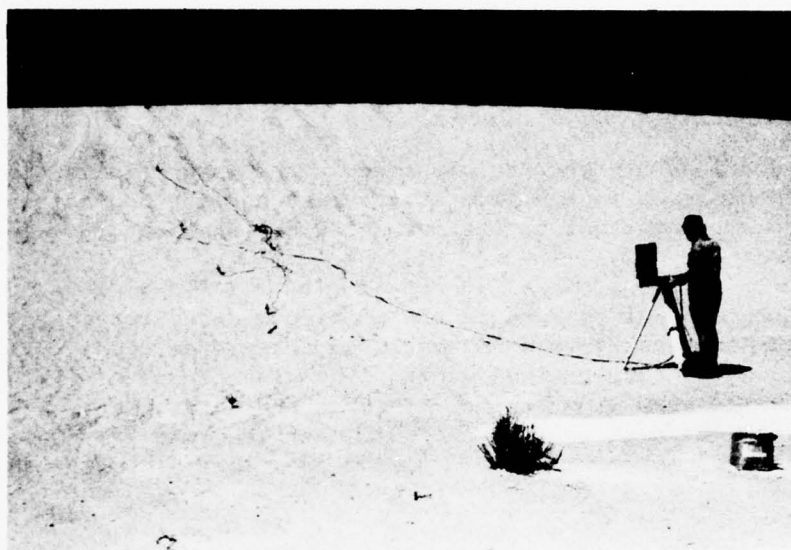


Fig. 3.1 The RIMCO Miniature-Cup Anemometers across the dune flank.

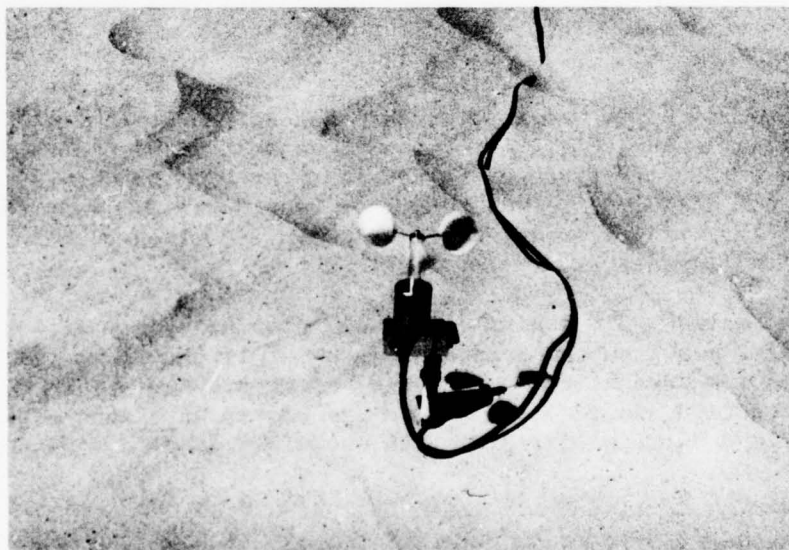


Fig. 3.2 Close view of an anemometer.

where changes in magnitude were measured across one flank or two flanks together; and measurements that were done along the length of the dune on one of the flanks. By these measurements it is possible to observe changes in magnitude at various points along the dune.

All the results of the measurements appear in Appendixes 6-13, and also in Table 3.2 and in Figs. 3.3-3.12 below. In the Figs. the anemometers location and the flags are seen in a cross section, or on a map (where there was measurement along the dune). The cross-sections in Figs. 3.3-3.9 represent parts of the cross-sections that were done with the aid of a level. The whole cross-sections from which the parts were taken appear in Appendixes 14-17. Fig. 3.13 represents the average direction of the wind on both dune flanks, for the measurements presented by Figs. 3.3-3.9.

Under the cross-section or the map are graphs which present the wind magnitude at the various measurement points. Each measurement unit covered a time of ten seconds to one minute. The average hourly wind magnitude, measured by a wind-recorder at the time of measurement, is also represented in this way. Beneath the wind magnitude graphs are graphs of the wind direction, which was measured simultaneously by flags. The general wind direction and the maximum interval of gusts are presented here, as they were measured at the same time by the wind-recorder.

### 3.3.2 Cross Profile Measurements

These measurements were done on a number of cross-sections at various points of the dune (Fig. 1.1) and during varied wind conditions and the results can be divided accordingly.

Figs. 3.3, 3.4 show the measurement results on the lee flank. The conspicuous phenomena in all these measurements are the sharp fall in velocity from the crest to a distance of 2-3 meters down the lee flank, and afterwards a slight rise in velocity for the remainder of the flank.

The rate of the drop in velocity on the lee flank, for a distance of 2-3 meters from the crest line, is not uniform and is dependent on a few factors which we will discuss below. The average rates of drop of the velocity are between 2.6-5.3 meters/second.

The rate of rise in wind magnitude, for the length of the lee slope (after the drop at a distance of 2-3 meters from the crest) is much smaller than the rate of decrease and amounts to an average of 1.2 meters/second at a distance of 6.9 meters from the crest in Fig. 3.3, and to 0.7 meters/second on the average at a distance of 6 meters from the crest in Fig. 3.4.

The results of the direction measurements, with the aid of the flags, showed that in every case there are significant differences (on the level

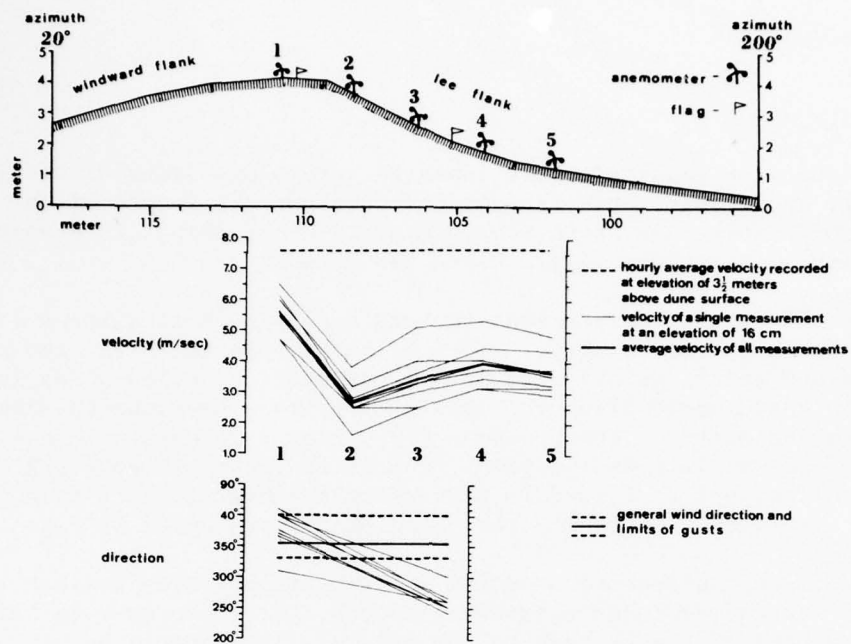


Fig. 3.3 Results of wind measurements taken across the dune flank at point no. 18.

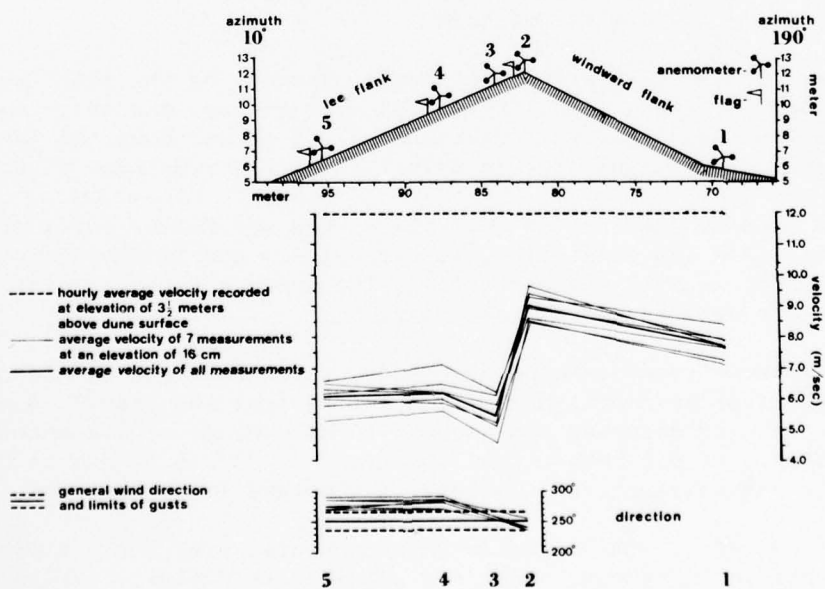


Fig. 3.4 Results of wind measurements taken across the dune flanks at point no. 5.

of 0.01) between the wind direction at the crest and at the lee flank. The change in direction has one transect parallel to the crest line. This is demonstrated by Table 3.1 where in all cases represented there,  $(A-D) > (B-D)$ . On the lee flank there are no significant differences (on the level of 0.05) between the directions measured on the upper part of the flank.

Table 3.1 Wind Direction Data on the Crest and on the Lee Flank

Point No.	Average wind direction on the crest (in degrees)	Average wind direction at a point on the lee flank (in degrees)	Difference between average wind direction on the crest and at a point on the lee flank (in degrees)	Distance between measurement point on the lee flank and the crest (in meters)	Angle between crest line [D] and wind direction (in degrees)	
					dune crest [A-D]	lee flank [B-D]
	[A]	[B]	[A-B]			
18	17	260	117	5.3	87	30
5	210	290	80	5.0	70	10
5	245	285	40	6.0	35	5
5	214	290	76	5.0	66	10
5	215	282	67	5.0	65	2

Figs. 3.5, 3.6, show the changes in wind magnitude and direction along the slope of the lee flank. A fall in the magnitude of the wind on the slope of the lee flank is observed, compared to the magnitude that is measured at the crest. ° (The differences are significant at the level of 0.01) In spite of the fact that the averages point to a tendency to a drop in the velocity on the slope of the lee flank, there is a variability in the wind magnitude in the above measurements and in some cases the wind magnitude on the lee flank is even higher than that at the crest. In other cases there is a sharp drop in the wind magnitude. In all the cases there are no differences (on the level of 0.01) between the various magnitudes measured on the lee flank itself.

The wind directions, on the lee flank at a distance of 5 meters from the crest, show a tendency to parallel the crest line that was observed previously (Table 3.1). At further distances from the crest (7½, 10 meters), this tendency is less obvious and here there is a tendency to try to return to the original wind direction as it was measured at the crest. From this we can see that the deflection in the wind direction on the lee flank is at its maximum at a distance of 5-7 meters from the crest, and that further down the slope of the lee flank, the wind strives to return to the general direction measured at the crest.



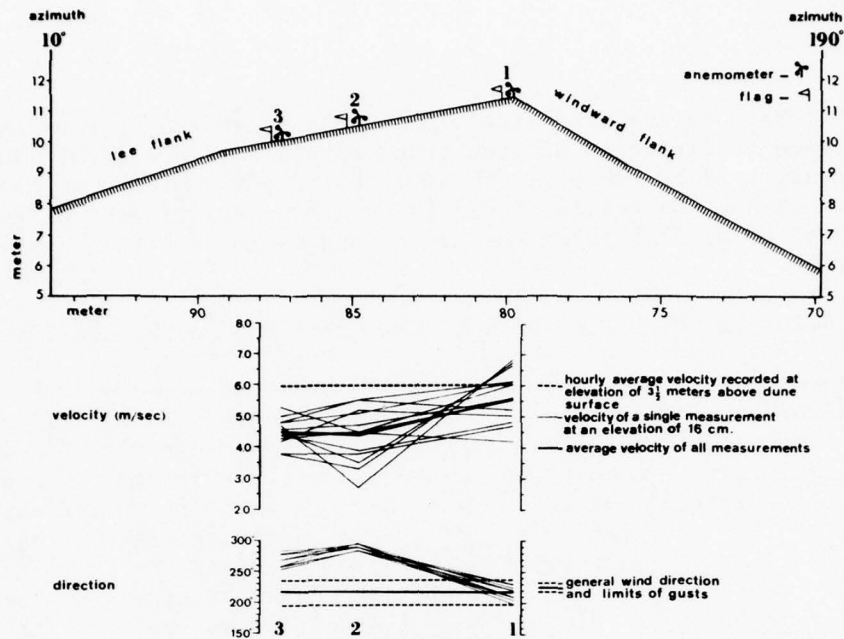


Fig. 3.5 Results of wind measurements taken across the dune lee flank at point no. 5.

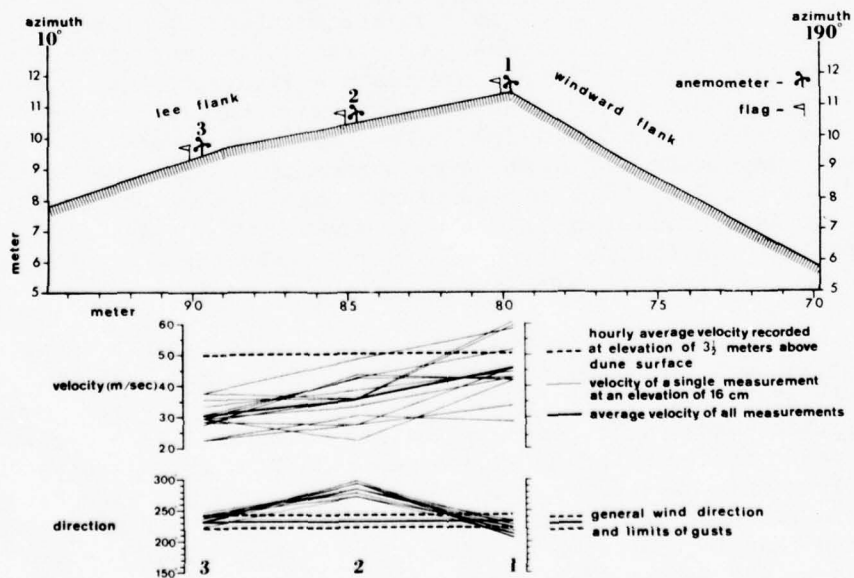


Fig. 3.6 Results of wind measurements taken across the dune lee flank at point no. 5.

Fig. 3.7 presents a measurement done across the lee flank from the crest to a distance of 8 meters, similar to the measurement done in Fig. 3.3. The results of the measurement are different from those in Fig. 3.3 and from other similar measurements (Figs. 3.4, 3.5, 3.6). These differences are: in most cases and on the average, there is a rise in the wind magnitude at a distance of 2 meters from the crest, compared with the magnitude that was measured at the crest itself. On the lee flank there are higher values of wind magnitude in contrast to the values at the crest.

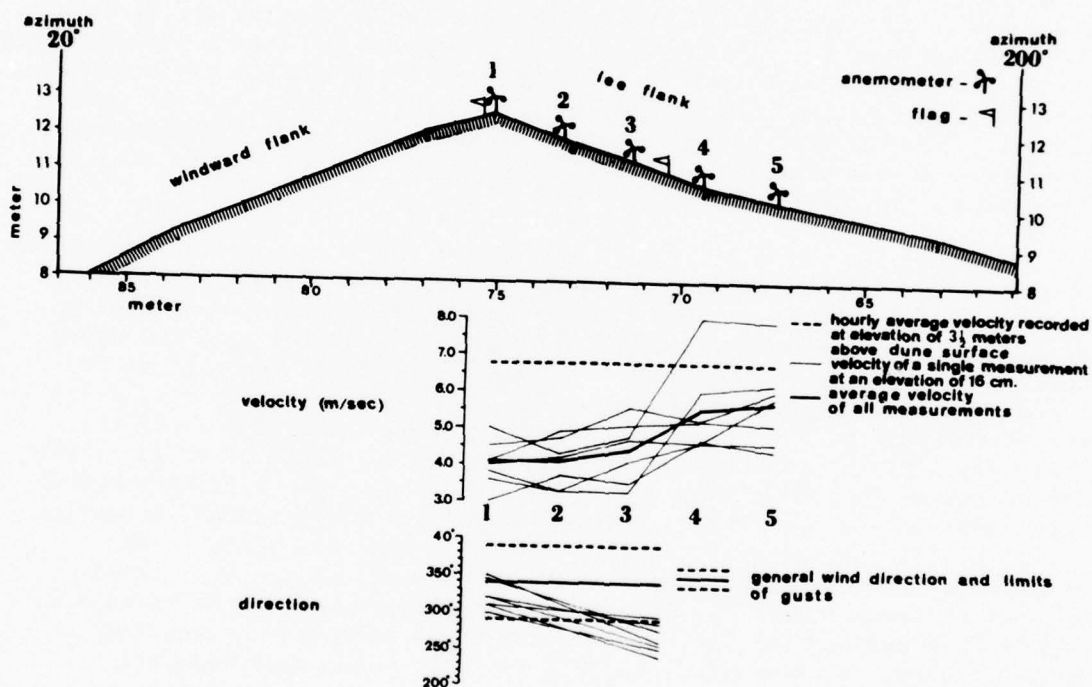


Fig. 3.7. Results of wind measurements taken across the dune lee flank at point No. 9.

If we compare the data of Fig. 3.7 with that given in Fig. 3.3, we can perceive that the outstanding difference is in the direction from which the wind comes (according to the direction of the wind on the crest). In the case of Fig. 3.3, the winds on the crest come from the average direction of  $17^\circ$  ( $310^\circ$  to  $50^\circ$ ), that is to say that the angle of encounter is almost a right angle ( $87^\circ$  average). In comparison to this, in the case shown by Fig. 3.7, the winds come from an average direction of  $315^\circ$  ( $295^\circ$ - $350^\circ$ ) and the average angle of encounter is  $25^\circ$ . We can conclude from this that the phenomena of the drop in wind magnitude at 2-3 meters down from the crest, and the rise that begins further down (Figs. 3.3, 3.4), occur when the wind encounters the crest line at a right angle or almost at a right angle. In cases where the wind encounters the crest line at an acute angle the magnitude at the lee side is higher than at the crest. The measurements, described in Fig. 3.7, show that in certain circumstances there is a drop in magnitude at a distance of 2 meters from the crest, and this happens when the wind is blowing almost perpendicular to the crest. In most cases the wind blows almost parallel to the crest line and the magnitude, at a distance of 2 meters from the crest, was higher than that measured at the crest itself.

Measurements carried out with the aid of three anemometers, one on the crest and the two others on the two flanks at a distance of  $6\frac{1}{2}$  meters from the crest, showed results similar to the results mentioned above (Table 3.2). The results in Table 3.2 can be classified into two groups according to the wind direction. In some of the cases the wind at the lee flank (anemometer # 1) blew from  $130^\circ$ - $160^\circ$  (measurements # 1, 8-15) and in the rest of the cases from the direction of  $240^\circ$ - $290^\circ$ . At the crest there are no significant differences (at the level of 0.01) in the directions of the above two cases. The magnitudes that were measured in both cases at the lee flank (anemometer # 1) are significantly different (level 0.01). At the crest (anemometer # 2) there are significant differences at the level of 0.05 in the wind magnitude in both cases, and not at level 0.01. At the windward flank (anemometer # 3) there are significant differences (at the level of 0.05) between the magnitudes in both cases. Accordingly, the data for both cases were presented separately. Fig. 3.8 demonstrates the first case and Fig. 3.9 demonstrates the second.

Here also the differences between the two cases are explained by the change in the direction from which the wind blows towards the crest. In the first case (Fig. 3.8) the average wind direction at the crest was  $10^\circ$  and in the second case (Fig. 3.9),  $357^\circ$ . The change in the wind direction at the lee flank is caused by the pronounced bend that exists at point # 9 where the measurements were carried out (Fig. 3.14 and Fig. 1.1). This bend causes the direction of the crest line to change substantially. Three main directions can be observed here: on the western side of the bend, the crest azimuth is from  $315^\circ$  to  $135^\circ$ . In the central portion

Table 3.2 Results of Wind Velocity and Direction Measurements on the Crest and on both Flanks (point # 9, Sep. 5, 1974)

No. of measurement	Wind Velocity (m/sec)			Wind direction (degrees)	
	1 Lee flank	2 Crest	3 Windward flank	1	2
1	1.7	4.5	5.5	160	360
2	3.1	5.1	4.6	240	340
3	6.7	6.7	4.8	250	360
4	4.9	5.8	3.7	250	350
5	4.7	5.6	4.2	260	350
6	4.7	6.1	4.0	250	360
7	2.4	6.6	7.6	260	10
8	1.4	5.9	5.7	160	10
9	2.0	5.6	6.3	150	20
10	1.7	5.9	5.1	140	10
11	1.5	5.7	4.4	140	10
12	1.7	5.5	4.3	130	360
13	1.4	5.4	5.2	150	30
14	1.7	4.8	3.8	140	360
15	1.2	5.5	4.9	130	10
16	4.0	4.7	3.1	290	360
17	4.2	5.6	3.6	240	360
18	5.6	6.8	4.4	250	350
19	7.1	7.6	4.8	250	330
20	7.7	6.5	4.5	290	20
21	5.3	6.5	3.4	280	10
Average of measurements 1; 8-15	1.6	5.4	5.0	140	10
Average of measurements 2-7; 16-21	5.0	6.1	4.4	260	357

(where the wind was measured) the azimuth of the crest is from 290° to 110° (parallel to the length of the dune). On the eastern side, the change in direction is greater and the crest continues from 250° to 70° (Fig. 3.14).

When the wind blows from 10°, it encounters the crest line at the western side of the bend at an angle of 55° and the eastern side at an angle of 60°. At each side there is a deflection in the wind direction towards the center of the bend. The winds come there from two opposite



directions and the result is a marked drop in the wind magnitude at the measurement point (anemometer # 1); these are all the cases presented in Fig. 3.8. The most common case, during the measurement period, was of a wind that came from the direction of  $350^{\circ}$ - $360^{\circ}$ . This wind encounters the crest line on the western side of the bend at an angle of  $35^{\circ}$ - $45^{\circ}$  and at the eastern side at an angle of  $70^{\circ}$ - $80^{\circ}$ . Accordingly the deflected wind that blew from the western side was of a higher magnitude than that which blew from the eastern side. These are all the cases presented in Fig. 3.9 where the average direction registered near anemometer # 1 is  $260^{\circ}$ .

The above explanation clarifies the average low magnitude measured by anemometer # 1 in all the cases presented on Fig. 3.8, and the relative higher magnitude in the cases presented on Fig. 3.9. A further phenomenon worth noting is that in most of the cases presented by Fig. 3.9, the wind magnitude that was measured on the lee flank (anemometer # 1) was higher than that measured on the windward side (anemometer # 3).

### 3.3.3 Measurements Alongside the Dune

Wind measurements alongside the dune were done on the lee flank in the area where the dune is bent.

Figs. 3.10, 3.11 and 3.12 present measurements that were made simultaneously on both sides of the deflection point of the saddle. The outstanding phenomenon in the above Figs. is the minimum magnitude in the area of the dune where the wind encounters it at a perpendicular, and the gradual rise in magnitude, with the change in direction of the dune to the east and west of this section.

In Figs. 3.10 a sharp fall in the magnitude can be observed between anemometer # 2 and # 3, which are 6 meters apart. The maximum magnitude is found between anemometers # 1 and # 2. The minimum magnitude is found between anemometers # 3 and # 4, where at # 4 the magnitude starts to rise gradually in the direction of anemometer # 6. Measurements of wind directions show a parallelism to the crest line, almost without exception.

Fig. 3.11 shows measurements that were done at the same point but with a wider deployment of the anemometers on the two sides of the deflection point. Here also the maximum magnitude was registered close to anemometer # 2, which is located close to its previous location in the measurements presented in Fig. 3.10. From this point there is a sharp drop in the magnitude at anemometer # 3, located at the deflection point. Afterwards there is a gradual and successive rise in the wind magnitude in the direction of anemometer # 6. Measurements of wind direction show a parallelism to the crest line with no exceptions.

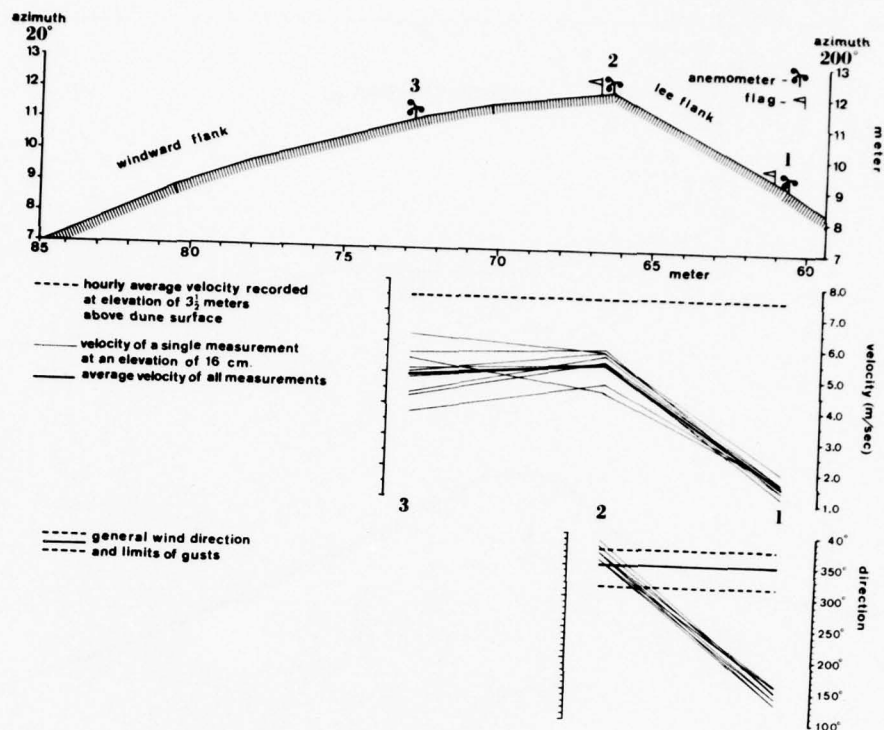


Fig. 3.8 Results of wind measurements taken across the dune flanks at point no. 9.

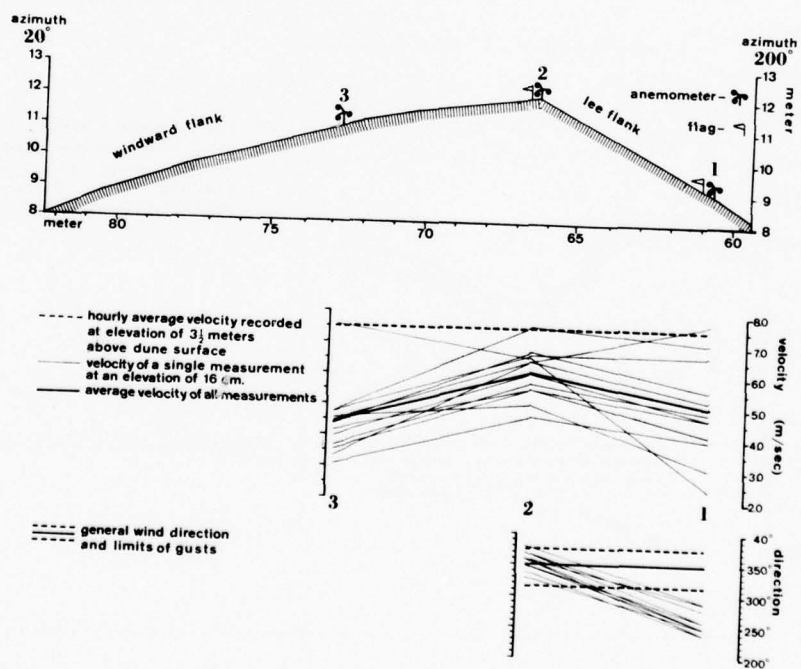


Fig. 3.9 Results of wind measurements taken across the dune flanks at point no. 9.

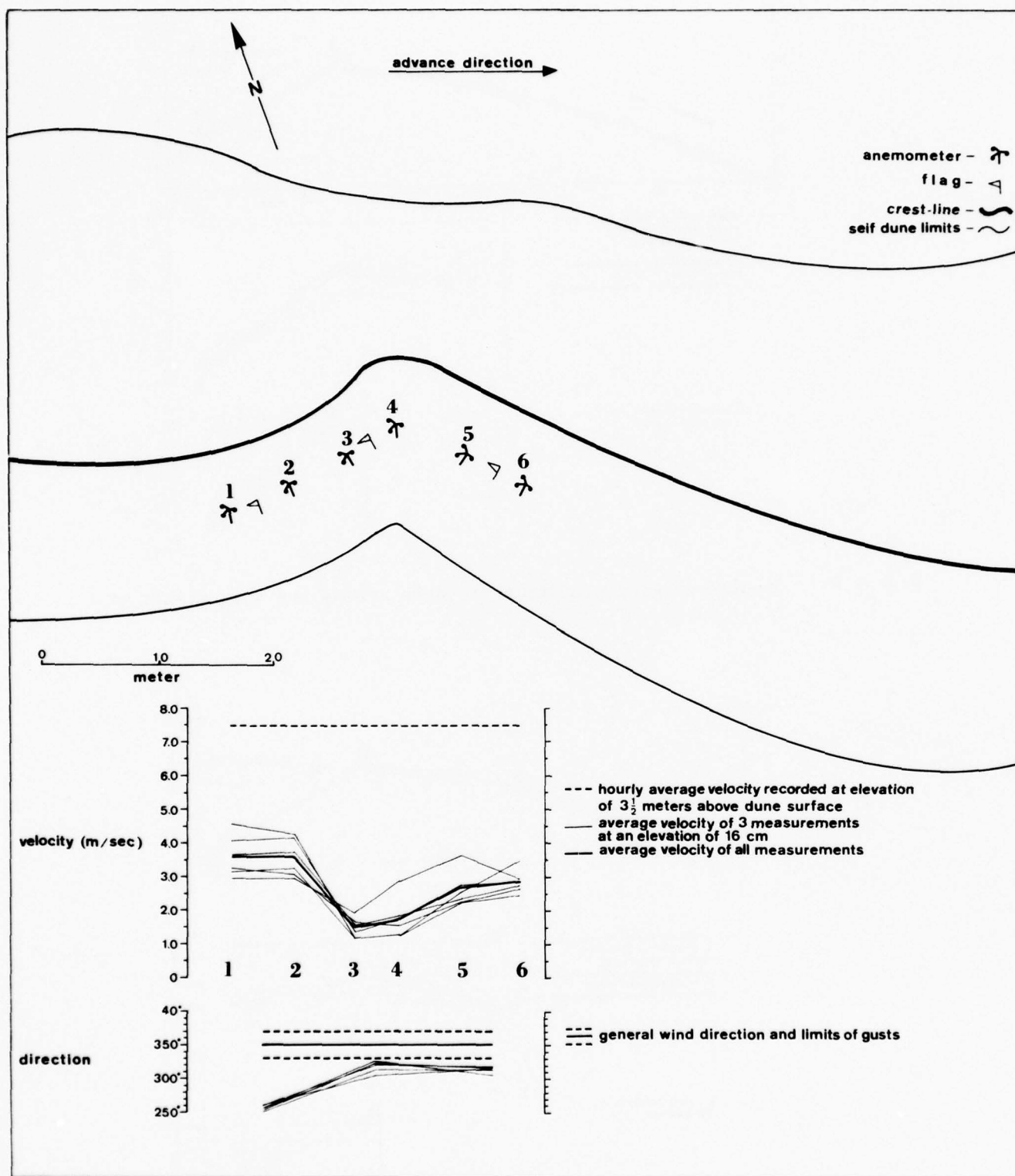


Fig. 3.10 Results of wind measurements taken along the dune lee flank at point no. 4.

Fig. 3.12 is similar to its two predecessors in that eastwards from the deflection point the magnitude rises, but here the rise is only until anemometer # 5, and from there to anemometer # 6 there is a sharp drop in magnitude. The reason for this is the change of  $20^\circ$  in the direction of the crest line in the area located between anemometers # 4 and # 5, and the area located between # 5 and # 6. In previous cases we found that the wind magnitude is in inverse proportion to the angle between the wind direction and the crest line. In the area between anemometers # 4 and # 5, the angle is more acute than that of the area between #5 and # 6, and therefore in the latter section there was a reduction in the magnitude. The results of the wind direction measurements indicate here also the tendency to parallel the crest line.

The rise in the wind magnitude, in the area where anemometer # 5 is located, in Fig. 3.12 is more noticeable than in the cases presented in Fig. 3.10, 3.11, and it is close to the wind magnitude measured by the wind recorder at a height of  $3\frac{1}{2}$  meters above the dune level. The rate of fall of the wind intensity, in the section situated to the left of the deflection point in Fig. 3.10, 3.11 is greater than the rate of rise in the wind magnitude in the section to the right. In Fig. 3.10 the drop in the wind magnitude in the left section is on the average 0.35 meters/second for each distance of one meter, and the rise in the right section is on the average at the rate of 0.09 meters/second to each distance of one meter. In Fig. 3.11 the rate of drop of the average wind magnitude is 0.18 meters/second for each meter, and the average rise is 0.09 meters/second.

#### 3.4 Tracing Eddies with Smoke Candles

Smoke candles have been used by a number of researchers to trace the eddies created on the leeward flank<sup>(9)(50)</sup>. They have also been used as a means of distinguishing directional changes in the various sections of the dune<sup>(53)</sup>.

There are two marked disadvantages to studying wind flow with the aid of smoke candles:

- 1) The obtained results cannot be determined quantitatively.
- 2) Smoke can only be traced by photography. The results are incomplete, since there is no third dimension and the quality is dependent on the angle of photography.

On the other hand, the observation point is on a continuous level and at a distance above the ground.

Smoke candles were used during the present research in order to distinguish and to trace the changes in the wind direction on the lee



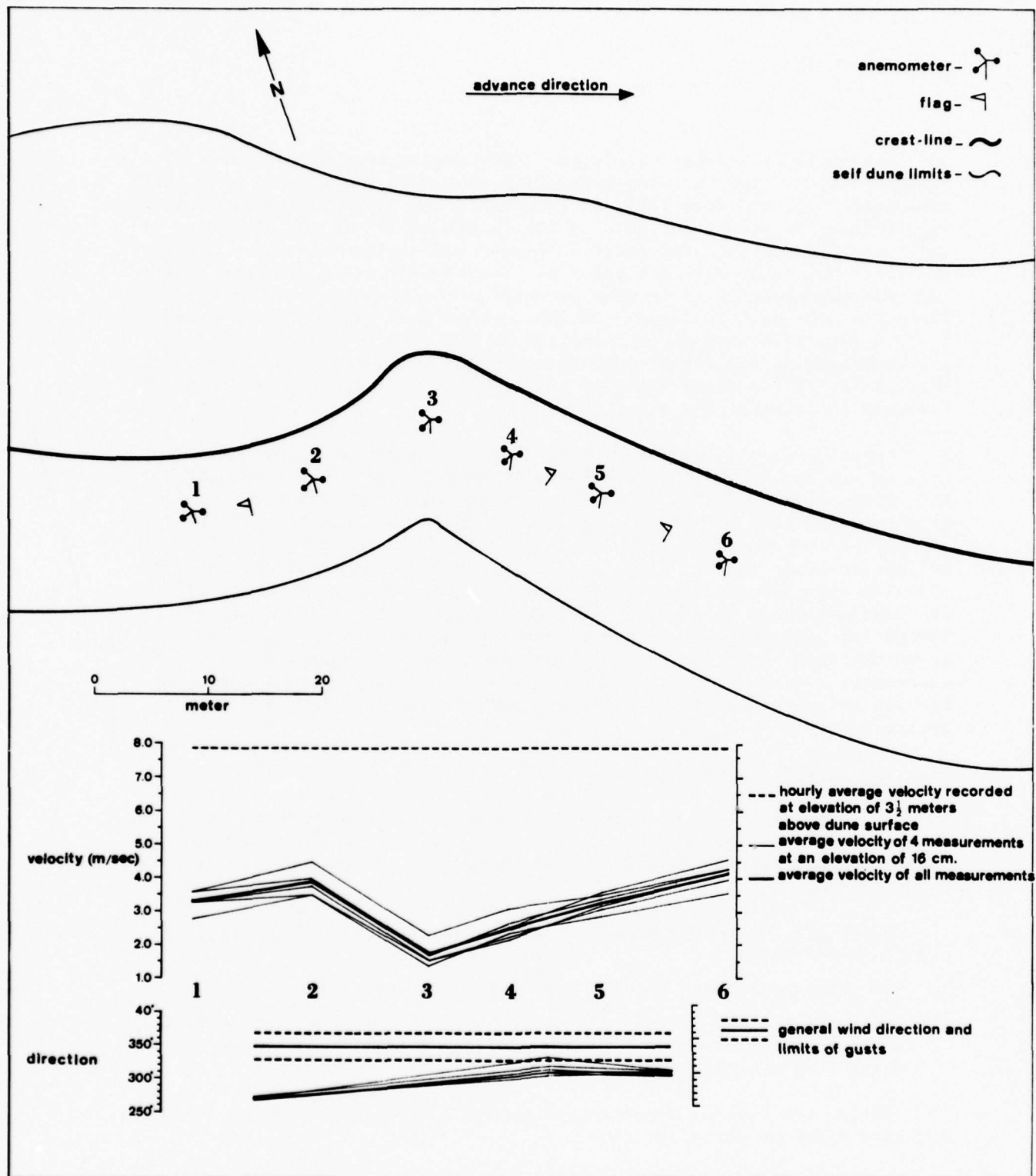


Fig. 3.11 Results of wind measurements taken along the dune lee flank at point no. 4.

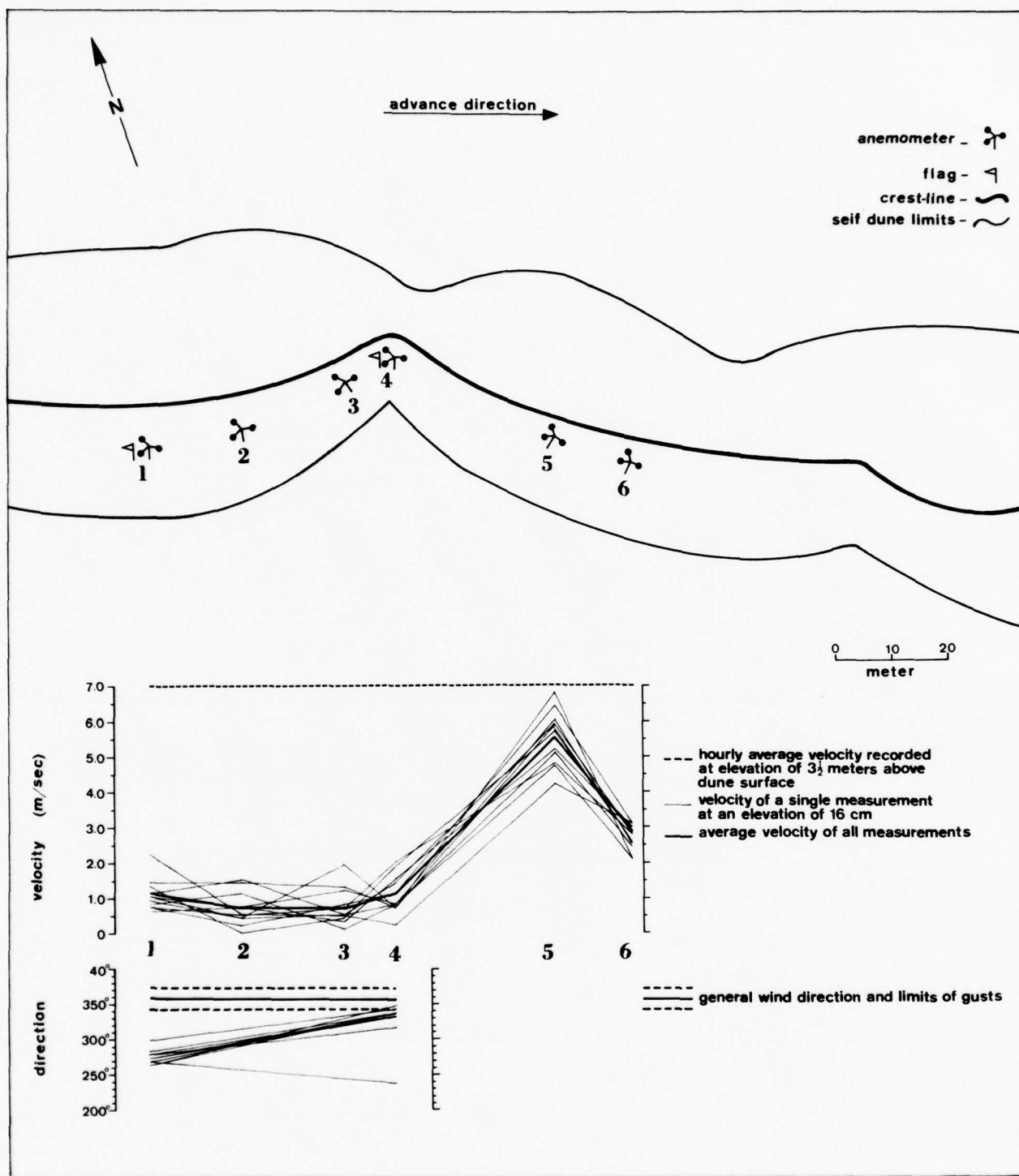


Fig. 3.12 Results of wind measurements taken along the dune lee flank at point no. 6.

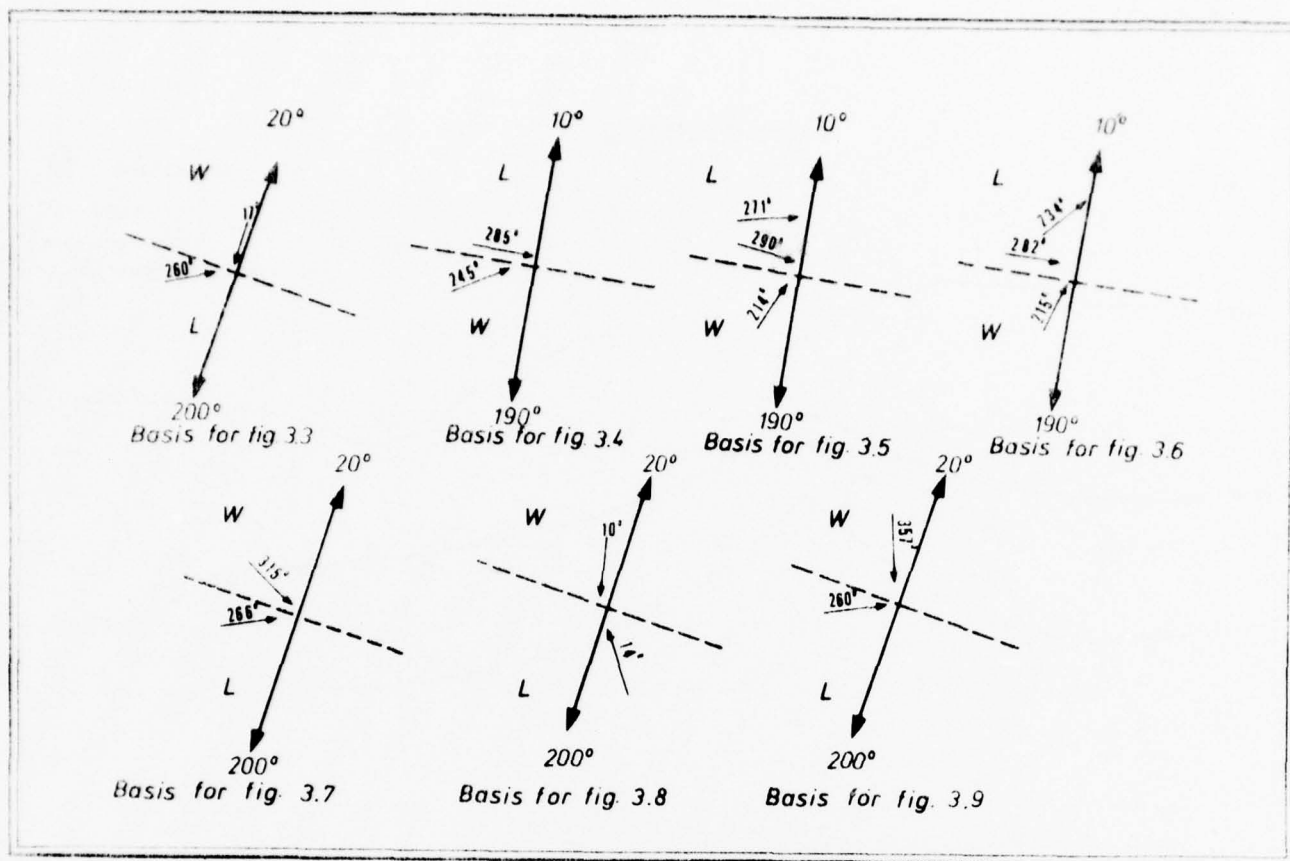


Fig. 3.13 Plan of average wind directions on both dune flanks for measurements presented by Figs. 3.3-3.9 (dashed line represents the dune axis; W = windward flank; L = lee flank).

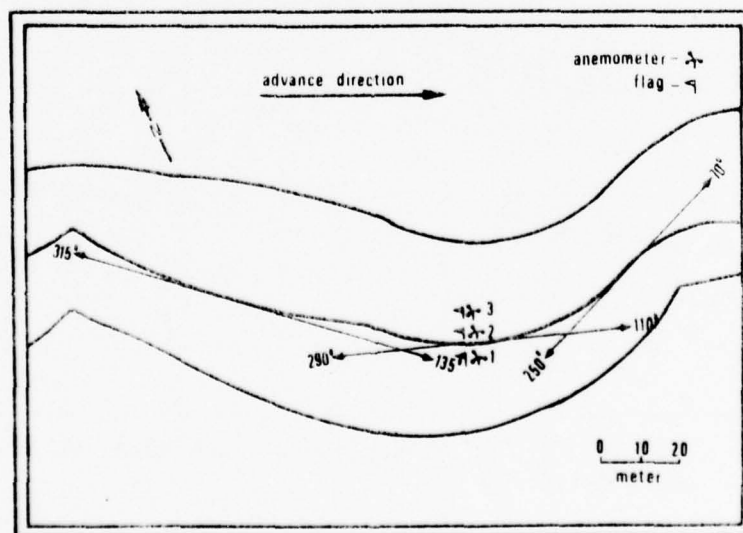


Fig. 3.14 Plan of the dune at point no. 9. The location of the anemometers and the flags as in Figs. 3.8 & 3.9.

flank (as already observed above at single points, with the aid of the anemometers and the flags), and to study the behaviour of the wind at the place where the magnitude drops and increases near the deflection points.

When any flow moves quickly above sharp edges, for example the crest of a longitudinal dune, it is separated from the ground level and enters the mainstream of the flow as a free shear layer. This layer returns and reattaches to the ground at a distance down flow (Fig. 3.15). This phenomenon is called "separation of flow". At the separation area two levels can be distinguished<sup>(54)</sup>: the higher is the separated boundary layer, the lower is a flow in the opposite direction to the mainstream (reverse flow region) and between the two there is an area of a marked shear (zero velocity surface) that separated the above flows (Fig. 3.16).

Fig. 3.17 demonstrates the formation of eddies above the slip-face of a barchan. The flow line, which ascends on the windward side of the barchan, does not turn or follow the sharp turn of the dune brink to the slip-face, but tends to persist and continue its previous path; so that it rises above the ground and returns to it at the slope of the slip-face. In the "vacuum" that is produced at the stream line, an eddy develops that causes a flow in the opposite direction up the slip-face.

There have been disagreements since the beginning of the present century as to the importance of the eddies in the determination of the morphology of dunes and ripples. Cornish<sup>(55)</sup> maintained that there is a fixed lee side eddy, which has a marked influence on the form and development of the dune. Several field studies contradicted his assumption (for example, King<sup>(56)</sup>) and others supported it (for example, Landsberg<sup>(57)</sup>). Bagnold<sup>(7)(58)</sup> did not have an unequivocal opinion on the subject. Cooper<sup>(9)</sup> conducted experiments with smoke candles, and came to the conclusion that eddies exist, but that they do not have enough strength to influence the shape or movement of the transverse dune. Sharp<sup>(50)</sup> had a similar opinion. After experiments with smoke he concluded that on the lee side of the transverse dune there is no fixed eddy of the type described by Cornish<sup>(55)</sup>. Inman et al<sup>(8)</sup> measured wind velocity on the lee side of barchan dunes and found that the flow existing there was in the opposite direction to the general wind direction. The magnitude of the flow was too weak to move sand grains, but their opinion was that this flow influences the settling of the grains which come from the windward flank on the upper part of the lee flank. Hoyt<sup>(59)</sup> found (when the wind velocity was 18-22 meters/second) eddies which raised sand, on the lee side, to a height of a few dozen centimeters. Allen<sup>(29)</sup> claims that the eddy on the lee side is a factor basically inherent to flow mechanics. Storm winds in sand dunes have high Reynolds numbers, which cause instability in the free shear layer. The result of this is that the eddies created do not stay in one position, so that it is difficult to study them with the aid of smoke candles. However, on



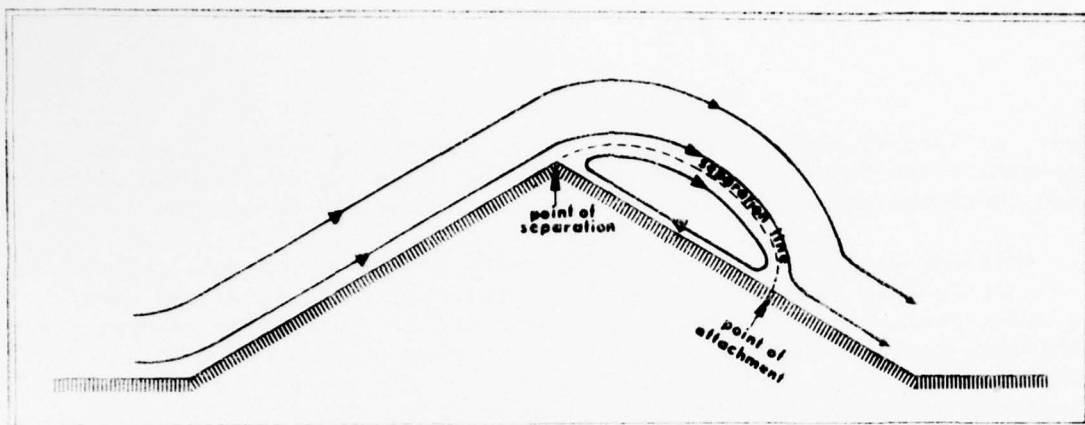


Fig. 3.15 Separation of flow above a profile of a longitudinal dune.

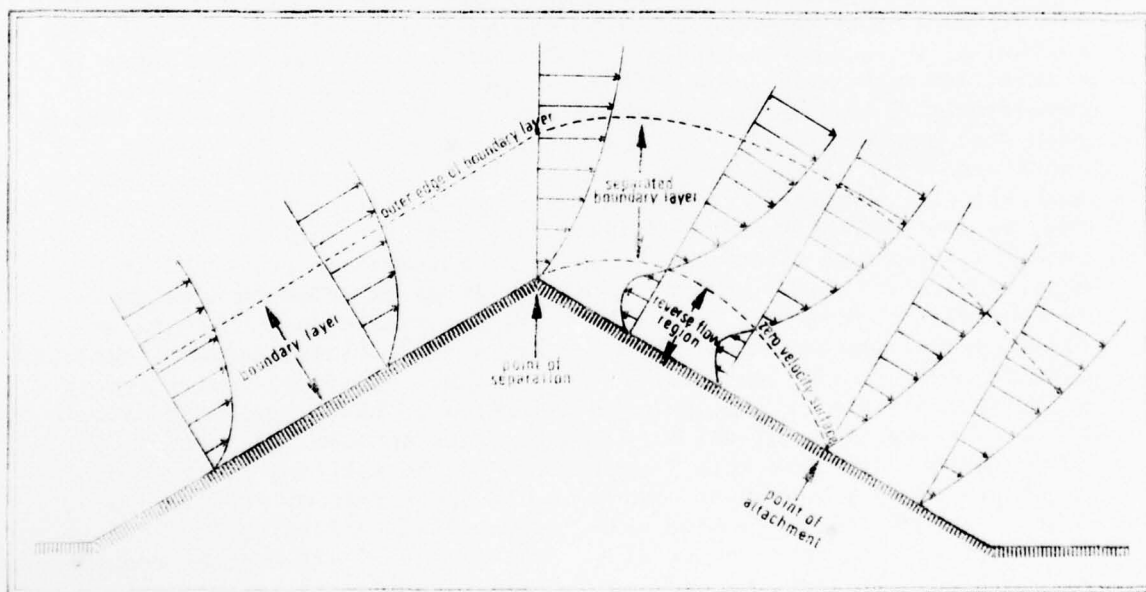


Fig. 3.16 Separation of flow above a profile of a longitudinal dune (with wind profiles).

the average, eddies do exist and under certain circumstances they have a constructive function in the formation of dunes and ripples.

In longitudinal dunes, the situation is different from that in barchans, transverse dunes and ripples, since there the wind encounters the crest line at an acute angle. Allen<sup>(49)</sup> claims that when a flow encounters a step at an angle between  $45^{\circ}$ - $90^{\circ}$ , a separated flow is formed on the lee side, which he calls "rollers", described and demonstrated above (Fig. 3.15, 3.17). When a flow encounters the crest line at an angle of  $0^{\circ}$ - $45^{\circ}$ , a vortex is formed which has stream lines in the shape of a helix which brings about movement of the flow down the axis of the eddy.

The last phenomenon was noticed several times during observations of smoke which arrives at the crest line obliquely, as well as at angles greater than  $45^{\circ}$ . Fig. 3.18 demonstrates a vortex in the shape of a helix which is moving along the lee flank of the dune as a consequence of a wind which meets the crest line at an angle of  $50^{\circ}$ . Since the eddies do not stay in one position, as was mentioned previously, in most cases it is generally possible to distinguish the wind deflection on the lee side, which parallels the crest line at a distance of 5-7 meters from the crest (Fig. 3.19), a phenomenon which was previously mentioned in the measurements done with the anemometers.

When the smoke issues from the candle it is very dense, and after a while, through movement, it gradually disperses. Smoke which travels with a wind with a steady magnitude and direction will disperse gradually through movement (Fig. 3.20). When the magnitude decreases, we expect to find a wide dispersion of the smoke in the same place.

Fig. 3.21 demonstrates the wind movement, according to a smoke candle located 3 meters to the left of anemometer # 1 in Fig. 3.11. The smoke moves at first almost parallel to the crest line and afterwards changes its direction and moves in an arc up the flank and descends in the direction of anemometer # 2. This movement is not steady and a few seconds later it changes to parallel the crest line (Fig. 3.22).

Figs. 3.23, 3.24, show successive photographs of smoke issuing from a candle located one meter to the left of anemometer # 2 in Fig. 3.11. Fig. 3.23 demonstrated the turbulence of the wind and therefore the widespread dispersal which took place during its movement, as a result of a sharp drop in the magnitude of the wind. As a result of this, part of the smoke ascends, leaves the sphere of influence of the lee flank and enters the sphere of the prevailing winds, whose directions are almost perpendicular to the crest line. Fig. 3.24 shows wind movement in the shape of an arc similar to that in Fig. 3.21. Here also a widespread



Fig. 3.17 A separation flow above a slip face of a barchan demonstrated by smoke.

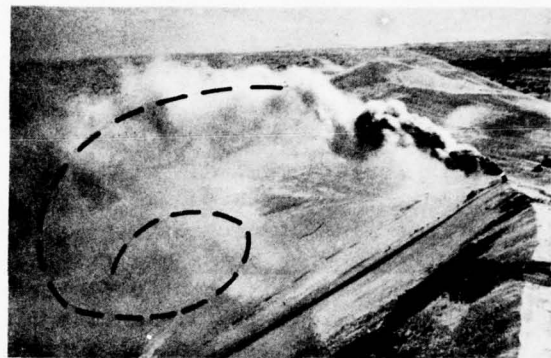


Fig. 3.18 A helix vortex on the lee flank of a longitudinal dune demonstrated by smoke. Dashed line designates the smoke movement.



Fig. 3.19 The wind deflection on the lee side of the longitudinal dune demonstrated by smoke.



Fig. 3.20 Smoke movement on the windward flank of the dune.

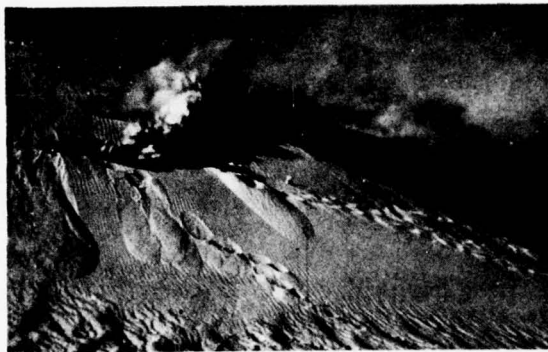


Fig. 3.21



Fig. 3.22

Wind movement along the lee flank in the deflection area demonstrated by smoke.



Fig. 3.23



Fig. 3.24

Wind movement along the lee flank in the deflection area demonstrated by smoke.



dispersal of the smoke can be seen close to anemometer # 3 in Fig. 3.11, which demonstrates a drop in wind magnitude at the same place.

### 3.5 Summary

The following is a summary of the phenomena observed and measured with the micrometeorological wind instruments.

- 1) When wind encounters the crest line at a perpendicular or obtuse angle, wind magnitude at the lee side, at a distance of 2-3 meters from the crest, decreases on the average by 20% to 70%. When wind encounters the crest line at an acute angle ( $20^{\circ}$ - $30^{\circ}$ ), the wind magnitude at a distance of 2-3 meters from the crest increases on the average by 5% to 20%. Because of the wind gusts, it is difficult to ascertain exactly and empirically the range of the impact angles where the wind magnitude increases at a distance of 2-3 meters from the crest, or the range within which it falls. It was found with the measurements that were performed, that when the wind encounters the crest line at an angle of  $10^{\circ}$ - $25^{\circ}$  (Fig. 3.7), the magnitude of the wind on the lee side increases. However, when the wind meets the crest line at an angle of  $40^{\circ}$  and above, the wind magnitude decreases on the lee side. Figs. 3.12, 3.25 clearly demonstrate the relation between the wind magnitude on the lee side and the angle formed by the wind and the crest line.
- 2) The wind magnitude, after dropping at a distance of 2-3 meters from the crest line, increases again until a distance of 5-7 meters from the crest line, and from there down the lee slope, it decreases.
- 3) In many cases (for example Figs. 3.7, 3.9) the wind on the lee side was of higher magnitude than the wind on the windward flank. This phenomenon was sometimes observed during isolated measurements (Figs. 3.5, 3.6) or during most of the measurements and on the average (Fig. 3.7).
- 4) In wind directions there is a conspicuous phenomenon of a deflection at the lee side to a direction parallel to the crest. This phenomenon is evident up to a distance of 5-7 meters from the crest line, in the area where the increase in magnitude starts on the lee flank (Fig. 3.3, 3.4 and Table 3.1). At further distances from the crest line, the wind direction changes and it attempts to return to the general wind direction as measured at the crest (Figs. 3.5, 3.6). These results are summarized in Fig. 3.26.
- 5) In the area where the wind magnitude decreases on the lee side (at a distance of 2-3 meters from the crest) there are often weak flows up the lee flank towards the crest (Figs. 3.21, 3.24).
- 6) The phenomenon of changes in the direction or magnitude of the wind

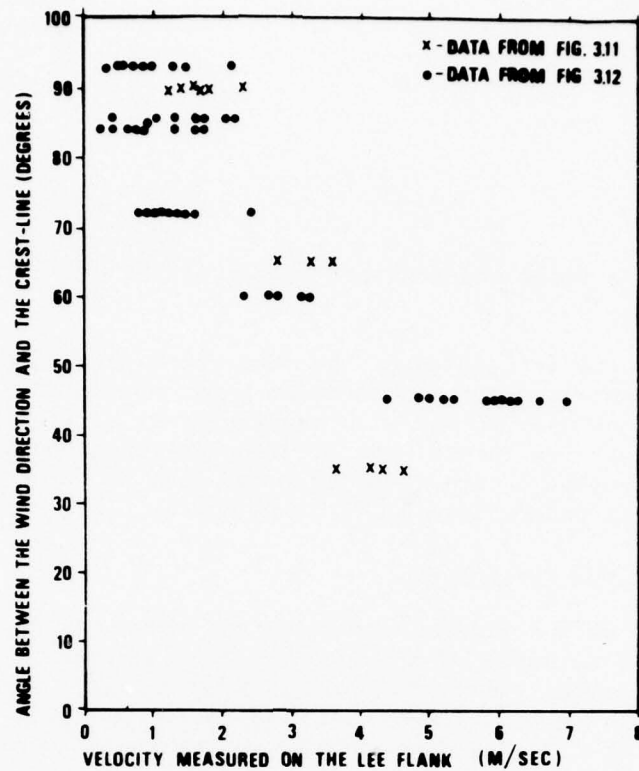


Fig. 3.25 Angle between the wind direction and the crest line versus velocity measured on the lee flank.

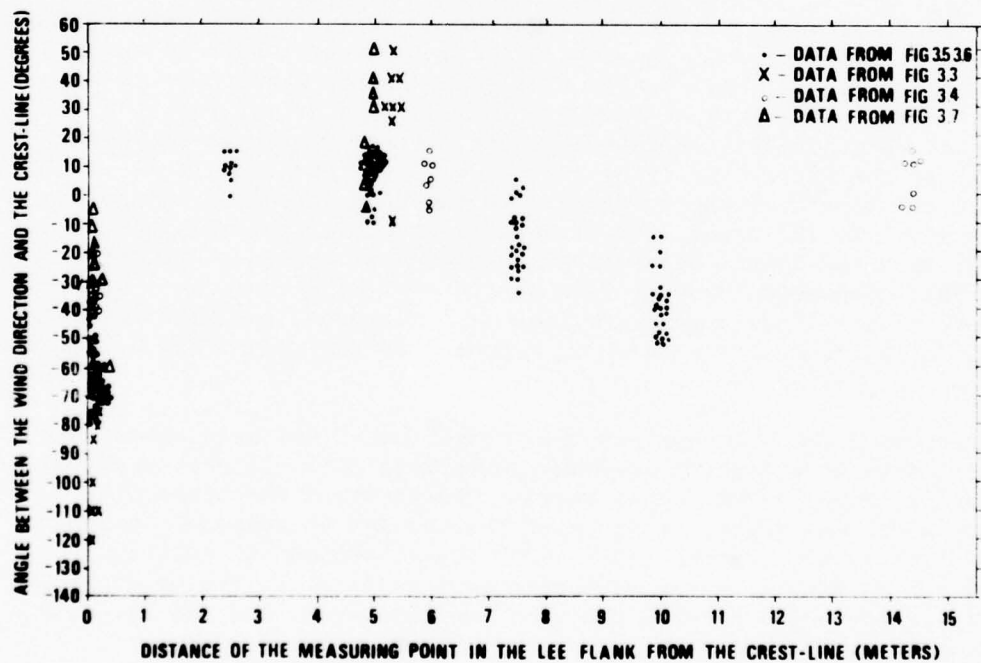


Fig. 3.26 Angle between the wind direction and the crest line versus distance of the measuring point in the lee flank from the crest line.

is limited to the lee flank and does not happen at the crest or on the windward flank.

7) In the area of the deflection of the dune there is a sharp drop in the wind magnitude until near the deflection point of the saddle. From there, there is an increase in the wind magnitude, at a rate which is relatively slower than the rate of the previous decrease, until the point where the crest direction changes, and this is close to the deflection point of the adjacent peak (Figs. 3.10, 3.11, 3.12).

### 3.6 Interpretation and Discussion

The phenomenon of the wind separation after encountering the body of the dune should be considered in order to explain the results of the measurements of wind magnitude and direction (Fig. 3.15). This phenomenon of separation also occurs when the wind meets the crest line at an acute angle. In this case the wind also has a horizontal component which is parallel to the crest line. As a result of this, we do not get a closed eddy like those that appeared in Fig. 3.15 and in Fig. 3.17, but a helix will be formed which will cause helicoidal flow along the lee flank (Fig. 3.18). At the attachment area, the separated wind meets the ground level obliquely to the contour lines. As mentioned, this wind has two horizontal components: one perpendicular to the crest line and the other parallel to it (Fig. 3.27). The component perpendicular to the crest line has a velocity of zero or close to zero at the point of attachment (Fig. 3.15). Therefore we are left only with the component parallel to the crest line (Fig. 3.27 no. 3). Accordingly it is possible to understand the deflection in the wind direction and in the flow parallel to the crest line at a distance of 5-7 meters, when this distance is actually the distance of the line of attachment from the crest line. This phenomenon happens only at the area of attachment. Down the slope of the lee flank beyond the line of attachment, the wind gradually returns to the general direction as measured at the crest (Figs. 3.5, 3.6, & 3.27 no. 4 & 5).

Every wind which encounters the crest line at an angle other than  $90^\circ$  will cause longitudinal movement whose magnitude will be dependent among other things on the angle between the wind and the crest line. The more acute the angle, the greater the horizontal component of the wind - which parallels the crest line. The trigonometric relation between the magnitude of the wind component parallel to the crest line and that of the angle between the wind and the crest line can be found according to the equation:

$$C_{p(z)} = V_{w(z)} \cos \alpha \quad (3.1)$$

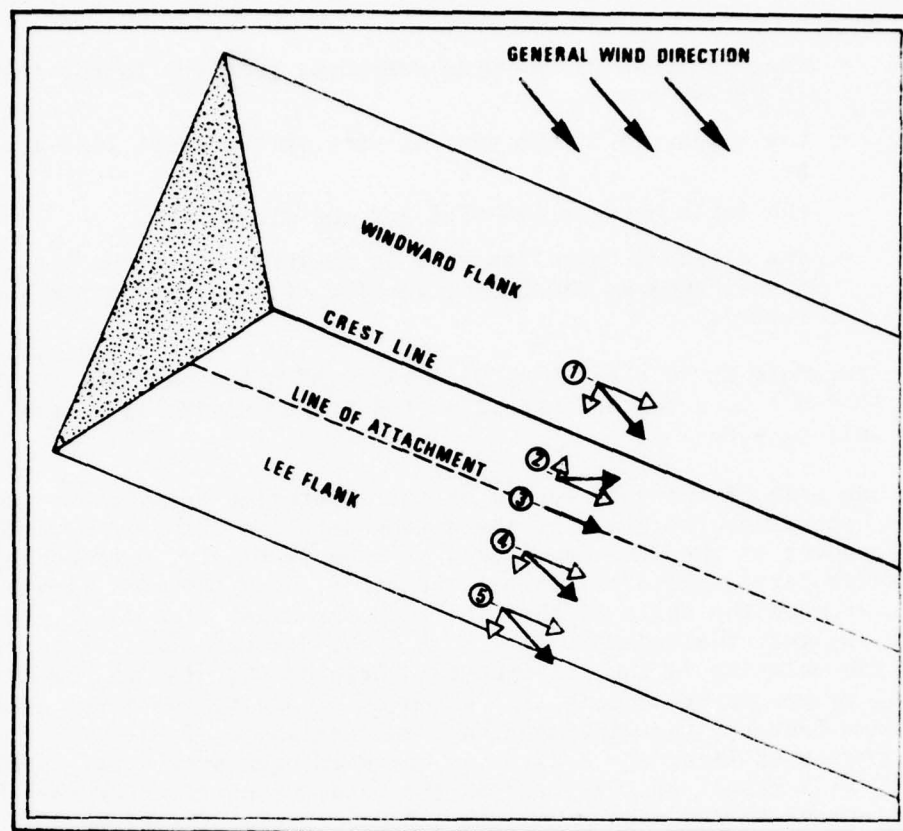


Fig. 3.27: Plan of the changes in the horizontal wind component that is perpendicular to the crest line. White arrows indicate wind horizontal components and black the actual wind direction. (1) - The situation before the separation. (2) - The situation in the reverse flow region. (3) - The situation on the line of attachment. (4) & (5) - The situation outside the separation area.



Whereas:

- $C_p(z)$  = the magnitude of the wind component parallel to the crest line at altitude  $z$ .
- $V_w(z)$  = the magnitude of the general wind at the crest line at altitude  $z$ .
- $\alpha$  = the angle between the wind and the crest line.
- $z$  = the altitude where the wind is measured above the level of the dune (found at the bottom section of the atmospheric boundary layer).

Therefore it is clear that when the wind blows parallel to the crest line ( $\alpha = 0^\circ$ )  $C_p = V_w$ , and when the wind is perpendicular to the crest ( $\alpha = 90^\circ$ )  $C_p = 0$ .

The size of the eddy formed at the separation area is the factor which determines the place of the attachment line (Fig. 3.15). The size is dependent on the wind magnitude, or more precisely, on the component perpendicular to the crest line. Therefore, when the wind magnitude is high, or when the angle of the wind with the crest line is at right angle, we get an attachment line at a great distance from the crest line. When the velocity is low, or when the angle of the wind to the crest is acute, we get an attachment line which is closer to the crest line. Both of these factors, the wind magnitude and the angle of the wind direction with the crest line, are subject to quick changes over a relatively wide range, as a result of the gusts of the wind, which are expressed by large oscillations in the wind magnitude and direction. Therefore when the degree of gustiness is larger, the line of attachment area will be wider. This is why the whole lee flank is covered with ripples up to a distance of 1/2 meter from the crest (Fig. 3.28). On the upper section of the lee flank at a distance of 2-3 meters from the crest line, there is sand movement only in cases when the wind (because of the gustiness) meets the crest line at an acute angle. In the rest of the cases there is no movement there, or there is only a weak movement towards the crest line. However, the ripples that were formed by the same gusts that were mentioned above remain. Only in cases where the wind blows parallel to the crest line, are there ripples on both flanks up to the crest line itself.

In the section between the line of separation and the line of attachment where the eddy is formed, the ground level wind has a weak flow which moves up the lee flank (Fig. 3.16). This movement is noticeable in Fig. 3.17, 3.21, 3.24. Fig. 3.3, 3.4 show the drop in wind magnitude at a distance of 2-3 meters from the crest line, in the area where the separation takes place. This section is a depositional area and a slip face begins to form there. The size of the slip face depends on the width of the separation vortex and the drop there in the

wind magnitude. It reaches its maximum size in areas where the wind is perpendicular to the crest line, that is to say, in the areas where the dunes meander. It is minimal in areas where the wind is at an acute angle to the crest, that is to say, the areas between the saddles and the peaks (Fig. 3.29).

Similarly we can understand the rise in wind magnitude which takes place at a distance of 5-7 meters from the crest line (Fig. 3.3, 3.4). This is actually the distance of the line of attachment from the crest line, where the flow of separation returns to ground level. As a result of this, the speed of the wind rises. Therefore, in the measurements performed, an increase in the wind magnitude was observed on the lee flank at the area where the wind is deflected to a direction parallel to the crest line.

As a result of the process of separation that is described above (Fig. 3.27), the stream lines assemble at the lee flank along the area of the line of attachment, after deflection of their direction. A concentration of streamlines at the line of attachment necessitates, according to the law of conservation of mass, an increase in the velocity of horizontal and vertical wind components. We know that the horizontal velocity component, which is perpendicular to the crest line, at the attachment line, approaches zero. The vertical component is directed downwards as a result of the separation process (Fig. 3.15), therefore, we are left only with the horizontal component parallel to the crest line, which must increase in magnitude because of the concentration of the streamlines at the line of attachment. This is the reason for the gradual increase in wind magnitude which starts at the deflection point of the saddle, as was observed in Fig. 3.10, 3.11 and 3.12. The greater the distance from the deflection point, the more streamlines assemble and the more wind magnitude increases. The increase in wind magnitude will continue as long as there is no change in the angle between the wind direction and the crest line. If the angle becomes less acute, because of the meandering of the dune, there will be a drop in the wind magnitude (Fig. 3.12). An increase in the magnitude will occur if the angle becomes more acute (Figs. 3.10, 3.11).

The explanation for the higher values of the wind velocity on the lee flank than on the windward one, and on the crest (Figs. 3.5, 3.6, 3.7) is also derived from the phenomenon of separation. Air that was on the ground rises to a greater altitude (Fig. 3.15, 3.16) and cuts off contact with the ground level. In this way, the ground surface resistance to the air movement is eliminated on one hand, and the separated flow gains momentum from the faster layers of air above on the other. Therefore equation 3.1 should be expressed as follows:

$$C_p(z) = V_w(z+\Delta z) \cos \alpha \quad (3.2)$$

Where:

$\Delta z$  = the addition of altitude to the wind flow as a result of the separation.

When the wind returns to the ground level (altitude  $z$ ) on the line of attachment, it has a velocity typical of a higher altitude ( $z+\Delta z$ ) which originated from the additional momentum gained when it was above the separation vortex.

We know that  $V_{w(z+\Delta z)} > V_{w(z)}$ . Therefore, in cases where angle  $\alpha$  is small and the value of  $\cos \alpha$  approaches 1, it is possible that  $C_p(z) > V_{w(z)}$ . Experimentally (Fig. 3.5, 3.7), it was found that the value of  $C_p(z) - V_{w(z)}$  in cases where  $\alpha \leq 40^\circ$  is between  $1\frac{1}{2} - 2.0$  meters/second. This value was obtained in wind measurements at an altitude of  $z = 16$  centimeters, and the magnitudes  $V_{w(z)}$  were between 4-6 meters/second.

There is no doubt that there is a relationship between  $\Delta z$  and angle  $\alpha$ . The less acute angle  $\alpha$ , the larger the wind component perpendicular to the crest (which determines the separation vortex) and the larger  $\Delta z$ . When angle  $\alpha$  approaches zero, the separation vortex is very small, and  $\Delta z$  is small, and the above phenomenon is weak. Accordingly, and as a result of the wind measurements, we can assume that angle  $\alpha = 30^\circ \pm 10^\circ$  is the optimal impact angle which causes the maximum increase in magnitude of the deflected wind on the lee flank.

The latter phenomena described above explain the high values of the wind magnitude on the lee flank of the dune sections, where the crest line is situated at an acute angle to the wind direction. In these sections there will be transport and removal of the sand, which will settle in the deflection area, where there is a sharp drop in the wind magnitude because of a change in the angle between the wind direction and the crest line.

It is worth noting, that in all the micrometeorological measurements there was no evidence of the existence of large helicoidal flows. When there were helical vortexes on the lee side, as a result of the separation phenomenon of the oblique wind, the diameter of their rotation was only up to 5-7 meters (Fig. 3.18). Thus they differ in their origin, in their essence and in their size from the helicoidal flows that were mentioned by Hanna<sup>(19)</sup>, Folk<sup>(14)</sup> and others.



Fig. 3.28 The lee flank of the longitudinal dune covered with ripples indicating flow parallel to the crest line up to a distance of half a meter from the crest.



Fig. 3.29 Different rates of slip face development on various sections of the lee flank.



#### IV. GRAIN SIZE CHARACTERISTICS

##### 4.1. Introduction

The grain size characteristics of the dune sand furnish important information for understanding the dynamic processes. In Chapter One and Two it was pointed out that the size of the grains determines the morphology. i.e., whether a high dune or a flat zibar is formed. Chapter Two describes the necessity for information about the size of the grains in order to calculate the threshold velocity of the wind. Folk<sup>(14)</sup> is certain that it is possible to deduce the direction of the sand movement of the dune by the sizes of the grains in various sections.

Relatively little work has been done on analyzing the grain sizes in desert dunes in general, and on longitudinal dunes in particular. Most of the work done was on coastal dunes in order to learn the changes taking place in sand grains moving from a coastal to an aeolian area <sup>(60)</sup><sup>(61)</sup>. Among the few granulometric studies published on longitudinal dunes, those of McKee and Tibbitts <sup>(17)</sup> and Folk <sup>(14)</sup> should be mentioned.

##### 4.2. Sampling and Sieving Methods.

Sampling is the first important step in any granulometric analysis. Even so, most researchers do not pay attention to this. The body of the dune is built up of laminae whose thickness is less than one or two millimeters. On the dune surface we find ripples built of both coarse sediment, which is concentrated near the crest of the ripple and on its windward flank, and of finer sediment which is in the ripple trough. <sup>(62)</sup>. The usual sampling is taken from the body of the dune itself and is done after removing the surface ripples seen as lag sediments. This kind of sampling takes sand from many laminae. Here there is also a chance that some of the sand from the removed ripples may be mixed in with the samples, while a true sampling must be taken from a single layer deposited under fixed and uniform conditions <sup>(63)</sup>.

Most of the granulometric studies done till now were for the purpose of definition and discrimination of sediments in the area of deposition. In dynamics research, it is more important to study and analyze the characteristics of the various grain size which are directly subjected to wind activity and are found on the surface, i.e., to analyze the top layer of sand which builds up the ripples and the slip face. A sampling of this layer is done with the aid of a glue spray by a method proposed by Tsoar <sup>(64)</sup>. The surface is sprayed and after the glue has been absorbed and dried, the top layer of sand is successfully peeled off. The sample is taken at various points along the length of the dune, at each point 5 different samplings are taken at different levels (Fig. 4J). Sample No. 1 at the base of the lee

flank; No. 2 in the middle of the lee flank; No. 3 at the crest; No. 4 in the middle of the windward flank and No. 5 at the base of the windward flank. The sand from the crest of the ripple and from the trough are collected separately with each sampling. In this way it is possible to study the differences in the grain characteristics in these parts of the ripple and to distinguish their influence on its morphometric characteristics. The samples were collected during the middle of the summer (July, August) and reflect the situation after three months of constant winds, blowing from the N-NW.

The weight of the sand in each sampling was from 5 to 10 grams. The sieving was done by means of standard sieves (3 Inches in diameter) suspended on a shaker. The apertures in the sieve were as follows :

- 1.0	φ	-	2.000	mm
0	φ	-	1.000	mm
0.5	φ	-	0.710	mm
1.0	φ	-	0.500	mm
1.5	φ	-	0.351	mm
2.0	φ	-	0.250	mm
2.5	φ	-	0.177	mm
3.0	φ	-	0.125	mm
3.5	φ	-	0.088	mm
4.0	φ	-	0.062	mm

Calculation of the 4 moment statistics of the sieve results was done arithmetically, <sup>(65)</sup> with the aid of a computer :

- 1) Mean,  $\bar{x}_\phi = \frac{\sum fm}{n}$
- 2) Standard deviation,  $\sigma_\phi = \sqrt{\frac{\sum f(m - \bar{x}_\phi)^2}{100}}$
- 3) Skewness,  $Sk_\phi = \frac{\sum f(m - \bar{x}_\phi)^3}{100\sigma_\phi^3}$
- 4) Kurtosis,  $Kg_\phi = \frac{\sum f(m - \bar{x}_\phi)^4}{100\sigma_\phi^4}$

Where : f = frequency percentage of each grain size grade

m = midpoint of each grain size grade in φ values

n = 100 percent

### 4.3. Results and Conclusions

#### 4.3.1. Introduction

A total of 92 samples were collected from various points along the dune where, as indicated, at each point 5 x 2 samples were taken (Fig 4.1). For each sample, calculation of moment was done on a computer and the results appear in Appendixes 18-20.

Appendix 18 gives the moment values for all the samples from the ripple trough and its crest separately. Appendix 19 gives the moment values calculated for the ripple trough and its crest together. Appendix 20 gives the moment values of the three top layers in three different areas. Table 4.1. presents the average moment of the five sampling points of each point sampled on the dune (not including the zibar).

Table 4.1. : The mean moments at the 5 sampling points on the dune (not including the zibar).

Point Moment	1	2	3	4	5
$\bar{x}\phi$	1.18	2.05	1.87	1.70	1.41
$\sigma\phi$	0.75	0.47	0.42	0.47	0.70
$Sk\phi$	0.52	0.32	0.80	0.31	0.68
$Kg\phi$	4.00	3.24	5.28	7.32	3.79

On the dune, we find, in addition to the regular ripples, larger ripples composed of coarse sand. These ripples are called "ridges" by Bagnolds (7), and "pebble ripples" by Sharp(62). In the present work they are termed "mega - ripples". They are found only near the dune base and therefor they are sampled only at points 1 and 5 (Fig 4.1)

The salient characteristics which differentiate the mega ripples from other ripples are their wave length and grain size . The usual ripples reach a length of 20 cm. and the mega-ripples are 25 cm. and longer (Fig 4.2). The ripple grain size is smaller than that of the mega-ripples. According to Fig. 4.2. it can be seen that there is no gradual transition on the dune from mega-ripples to the regular ripples and that they are two separate types.

#### 4.3.2. Means of Troughs and Crests in Ripples and Mega-Ripples

In all the samples (except one) it was found that the mean grain size of the ripple crest was larger than that of the ripple trough.

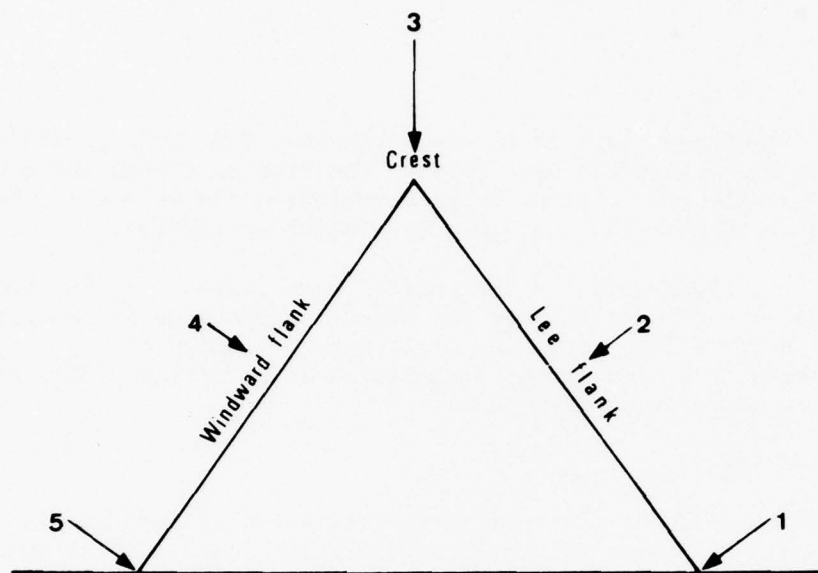


Fig. 4.1 Location of sampling points on a cross section of the dune.

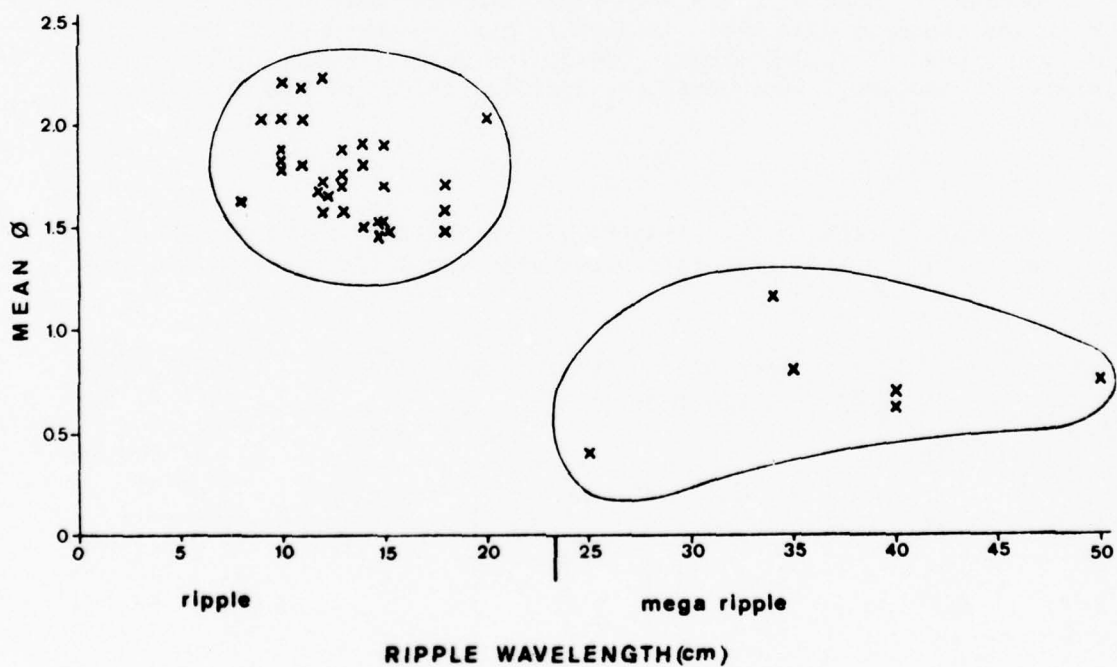


Fig. 4.2 Mean ( $\bar{X}_\phi$ ) versus ripple wavelength.



The spread is more obvious in the mega-ripples. Fig. 4.3. presents the differences in the mean grain size between the ripples trough and crest compared to the wavelength. A significant correlation can be noticed here (a possibility of less than 1% that the correlation is random).

Fig. 4.4. represents the same differences compared to the mean value. Here it can be noticed that when the average grain size of the ripple is lower, the difference between the crest and the trough of the ripple is smaller. There is a significant correlation (a possibility of less than 1% that the correlation is random).

#### 4.3.3. Mean ( $\bar{x}\phi$ )

The mean values of the various samples shown in Appendix 19 appear in a wide range from 0.41  $\phi$  (0.75mm) to 2.22  $\phi$  (0.22 mm) and the mean is 1.62  $\phi$  (0.33 mm). The separate samples from the crest and the trough give more extreme values (Appendix 18) whereas in all cases (except one) the crest has coarser sand than the trough. The large range of values results from the fact that the samplings were taken in various sections of the dune and included samplings from ripples and mega - ripples. Therefore it is desirable to show the results in agreement with the different sampling sites (Table 4.2).

According to Table 4.2, the mega ripples appear only at the base of the dune and the mean size there is the highest. In the rest of the locations, where mega - ripples are not found, the smallest mean is found at the center of the lee flank, where the smallest values of the wave are also found.

Table 4.2 Distribution of wave lengths of ripples in various sampling sites (according to Fig. 4.1.), mean values and size range including 90 % of the sampling.

Sampling site according to Fig. 4.1	Ripples wavelength (cm)	The number of ripples according to the various wave lengths.							Mean $\phi$	Size Range (in $\phi$ ) in- cluding 90% of the sam- pling.
		Ripples			Mega-Ripples					
		0-10	11-15	16-20	21-25	31-35	36-40	46-50		
1			3	1	1	1		1	1.18	0.06-2.42
2	4		2	1					2.05	1.27-2.83
3	1		6						1.87	1.18-2.50
4	1		6						1.70	0.92-2.40
5			3	2		1	1		1.41	0.25-2.57

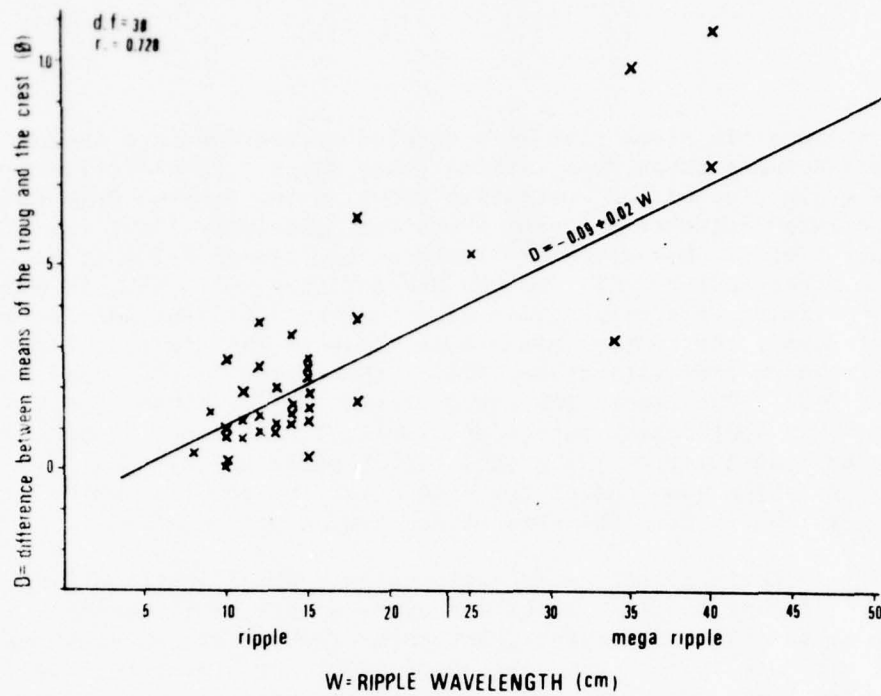


Fig. 4.3 Difference in mean grain size between the ripple crest and the trough versus the ripple wavelength.

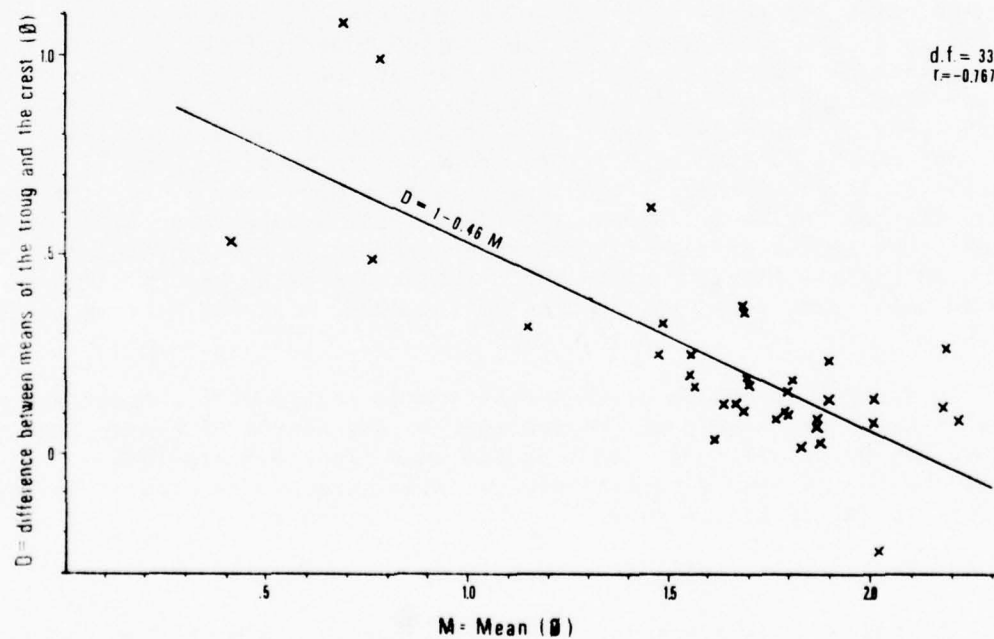


Fig. 4.4 Difference in mean grain size between the ripple crest and the trough versus the mean grain size of both together.

The average grain sizes that were sampled at the dune are larger than the known grain sizes taken from various other dunes. Folk<sup>(14)</sup> found that the average grain size of the Australian dunes in the Simpson Desert was 2.7  $\phi$ . He pointed out that the sand there was relatively finer than the sand in other places. Mabeoone<sup>(66)</sup> found an average of 2-2½ $\phi$  in the coastal dunes in North-East Brazil. On the Barrier Coast of N.S.W. in Australia, Hails<sup>(67)</sup> found an average grain size between 1.6-2.4 $\phi$ . At the internal dunes of Sinai, the average grain size close to the crest is 2.21 $\phi$ <sup>(68)</sup>. In most cases known from literature, 90% of the grains in the dunes are in the range of 2-3 $\phi$ . The reason for the different values found in our present research, is a different method of sampling. The sampling here was done on the topmost layer of the ground, which build the ripples. In other studies, the sampling was done of the sand under the ripples, which build the laminae, which are from the area of deposition of the dune.

In order to learn about the differences in average characteristics in the various different sampling sites the average data ( $\bar{x} \phi$ ) was tested with F-tests for differences in variance, and t-tests for differences in means, whereas the variance in both sampling sites is equal. The t-tests were also performed where there was an assumption (from the results of the F-tests) that the variance was not equal<sup>(69)</sup>. The results are summarized in Table 4.3.

From Table 4.3 we can see that with the exception of the differences between sites 1-5 and 4-5, there are significant differences in the characteristics of the grain size. In the Simpson Desert, Folk<sup>(14)</sup> found that the sand grains at the crests were larger than at the flanks. In many other cases, fine sand was found at the crests and coarse sand was concentrated at the base of the dune. Bagnold<sup>(7)</sup> believes that coarse sand collects at the base of the dune because of its inability to move onto the flank slope. Sharp<sup>(50)</sup>, in California, found fewer coarse grains at the crest of the dunes than at the base, whereas the finest grains were more common on the flanks than on the crest. In the present research, the finest grains were found on the lee flank, then on the crest, and finally on the windward flank. The coarsest were found at the base of the dune, with the maximum on the lee flank.

In general it can be assumed that coarse grains will concentrate at the base of the dune because of the nearness to the source of coarse sand - the zibar, due to inability to climb up the dune flank and also due to the seasonal changes of wind direction and the slow movement (a form of surface creep) typical of coarse sand.

#### 4.3.4. Standard Deviation (sorting) ( $\sigma \phi$ )

The values of the standard deviation (sorting) are related to the size of the grain and the type of ripple. The mega-ripples have a wide range of sand, from very coarse to very fine, and therefore have a high standard

Table 4.3 Results of F and t Tests of Different Groups of Sampling Sites.

Sampling groups (as of Fig. 4.1)	F-Test		t-test, pooled variance estimated			t-test, separate variance is estimated			Conclusions
	F Value	Probability that difference between groups is random (2 tails prob.)	t Value	Degree of freedom	Probability that difference between group mean is random (2 tails prob.)	t Value	Degree of freedom	Probability that difference between group mean is random (2 tails prob.)	
1 vs 2	10.47	0.012	4.32	12	0.001	4.32	7.14	0.003	Significant difference
1 vs 3	43.49	0.000	3.59	12	0.004	3.59	6.28	0.012	Significant difference
1 vs 4	19.23	0.002	2.65	12	0.021	2.65	6.62	0.033	Significant difference
1 vs 5	1.88	0.461	1.00	12	0.339	1.00	10.97	0.341	No significant difference at 0.05
2 vs 3	4.15	0.107	2.59	12	0.024	2.59	8.73	0.029	Significant difference
2 vs 4	1.84	0.478	4.70	12	0.001	4.70	11.04	0.001	Significant difference at 0.05
2 vs 5	5.56	0.056	4.15	12	0.001	4.15	8.09	0.003	Significant difference
3 vs 4	2.26	0.344	3.33	12	0.006	3.33	10.44	0.008	Significant difference
3 vs 5	23.10	0.001	3.22	12	0.007	3.22	6.52	0.015	Significant difference
4 vs 5	10.22	0.012	1.94	12	0.076	1.94	7.16	0.093	No Significant difference



deviation, above  $1\phi$ , which shows bad sorting. The ripple sand is better sorted; its standard deviation averages between  $0.42\phi$  and  $0.47\phi$ . This value is similar to the standard deviation values that Folk<sup>(14)</sup> found for ripples sampled on flat surfaces (and not on dune flanks) and also for dune sand in the Simpson desert and other places <sup>(66)</sup>.

Fig. 4.5 presents the relationship between the average and the standard deviation of the samplings taken at various places on the dune. The results of the sampling are concentrated separately where in sites 1-5 there is an overlap, and in sites between 4 to 1+5, 2 to 3 and 3 to 4 there is a partial overlap. The results are understandable in light of the results of the t-tests for the values of the averages (Table 4.3) and in light of the fact that there is a significant correlation (at a level of 1%) between the values of the average ( $\bar{x}\phi$ ) and the values of the standard deviation ( $\sigma\phi$ ).

According to the averages (marked in Fig. 4.5 by a circle) it can be seen that at point no. 1 the largest sand grains and the worst sorting are found and the next point is no. 5. At the time the sampling was done, in the summer, point no. 5 was at the base of the windward flank and no. 1 at the base of the lee flank. The coarse sediment that comes from the windward side during the summer collects at the base of the lee flank and is not carried away from there because of the weak winds which exist at this season. The sand at point no. 4, at the middle of the windward flank, is coarser than the sand at point no. 2 which is found at the same level on the lee flank, since it gets additional coarse sand from point no. 5 (this explains the lack of significant difference between the averages of points 4 and 5 in Table 4.3). Mostly finer material gets to point no. 2 and the coarse material which succeeds in crossing the crest tends to slide and roll to the base (point no. 1). Point no. 2 is similar to point no. 3, although the former has finer sand. Point no. 2 has ripples with the shortest wavelengths (Table 4.2). The sizes of the sand grains there are within the range of sizes found in the body of the dune ( $2-3\phi$ ). This indicates that point no. 2 is found in the depositional area of the dune or close to it. Coarser material does not succeed in crossing the crest; or if it does, it does not move with the direction of the flow along the dune. Because of its relatively greater weight and the steepness of the lee side, it falls to the base of the flank. We know from data on the wind regime (Chapter 2) that the magnitude of the wind in the summer is relatively lower. Therefore, less sand succeeds in crossing the crest to sink to the lee side.

#### 4.3.5. Skewness ( $Sk\phi$ )

Skewness is considered one of the more delicate parameters for distinguishing between the various depositional layers<sup>(70)</sup>. In all cases, in dunes, positive skewness is found, which indicates a "tail" of fine-grained sediments in a distribution curve (Fig. 4.6). The source of these fine sedi-

ments is dust which settles on the dune after storms. In separate samplings of the crest and troughs of the ripple (Appendix 18), 84 % had a positive skewness. Among the 13 cases where the skewness was negative, 11 were samplings of the ripple trough, where most of the sand is fine and the "tail" is of coarse sand (Fig.4.7). In 90 % of the results, the skewness of the crest and trough together had positive values (appendix 19). Four cases of negative skewness were found at sampling points no.2 and 4 on the dune (Fig. 4.1 ).

Averages of skewness (Table 4.1.) show that the lowest values are found at the two flanks and that the crest has the highest skewness. Folk (14) obtained an identical result using a different sampling method. He points out that the differences are not meaningful because of the great overlapping between all the sublayers of the dune.

The skewness values of each sampling on the dune have a wide distribution along the scale of results. T-tests that were done on the results of the various sampling sites show that there are no significant differences between the results of the various layers. In view of this, it seems that the skewness values have no dynamic or sedimentological importance in the environments of the longitudinal dune.

#### 4.3.6. Kurtosis ( $Kg\phi$ )

Kurtosis measures the amount of peakedness of the distribution curve. On its own, it has no importance and few conclusions can be drawn from the kurtosis values. Its importance lies mainly in integrated analysis<sup>(71)</sup>.

All the kurtosis values (Appendixes 18,19) are above 1; that is to say, they are all of the leptokurtic type.

Fig 4.8. presents the relationship between the average and the kurtosis of the various subenvironments samplings on the dune. The discrimination between the subenvironments (except for nos.1 and 5) is made possible due to the significant differences that exist in the average values (Table 4.3), and also due to differences in the kurtosis values between the windward flank (no.4) and the rest of the subenvironments. No reason is seen for the high values on the windward flank. There is no significant correlation between the mean values and the kurtosis values ( $r = 0.19$ ; d.f.=33).

#### 4.3.7. Grain Size Distribution Curves.

Fig 4.6, 4.7, and 4.9-4.15 present distribution curves of some of the results of the sieving at various points. In the presentation of distribution curves of this sort there is an error in the fact that we are taking the midpoint of each class interval as being representative of the average of each class. However, the purpose of the presentation of these curves is

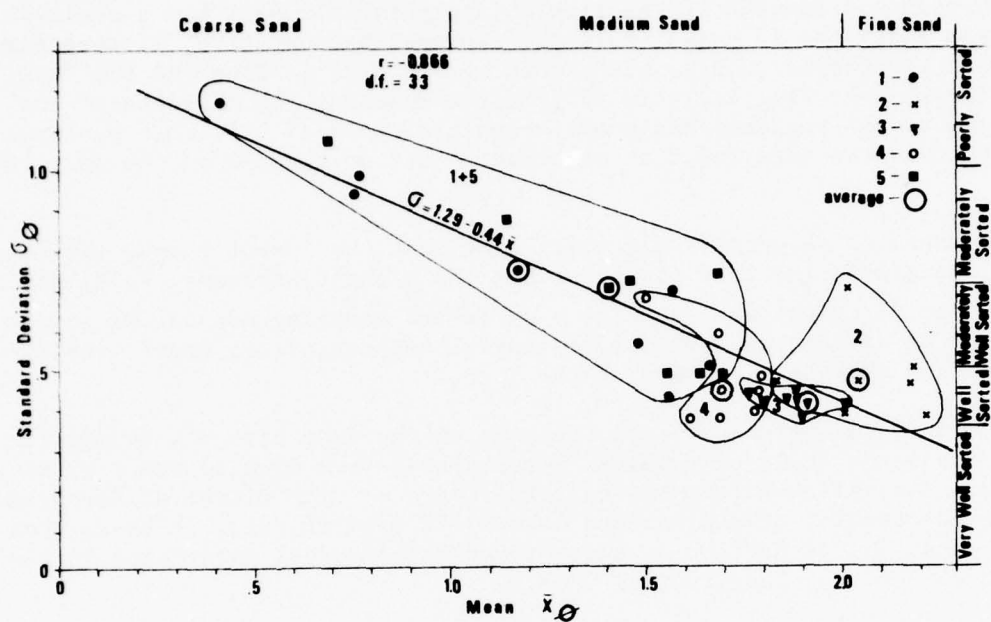


Fig. 4.5 Standard deviation (sorting) versus mean ( $\bar{x}_\phi$ ) (Numbers designate the sampling points according to Fig. 4.1).

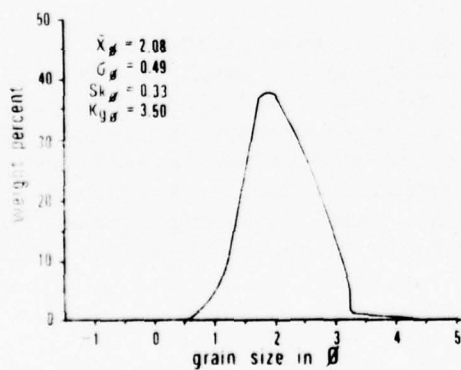
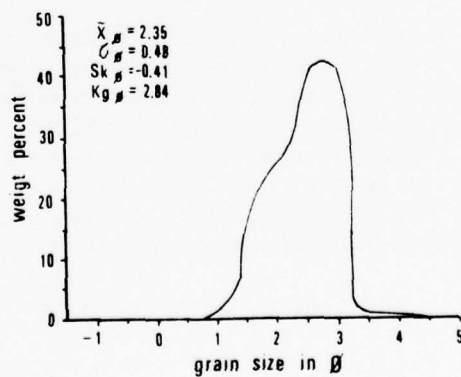


Fig. 4.6 Grain size distribution curve, Fig. 4.7 sample no. 45.



Grain distribution curve, sample no. 46.

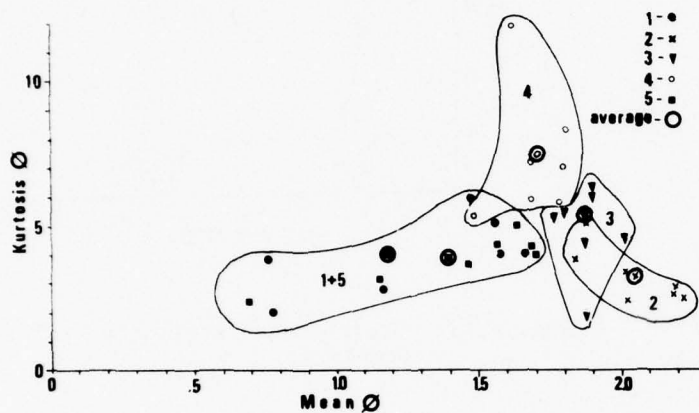


Fig. 4.8 Kurtosis ( $Kg_{\phi}$ ) versus mean ( $\bar{X}_{\phi}$ ).  
(Numbers designate the sampling points according to Fig. 4.1).

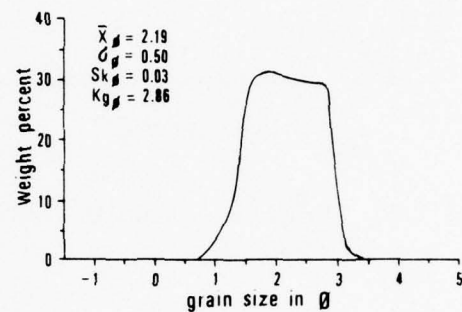


Fig. 4.9 Grain size distribution curve,  
sample no. 45 + 46.

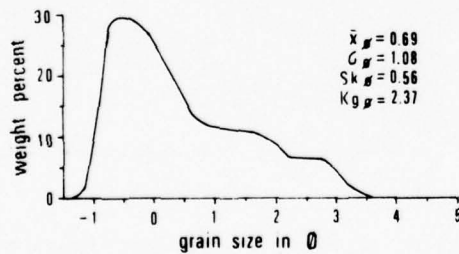


Fig. 4.10 Grain size distribution curve,  
sample no. 23 + 24.

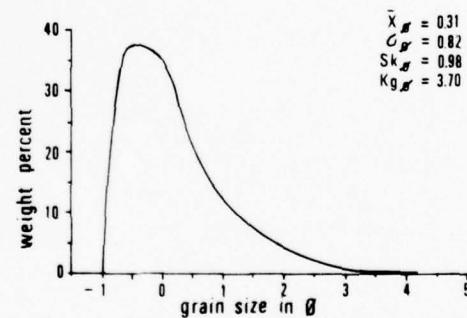


Fig. 4.11 Grain size distribution curve,  
sample no. 23.



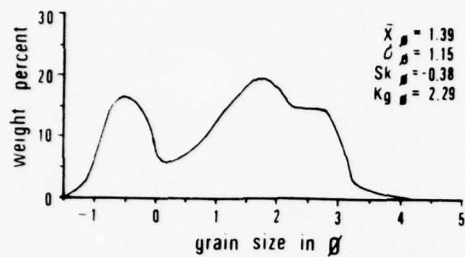


Fig. 4.12 Grain size distribution curve, sample no. 24.

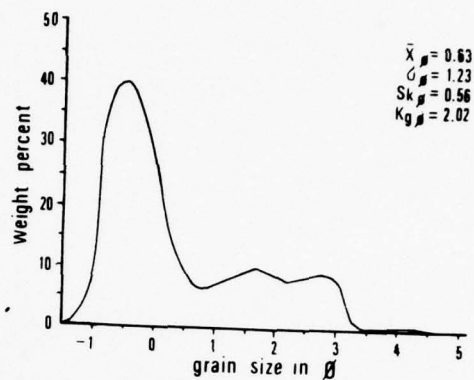


Fig. 4.13 Grain size distribution curve, sample no. 1 + 2.

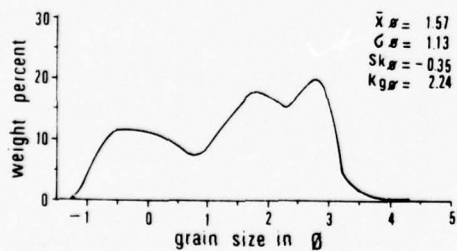


Fig. 4.14 Grain size distribution curve, sample no. 3 + 4.

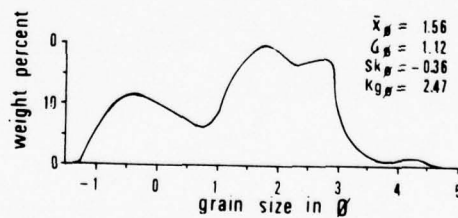


Fig. 4.15 Grain size distribution curve, sample no. 5 + 6.

to distinguish between the various modes. Their presentation on the same scale with the same size groups permits a visual comparison of the distribution at the various sampling points.

Fig. 4.9 presents a large distribution of regular ripple grains, and Figs. 4.6 and 4.7, the distribution of the crests and troughs respectively of the same ripple. The distribution of the grain size of the ripple is almost symmetrical. The distribution of the ripple crest is coarser, with positive skewness, and the distribution of the trough is finer, with negative skewness.

Fig. 4.10 presents the distribution of the mega-ripple, and Figs. 4.11 and 4.12 show the distribution of the crest and trough, respectively, of that mega-ripple. The mega-ripple has a distinctly asymmetrical distribution, which is even more pronounced at the crest of the mega-ripple (Fig. 4.11), where the coarse fraction is marked. In the mega-ripple trough (Fig. 4.12) we find two major components - coarse and fine, where the coarse is the lesser component and the major part is medium and fine.

#### 4.3.8. Grain Size Characteristics in Laminae Below the Top Surface.

During three samplings, two additional layers were taken in addition to the upper layer of sand grains, in order to check the variation in size of the grains between the grain layer subjected directly to wind action and the two layers beneath it. The results appear in Appendix 20. In all three examples there is a marked difference between the upper layer and the two layers below it in all 4 moments. The two layers are almost exactly identical in the characteristics of grain size and distribution. This fact justifies the method of sampling the upper layer of grains without any mixing in of the lower layers.

Fig. 4.13 presents the mega-ripple (similar to the distribution of the mega-ripple in Fig. 4.10). Figs. 4.14 and 4.15 present the distribution of the two layers found underneath that particular mega-ripple. Here the acute decrease of the component of coarse sand is marked; that is to say coarse sand is the modal size only on the surface. Under the surface, the medium and fine sand are the modal size. It is clear that the very coarse component appearing in Fig. 4.13 is in fact the lag sediments typical of ripples and mega-ripples.

It is to be noted that the distribution of the two layers under the mega-ripple (Figs. 4.14, 4.15) is identical to that of the grains in the trough of the mega-ripple (Fig. 4.12). From this we can conclude that the characteristics and distribution of the two layers underneath the surface of the ripple are identical to those of the grains on the surface of the ripple trough.

## V. TRACING SAND MOVEMENT BY FLUORESCENT DYE

### 5.1 Introduction

During the last few years, the use of tracers in dynamic geomorphology and sedimentology has become more common. This method was devised in response to the problems arising from attempts to reconstruct processes with the aid of natural models. The use of tracers was introduced into the measurements of the course of sediments in streams and rivers<sup>(72)</sup> and also on beaches<sup>(73)</sup>.

The data, techniques and results of the use of tracers in aeolian sediments has not yet appeared in the literature. Therefore, the technique of using tracers for dune research was utilized by relying on the knowledge and experience gained by Yasso<sup>(74)</sup> in his summary of fluvial and marine environments.

It is much easier and simpler to use tracers for aeolian sand dunes, since the marked sand and its sampling were introduced both before and after a storm. In this way, we are able to avoid technical problems and those errors relating to the introduction of material and sampling during actual movement, as in streams and beaches.

Of the two methods of marking sand - radioactive and fluorescent - the latter was chosen because it is cheaper, entails no danger to humans, and also because various colors can be used, thus providing more information in each experiment.

### 5.2 Techniques Used

The technique includes: dyeing the sand, releasing it on the dune, sampling, and counting the grains.

a) Dyeing: The dyeing is done with the aid of fluorescent pigments (manufactured by the Dayglo Co., Ohio, U.S.A., Series A) containing 10 different colors. The solvent used was "Supercryl" - a white acrylic exterior emulsion paint (manufactured by the Tambour Co., Haifa, Israel). The sand which was dyed was taken from the dune itself, in order to maintain the sand characteristics (shape, density, roundness and size). A quantity of 25-30 kilograms of sand was dyed, equivalent to a medium-sized sand storm lasting from 7 to 15 hours. The necessary quantities for dyeing 25-30 kilos of sand are: 250 grams of fluorescent pigment and 500-600 cubic centimeters of Supercryl paint diluted in 80-100% water. The dyeing is effected by mixing all the above materials in a receptacle and by drying them. The dry colored sand is very fragile to the touch and is easily crumbled. It contains some aggregates created by insufficient mixing of the sand, and therefore the colored sand, after crumbling, is put through

a  $\frac{1}{2}$  mm sieve in order to remove the aggregates. Sieving the sand through a  $\frac{1}{2}$  mm sieve does not change its granulometric characteristics because it has been found that on the average, only 0.2% of dune sand is larger than  $\frac{1}{2}$  mm.

Examination of the dyed sand showed that it maintained the same characteristics as before dyeing. From the granulometric point of view, the size distribution of the sand before and after dyeing was almost identical (Fig. 5.1). Examination by means of a microscope revealed that the fluorescent color tended mostly to concentrate in concavities on the surface of the grains and therefore had almost no effect on its aerodynamic qualities. Nevertheless, the specific weight of undyed sand in bulk is 1.44 grams/cm<sup>3</sup>, and that of dyed sand is 1.26 grams/cm<sup>3</sup>. The difference in the bulk weight of the sand reveals that during the dyeing, the shape of the grains changes somewhat, and that in a lump of dyed sand there are more spaces between the grains than in a lump of undyed sand.

b) Release of the fluorescent sand: The fluorescent sand is released on the surface of the dune in places where its movement on the surrounding area is of interest. The release of the sand can be in an elongated narrow strip or around a particular point. The depth of the fluorescent sand released is not more than 2-3 cm, in order not to make obvious changes in the morphology of the dune. It is important to make every effort to prevent obvious changes on the dune while releasing the sand, in order to reconstruct the natural conditions in the best possible manner. Reference pegs are sunk at places where the sand is released, and their height and azimuth are measured in relation to a central reference point. They are used after sampling as the basis for mapping the dune in the area under investigation.

c) Sampling method: Sand sampling is done starting from the area next to the sand release area and in the direction of the movement of the last sand storm. It has been found that in most cases, the general direction of the movement of the sand is towards the east (except for western sand movement in small amounts in different cases). The sampling is systematic and is done in strips across the dunes; the distance between one strip and another is between 3-5 meters. Sampling is taken along the entire strip at intervals of 1-3 meters, according to the height of the dune. Every strip sampled is marked for mapping.

The sampling method is according to Ingle<sup>(73)</sup>. A sampling card (3 by 3 inches), one side of which is smeared with a light coating of vaseline, is then attached to the sampling post by means of two rubber bands (Figs. 5.2, 5.3). The sampling cards are kept, before and after sampling, on a board and are attached to it by clips (Fig. 5.4). Each sampling is marked according to the sampling strip, the face of the slope, and its location on the strip. At the end of each sampling, the cards are placed in a plastic bag.



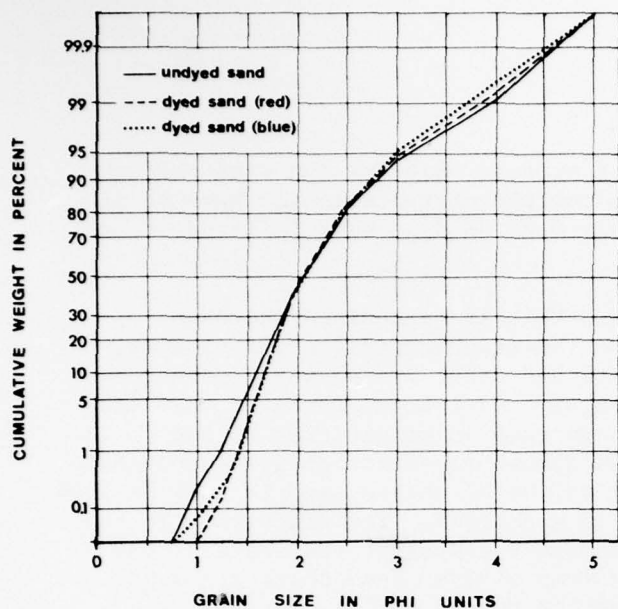


Fig. 5.1 Distribution of grain size in the dune before and after dyeing.

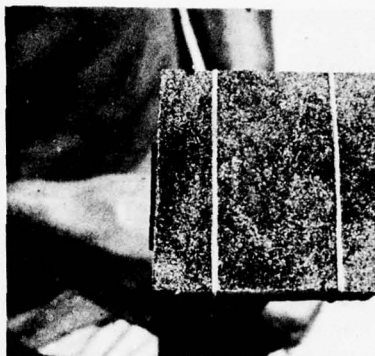


Fig. 5.2 Sampling card (after taking a sample) attached to post by rubber bands.



Fig. 5.3 Sampling post to which sampling card is attached.

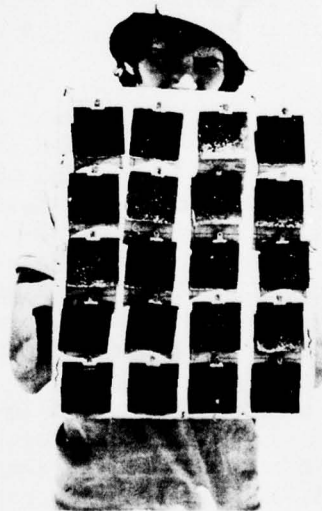


Fig. 5.4 Board holding the sampling card system.

During the entire sampling activities, care must be taken to avoid the introduction of errors which can arise from scattering of sand by the samplers' shoes (while the samplers are walking on the dunes), and by sand avalanches on slopes whose angles are near the angle of response of the sand. Also to be avoided are errors caused by lack of attention to the cleanliness of the sampling posts, the sampling system board and the samplers' hands. In order to prevent this, long posts must be used (Fig. 5.3); the sampling post should be cleaned after each sampling, and the rubber bands holding the sampling cards in place on the post should not be used more than once. It is also impossible to take samplings during a sand storm - even the slightest - because the cards become filled up with the sand blowing around the dune. After the sampling, an accurate mapping of the entire sampling area is carried out, using a level.

d) Counting procedure: The sampling cards were checked under an ultra-violet lamp (UVL-56-Black-Ray), which, on one hand, illuminates each colored grain, and on the other hand, presents no hazard to the human body. All the colored grains were counted and were used as a basis for a map showing the grains movement.

### 5.3 Releasing the Fluorescent Dyed Sand

The data obtained from tracing the dyed sand can be tested both qualitatively and quantitatively. Qualitatively, it is possible to learn about the movement and the major deposition areas of the sediments, and quantitatively, data can be obtained on the sediment yield in the same directions of movement. Most of the research done up to now on this subject, mostly on coasts, shows the changes in the dispersal of the tracers in conditions of various surroundings<sup>(73)</sup>. The few quantitative research works that have been done have stressed that the accuracy of the quantitative data is dependent upon many factors, among which is the method of collecting sand or sampling<sup>(75)</sup>. In addition to this, information on the velocity and direction of the flow moving the sediment is necessary. Any change in velocity or direction is likely to introduce an error into the calculation. Any transfer of the sediment from one place to another (as from the windward to the lee flank of the dune) changes the characteristics of its transportation.

In spite of the existence of data on the general direction and velocity of the wind, in all tracers work of dyed sand done in the present research there were also micro-changes in the wind direction and velocity of the dune itself. In a few sections there is increased erosion of sand, and in other sections, deposition. Therefore we should disregard a priori all attempts at quantitative measurement of colored sand movement on the sand dune, and the results are limited to the qualitative results of the directions of movement and areas of deposition.

Movement of the colored sand, in all the cases sampled, was in a strip with a width of 2-6 meters. In uni-directional sand movement with a steady rate, the concentration of colored grains was found to fall gradually with the increasing distance. In instances where the sand movement stopped or decreased, for any reason whatsoever, we find a dispersion of sand over a wide area, and from there onwards a sharp decrease in the sand concentration. Therefore the shape of the sand dispersion and its concentration, as found after sampling, can indicate the following data: a) direction of the sand movement and changes in the direction of this movement; b) cessation or slowing-up in the rate of the sand movement (in the deposition area).

#### 5.4 Graphical Representation of Dyed Sand Movement

The number of colored grains found in each sample was recorded on the map of the sampling area. With the help of interpolation, isolines of the number of grains were drawn on a map with the following values: 4,10,20,25,50,100,250,500,750,1000,1500. Each number indicates the amount of dyed grains found in an area of 9 square inches (the area of the sampling card). Values of less than four were not counted in order to prevent errors that might arise from artificial dispersal of the sand by the samplers' shoes, and sticking of the sand to the sampling pole or to the samplers' fingers. Only in one instance (Fig. 5.10), were various values smaller than four taken, and this was after a storm which lasted for seven days, which dispersed and buried most of the sand and the highest number of colored grains sampled was 8. Isolines of dyed grains show the direction of the sand movement, the width of the moving sand strip, the shape of the sand dispersal, and the deposition areas. Measurements of dyed sand movement were done in various areas of the dune, mainly in places where the dune meanders, in order to ascertain the course of the sand movement there. The wind recorder supplied the general data on the wind regime for the period between the release of the sand and its sampling. All the measurements except one were done in a period when the wind blew north or northwest - that is to say, in a typical summer wind regime, where there are weak and medium sand storms at fixed hours during the day. All the experiments done in the winter, during a stormier wind regime, failed because of the almost total disappearance of the colored sand. Only in one instance (Fig. 5.10) was there a successful sampling after a winter storm, but, as already mentioned, we obtained a sample with a very low number of dyed grains.

In all the measurements, two different colored sands were released on the dune, one on the lee side and the other on the windward side. In order to distinguish between the dispersal of the two colors of sand, the isolines were drawn with dashes for the windward flank and with continuous lines for the leeward flank.

## 5.5 Results and Discussion

### 5.5.1 Grain Movement Under Northern Winds (Summer Condition)

Summer winds, which have a velocity above the threshold velocity, are actually sea breezes which blow every day from noon until evening. These breezes have a northerly component and a high degree of constancy.

Fig. 5.5 presents the sand movement after a windstorm of magnitudes up to 10 meters/second from two main directions,  $360^\circ$  and  $340^\circ$ . The sand released on the windward flank moves parallel to the wind blowing from  $340^\circ$ . This is because the storm started with wind from  $360^\circ$  and ended with wind from  $340^\circ$ , which left the final impression in the course of the sand. On the lee side, there was a change in the sand direction which was a result of the change in the wind direction. At a distance of 2 meters from the crest, the direction of the sand movement gradually changed to parallel to the crest line. This movement took place in a belt with a width of 8 meters, whose center is at a distance of 5 meters from the crest. The sand released on the lee flank also moved in this direction, which is at an angle of  $70^\circ$  -  $90^\circ$  from the general wind direction. It is interesting that the sand coming from the windward flank moved a greater distance than the sand released on the lee flank. This phenomenon repeated itself in most of the similar instances. This results from the fact that on the windward flank removal of sand only takes place while on the lee flank there is deposition as well as movement. Therefore, the sand coming from the windward flank buries a portion of the sand moving on the lee flank.

An additional phenomenon is a secondary concentration of sand (50 grains) downwind on the lee flank. This kind of concentration could indicate sand deposition, possibly stemming from a change in the orientation of the continuation of the dune, because of its meander. This can be seen in Fig. 5.6, which describes a section in the meander area which is found to the east of the section appearing in Fig. 5.5. In Fig. 5.6, we can distinguish a change of  $20^\circ$  in the direction of the crest line. Because of this, the relationship between the wind direction and the direction of the crest changes. The sand starts to move in a manner similar to the aforementioned case (Fig. 5.5), that is to say, parallel to the crest line on the leeside, where most of the movement happens also at a distance of 5-6 meters from the crest. When the sand approaches the area where the dune changes its direction, it spreads out along a very wide area that includes almost the whole southern flank of the dune. Smoke candles showed (Figs. 3.21 - 3.24) that in this area eddies are found which are caused by a decrease there in the wind magnitude and from wind flows to the west (upwind), since the general winds from N-NNE get a western deflection. On the western part of the lee flank, the same wind tends to blow to the east (Fig. 5.5). In the area where the crest line direction changes, these two opposite wind directions (which are from the same source)





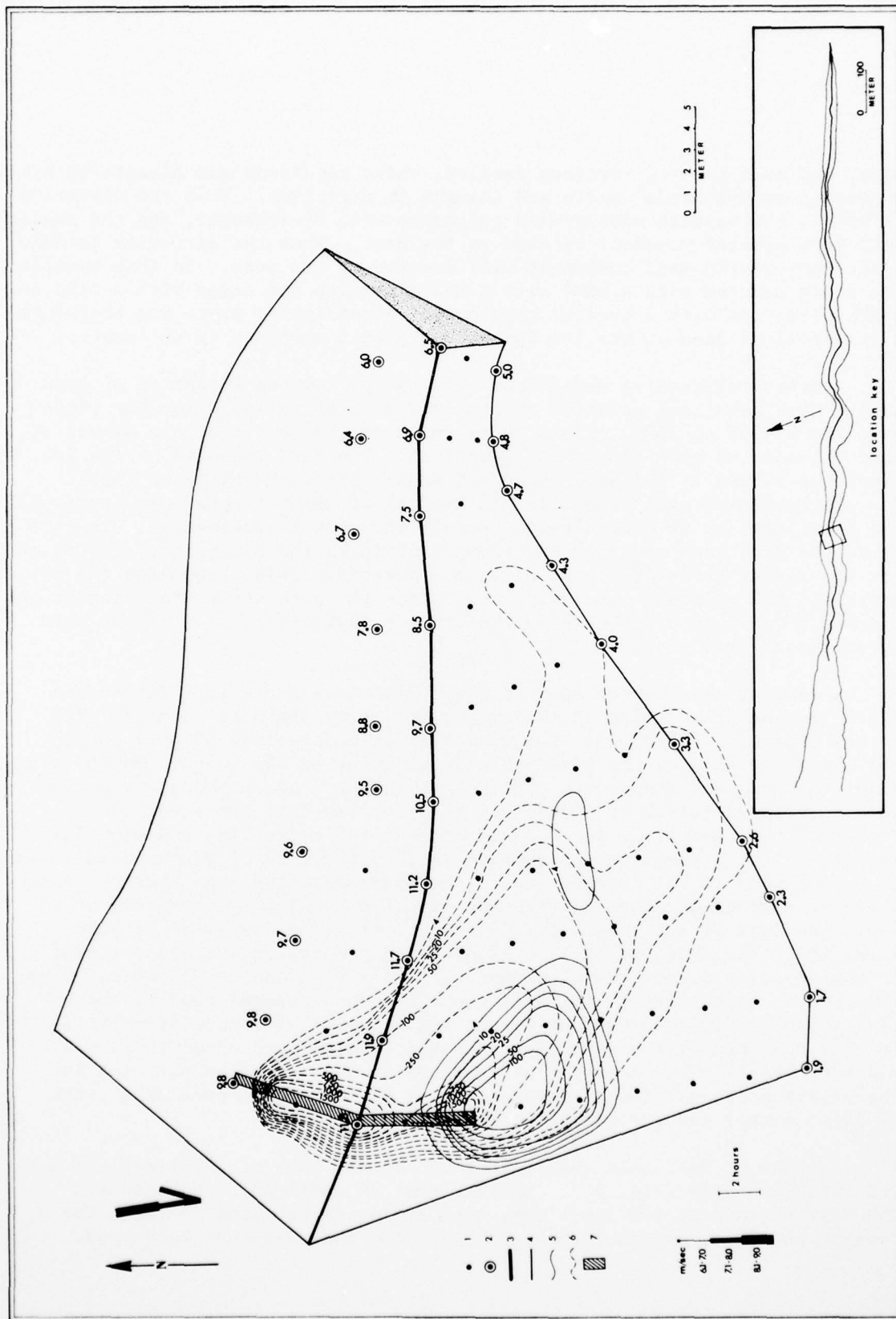


Fig. 5.6 Sampling map of released fluorescent dyed sand on both flanks of the dune between points no. 5 and 6. For key see Fig. 5.5.

meet, and as a result, vortices develop, whose magnitude and directions are dependent on the winds' gusts and changes in direction. When the direction is NNW-N, the eastern moving wind component will be stronger, and the result will be a greater movement of sand to the east. When the direction is NNE, a stronger moving wind component will develop to the west. In this example, the storm started with a wind with a NNE direction and ended with a wind in a NNW direction with a greater magnitude. Accordingly, there was therefore a dispersal of sand on the lee flank, but also a movement to the east.

Another outstanding phenomenon here is the low concentration of dyed sand on the lee flank relative to the dyed sand which came from the windward flank (100 to 1500). This is in spite of the fact that the amount of sand released on both flanks was identical. The sand released on the lee flank was buried by the sand (dyed and undyed) from the windward flank. The phenomenon of sand deposition is typical of the two uppermost meters of the lee flank (as we have already seen in the wind measurements). In this case, the dyed sand was released along a strip on the 5 uppermost meters of the lee flank; therefore, most of it was covered. This phenomenon did not happen in the previous case (Fig. 5.5) since the sand there was released on the lee flank 4 to 6 meters from the crest - that is, outside of the main depositional area.

A similar case can be seen in Fig. 5.7, where there is a difference of  $40^\circ$  in the orientation of the crest line (from the direction  $130^\circ$ - $310^\circ$  to the direction  $90^\circ$ - $270^\circ$ ). The wind blew at a direction of only  $360^\circ$ , and moved the sand on the windward side straight to the south. On the lee side, the movement changed to parallel the crest line, although this time it concentrated itself at a distance of  $2\frac{1}{2}$  meters from the crest (as a result of the relatively acute angle between the crest line and wind direction). The predominant phenomenon in the direction of the sand released on both flanks is the movement up to the area where the dune changes course. There is a stoppage there in the sand direction, which is expressed by a sharp gradient of isolines. In addition, there is a dispersal of sand along the whole width of the lee flank in an almost homogeneous pattern: in two opposite directions of movement, to the west and to the east. From this we can learn that in the area where the dune changes course, there is a stoppage of sand movement due to the opposite wind direction there. In this same place, the sand disperses and is deposited along the whole width of the flank as a result of vortices in this area, as was seen in the previous cases. The dispersal area is limited to an area of a length of 10-15 meters and the width of the lee flank.

Samples of dyed sand that were taken at the base of the lee flank in the interdune area (Fig. 5.7) indicate that in spite of turbulence and dispersal of sand on the lee flank, sand grains do not tend to leave the body of the dune, and therefore, in fact, the dune does not lose sand.

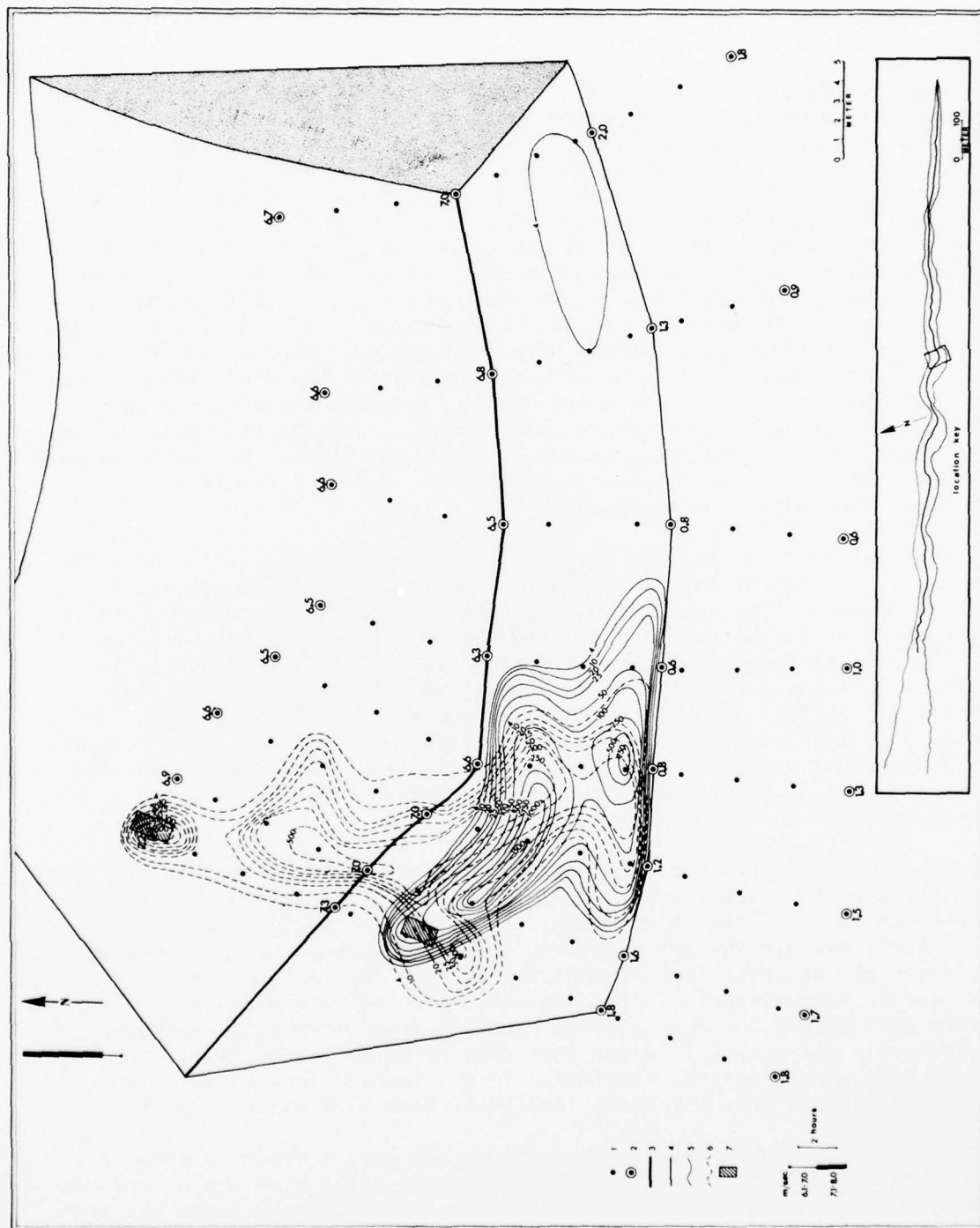


Fig. 5.7 Sampling map of released fluorescent dyed sand on both flanks of the dune at point no. 11. For key see Fig. 5.5.



Fig. 5.8 describes an additional case of colored sand movement in the dune deflection area, between points 9 and 10 (Fig. 1.1). The sand released on the windward flank moves parallel to the wind and is deflected in its direction at the lee flank at a distance of 5 meters from the crest, as we have already seen in previous cases (Figs. 5.5, 5.6). The deflection is to the east, according to the wind direction in relation to the crest line. The crest line here is deflected  $20^\circ$  in direction (from  $90^\circ$ - $270^\circ$  to  $70^\circ$ - $250^\circ$ ). In this area, the western component of the wind is weakened and the sand begins to settle and scatter over the whole lee flank. Proof of this can be found also in the movement of the sand released on the lee flank itself. This sand was partly scattered and partly buried and covered. On the other hand, it concentrated itself in the same place where the sand from the windward flank was scattered. The storm, which blew here for 15 hours and reached a magnitude of 10 meters/second, caused dispersal and burial of most of the dyed sand that had been released on the lee flank. The sand remained only where we found a deflection in the crest line which resulted in a deposition and concentration of sand.

Fig. 5.6 and 5.8 show two similar cases of sand movement in the deflection area. The result in both cases is identical, namely deposition of sand in the deflection area. However, in Fig. 5.6, the sand deposition is concentrated in the part near the deflection point of the dune peak, and in Fig. 5.8 - in the center of the deflection area. The differences in the positioning of the deposition area derive from differences in the wind directions. In Fig. 5.6, the winds were from NNE and NNW directions, and in Fig. 5.8, from the NNW only, at higher magnitudes. Therefore the eastward directional component was stronger in the case presented in Fig. 5.8 and as a result of this, the deposition was concentrated more to the east than in the case described in Fig. 5.6.

Fig. 5.9 describes the sand direction in the section found in the area where the sand is concentrated (in Fig. 5.8). The crest line changes its course here by  $75^\circ$  (from  $70^\circ$ - $250^\circ$  in the west to  $145^\circ$ - $325^\circ$  in the east). The wind that was blowing was northerly ( $360^\circ$ ), and therefore encountered the length of the crest line at various angles. The expected result in this case is sand movement at the lee flank in a western direction at the western side of the section. Though sampling results show the sand movement in a westerly direction, it seems that this movement was mainly in the central area of the section examined. In the western area there is a scattering of sand over the whole lee flank, with some easterly movement.

In general, the lengthwise movement of the sand in this section is very short, relative to the magnitude of the wind which blew there (see the wind rose case in Fig. 5.9 and compare with other cases where the magnitude was lower, as in Figs. 5.6, 5.7). Therefore, it seems that this is an area where there is mainly sand deposition. The sand released on the lee flank moved mainly to the west. The shorter movement was to the east,

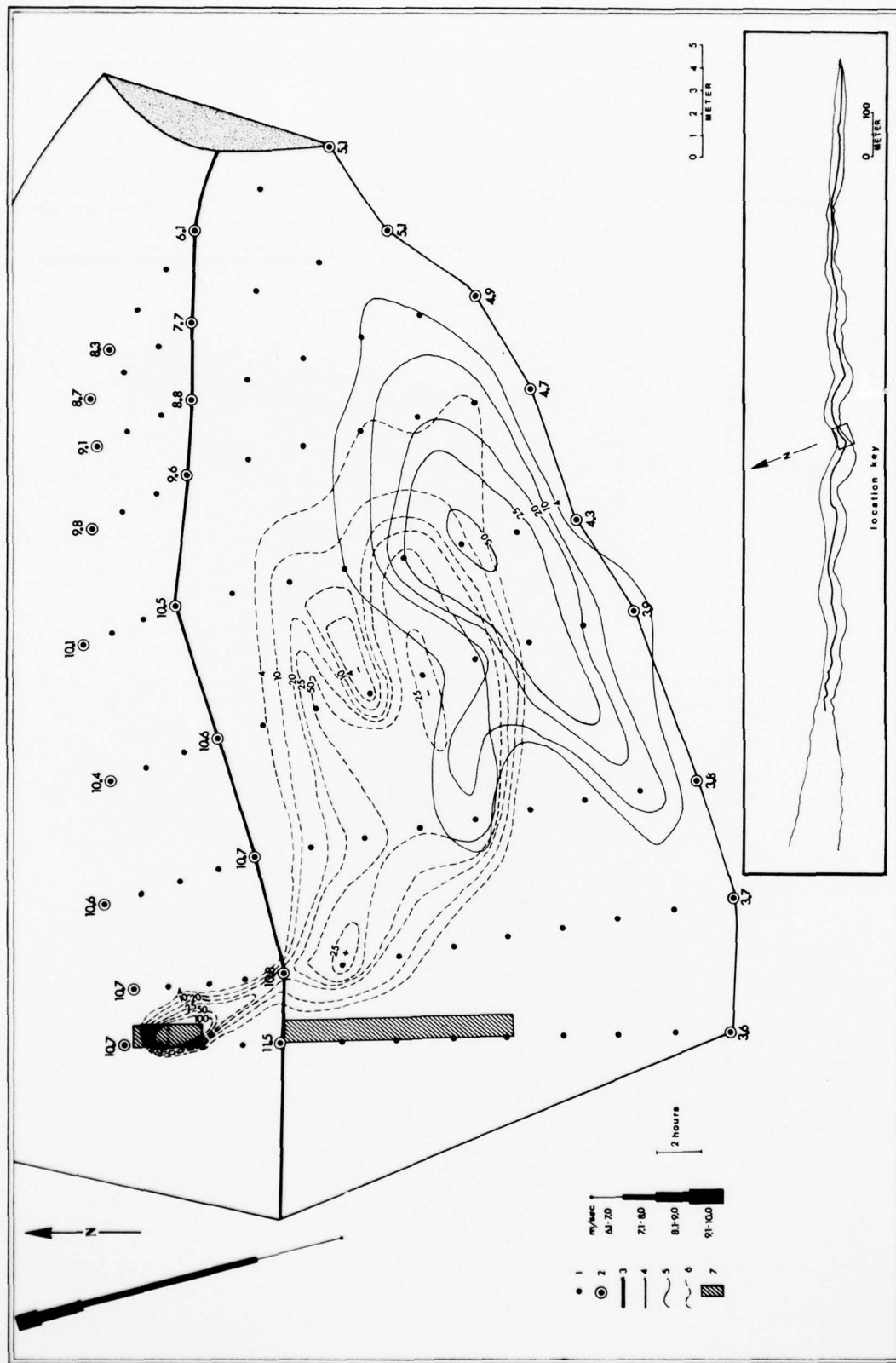


Fig. 5.8 Sampling map of released fluorescent dyed sand on both flanks of the dune between points no. 9 and 10. For key see Fig. 5.5.



where there are signs to show that sand in this area crosses the crest and settles on the windward flank, in a movement whose direction is almost opposite to the general wind movement.

These phenomena are to be seen as a result of eddies which form at the lee flank and which are derived from the deflection here of the wind direction to two opposing directions. In the area being examined, the wind has a western tendency when there are winds blowing from a general northern direction. This western tendency takes place at a limited section of the dune located in the deflection area. In a longer section located to the west of this area (on the section presented in Fig. 5.8) on the lee flank, according to the angle between the crest line and the northern wind, there is deflection and movement to the east. When the wind, deflected to the east, encounters the deflection point of the peak, it has a greater magnitude since it has come a relatively long distance from where there was a concentration of flow lines. Therefore, at the deflection point of the peak, two opposite wind directions meet, and the eastward wind direction is the stronger. At the encounter area, eddies are formed whose direction and magnitude are dependent upon and change according to the gusts of the wind. However, they have a stronger eastward component. The longer the wind moves to the east, the more the westward component gains strength and the eastward component weakens. The result, as we see it, is that the sand on the western side scatters over the width of the lee flank and tends to move somewhat to the east, while the sand released on the eastern side tends to move to the west.

#### 5.5.2 Grain Movement Under Western and Southern Winds (Winter Condition)

The results presented in the previous section relate to northern wind conditions typical of summer. In the winter, the conditions are different; the storms are limited for the most part to the invasion by barometric depressions of the eastern Mediterranean. The passing of a barometric depression is accompanied by circling winds from a S-SW to W-NW direction, where the S-SW has the higher magnitudes (Appendix 2).

Fig. 5.10 gives the results of such wind condition on the movement of dyed sand. Wind directions during the passing of the depression ranged from SW to NW, where the strongest magnitudes were in the SW and W. The dyed sand was released on the dune on May 11, and the sampling was taken on May 18. For seven days the area had been affected by winds of medium to high magnitudes (Fig. 5.10), with the sand movement beginning during a relatively light wind (a magnitude of 6-8 meters/second) from the north - actually a sea breeze. Later, with the invasion by barometric depression of the area, strong westerly and south-westerly winds began to flow (14 meters/second).

The movement that began with the northern winds caused a scattering



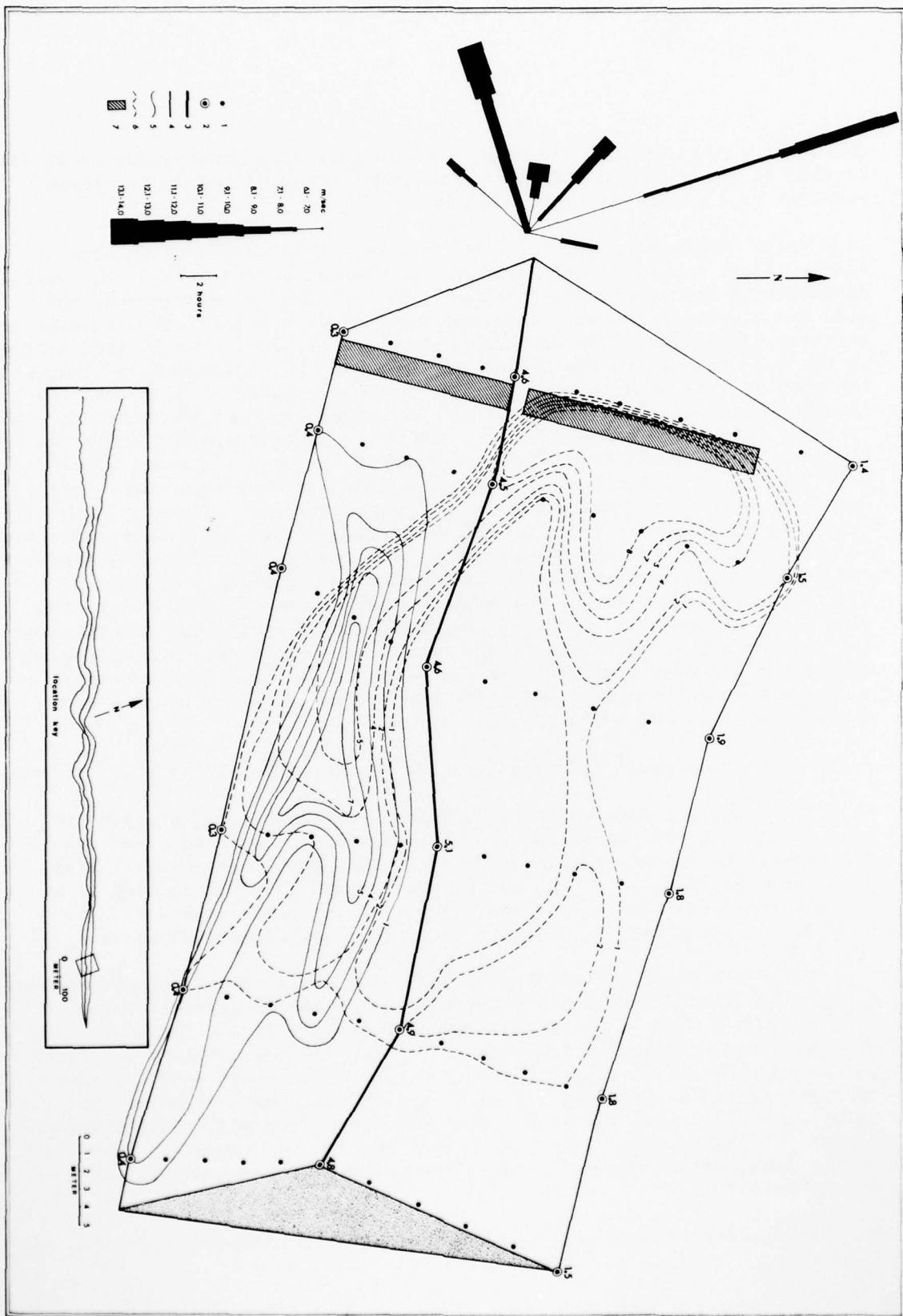


Fig. 5.10 Sampling map of released fluorescent dyed sand on both flanks of the dune at point no. 18. For key see Fig. 5.5.

of the sand, as in the summer cases already discussed (Figs. 5.5-5.8). The sand released on the southern flank was scattered in the area where it was released and completely covered. Further on, it concentrated in the area where the crest line changes course at  $20^\circ$  (from  $290^\circ$  to  $270^\circ$ ). As a result, there was a slowing down in the wind magnitude and the sand was scattered along the whole width of the lee flank. We assume that during the blowing of the northern wind (16 hours) before the beginning of the winter storm with the SW and W wind, most of the sand released on the southern flank was scattered and buried. For this reason, we do not find any of this sand contributing to the northern flank. On the other hand, the sand released on the northern flank was scattered by both the northern and southern winds and in both cases, show signs of concentrating in places where there is a change in the crest line which results in the weakening of the magnitude of the wind parallel to the crest line of the dune.

The distribution of the wind directions and magnitude during the time in which the sand is scattered (Fig. 5.10) is similar in general to the wind rose of the yearly winds (Fig. 2.7). This example shows the average state of sand movement throughout the year. The outstanding phenomenon is the sand movement parallel to the dune line and its concentration in the areas where the dune meanders. Lengthwise sand movement takes place in strips at a distance of 5-7 meters from the crest. The nature of the movement is determined by the relation between the general wind direction and the direction of the crest line. This relationship also determines the magnitude of the sand movement, as we have seen in Chapter III.

### 5.5.3 Grain Movement on the Zibar

The zibar, as described in the previous chapters, is a sandy body different from the dune in its morphology, which is flat and wider (Fig. 1.1), and also in its grain size (Fig. 1.2).

Tracing of the sand movement on the zibar, done at point no. 1 (Fig. 5.11), showed that the sand crosses the crest line (which has no sharp morphological expression) and continues without any change in the same direction on the lee flank, in complete accord with the wind direction. The width of the moving sand strip grew with the distance from the sand release area. However, this is an expected phenomenon of sand scattering by a gusty wind and no importance should be attached to it. In the lower part of the lee flank we find a concentration of sand which indicates deposition. There is also some change in the direction of the movement of the dyed sand released on the lee flank. It is difficult to attach any special importance to these two phenomena, especially because of the fact that in the lower parts of the zibar we find a high concentration of flora which traps the sand and causes unexpected deposition. It is possible also that the change in the direction of the movement of the sand released

AD-A063 612

BEN-GURION UNIV OF THE NEGEV BEERSHEBA (ISRAEL)  
THE DYNAMICS OF LONGITUDINAL DUNES.(U)  
JUL 78 H TSOAR

DEPT--ETC F/G 8/6

DA-ERO-76-G-072

NL

UNCLASSIFIED

2 OF 2

AD  
A063612



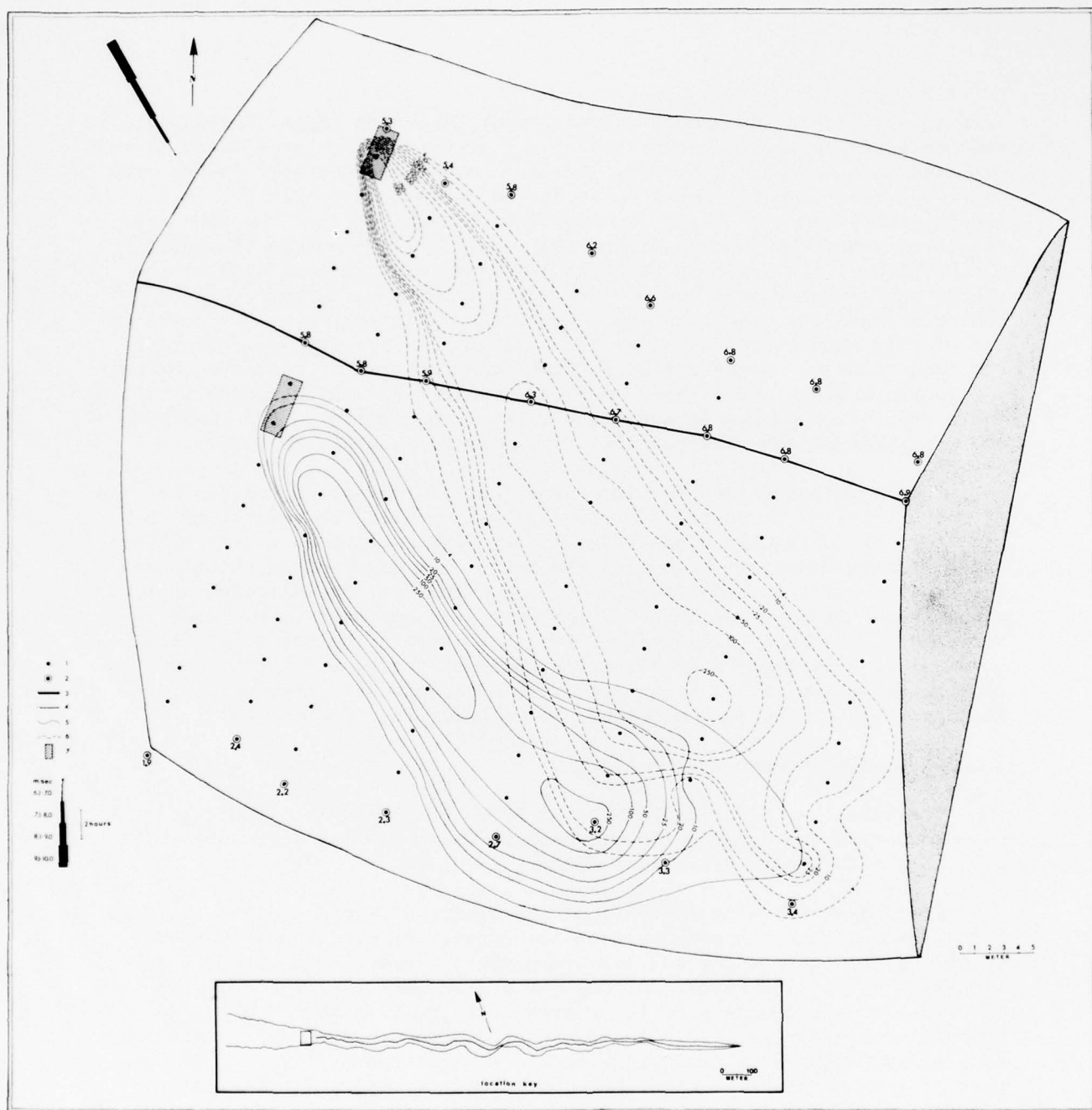


Fig. 5.11 Sampling map of released fluorescent dyed sand on both flanks of the zibar at point no. 1. For key see Fig. 5.5.



on the lee flank may be local, since there is no similar change in the direction of the sand released on the windward flank.

## 5.6 Summary

The outstanding and important phenomenon in the movement of sand upon the longitudinal dune is that the movement on the lee flank is always parallel to the crest line, irrespective of the direction of the wind. This phenomenon is caused by the change in the wind direction at the lee flank, according to the laws explained in Chapter Three. In this way the dune continues to grow longitudinally in one direction and any real lateral movement of the dune body is prevented.

On the windward flank, the wind movement is parallel to the wind direction while the longitudinal movement on the lee flank is at a distance of 5-7 meters from the crest line. At a distance of 2-3 meters from the crest line, on the lee flank, there is deposition of sand coming from the windward flank. This deposition brings about the beginning of a creation of a slip face at the head of the flank. In certain cases, this will grow with the addition of sand at the head of the flank and its avalanche on the slope, until the entire flank has a steepness of  $34^{\circ}$ , typical of a slip face. This phenomena is limited only to those sections where the wind encounters the crest line at almost a right angle, which are the deflection areas of the dune.

The phenomenon which is related to the changes in wind direction on the lee flank, parallel to the crest line, only takes place in cases where the dune has a typical sharp crest. On the other hand, where there is a flat low dune such as a zibar, which has no sharp outstanding crest line, this phenomenon does not take place, and the sand on the lee flank moves parallel to the general wind direction.

We saw in Chapter Three that there are changes in the deflected wind magnitude on the lee flank which are related to the impact angles of the wind. When the angle is right or nearly right, the wind magnitude on the lee flank is relatively low and it increases when the angle becomes acute. Accordingly, changes occur in the wind magnitude and as a consequence, changes in the rate of the sand movement according to the deflection of the dune. When the impact angle is acute, but changes to almost a right angle because of the deflection of the dune, there is a slowing of the wind at the deflection point, and consequently a stoppage of the sand movement - or in other words, deposition (Fig. 5.7). Where the impact angle is close to a right angle and becomes acute, we find an acceleration of the wind speed in the transition area, and consequently a faster sand speed (erosion) up until the next deflection of the dune. In that area, the angle between the wind and the crest line again changes to a less acute angle and there is sand deposition, etc., etc. An example of this

can be seen in the sand distribution on the northern flank in Fig. 5.10, where on the western part of the flank the angle of the storm wind from the SW was relatively less acute, and became more acute because of the deflection of the crest line.

When the angle between the crest line and wind in the deflection area is greater than  $90^\circ$ , sand movement in an opposite direction begins on the lee flank. As a result of this there is an encounter on the lee flank between two opposite stream lines, which leads to the formation of eddies and to a drastic decrease in speed (as we have already seen in Chapter Three). The two wind directions constitute two vectors in different directions. During summer the vector of the wind coming from the west in the direction of the dune movement is greater because this part of the dune, situated at an acute angle to the wind, is longer than the section of the deflection area (Fig. 1.5). Therefore, we do not find a change in the direction of the sand movement immediately at the sharp change in the crest line, but rather at some distance to the east - as shown in Fig. 5.9. However, because of the marked gustiness of the wind, it is possible to "feel" a change in the crest before the deflection, as in Fig. 5.5.

Eddies formed on the lee flank where the deflected windspeed is slowed down and in places where two opposite wind directions meet tend to scatter the sand and to deposit it in a uniform manner over the whole flank of the dune. In most cases, examined, it was found that deposition of sand takes place only on the lee flank, and there is no contribution from that flank to the interdune area. We can assume that every grain of sand that arrives at the dune - either from the zibar or from the interdune area - remains on the dune and does not leave it.

#### 5.7 A Model of Grain Movement on a Longitudinal Dune

The model prepared as a summary of the measurement of the dyed sand movement (Fig. 5.12) is of a typical longitudinal dune, which stretches in a direction of  $110^\circ$ - $290^\circ$  (similar to the longitudinal dune upon which the research was carried out), and is influenced by a wind from the N, which is a common summer wind direction. The course of the sand movement is demonstrated with the aid of arrows indicating the direction of the movement and its changes. The directions of the arrows were determined by the results of the measurements of the dyed sand carried out at various points along the dune. There are two kinds of arrows: a wide arrow indicating the dominant movement of the grains and a thin arrow indicating the secondary grain movement. These directions are derived from the wind gusts, which, according to the data of the wind recorder, move on the average between  $20^\circ$ - $30^\circ$  around the average direction.

This hypothetical longitudinal dune is divided into 4 parts: it starts from a wide flat section which forms the zibar, after which there is a

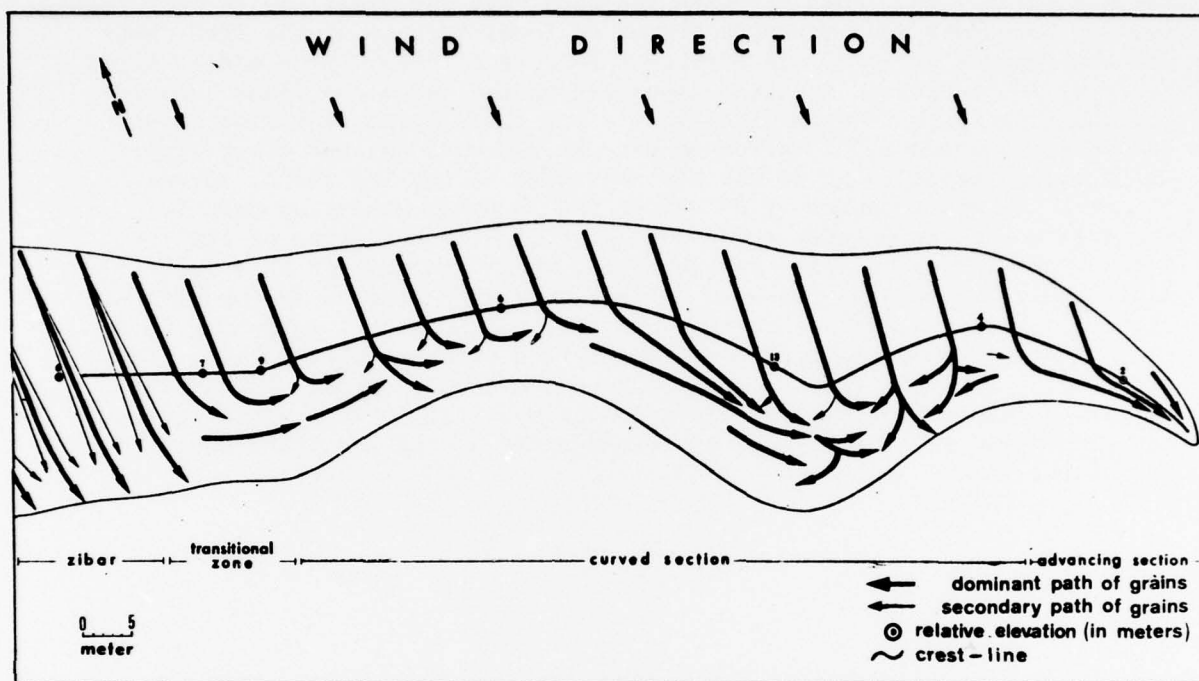


Fig. 5.12 Model of sand direction movement on a longitudinal dune.

short section which constitutes the transitional area to the developed dune. The central section, in which the developed longitudinal dune is found, has two meanders - one (western), moderate, and the other, sharper. The last section constitutes the end of the dune.

The movement on the zibar is parallel to the wind, and there is no real influence of the morphology on the wind direction. Small changes in direction, which are caused by wind gusts, bring about a wider scattering of the lee side of the zibar. On the narrow transitional area, the dune is beginning to form and to change from a wide flat zibar to a longitudinal dune with a narrow steep profile. Here we begin to notice the morphological influence on the wind that encounters the crest at an angle of  $70^\circ$  changes its direction on the lee flank and causes sand movement parallel to the dune axis. This movement along the lee flank progresses along a strip 5-7 meters from the crest line, and continues until the area where the first meander begins (next to the 9 meter elevation point). Here, because of the change in the direction of the crest line, the winds encounter

the dune at almost a right angle. The longitudinal movement on the lee flank naturally continues the same tendency, but the magnitude is much lower. Secondary sand movement begins to form, because of the wind gusts and the changes up to  $30^\circ$  in direction because of them. Here eddies begin to form, which scatter the sand deposited on the whole lee flank. Further on, the dune again changes direction (after the 6 meter elevation point) and an acute angle ( $45^\circ$ ) is formed between the wind and the crest line, which brings about longitudinal sand movement on the lee flank, increasing up until the next meander (found after the 13 meter elevation point). There is a sharper meander and a change of  $50^\circ$  in the course of the crest line. The wind encounters the crest line after the meander at a less acute angle, which also causes a deflection of the wind to an opposite direction. Sizeable eddies are again formed, which cause a lessening in the wind velocity, sand deposition and scattering over the whole flank. Here also there is considerable secondary movement caused by the wind gusts. Further on (after the 4-meter elevation point), the dune is again deflected and sand movement toward east is formed again on the lee flank until the end of the dune.



## VI. DEPOSITIONAL SURFACE AND INTERNAL STRUCTURE OF THE DUNE

### 6.1 Introduction

The body of the dune is built of sand laminae deposited by different wind regimes. The laminae are found on the slopes which were the depositional surfaces at the time sand was deposited. They cannot be seen on the surface and are covered by ripples. Bagnold<sup>(7)</sup> differentiated two types of laminae:

- 1) those deposited as a result of sand avalanches on the slip-face, which generally have a dip of more than  $30^\circ$  - which he termed "avalanche laminae";
- 2) laminae deposited as a result of the usual sand movement when in addition to the movement there was also deposition of the sand - termed "accretion laminae". This deposition is characterized by slopes much smaller than  $30^\circ$ . Yaalon and Laronne<sup>(76)</sup> also discern low angle lee sets smaller than  $20^\circ$ .

The internal structure of the sand dune serves as a means of identifying and describing fossil aeolian sand bodies and therefore furnishes information about the wind direction at the time the sand body was deposited. For this reason, a number of studies have been conducted on the internal structures of recent dunes and the subject has been recently summarized by Bigarella<sup>(77)</sup>.

### 6.2 Previous Work on the Internal Structure of Longitudinal Dunes

There is very little information on the internal structure of these dunes, especially in view of the fact that developed longitudinal dunes are widespread only in deserts. Most of the various dynamic theories assume that the slip-face of the longitudinal dune is produced alternately on both flanks of the dune. Therefore it appears to most researchers that the ideal internal structure must be avalanching beds at an angle of  $30^\circ$  found alternately on both flanks (Fig. 6.1). Bagnold<sup>(7)</sup>, who described this characteristic, indicates however that the depositional stages are very irregular, but his investigations confirm this order of layers. Glennie<sup>(25)</sup> sees this ideal internal structure as an expression of processes related to helicoidal flow which affect the longitudinal dune. He admits however that lamination on fossil dunes is often very rare, and he merely offers it as an ideal example. Yaalon and Laronne<sup>(76)</sup> are certain that the lowest percent of avalanche laminae is found on seif dunes exposed to winds from different directions.

The only comprehensive research on this subject has been done by McKee and Tibbetts<sup>(17)</sup>, who worked in Libya on seif dunes which have morphological characteristics very similar to those we have investigated in this present inquiry. Their results have shown that all the laminae

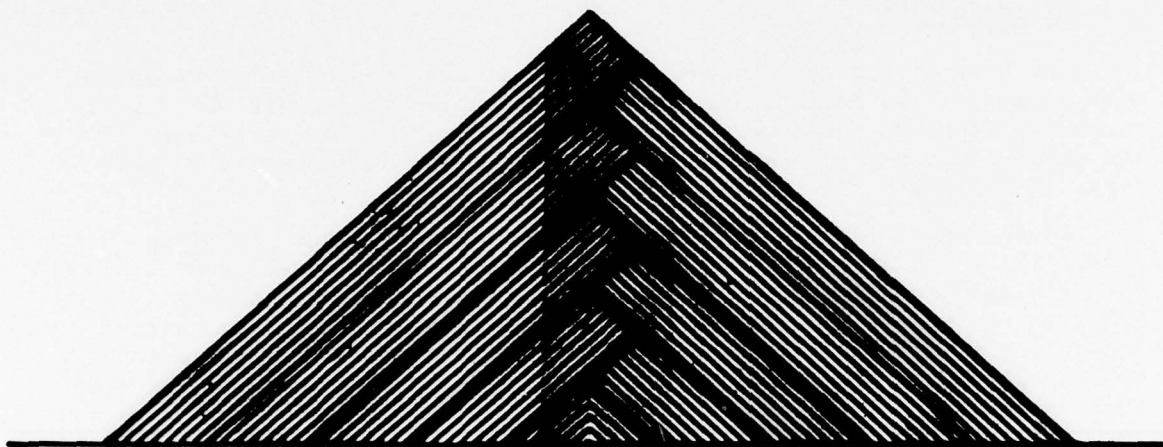


Fig. 6.1 Cross section showing the ideal internal structure of a longitudinal dune (according to Bagnold<sup>(7)</sup>, Glennie<sup>(25)</sup> and McKee & Tibbitts<sup>(17)</sup>).

slope at a direct angle to the crest line at a dip of  $10^{\circ}$  to  $33^{\circ}$ , except next to the dune base, where the dip is less. Their conclusion is that the self dune which they examined was created by dominant bi-directional winds, each one at  $45^{\circ}$  from the dune axis. The dune laminae are slip-face depositions at an opposing direction of  $180^{\circ}$ , determined by the state of the dune crest. These conclusions in fact support the ideal structure described above.

### 6.3 Research Method

Works dealing with studies of internal dune structure are faced with the problem of active dunes, covered by ripples or by avalanche beds which hide the internal structure. In order to uncover the internal structure, it is necessary to dig deeply, to locate the laminae and to measure the dip and its direction. This is very difficult, especially in arid areas where the sand is dry to a great depth and a great deal of water is needed to wet it in order to preserve the vertical walls. This activity has its limitations and it is not possible to dig down deeper than one or two meters, especially in the steep sections of the dune, because of the danger

of the walls caving in. Digging of deep pits is possible in stabilized or half-stabilized dunes, which are very rare in the desert. Therefore, most of the work done on this subject in deserts<sup>(17)(50)</sup> suffers from meagre information on depths of one or two meters and from the inability to dig at every place on the dune surface.

The main study of the internal structure in the present research was not achieved by digging pits. Because of the limitation mentioned, we were not able to dig more deeply than a meter and a half, and not at all in the steep sections of the dune. A rare opportunity to discern the contact of the laminae with the surface occurred on February 21, 1975. On that day and the two preceding days, there was a very heavy rainfall in the Negev, which caused severe flooding in the wadis. During the rain and afterwards, there were winds blowing in the area from the S and W at a velocity of more than 10 meters/second, which caused masses of wet sand to erode from the dune surface, uncovering the laminae which composed the internal structure along the entire southern flank of the dune, from the crestline to near the base. The differential drying of the various laminae and the differential erosion of sand from the same laminae made the structures very evident (Figs. 6.2, 6.4). A similar phenomenon was also described by McKee<sup>(78)</sup> and sharp<sup>(50)</sup>, although they did not attribute much importance to it.

This exposure allowed us to obtain a good evaluation only on the azimuths of the laminae, but in addition, gave a comprehensive picture of the extent of the laminae along the length of the southern flank and enabled us to distinguish the depositional systems which belong to the different periods. However, the knowledge gained from these exposures was compounded by information gained from the pit diggings at the various points on the dune and we were thus able to arrive at a better evaluation of the internal structure.

The pit diggings were done after a rainfall of several scores of millimeters which wet the dune to a depth of a meter to a meter and a half. After the true dip was located, it was measured by a Branton compass. In a few instances, peels were taken according to Yasso and Hartman<sup>(79)</sup>.

#### 6.4 Results and Discussion

Figs. 6.3 and 6.5 were prepared according to Figs. 6.2 and 6.4. The figures show the contact of the laminae with the surface of the southern flank of the dune at points 5 and 7. In both cases, the picture is the same and, along the entire length of the flank, we obtain the contact lines of the laminae with the surface, arched and concave in the direction of the dune's advance. Close to the dune crest there is a sharp unconformity line with laminae, whose contact lines are parallel to the crest line. It is possible to discern this phenomenon clearly in Fig. 6.6



Fig. 6.2 Contact lines on the laminae with the surface (on the southern flank of point no. 5), as exposed after a severe rainstorm accompanied by strong winds from the S and W.

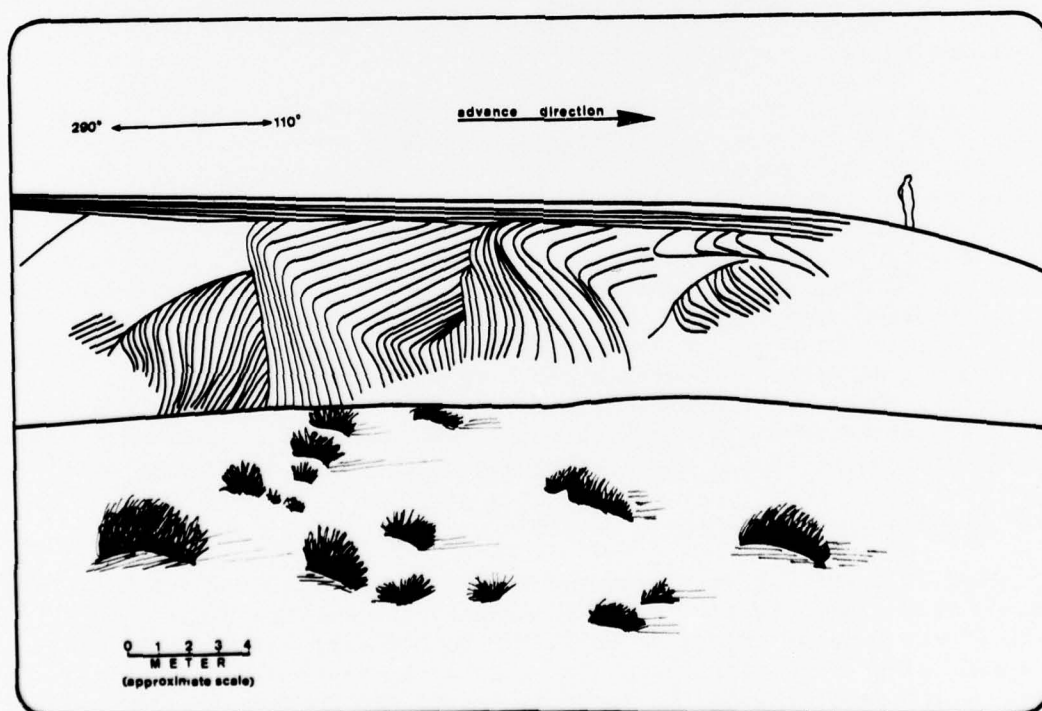


Fig. 6.3 Contact lines of the laminae with the surface (on the southern flank of point no. 5) according to Fig. 6.2.





Fig. 6.4 Contact lines of the laminae with the surface (on the southern flank of point no. 7), as exposed after a severe rainstorm accompanied by strong winds from S and W.

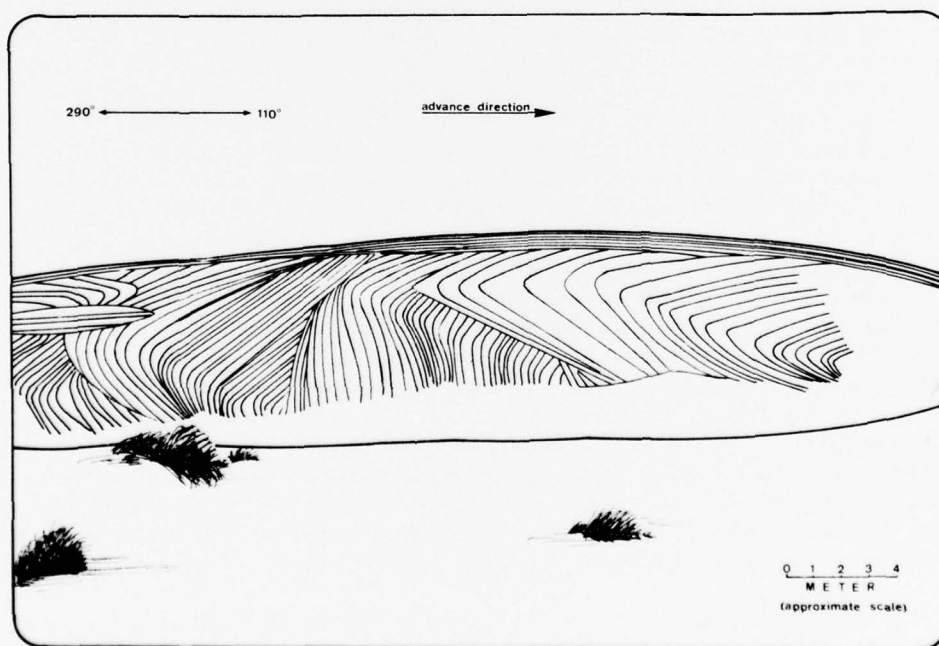


Fig. 6.5 Contact lines of the laminae with the surface (on the southern flank of point no. 7), according to Fig. 6.4.

taken at the crest line. From here, the laminae are arranged in both systems: one, the main one, found all along the length of the dune flanks; and the second, close to the crest line. In both examples (Figs. 6.3 and 6.5), we find along the flank about 4 separate systems of contact lines of the main laminae with the surface, all with the same appearance, although they relate to each other in unconformity. These contact lines, whose appearances were determined by the eroding angle of the laminae with the surface, show clearly that they were all deposited obliquely to the longitudinal axis of the dune. That is, the deposition was in places where the dune meanders and as a result, the wind velocity there decreased (as we have already seen in the smoke candle measurements, measurement of the wind velocity and tracing the dyed sand). Fig. 6.7 presents the situation in 3 dimensions. Because of the stormy winds which accompanied the rain, considerable erosion began at the top part of the windward flank and the entire flank was convex (Fig. 6.6). The laminae deposited in earlier seasons at the deflection area are oblique to the longitudinal axis of the dune and were bared as a result of it in an arched form on the flank surface. At the cross section all the laminae (except those connected to the crest line) are in the apparent dip. Each laminae system underwent erosion after its deposition. In every case, we find that the laminae which were deposited first in the same system were relatively less eroded than those deposited after them. This phenomenon occurs in the following way: the laminae which we see in Figs. 6.3, 6.5 were deposited in the summer season by NW-N winds, which transported the sand along the southern flank of the dune, and deposited it in places where the dune meanders. After constant deposition in the summer, the wind regime changed to SW-S winter winds. These winds directly affected the southern flank including the deflection area facing southward, where the laminae of the previous summer had been deposited and caused erosion of these laminae. The lamina deposited last, unprotected by other laminae, was the most eroded, with most of the erosion close to the crest. The one deposited first during the summer and protected by the many laminae above it was relatively less eroded. After the winter, and with the beginning of another summer season, another deposition cycle starts in the same area, however, in marked erosional unconformity on the eroded laminae. For this reason we find that the entire laminae system lies one on top of the other in erosional unconformity, and in each area there is a maximal erosion of the lamina nearest to the direction of the advance of the dune, and minimal erosion to the further lamina. In this way it is possible to come to some kind of evaluation of the rate of advance of the dune each summer.

The laminae parallel to the crest line were deposited in a belt 2 meters from the crest line, where we found a sharp decrease in the wind speed (Fig. 3.3, 3.4). This is a secondary deposition on the dune, and is limited to sections close to the crest line. In the summer when there are NW, N winds, there is a deposition on the southern flank, and in the winter, with W, SW, S winds, there is deposition on the northern flank.

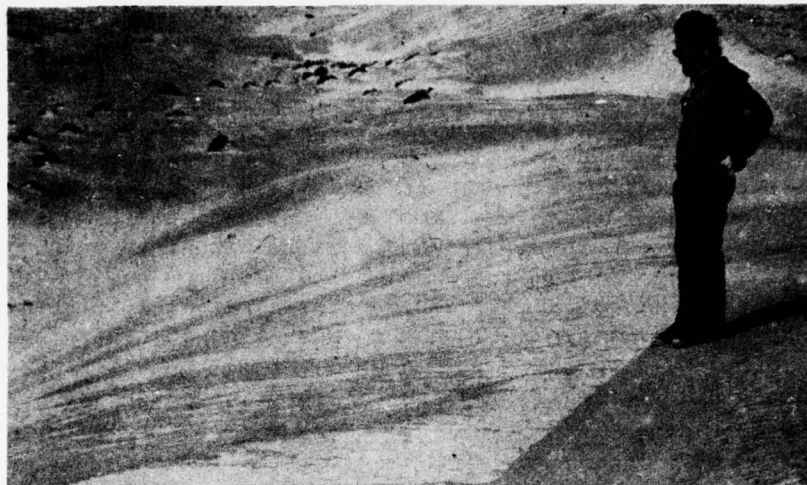


Fig. 6.6 Contact between the main laminae and the laminae parallel to the crest line (point no. 7).

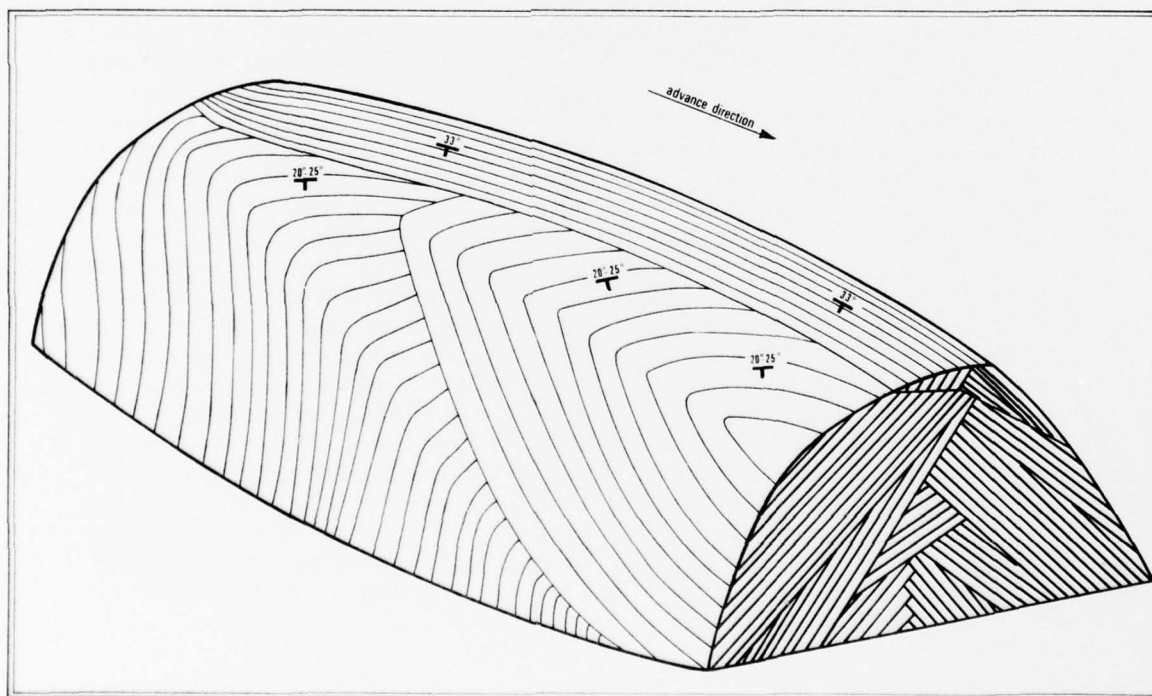


Fig. 6.7 Model of Fig. 6.5 in three dimensions.

Fig. 6.8 shows the secondary deposition near the crest at point 5 (at the same place as Fig. 6.2). In Fig. 6.8 we can also see the area where the dune meanders, where the main area of deposition is found. In this section, the azimuth of the laminae deposited close to the crest line is identical with the azimuth of the main laminae deposited on the area.

The magnitude of the deposition, which is parallel to the crest line, is dependent upon the angle between the crest line and the wind. When the angle is acute, the deposition is minimal, and it is maximal when the angle is a right angle (Fig. 3.29). Therefore this deposition is not uniform along the whole length of the dune. Even these laminae are prone to erosion, as we have already seen in Fig. 6.6.

A number of measurements of the dip of the various laminae and their azimuths, obtained by means of digging pits, give some quantitative data on the dip of the different laminae. In these also one can always distinguish the laminae deposited parallel to the crestline and limited to the upper parts of the flank, from the basic laminae deposited in the deflection area. In a number of pits dug at the upper part of the flank one can discern the contact line between two kinds of laminae (Fig. 6.9).

The results of the laminae dip measurements appear in Table 6.1 and in Fig. 6.10. Most of these were taken on the northern flank of the dune because the dampness of the very deep sand is better preserved there. The sand on the southern flank, facing the sun, is dryer and this makes it difficult to dig pits with vertical walls. The results of dip measurements done at a depth of a meter and a half show that on each flank there are two basic groups of laminae. One was deposited in the deflection area and was uncovered mainly in the middle and lower sections of the flank; these are the measurements from nos. 1 to 7 inclusive (on Fig. 6.10 they appear as a point). The second group are laminae parallel to the crest line and they are found near it; these are from nos. 8 to 12 on the Table (on Fig. 6.10 they appear as a point within a circle). In the first group we obtain slopes from  $15^{\circ}$  to  $32^{\circ}$ . From this we can deduce that most of the laminae from the deflection points are deposited as a result of the decrease in wind velocity, and are therefore "lee side accretion laminae". At some stages it is also possible to obtain there "avalanche laminae", when a slide begins from the crest to the base of the dune. The azimuth of the basic dip of the laminae (from no. 1 to 7) on the northern flank faces a direction of  $40^{\circ}$  to  $90^{\circ}$ , and on the southern flank  $160^{\circ}$  and  $170^{\circ}$ . On both these flanks, the surface deposition is found at an oblique to the dune axis, continuing in the direction of  $110^{\circ}$ .

The laminae which were deposited parallel to the crest line (from Nos. 8-12 in Table 6.1) are at different dips from  $11^{\circ}$  to  $30^{\circ}$ . It must be noted that in all cases the dips were identical to the surface slopes and perpendicular to the crest line. From this it is possible to deduce





Fig. 6.8 Slip face development next to the crest line which represent the secondary deposition which creates the laminae parallel to the crest line (point no. 5).



Fig. 6.9 Contact between the main laminae and the laminae parallel to the crest line, in a 1-meter pit on the upper part of the flank. The upper laminae (in an apparent dip) are part of the laminae deposited parallel to the crest line. The lower ones (in a true dip of  $28^\circ$ ) are part of the main laminae.

Table 6.1 Summary of Data on Measured Dips and their Azimuths

Measurement No.	Point	Pit Site	Dip	Azimuth	Comments
1	9	Southern flank (middle section)	30°	160°	
2	7	Northern flank (middle section)	32°	80°	
3	3	Northern flank (middle section)	23°	60°	
4	3	Northern flank (upper section)	28°	90°	
5	4	Northern flank (middle section)	16°	80°	
6	4	Northern flank (middle section)	15°-18°	40°	
7	9	Southern flank (middle section)	24°-25°	170°	
8	3	Northern flank (upper section)	15°	20°	Dip identical to surface slope
9	5	Northern flank (upper section)	30°	20°	Dip identical to surface slope
10	3	Northern flank (upper section)	16°-21°	360°	Dip almost parallel to sur- face slope
11	2	Northern flank (upper section)	11°-12°	340°	Dip identical to surface slope
12	3	Crest	10°	20°	Dip identical to surface slope

that these laminae were deposited during the season when the measurements were taken. Measurements Nos. 4&8 in the Table were taken from the same pit (Fig. 6.9) where the upper dip sets (on the picture with the apparent dip) are the laminae deposited parallel to the crest line, and the lower ones are related to deposition in the deflection area.

The dip of the laminae parallel to the crest line was measured only on the northern flank of the dune. It was impossible to dig pits on the upper southern flank for the reasons already mentioned, but one can discern these laminae on the southern flank in Fig. 6.6.

#### 6.5 A Model for the Internal Structure of a Longitudinal Dune

On a longitudinal dune there are 4 stratified units, the two basic ones being found in the deflection area on both sides of the dune, and the two secondaries on both sides of the crest line and parallel to it. These deposition units are seasonal; in each season there is deposition on the lee flank.

Near the crest line, sand is deposited in a section with a width of one to two meters, where a considerable fall in the wind velocity begins (Figs. 3.3-3.4). The existence of this section depends on the impact angle of the wind with the crest line. In cases where the wind comes almost parallel to the crest line, there is no decrease in the wind velocity on the lee flank; on the contrary, it increases. When the crest line is perpendicular to the wind, the decrease in wind velocity is very evident. Therefore, the deposition units parallel to the crest line will be very thick and extensive at the place where the dune meanders and where the crest line is found perpendicular to the prevailing seasonal wind. At the same place, there occurs also the main deposition, following the quick abatement of the wind, which moves along the lee flank (as we have already seen in Chapter Three). As a result, "lee side accretion laminae" deposition begins there. Over a period of time the secondary deposition spreads out there, beginning near the crest line, and towards the end of the season it covers the entire lee flank in the deflection area. Then the deposition is from both directions; from the crest of the avalanching sand - the "avalanche laminae", mixing with the "lee accretion laminae" of the sand moving along the lee flank.

Since the laminae deposited on the dune are of both types, the "lee side accretion laminae" and the "avalanche laminae", one expects to find laminae at various dips. The "lee accretion laminae" take on the declination of the surface on which they are deposited. At the beginning of each season, the deposition is on the erosional surface, sloping mostly at an angle of  $10^{\circ}$  to  $20^{\circ}$ . The deposition occurring near the crest line becomes thicker and steeper over a period of time and turns into

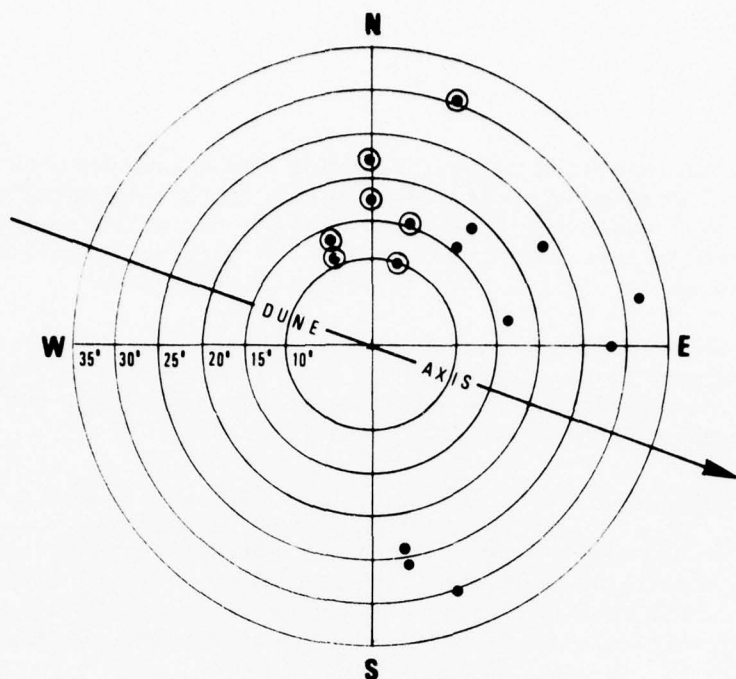


Fig. 6.10 Distribution of the condition of the dip and the azimuth of the investigated laminae. A dot indicates the main laminae; a circled dot, laminae deposited parallel to the crest line.

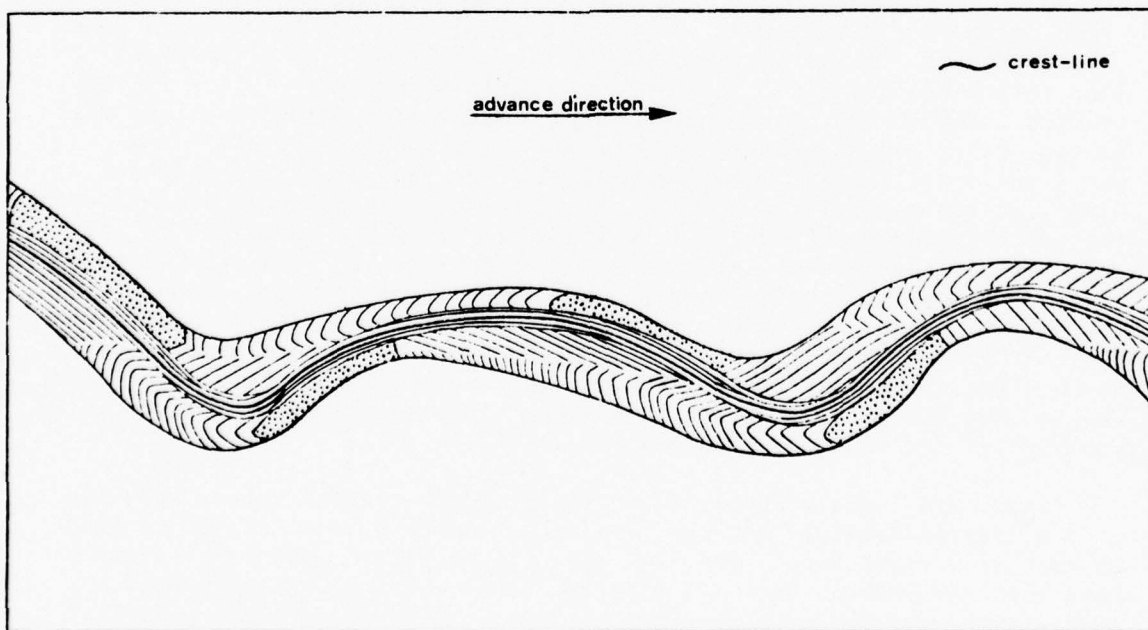


Fig. 6.11 Model of the internal structure of a longitudinal dune. The lines represent the contact of the laminae with the surface, and the dots, the depositional areas.



"avalanche laminae" especially at those sectors where the crest line is perpendicular to the prevailing seasonal wind. Main depositional layers will be found at angles of  $20^{\circ}$  to  $70^{\circ}$  on both sides of the dune axis and the secondary deposition will parallel the crest line and change its direction in accordance with the tendency of the situation of the dune.

Figure 6.11 is a hypothetical model of the stratified layers of a longitudinal dune, as they would appear if we took off all the lag deposits and could discern the contact on the erosional surface on both flanks. The model does not show the erosional unconformities which exist between the various seasonal depositions. The dotted sectors denote the present depositional areas of the deflection areas on both sides of the dune. It is possible here to distinguish two main depositional systems on both sides of the dune and two secondary depositional systems on both sides of the crest line, and their relationships.

The appearance of the laminar systems, as they are seen in Figs. 6.2 and 6.4, characterizes the wind regime in the research area, with its seasonal changes in the wind direction on both sides of the dune. In places where the changes in the wind direction are not seasonal but daily<sup>(17)</sup> or without order, the relationships between the systems would be different. The same processes would have an effect on the dune, but because of changes in the regularity of the erosion and deposition on both flanks of the dune, it would have a much more complex structure than the present one.

The cross section in Fig. 6.7 shows the characteristic structure of cross-bedding which is identical in appearance to similar cross-sections made by Bagnold<sup>(7)</sup>, McKee and Tibbitts<sup>(17)</sup> and others (Fig. 6.1). There is an important essential difference between the cross section in Fig. 6.7 and that in Fig. 6.1. In the latter, all the dips are true dips and in Fig. 6.7, all the dips are apparent, except for the laminae near the crest line, found in the true dip. One can discern the true dip only in a cross section done perpendicular to the strike line, which is parallel to the crest line of the dune in the deflection area. It may be that the reason for the conclusions of Bagnold<sup>(7)</sup>, McKee and Tibbitts<sup>(17)</sup> and Glennie<sup>(25)</sup> is that in cross-section they saw the same situation as in Fig. 6.7, but did not succeed in noticing that the strike of the laminae is not parallel to the crest line, but strays from it by a few degrees.

## VII. MEASUREMENTS OF ELONGATION AND MOVEMENT OF THE DUNE

### 7.1 Introduction

The actual movement of longitudinal dunes is not sufficiently clear. According to its appearance and the usual assumption that longitudinal dunes are a depositional form of sand, it is clear that the dunes become elongated and this is the reason for finding dunes of various lengths. Bagnold<sup>(7)</sup> found three different kinds of movement of longitudinal dunes: a) extension of the dune itself; b) longitudinal displacement of the summits; c) transverse shift as a result of the directional component (lateral) of the crosswinds.

Measurements were made to determine the rate of the three above forms of movement; the data on the transverse shift appear in Chapter Eight.

Measurements of a longitudinal dune were done through mapping the end of the dune at different periods by level and staff, with the pegs at point # 19 (Fig. 1.1) used as points of reference. With the aid of reference points denoting the sites where peaks and saddles were found in the beginning of the research, it was possible to measure the rate of longitudinal displacement of sections of the dune. Additional measurements made with two sets of aerial photographs taken 4 years apart furnished additional data on the rate of displacement of the peaks and saddles.

### 7.2 Results

#### 7.2.1. Elongation at the Far End of the Dune

Fig. 7.1 summarizes the changes at the far end of the dune and the elongation measured at different times. Table 7.1 summarizes the values of the dune elongation starting from January 19, 1973. The far end becomes elongated at different rates in the winter and summer. It also moves laterally with the direction of the wind. The lateral movement is limited only to the segments where the slip-face is found; where the slip-face disappears, there is only dune elongation.

#### 7.2.2 Longitudinal Movement of Dune Segments

The rate of longitudinal movement of the dune segments, as measured according to the changes in the sites of the peaks and saddles, is presented in Table 7.2.

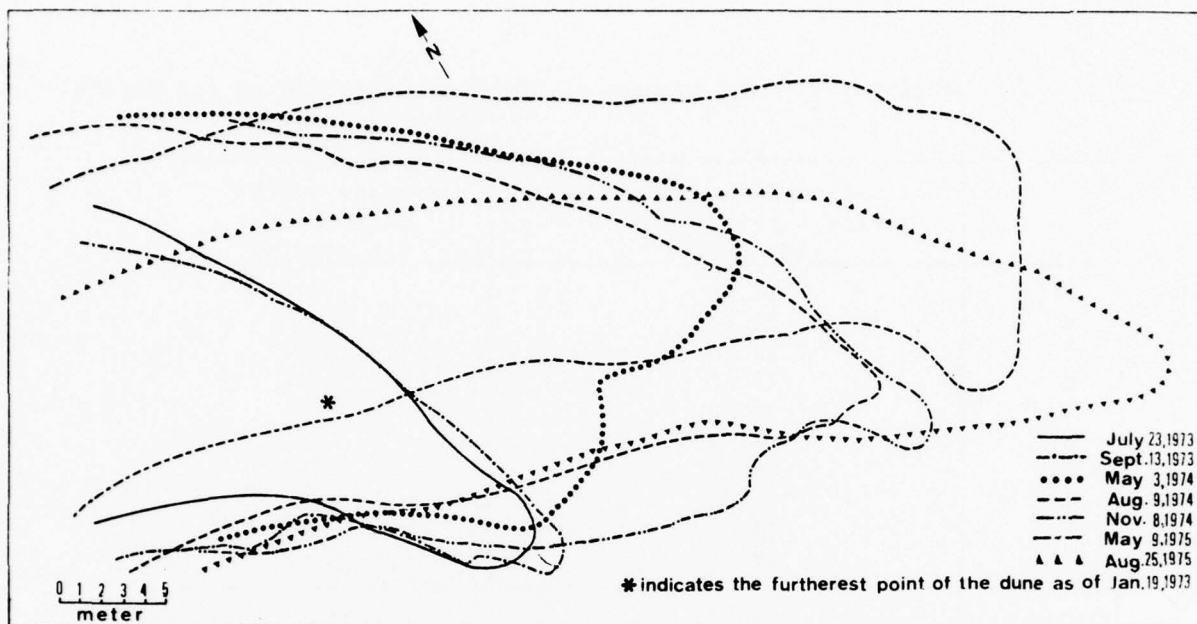


Fig. 7.1 Elongation at the far end of the dune.

Table 7.1 Dune Elongation (in meters)

Period	Season	Periodic Elongation (in meters)	Accumulated Elongation (in meters)	Monthly Average Elongation (in meters)
1.19,73- 7.23,73	Winter & Summer	11.5	11.5	1.88
7.23,73- 9.13,73	Summer	1.5	13.0	0.89
9.13,73- 5.3,74	Winter	7.5	20.5	0.98
5.3,74- 8.9,74	Summer	5.5	26.0	1.72
8.9,74-11.8,74	Summer	2.0	28.0	0.67
11.8,74- 5.9,75	Winter	4.5	32.5	0.75
5.9,75- 8.25,75	Summer	6.5	39.0	1.85
Total for period of 1.19,73 to 8.25,75	Winter & Summer	39.0	39.0	1.21

Table 7.2 Longitudinal Displacement of the Peaks and Saddles (in meters)

Point No.	Total displacement for the period 1.19,73-8.25,75 (in meters)	Average monthly displacement (in meters)
3	21.60	.67
4	21.80	.68
5	27.20	.85
6	17.40	.54
7	20.80	.65
8	24.50	.76
9	25.00	.78
11	25.00	.78
13	21.90	.68
15	18.30	.57
Mean	22.35	.70

The displacement rate is not equal at all points. This phenomenon does not necessarily arise only from the different rates of movement of the various segments, but also from changes in the relative sites of the peaks or the saddles on the segment itself.

Measurements of the elongation of the peaks and saddles, made with the aid of two sets of aerial photographs taken on November 27, 1970 and January 9, 1975 at points # 4, 7, 8 and 12, showed an elongation of 30 meters for this period, i.e. an average monthly elongation of 0.61 meters, slightly lower than the average measured elongation.

### 7.3 Discussion and Summary

It is clear that in most cases, elongation during the summer was greater than during the winter. In summer, a slip-face is created on the lee flank of the far end of the dune. This is evidence of the fact that summer winds do more total work than winter winds and that they are more constant in their directions and therefore make possible the creation of the slip-face at the end.

The elongation rate of the dune is faster than the rate of movement of the segments comprising it. Therefore new segments are created; on one side of the advancing section at the end of the dune, and on the other side, at the area where the dune begins from the zibar. The elongation rate is almost uniform, as the monthly maximum is less than three



times the monthly minimum and the average is 1.2 meters (Table 7.1).

It is not clear if the zibar also becomes longer at the expense of the dune. It is assumed that the zibar must become longer (although at a much slower rate), because the coarse sand in it moves at periods when there are storms with high wind velocities. On the other hand, it is possible to assume that the supply of fine sand ( $1/8 - 1/4$  mm) from the zibar to the dune does not amount to the rate of transport along the length of the dune. Therefore it must remain stable after the longitudinal dune is created from it.

## VIII. LATERAL MOVEMENT AND CROSS SECTION DECLINATIONS

### 8.1 Methods

At various points along the dune (peaks and saddles), cross sections were made with the aid of a staff and level at different times, mostly at the end of the summer and winter seasons. The section line was determined by means of a cord connecting the 4 pegs marking each point on both sides of the dune (Fig. 1.1), and continuing perpendicular to the dune axis - that is, from the 200° to the 20° direction.

Each reading of the level gave three values, the middle one of which gave the height, and the difference between the upper and lower ones giving the horizontal distance of the staff from the level. In a true reading, there is an equal difference between the middle reading and the outer ones. In this way, one can check the correctness of the reading. The reading is accurate up to 1 mm. In the horizontal distance reading, 1 mm = 10 cm, so that in a true reading, an error of 10 cm can occur in the horizontal reading. An additional error can occur as a result of the staff settling in the sand. It is difficult to prevent settling of up to 5 cm in the sand, which caused an error of 5 cm in the height reading, but does not affect the horizontal reading.

The horizontal error is more of a problem than the vertical because it can accumulate during the entire reading taken along the length of the section. In each section, an average of 20-30 readings were taken and theoretically, there can be an accumulated horizontal error of up to 3 meters. The sections were made along a line, with 4 fixed pegs so that it was possible to determine the amount of the accumulated horizontal error. In 68 sections done at 13 points, an accumulated horizontal error was found, ranging from 0.2% to 1%, and in an absolute evaluation, from 40 cm to 210 cm.

Presentation of the results was made with the aid of a plotter which originally drew the cross-section in a scale of 1:500 (Appendixes 14-17). The plotter has an accuracy of  $\frac{1}{2}$  mm, and on the scale of the original cross-section, it can cause a deviation of up to 25 cm in the horizontal and vertical readings. The accuracy of the vertical reading can be improved by exaggerating the vertical scale of section 3 times. Vertical error will then be up to 8.3 cm (Appendixes 21-26).

The lateral dune movement begins at the crests and changes in accordance with the seasons of the year. In summer with the northern and north-western winds, the lateral movement is in the 200° direction, and in winter, mostly 20°.

## 8.2 Results

The cross-sections appearing in Appendixes 14-17 and 21-26 present the dune profile at various points during different periods. Towards the end of the summer, we obtain mostly evident asymmetry in the cross-sections (Fig. 1.1 and Appendixes 24,26) which is mostly evident in the saddles, where the slip face reaches its highest development (Fig. 3.29). Asymmetry also develops in the reverse direction in the winter (Appendixes 24,27). During the change of seasons - mainly from winter to summer - a symmetrical profile is developed (Appendix 22).

From the cross section we can study the lateral movement of the dune. Due to the sinuous pattern of the dune, the longitudinal movement of the various sections also causes lateral changes. For this reason, it is difficult to evaluate measurements of the lateral movement which arises only from the cross-winds on the crest line that deposit sand near it. In extreme cases, the measurement shows profile changes at the fixed point arising from a considerable addition of volume, or a reduction in volume, as a result of the longitudinal movement. Fig. 8.1 presents 2 cross-sections made at the saddle of point # 4 ten months apart. As a result of the lengthening of the dune, the cross section which was made later is closer to the nearby peak. The saddles are found near the peaks (Fig. 1.5), therefore in the cross section made in the saddles, there were rapid changes found with time, as in Fig. 8.1, but slower changes with time in cross sections made at the peaks. Therefore, in order to follow up the lateral movement, it is desirable to compare only short periods, such as the beginning and the end of a season and then to pay attention mainly to cross sections made in peaks.

Fig. 8.2 shows 9 cross sections (on one scale) made during a period of 27 months at point # 1. This point is situated at the end of the zibar section of the dune. The results show that there is no significant change in the profile during the measured period. This result is evident in the light of the changes investigated at the sections of the dune itself (Fig. 8.3-8.5). It appears that the grain size and the surface morphology bring about stability of the zibar structure.

The lateral movement of the dune is in agreement with the winds at the various seasons. In summer, with winds from N and NW, the movement is in the  $200^{\circ}$  direction, and in winter, the main movement is in the  $20^{\circ}$  direction. Fig. 8.3-8.5 show that the principal lateral movement takes place in the upper parts of the dune, but in the lower parts there is very little change and they resemble the zibar in Fig. 8.2 from this point of view.

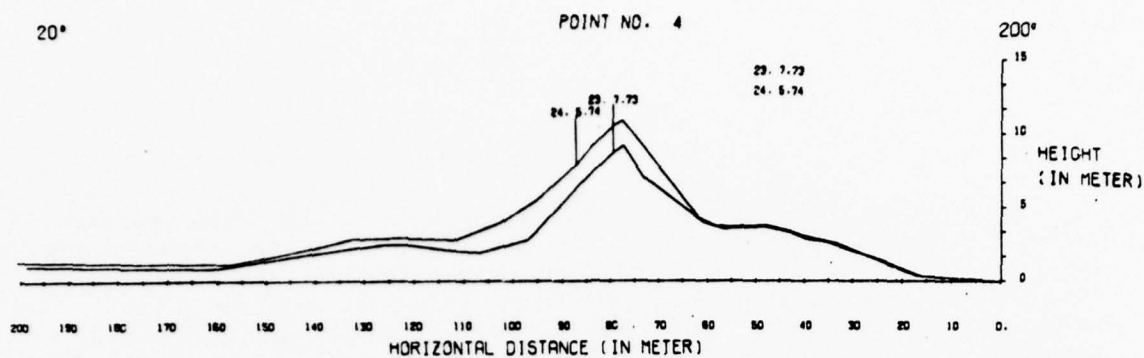


Fig. 8.1 2 cross sections at different periods at point no. 4. Note changes in dune volume.

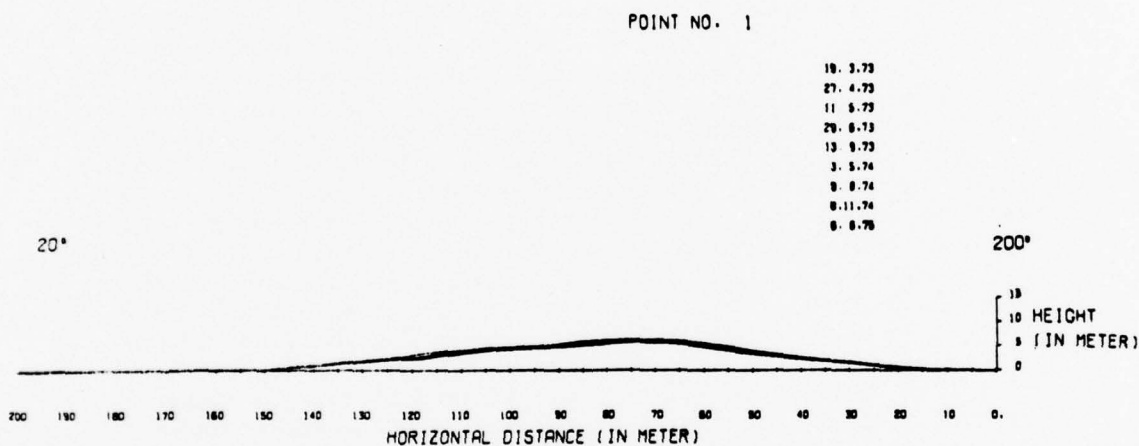


Fig. 8.2 9 cross sections at different periods at point no. 1 (zibar).

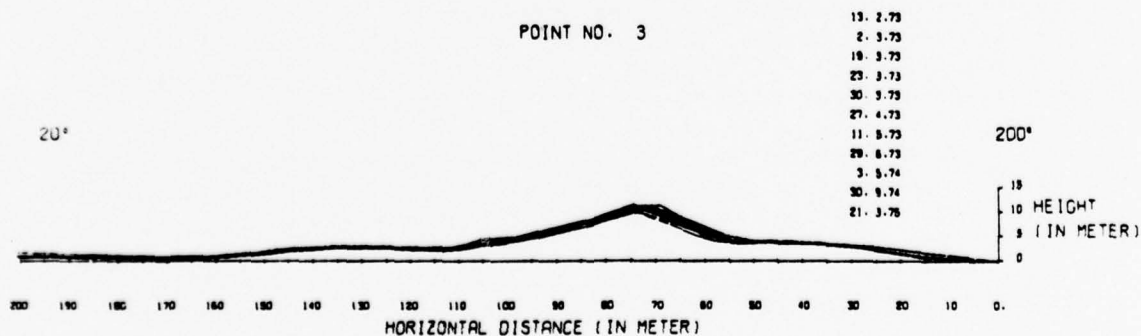


Fig. 8.3 11 cross sections at different periods at point no. 3.



Fig. 8.6-8.9 present the profile changes of the dune from the end of winter to the end of summer. In all the above cases, it is possible to discern in the crest movement to the  $200^\circ$  direction of about 5-9 meters, which began as a result of sand erosion on the flank facing  $20^\circ$  and deposition on the flank facing  $200^\circ$ . Therefore, the flank facing  $200^\circ$  became steeper at the end of the summer. In Fig. 8.6, for example, it is possible to distinguish between the steepness of  $18^\circ$  in the slope facing  $200^\circ$  at the end of the winter (May 3rd) and  $30^\circ$  at the end of the summer (Sept. 30). Any such change is limited to the top section of the dune at a height of 4 meters and over.

Fig. 8.10 shows the profile changes which occurred at point no. 6 over a period of 2 months. The summer slip face which began to develop from the crest line can be discerned. The flank facing  $20^\circ$  became more gentle ( $13^\circ$ - $24^\circ$ ) in contrast to its situation at the end of the winter ( $27^\circ$ ) but received additional material. On the flank facing  $200^\circ$  the declinations at the end of the winter (April 27th) were  $11^\circ$  and 2 months later  $-28^\circ$ . At this point, rapid changes began in the profile during the change of seasons, since it is found in the saddle.

In the same manner, there is a change in the profile from the end of summer to the end of winter. Fig. 8.11-8.12 show the changes from the summer to winter profiles, accompanied by movement of the crest in a  $20^\circ$  direction.

### 8.3 Declination of the Flanks

The declination in degrees of the dune flanks was calculated according to the data from the cross sections. Appendix 27 resents the distribution in degrees of the declination values all along the flanks (northern and southern) and of both together, at a number of measured points.

Just as there is a possibility of a certain error in the measured horizontal and vertical values of the cross section, so there is a possibility of error in the slope values. According to the percentage of probable error of the measurement, these errors can reach a value of  $\pm 3^\circ$ . If the calculations give slopes of values over  $34^\circ$  - this signifies an error, because dry loose sand cannot create a slope at an angle greater than  $34^\circ$ . Only in 3 cases, out of all the cross sections made, were values of higher than  $34^\circ$  obtained, where the maximum value came to  $37^\circ$  - and this is within the area of probable error.

#### 8.3.1 Declination of the Zibar Flanks

Figure 8.13 shows the frequency distribution in percentages of the slope declinations for both zibar flanks and separately, for the southern

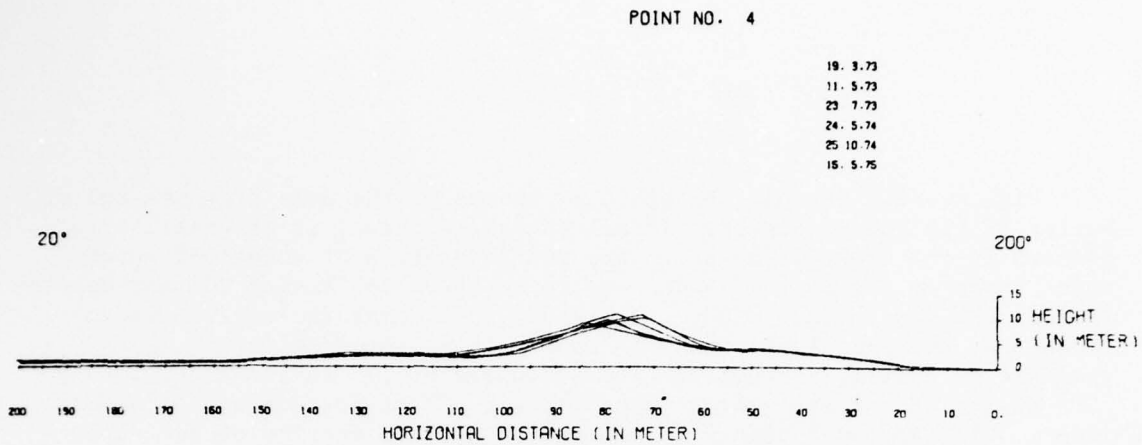


Fig. 8.4 6 cross sections at different periods at point no. 4.

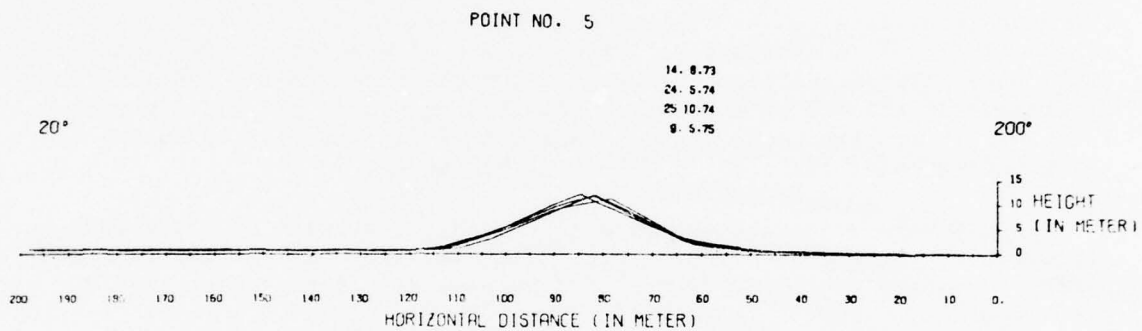


Fig. 8.5 4 cross sections at different periods at point no. 5.

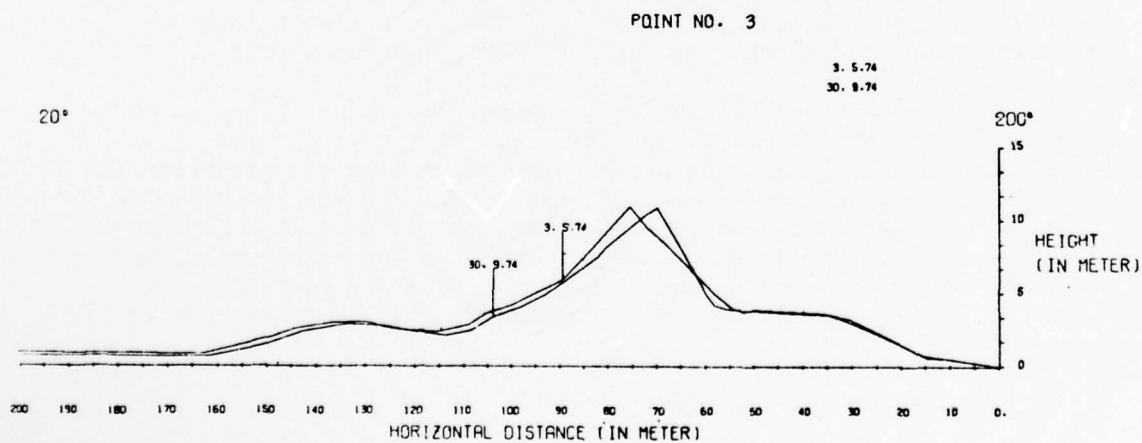


Fig. 8.6 2 cross sections at the beginning and end of the summer season at point no. 3.

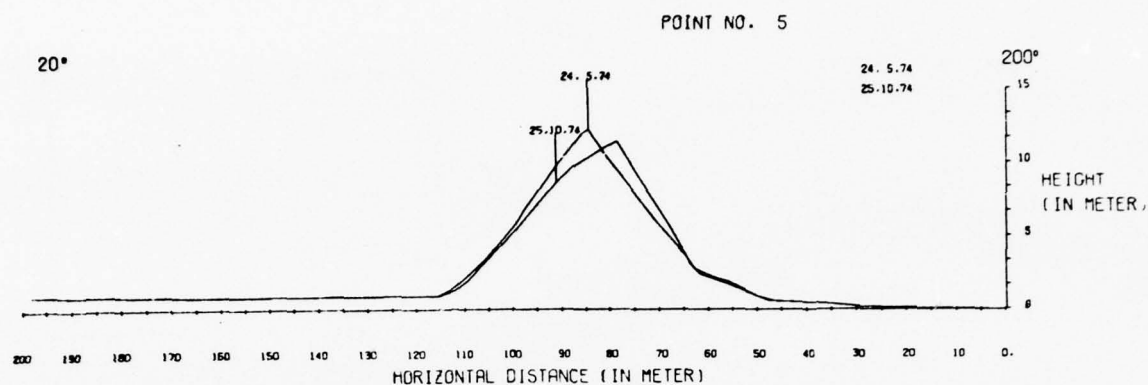


Fig. 8.7 2 cross sections at the beginning and end of the summer season at point no. 5.

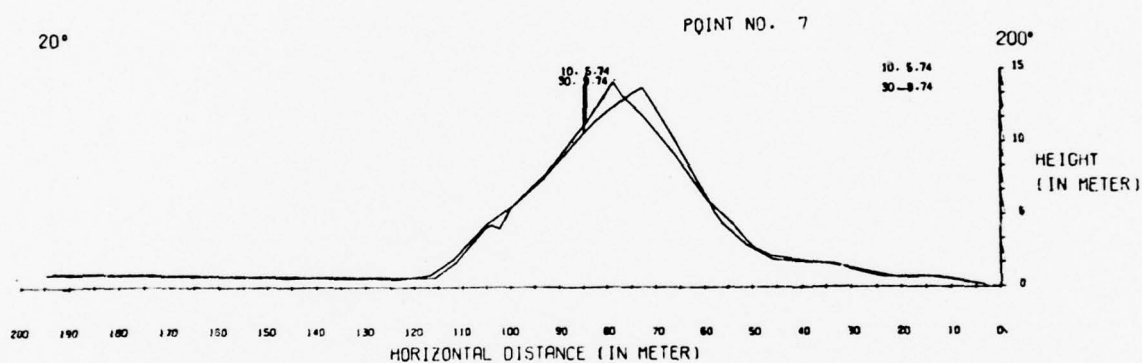


Fig. 8.8 2 cross sections at the beginning and end of the summer season at point no. 7.

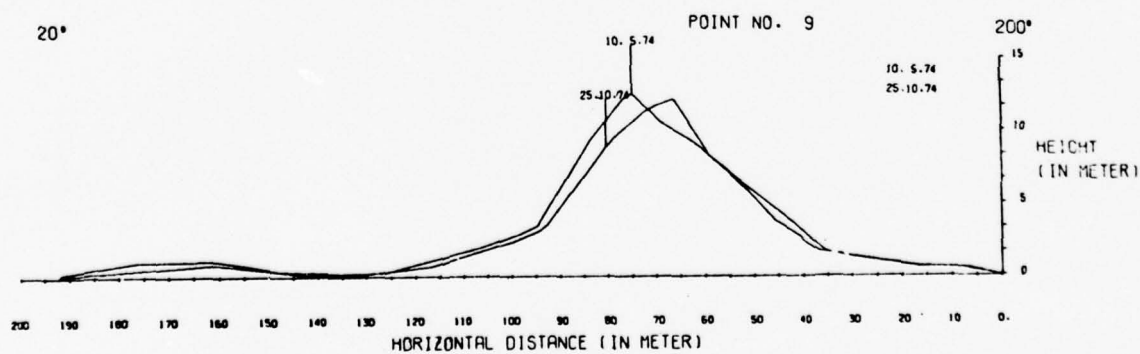


Fig. 8.9 2 cross sections at the beginning and end of the summer season at point no. 9.

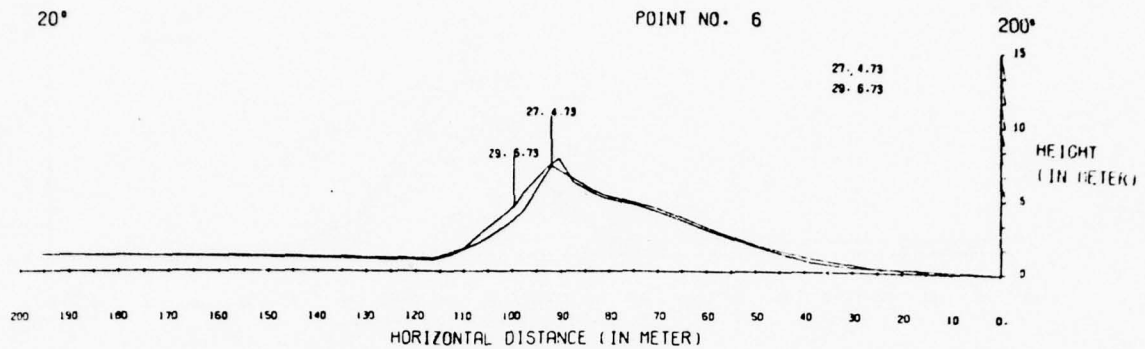


Fig. 8.10 2 cross sections at the beginning of the summer season at point no. 6.

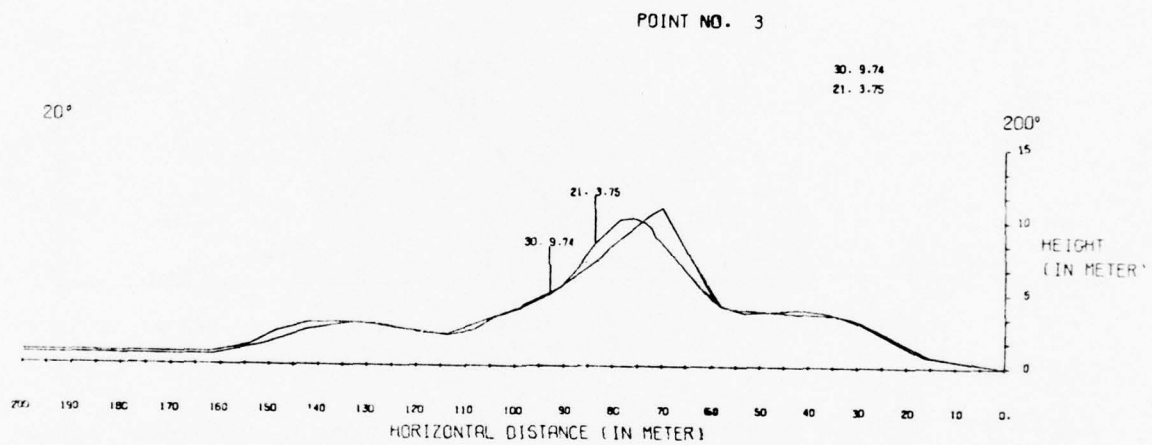


Fig. 8.11 2 cross sections at the beginning and end of the winter season at point no. 3.

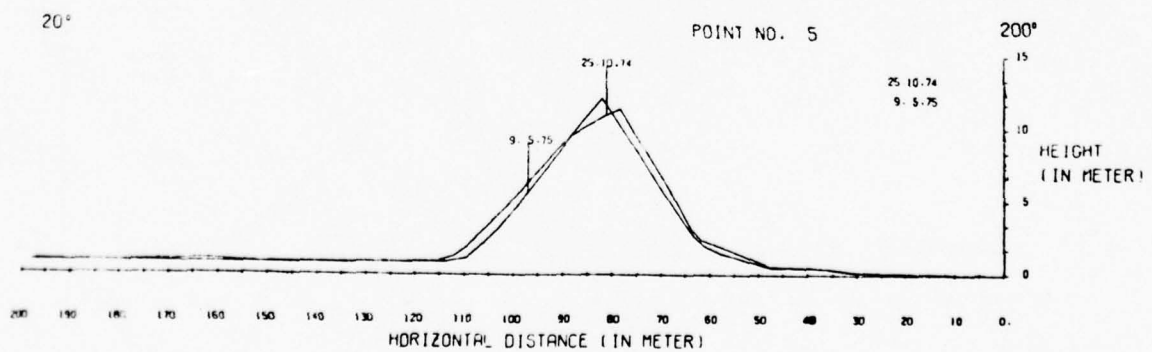


Fig. 8.12 2 cross sections at the beginning and end of the winter season at point no. 5.



flank in Fig. 8.14, and the northern flank in Fig. 8.15. The data are from the end of summer. All slopes of the zibar are less than  $10^{\circ}$ . There is an evident phenomenon of a greater percentage of steep slopes on the southern flank. This phenomenon, which generally takes place in the summer, is the result of northern winds with a high degree of constancy. The gentler slopes of the zibar arise from the medium and coarse sand which composes it and which cannot create a slip face.

### 8.3.2 Declination of the Dune Flanks

The dune declination (Appendix 27) changes from point to point and from season to season. In most cases, the lee flank is found at a declination of  $26^{\circ}$ - $30^{\circ}$  and the windward flank, at  $11^{\circ}$ - $25^{\circ}$ . Declinations with values above  $30^{\circ}$  (the slope of the slip faces) are rarer in longitudinal dunes, and in most cases measured, do not come to 10% of the flanks, on the average.

Fig. 8.16 shows the frequency distribution in percentages of the slope declinations, of both flanks of point # 3, and separately, for the southern flank, in Fig. 8.17 and the northern flank, in Fig. 8.18, at the end of summer. Fig. 8.16 shows bi-modal distribution when one mode is found between  $11^{\circ}$ - $15^{\circ}$  and the second between  $26^{\circ}$ - $30^{\circ}$ . The first mode belongs to the northern flank (Fig. 8.18) and the second to the southern (Fig. 8.17). The evident difference in the slopes is the result of the constant summer breeze which causes obvious asymmetry of the dune near the end of summer (Appendixes 24, 26, and Fig. 1.1).

Fig. 8.19 shows the frequency distribution in percentages of the slope declinations, along both flanks of point # 3; and separately, for the southern flank in Fig. 8.20, and in Fig. 8.21 for the northern flank, at the end of winter. There are no differences in the modal size of the declinations of the northern flank at the end of winter (Fig. 8.21) and summer (Fig. 8.18). On the southern flank (Fig. 8.20) there is a considerable decrease of the slope values vs. the situation existing in the summer (Fig. 8.17). The mode found is in the declinations range of  $16^{\circ}$ - $25^{\circ}$ . The bi-modality, which characterizes the slope values on both flanks at the end of summer (Fig. 8.16) and was the result of asymmetry - evident at this season - does not exist at the end of winter (Fig. 8.19). The profile of the longitudinal dunes tends more to asymmetry during winter and at its end (Appendix 22). The relatively steeper slopes of the southern flank of the dunes during the different seasons of the year (Appendix 27) are evidence of more work done by the northern winds (especially in summer) compared to the southern and the southwestern winds.

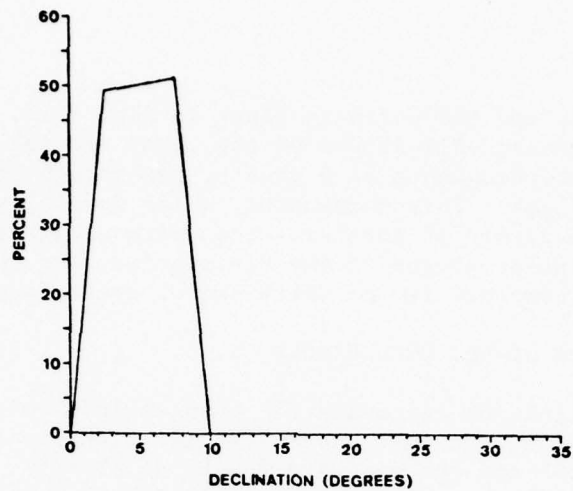


Fig. 8.13 Frequency distribution of declinations of the flanks at point no. 1 (zibar); Nov. 8, 1974.

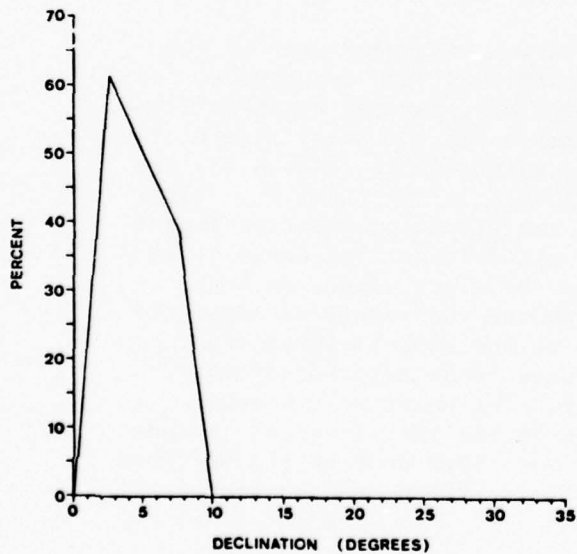


Fig. 8.15 Frequency distribution of declinations of the northern flank at point no. 1, Nov. 8, 1974.

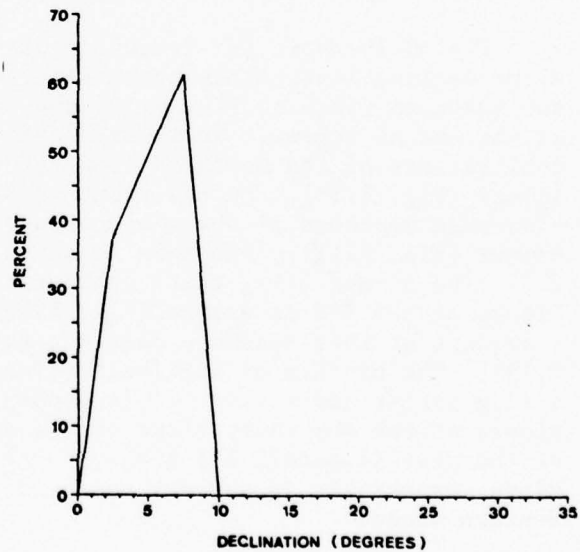


Fig. 8.14 Frequency distribution of declinations of the southern flank at point no. 1 (zibar); Nov. 8, 1974.

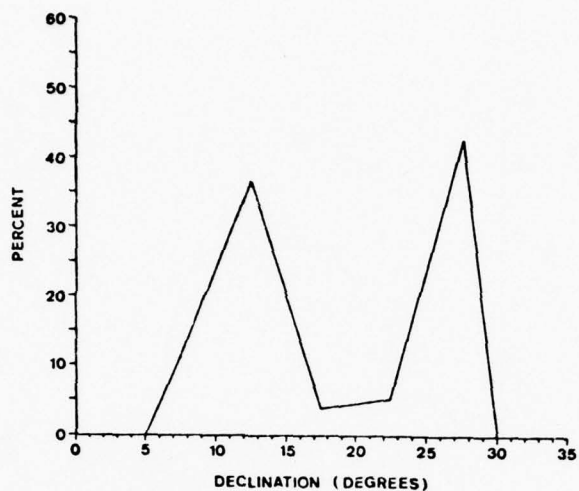


Fig. 8.16 Frequency distribution of declinations of the flanks at point no. 3, Sept. 30, 1974.

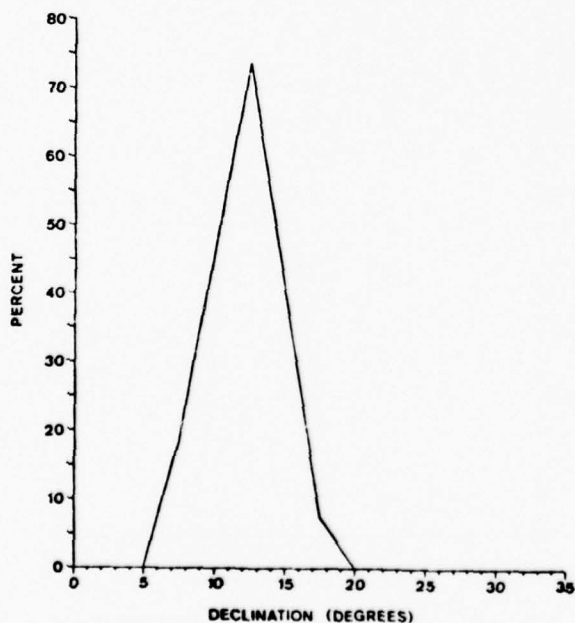


Fig. 8.18 Frequency distribution of declinations of the northern flank at point no. 3, Sept. 30, 1974.

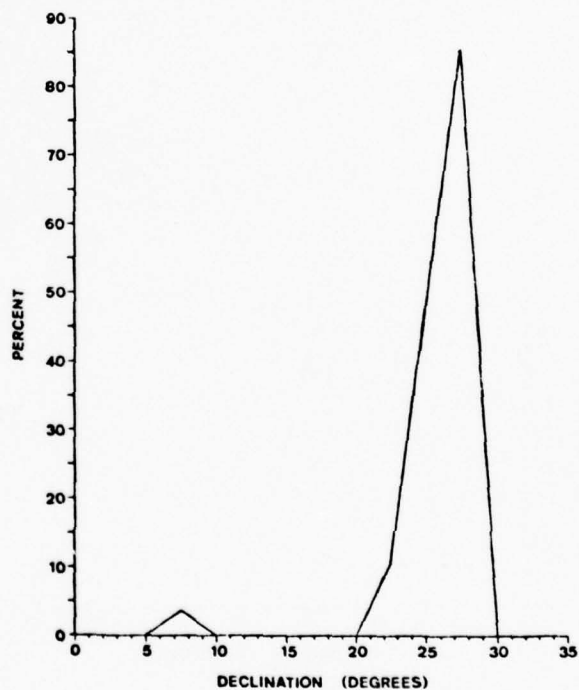


Fig. 8.17 Frequency distribution of declinations of the southern flank at point no. 3, Sept. 30, 1974.

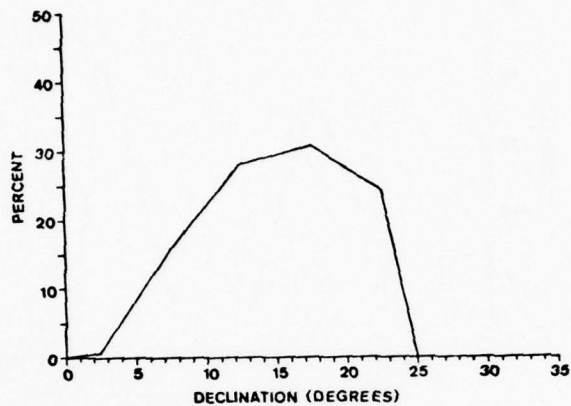


Fig. 8.19 Frequency distribution of declinations of the flanks at point no. 3, April 27, 1973.

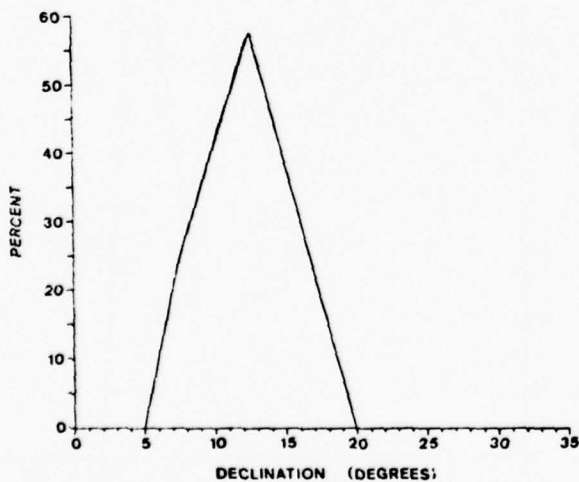


Fig. 8.21 Frequency distribution of declinations of the northern flank at point no. 3, April 27, 1973.

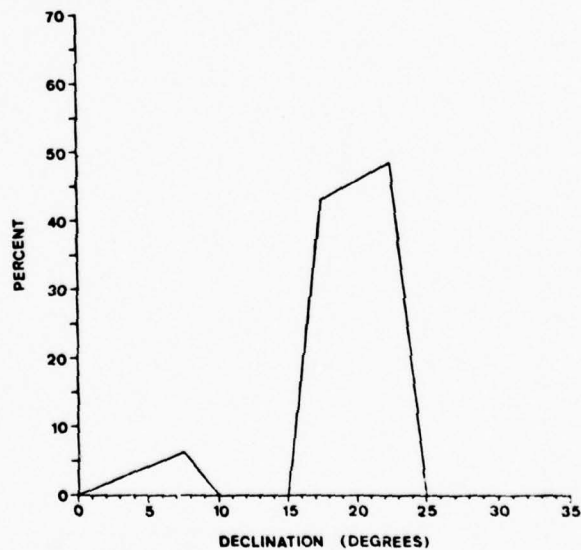


Fig. 8.20 Frequency distribution of declinations of the southern flank at point no. 3, April 27, 1973.



#### 8.4 Summary

The results of the measurements of the cross sections, done in a systematic manner, verify some conclusions of the previous chapters:

- a) The dunes undergo seasonal lateral changes, which are emphasized towards the end of each season (winter and summer);
- b) The main lateral changes begin near the crest, at a range of up to 5-7 meters from the crest line where the separation phenomenon occurs. The dune base does not move laterally.
- c) The slopes of the dune flanks are very rarely more than above  $25^{\circ}$  on the windward flanks, and above  $30^{\circ}$  on the leeward. These results resemble the slope values of the measured laminae (Table 6.1, Fig. 6.10).
- d) Because of the high degree of constancy of the summer winds from the N-NW, the asymmetry towards the end of this season is much more obvious than at the end of winter.

## IX. SUMMARY

### 9.1 Genesis of Longitudinal Dunes

The data and results presented in this paper are based on measurements and observations which took place over a period of 2 to 3 years. The measurements provide us with information about the processes affecting the dune and the mutual relationships which exist between the typical morphology of the longitudinal dune and its dynamics. From the results it is not possible to make direct deductions about the reasons for the formation of the initial typical longitudinal formation. In order to follow up the factors and reasons for the initial formation of the longitudinal dune, it would be necessary to measure and observe them for a much longer time period or to study the subject with the aid of a simulation model. In the framework of the present research, it was not possible to carry this out, therefore this step in the research is in part speculative. It was possible to evaluate the reasons and the factors for the initial creation of the longitudinal dune by means of aerial photographs of the dunes in the area of their formation, by various examples from the literature, and also with the aid of some of the data presented in this research.

Bagnold<sup>(7)</sup> considers that strong winds cause concentration of sand in longitudinal strips above the initial random sandy spots. He assumes that under the influence of favorable conditions such as storms passing in succession from the same direction, strips of several relatively thick strips are built up, so that they even outlast subsequent periods of opposite wind direction, and finally develop into a chain of long dunes. In the Libyan desert, he observed long narrow strips, 1-3 meters and 1-2 cm thick, found parallel to each other at spaces of 40-60 meters, and half a kilometer long.

Gorycki<sup>(80)</sup>, who explained the formation of the beach cusp by means of the sheet-flood mechanism, tries to attribute this also to the formation of the longitudinal aeolian sand strips, even though it does not seem that wind has a sheetflood structure such as the swash of sea waves in contact with the shore line.

From our research results it is clear that for a dune to develop and function as a longitudinal dune, two basic things are necessary: a) a bi-directional wind regime, where the two wind directions do not create an angle larger than  $150^{\circ}$ - $180^{\circ}$  (and the dune stretches between them), b) a dune with a sharp profile, i.e., the declination of each flank is at least  $16^{\circ}$ - $20^{\circ}$ , so that the flow of separation can be developed on the lee flank.

The bi- or multi-directional wind regime is the most widespread on the face of the earth<sup>(81)</sup> and therefore in a considerable area of the world's deserts there are suitable wind conditions for the formation of such longitudinal dunes. The sharp dune profile is created at the "horns" of barchans and transverse dunes. In cases where the wind regime existing in barchan fields answers the above requirements, the "horn" of the barchan will elongate at a faster rate than the barchan body advances, and will finally change to a linear longitudinal dune. For this reason, it was found that in most of the barchan fields and the transverse dunes of the world there exists an elongation of one of the horns<sup>(1)(2)(82)(83)</sup>. This consideration brought Bagnold<sup>(7)</sup> to the assumption that the origin of the longitudinal dune is from a barchan exposed to a bi-directional wind regime, one of whose horns (found on the side exposed to the storm) is elongated by a non-constant stormy wind. In a research carried out in Arabia<sup>(40)</sup> and in northern Sinai<sup>(2)</sup>, the same phenomenon was discerned, although the elongated horn was the one opposite the direction the wind was blowing. Therefore, one may regard barchans and transverse dunes as the origin of the longitudinal dune.

An additional and probably more important source of the longitudinal dune is the zibar (Fig. 1.1, 1.3). As noted in Chapter One, the zibar is built from bi-modal sand (Fig. 1.2). With time, there takes place winnowing of the fine mode of the sand (2-3  $\phi$ ) and concentration at the end of the zibar. The bi-directional wind regime creates a sharp profile there, upon which work all the processes which bring about its elongation.

Even so, the problem of the genesis of the longitudinal dune has not yet been solved, because there still remains the question: how are the sand strips of the zibar formed, and what determines the definite spacing between them? It may be that the explanation for this can be found in Bagnold's<sup>(7)</sup> hypothesis or in Groycki<sup>(80)</sup>, both of whom noted the above. From all this, it appears that the longitudinal dune is a secondary formation of a barchan, a transverse dune, or a zibar.

## 9.2 The Zibar as a Source for Longitudinal Dunes

According to aerial photos of the Sahara<sup>(41)(42)</sup> (Fig. 1.3), it is possible to see that the source of most longitudinal dunes is from the zibar strip. The fact that transverse dunes and barchans are rare in deserts<sup>(4)</sup> supports the assumption that the zibar form is the source of most of the longitudinal dunes of the world.

Folk<sup>(14)(15)</sup> sees the source of the bi-modal sand which characterizes the zibar as the creator of the sand sheet which undergoes deflation by the wind, which selectively removes the fine grains (2-2½  $\phi$ ) and piles them on the dune. Warren<sup>(41)</sup> is certain that among the grains which move by saltation on the zibar are also grains fine enough to suit

the inter-grain spaces between the very coarse grains which move by creep. In this way these fine particles are protected from the impact of the medium particles which move quickly by saltation and finally concentrate at the end of the zibar and form the longitudinal dune. He bases his claim on the fact that the longitudinal dune sand has the mode found in the gaps between the two modes of zibar sand<sup>(1)</sup>. A similar discovery was made by Wilson<sup>(44)</sup>.

The zibar which serves as a source of the dune in this present work has a coarse mode ( $1-1\frac{3}{4} \phi$ ) and a fine mode ( $2-2\frac{1}{2} \phi$ ) which is also the mode of the sand found in the body of the longitudinal dune (Fig. 1.2). This zibar is different from the zibars that Warren<sup>(41)</sup> and Wilson<sup>(44)</sup> sampled, in that it has a potential of a great amount of fine dune sand. It appears that this zibar furnishes sand to the dunes for a relatively short period.

The morphology of the zibar arises from the fact that a considerable part of the sand which builds it is medium to coarse, as contrasted to the fine sand which characterizes the dune. Warren (in his lecture at the International Symposium on Geomorphic Processes in Arid Environments held in Jerusalem, March 1974) is certain that the coarse size of the zibar grains has a longer saltation path and as a result, cannot form a slip face on a zibar whose height is less than 13 meters. In Chapter Two we explained, according to Fig. 2.2, why a dune built of coarse sand, has a lower and flatter morphology. From this we can understand that the flat morphology, which cannot create a slip face, prevents the formation of separation flow and development of the dynamic processes as those which work on the longitudinal or transverse dunes. From this, one can perceive why the zibar does not change its profile during the different seasons (Fig. 8.2).

In a few places like the Sahara<sup>(84)</sup> we find that longitudinal dunes formed from zibars change in their general direction from the zibar's direction. One should not see this as evidence of a climatic change, as Bagnold<sup>(7)</sup> thought, but rather as a fact that the threshold wind velocity needed to carry the medium and coarse zibar sand is higher than that carrying the fine dune sand (Fig. 2.2). Therefore the zibar sand moves only under a wind regime which is above the threshold velocity needed to carry the medium and coarse sand. In certain cases, this wind regime is different from that needed to carry the fine sand. The result would be a different direction of movement to the zibar and to the longitudinal dune built from it.

From Fig. 1.1 it can be seen that in places where the longitudinal dune became fully developed, the interdune area between them is free of all signs and remains of the zibar. The reason arises from the fact that when the developed dunes were formed, they served as traps for sand



moving obliquely or perpendicularly in the interdune area. The longitudinal dune, as we have already seen (Figs. 5.5, 5.7) does not furnish sand to the interdune area because of the deflection in the direction of the wind on the lee flank. The fact that the zibars in the interdune area furnish sand to the longitudinal dune, although without receiving sand from them, finally brings about their disappearance. This is the secondary contribution of the zibar to the longitudinal dune. The coarse sand furnished in this manner is concentrated along the base of the dune and there forms mega-ripples, as we saw in Chapter Four.

### 9.3 The Morphodynamic Model of a Longitudinal Dune

The basis of the dynamics of the longitudinal dune is the phenomenon that the path of the wind flow, when crossing the crest line at any angle whatsoever, is deflected on the lee flank in the direction parallel to the crest line. As a result of this process, all the winds which arrive at the dune from a sector of  $180^\circ$ , whose center is at the place where the dune begins, cause a longitudinal movement of the sand and an elongation of the dune. Because of the separation process, we get, with wind which meets the crest line at an acute angle, high velocities of the deflected wind on the lee flank, higher than those of the windward flank and the crest. In these cases, the sand eroded from the windward flank is not deposited on the lee flank but continues to move along the dune with the deflected wind. Because of the increase in the deflected wind magnitude, it also erodes sand from the lee flank and carries it along its path. This process exists as long as the wind magnitude continues to increase. Deposition begins only when the wind magnitude drops. This occurs only when the angle between the wind direction to the crest becomes less acute (Equation 3.2).

In each section of the dune there exist processes of erosion and deposition (Fig. 9.1). With N-NW winds (summer), erosion is from the long part of the section (from the saddle to the peak) and deposition is in the deflection area (short part). With wind from the SW (winter), erosion is from the short part and deposition at the long one. The cycle of sand movement on a longitudinal dune occurs in this manner resulting in transportation-deposition-burying by additional deposition, and subsequent exposure. The sectors undergoing erosion in the longitudinal dune are equivalent to the windward slope of the transverse dune and the barchans. The sectors where depositions occur in the longitudinal dunes, to the slip face of the transverse dunes. Deposition on the longitudinal dune differs from that on the transverse dune in that it is essentially a "lee side accretion", in contrast to the "avalanche type" which characterizes transverse dunes and barchans. For this reason, the slip face is not a widespread form on longitudinal dunes, and the flanks there are not so steep as the lee flanks of transverse dunes. Slip faces on longitudinal dunes develop only on the upper segments of the sloped sections undergoing

erosion, and also cover considerable parts of the slopes in the sector where the sand deposition starts (Fig. 3.29).

Fig. 9.2 is an example of the erosion on the long part of the dune segment, which undergoes considerable erosion during the summer. One can distinguish the lack of ripples on the surface and the exposure of the contact lines on the laminae with the surface (as we saw in Chapter Six). This phenomenon can be noticed only at the beginning of the summer (the case presented in the above Fig.) when the dune sand is still wet at shallow depth. In summer, when the sand is dryer, it is hard to recognize this phenomenon on the surface.

Figs. 6.8 and 9.3 (close-up of Fig. 6.8) are examples of the depositional phenomenon of the "lee side accretion" type at the deflection point. The deposition here is demonstrated by a concentration of lightweight 'chips', created by decomposition of the branches and leaves of the shrubs in the dune area. One can distinguish them by the dark color in the center of the flank. Fig. 9.4 is a close-up of these chips, which appear in Figs. 6.8 and 9.3. Attention should be paid to the chip concentration in the trough of the ripples and also to the surprising symmetry of the ripples - evidence of the uniform flow from both directions. From the wind data it is clear that the sector where the chips began to be deposited is perpendicular to the direction of the last storm wind. As a result, the winds at that same segment blew alternately from both directions, their velocity abated, the chips (and therefore also the sand which they carried) were deposited and the ripples became symmetrical. This phenomenon resembles the case shown in Figs. 3.8 and 3.9.

The initial linear longitudinal dune is subjected to a gradual rise in the magnitude of the wind deflected along the lee flank as a result of the concentration of the stream lines, as explained in Section 3.6. The rise in wind velocity brings about a gradual increase of erosion of sand on the lee flank. The increasing erosion of the sand causes a "gnawing away" in the linearity of the dune and formation of the first meander at the crest line (Fig. 9.5). The distance from the beginning of the dune to the place where the "gnawing" begins depends upon the wind magnitude at the lee flank, which is also dependent upon the angle between the wind and the crest line. At the place where the first meander is created, the angle between the wind and the crest line is made less acute. After a certain distance, which is related to the reaction time between the change in morphology and the corresponding drop in the wind velocity (Figs. 3.10, 3.11), the erosion stops, the sand deposition starts and the situation returns to the previous stage. Afterwards, the process repeats itself, and actually it forms at the same time the lengthening of the initial longitudinal dune starts.

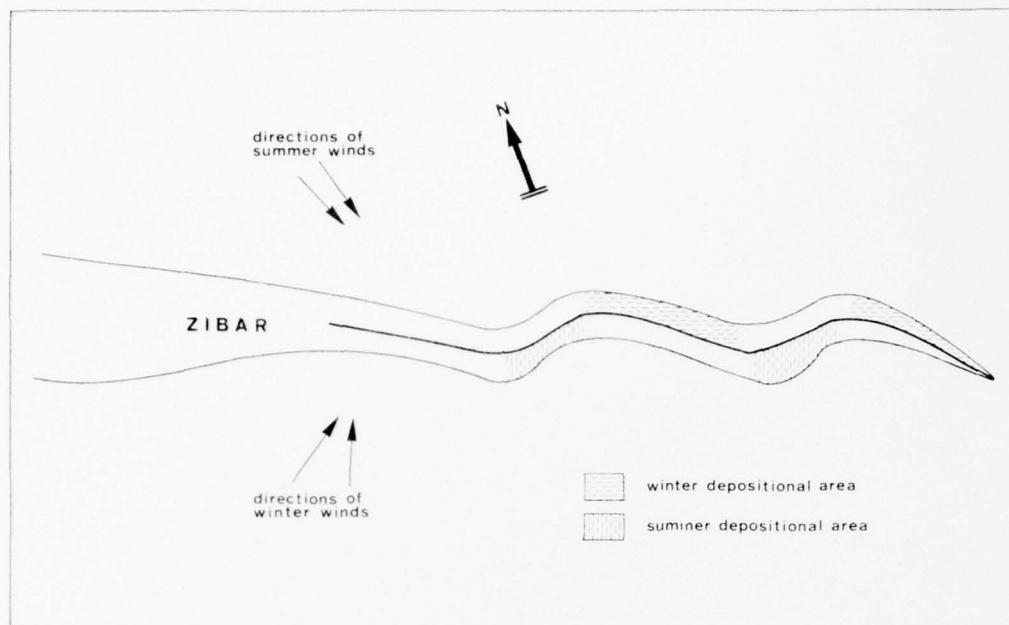


Fig. 9.1 Plan of the longitudinal dune showing the depositional areas in two seasons. All other areas are subjected to erosion.



Fig. 9.2 Erosion along the lee flank by wind blowing at acute angle to the crest line. The erosion is demonstrated by means of laminae exposures.



Fig. 9.3 Concentration of light chips (dark color) on the deflection point (point no. 5).

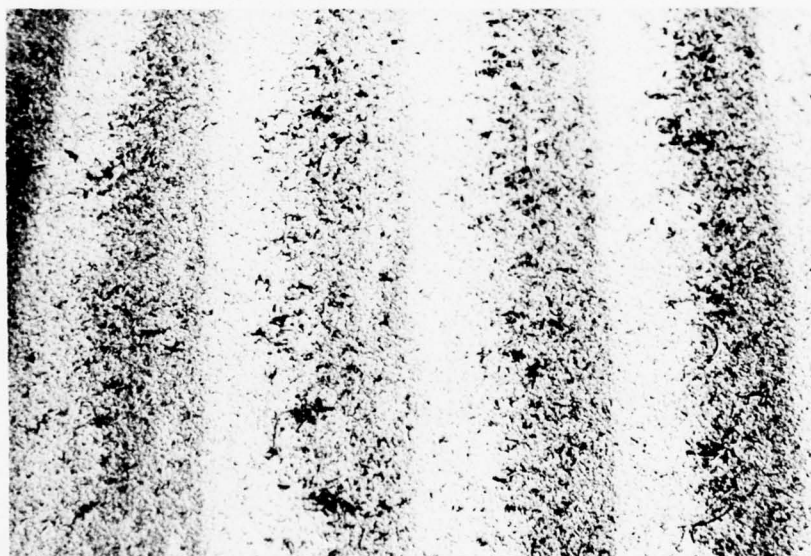


Fig. 9.4 Close-up of the symmetrical ripples and the chips appearing in Fig. 9.3.



To summarize, we see that the rise in wind velocity along the lee flank brings about a morphological response<sup>(85)</sup> of the dune. This is expressed in the continually increasing erosion of the lee flank, which brings about a change in the direction of the crest line. This change checks the acceleration of the wind and lowers its velocity. As a result, erosion stops and deposition begins. The crest line, afterwards, returns to its former state and the entire process begins anew.

The reason for the formation of peaks and saddles along the sinuated dune is related to the fact that there is no uniformity in the velocity and the direction of the winds on both sides of the dune. The summer winds are from the N and NW, with a high degree of constancy, high frequency (winds above the threshold velocity occur daily), and low velocity. In winter, the winds are generally from the S, SW and W, with a low degree of constancy, low frequency, and higher velocity. We have seen (in Chapter Two, Table 2.2) that there is more total work done by the summer winds of high frequency and low magnitude<sup>(86)</sup>. In winter, the rain is often accompanied by storms and the sand movement in these cases is drastically reduced<sup>(2)</sup>. The lee flank in winter is the northern slope, which retains its moisture for a long time, since there is less sun and the slope is shaded. Thus an additional factor makes sand movement difficult during this season.

The lack of uniformity in the effects of the wind on both sides of the dune brings about a lack of uniformity in the rate of erosion and deposition. A model developed to illustrate this phenomenon is presented in Fig. 9.6. In this figure, one can distinguish the sinuated longitudinal dune, where the pair of no. 1 lines marks its parallel limits. The drawing describes the state of the dune (line no. 3) after 2 phases of deposition (symbol no. 4) and erosion (symbol no. 5) on each flank (a total of two years' activity). In order to simplify the schematic model of Fig. 9.6, erosion and deposition are designated on it as taking place on the lee flank only. Not shown is the continuous erosion on the windward flank (especially on the upper part), as can be seen in Figs. 8.6 - 8.9 and 8.11, 8.12. Because of the seasonal changes in wind direction, this erosion occurs almost equally on both sides of the dune; therefore in this case, it may be disregarded. It is shown that in each phase the rate of erosion and deposition on the southern flank is greater than that on the northern flank, because the erosional processes and deposition on the southern flank are related to summer winds, whereas on the northern flank to winter winds. Line no. 2 in Fig. 9.6 marks the limits of the dune after the first phase, and line 3, after the second one. It can be seen that the pair of lines (no. 3) are not parallel (unlike that of the pair of lines no. 1). As a result of the greater deposition on the southern flank in proportion to the lesser erosion on the opposite northern flank, the dune becomes wider in that place. In another segment,



the dune is made narrower as a result of greater erosion on the southern flank and lesser deposition on the opposite northern flank. The wide area in Fig. 9.6 characterizes the sector found between the convex and concave parts facing south. On the surface of the dune, this widening is expressed also in greater height, which forms the peaks along the dune. The part which is made narrower is found between the concave and convex parts facing south and forms the saddles along the dune. In this manner, one can explain the typical morphology of the dune with peaks and saddles, which is characteristic of all meandering longitudinal dunes.

According to the above rule this process should continue and cause a widening of one part of the dune and a narrowing of the other. In practice, the wide part becomes higher and the narrow one lower. Inasmuch as the wide part becomes higher, the sand which reaches there by a longitudinal movement must disperse and be deposited on a wider surface, and the total addition after deposition becomes less per unit area. However, at the lower part, the sand which is deposited disperses on a smaller area, and the total addition, after deposition, is greater per unit area. Finally, the rise in one part and the lowering of the other is checked by the increase and decrease of the depositional area, respectively. The process of lowering on one side and rising on the other continues until the dune reaches dynamic equilibrium, where the additional sand per unit area in the high depositional section equals the additional sand per unit area on the lower depositional section.

The sections of the dune which reach full development and are found in a state of dynamic equilibrium will always be of uniform height, which is the height they reached at the time the dynamic equilibrium was achieved. This is the reason why the peaks of the longitudinal dune in the research area range from 12-14 meters in height, and the saddles, from 5-8 meters (Fig. 1.4). However, only in the central part of the longitudinal dune, where the measurements were taken (Fig. 1.1), are there peaks and saddles of maximum height. This section is found in the center of the dune and it is the earliest segment of the dune, which has already reached dynamic equilibrium. In order to reach this stage, a certain time is necessary for the processes described in Figs. 9.5 and 9.6 to take place. Together with these processes, the dune, on one side - (the end) becomes longer, and the other - (the beginning) the sectors advance, and a new sector is formed from the zibar. As we have seen in Chapter Eight, the advancement rate is greater than the rate of movement of the dune segment. Therefore on the end of the dune there are many segments which are not in dynamic equilibrium, starting from point no. 11 (Fig. 1.1), which has a peak at a height of 7 meters. Point no. 3 at the beginning of the dune is closer to dynamic equilibrium and its height is about 10 meters.

In agreement with the above model, the heights reached by the peaks and saddles of longitudinal dunes found in a state of dynamic equilibrium, are a function of a degree of lack of uniformity between the 2 dominant wind directions. References to this can be found in places where two sets of longitudinal dunes can be found, where each one continues in a different direction<sup>(1)</sup>. In such a case, the relationship between the wind directions on both sides of the dune would be different for each situation. As a result, the heights of the dunes, the length of the sinuated sections and the size of the meanders will be changed from one set to the other.

In this way, we can understand the reason for the formation of the "tear-drop" which characterizes many longitudinal dunes of the world<sup>(7)(39)</sup>. Each "drop" is an asymmetrical section of the dune which begins in the saddle and ends in the next saddle in the direction of the dune trend (Figs. 1.4 and 1.5). In agreement with the process described above (Fig. 9.6), the high point of each sector is found at its end in the direction of the dune end (deflection point) and here there is a structure which resembles a "tear drop" when viewed from the side.

In order to obtain dune meanders in a regular form and at equal distances, a high degree of constancy of wind direction and velocity is necessary. This type of wind regime exists in the summer (sea breeze) and therefore, the meanders of the dune are evident and clearer on the southern flank, which is on the lee flank to the sea breeze winds (Fig. 1.1). The summer wind in fact determines the trend of the dune which is in an angle of  $50^\circ$  with the dominant wind. The meander of the dune lessens this angle to  $20^\circ$ - $30^\circ$ ; this is the optimal impact angle which brings about maximum erosion on the lee flank (see Section 3.6).

The strong and variable winter wind in fact preserves the symmetrical profile which is necessary for the dynamic mechanism of the longitudinal dune. This wind also causes transportation along the dune, together with deposition parallel to the crest line, but the direction of this wind does not have to be at the optimal impact angle.

Therefore, if on the longitudinal dune there appear saddles and peaks, the direction opposite the place where the peak is convex and the saddles concave is the direction from which the uniform dominant wind comes, with a constant direction. In theory, we do not get peaks and saddles only in places where two wind directions and velocities from both sides of the dune are uniform and fixed at an angle between the wind direction and the dune axis.



#### 9.4 Spacing Between the Dunes

The uniform spacing between the parallel belts of the longitudinal dunes is one of the most outstanding phenomena of the characteristics common to the longitudinal dunes of the world's deserts<sup>(14)(19)(31)</sup>.

There are some who see the appearance of the spaces as irregular statistical occurrences<sup>(38)(87)</sup> and others even tried to attribute to it dynamic significance. Hanna<sup>(19)</sup> and Folk<sup>(14)(27)</sup> see the spaces between one dune and the other as related to the diameter of the two helicoidal eddies, which according to them, create the longitudinal dune. Not in every case where the helicoidal eddies are considered as the origin of the dune is it clear whether these determine the size of the spaces or if the size of the eddies are determined by the existing spaces<sup>(25)</sup>. Twidale<sup>(31)</sup> lists several theoretical reasons for the equal spaces, not all of which stand up to the test of reality. The data he presents point to the correlation between the height of the dune and the interdune space.

In the present research, no proof was found that the longitudinal dune is formed by the helicoidal flow or by a uni-directional wind. Since the oblique cross winds are the main factor required for its dynamics and morphology, one must see in them also the reasons for the interdune spaces.

The space between one dune and the other in the research area was from 200-300 meters (Fig. 1.1). This is not the space existing between the zibar belts from which the dune is formed. A glance at the aerial photograph of the research area reveals that "initiations" of longitudinal dunes develop in an irregular form on the surface covered by zibars (Fig. 1.1). However, the full development of the dune exists only in the spaces noted. From this it is possible to deduce that a fully developed longitudinal dune, which reaches a height of 12-15 meters acts as a wind-break for the surfaces found on both sides. In the literature dealing with wind-breaks<sup>(88)(89)</sup>, it is usual to consider the length of the protected area as 12-15 times the height of the wind-break (including wind-breaks built of earthen banks). This size fits the interdune spaces existing in the research area and also the spacing data which Twidale<sup>(31)</sup> found in the Simpson desert of Australia. Therefore it is possible to assume that the dune height determines the size of the space between one dune and the other.

The spaces begin to be determined from the initial developed longitudinal dune, which does not permit other longitudinal dunes to develop in a space less than 12-15 times its height. The next developed dune will therefore develop at a distance of 12-15 times of the height and therefore the uniform space will spread out laterally on the sand field.

Fig. 1.1 permits us to see that in places where the dune reaches full development, the spaces are 200-250 meters in size. In the southern part of the photo (Fig. 1.1) in the place where the dunes do not reach the final development stage (dynamic equilibrium), the spaces reach about 150 meters. After one of the dunes there reaches its maximum height, an additional dune will develop at a distance of 200-250 meters, and the dune existing today at a distance of 150 meters will then decline and disappear. Evidence of this process is given in several signs which can be found in Fig. 1.1.

#### 9.5 Dynamic Implications of the Distribution of Longitudinal Dunes in Deserts

The longitudinal dunes and other dune types in the world have similar profiles - i.e., mega-dunes (draa) are the most widespread forms in the great sand desert of the world (Sahara, Arabia, Australia).

The longitudinal dunes are not the creation of the initial response of the sand to the wind. The first forms of the initial contact are barchans, transverse dunes, parabolic dunes, foredunes and zibars. The longitudinal dunes develop from these initial aeolian bedforms, mostly from zibars, barchans, and transverse dunes.

Longitudinal dunes are formed and developed only in cases where the bulk of the sand piles up with a sharp profile - which is the one capable of elongation in response to oblique winds, through processes described in the preceding chapters. The initial contact between the wind and the sand, forms rounded sand piles which in deserts turn into barchans or transverse dunes<sup>(7)</sup>, and into parabolic dunes in more humid places. In places where the sand is not sorted, we get the zibar. A longitudinal dune will be formed only after these aeolian forms are developed, at a later stage.

In the case where the development of the longitudinal dune is from the zibar, we saw in Section 9.2 and in Figs. 1.1 and 1.3 that after the zibar has lengthened and the wind winnowed the fine sand from it, a longitudinal dune begins to be formed at its end, as a secondary product. In cases where the longitudinal dunes develop from transverse dunes or barchans, their development is dependent on the crescent-like structure of the barchan and the transverse dune, whose horns have a sharp profile, able to elongate under dynamic processes into longitudinal dunes.

When a longitudinal dune is formed from a barchan or a transverse dune, we have in one system two aeolian bedforms, each of which has a different movement mechanism. The volume of the transverse dune (or barchan) advances by means of erosion on the windward flanks and its deposition, through slides and avalanching, on the slip face. Therefore

the movement rate of the transverse dune is found in a direct relation to the wind and in reverse relation to its height<sup>(7)</sup>. The longitudinal dune does not advance, but elongates, its elongation dependent only on the wind velocity and the angle that the wind makes with the crest line. From the dynamic point of view, the longitudinal dune has an advantage over the transverse in that any wind direction from a sector of  $180^\circ$ , whose center is at the beginning of the dune, brings about its elongation. On the contrary, in transverse dunes, only winds whose direction coincides with the direction of the dune movement can bring about an optimal advance rate. Cross winds cause most of the morphological changes and considerable abatement in the advance rate<sup>(2)</sup>. Therefore one can say that the longitudinal dune "utilizes" winds from all directions much better and elongates in any wind direction at all.

When a transverse dune receives a considerable addition of sand, it becomes higher and the advance rate is correspondingly smaller. The longitudinal dune, on the contrary, does not become higher as a result of additional sand; it only elongates.

The result of the above process is that the longitudinal dune, after its formation, (from a transverse dune or barchan) elongates faster than the advance rate of the part of the transverse dune connected to it. Therefore, if a barchan field or transverse dunes begin to develop longitudinal dunes, it is because of the faster relative elongation rate of the longitudinal dunes; their dominance in the sand dune fields will be only a question of time. From this, we understand that dominance of the transverse dunes in coastal areas comes about because they are younger. Goldsmith<sup>(90)</sup> is certain that coastal dunes of the world are only from 3000 to 4000 years old, since the end of the last rapid rise in sea level. In the deserts, on the contrary, the age of the dunes can be and is greater, and the longitudinal dunes are thus widespread.

#### LITERATURE CITED

- (1) Cooke, R.U., and Warren, A., "Geomorphology in Deserts", Batsford, London, 1973, 394 pp.
- (2) Tsoar, H., "Desert dunes morphology and dynamics, El-Arish (Northern Sinai)", Zeit. Geom. Suppl., Vol. 20, 1974, pp. 41-61-
- (3) McKee, E.D., and Breed, C.S., "Sand seas of the world", U.S. Geological Survey, Prof. paper, Vol. 929, 1976, pp. 81-88.
- (4) Jordan, W.M., "Prevalence of sand-dune types in the Sahara Desert", Geol. Soc. Am. Spec. Pap., Vol. 82, 1964, pp. 104-105.
- (5) Bagnold, R.A., "Sand formation in south Arabia", Geog. Jour., Vol. 117, 195 , pp. 77-86.
- (6) Mabbutt, J.A., "Aeolian landforms in Central Australia", Australian Geog. Studies, Vol. 6, 1968, pp. 139-150.
- (7) Bagnold, R.A., "The physics of blown sand and desert dunes", 2nd ed., Methuen, London, 1954, 265 pp.
- (8) Inman, D.L., Ewing, G.C., and Corliss, J.B., "Coastal sand dunes of Guerrero Negro, Baja, California, Mexico", Geol. Soc. Am. Bull., Vol. 77, 1966, pp. 787-802.
- (9) Cooper, W.S., "Coastal sand dunes of Oregon and Washington", Geol. Soc. Am. Mem., Vol. 72, 1958, 169 pp.
- (10) Aufrère, L., "L'orientation des dunes continentales", Proc. 12th Int. Geog. Cong., Cambridge, 1928, pp. 220-231.
- (11) King, D., "The sand ridge deserts of South Australia and related aeolian landforms of the Quaternary arid cycles", Trans. Roy. Soc. S. Australia, Vol. 83, 1960, pp. 99-108.
- (12) Melton, F.A., "A tentative classification of sand dunes and its application to dune history in the Southern High Plains", Jour. Geol., Vol. 48, 1940, pp. 113-174.
- (13) Verstappen, H.Th., "On the origin of longitudinal (seif) dunes", Zeit. Geom., N.F., Vol. 12, 1968, pp. 200-220.
- (14) Folk, R.L., "Longitudinal dunes of the northwestern edge of the Simpson Desert, Northern Territory, Australia. I. Geomorphology and grain size relationships", Sedimentology, Vol. 16, 1971a, pp. 5-54.
- (15) Mabbutt, J.A., and Sullivan, M.E., "The formation of longitudinal dunes: evidence from the Simpson Desert", Aust. Geographer, Vol. 10, 1968, pp. 483-487.



- (16) Wopfner, H., and Twidale, C.R., "Geomorphological history of the Lake Eyre basin", in J.N. Jennings and J.A. Mabbutt (eds.): Landform Studies from Australia and New Guinea, ANU Press, Canberra, 1967, pp. 118-143.
- (17) McKee, E.D., and Tibbitts, G.C., "Primary structures of a seif dune and associated deposits in Libya", Jour. Sed. Petrol., Vol. 34, 1964, pp. 5-17.
- (18) Smith, H.T.U., "Nebraska dunes compared with those of North Africa and other regions", in: Loess and related eolian deposits of the world, ed. by C.B. Schultz and J.C. Frye, Proceedings 7th Congress International Association for Quaternary Research, Vol. 12, 1968, pp. 29-47.
- (19) Hanna, S.R., "The formation of longitudinal sand dunes by large helical eddies in the atmosphere", Jour. Appl. Meteorology, Vol. 8, 1969, pp. 874-883.
- (20) Wilson, I.G., "Journey across the Grand Erg Oriental", Geog. Mag., Vol. 43, 1971a, pp. 264-270.
- (21) Wilson, I.G., "Aeolian bedforms - their development and origins", Sedimentology, Vol. 19, 1972a, pp. 173-210.
- (22) Warren, A., "Desert dunes", in: The study of desert geomorphology: Peel, R.F., Cooke, R.U., and Warren, A., Geography, Vol. 59, 1974, pp. 127-133.
- (23) Bagnold, R.A., "The surface movement of blown sand in relation to meteorology", Desert Research, Int. Sym. Res. Coun. of Isr. and UNESCO, Spec. Pub., Vol. 2, 1953, pp. 89-96.
- (24) Angell, J.K., Pack, D.H., and Dickson, C.R., "A lagrangian study of helical circulations in the planetary boundary layer", Jour. Atmos. Sci., Vol. 25, 1968, pp. 707-717.
- (25) Glennie, K.W., "Desert sedimentary environment", Development in sedimentology 14, Elsevier Pub. Comp., 1970, 222 pp.
- (26) Mabbutt, J.A., Wooding, B.A., and Jennings, J.N., "The asymmetry of Australian desert sand ridges", Aust. Jour. Sci., Vol. 32, 1969, pp. 159-160.
- (27) Folk, R.L., "Genesis of longitudinal and oghurd dunes elucidated by rolling upon grease", Geol. Soc. Am. Bull., Vol. 82, 1971b, pp. 3461-3468.
- (28) Folk, R.L., "Rollers and ripples in sand, streams and sky; rhythmic alteration of transverse and longitudinal vortices in three orders", Sedimentology, Vol. 23, 1976, pp. 649-669.
- (29) Allen, J.R.L., "Current Ripples", North Holland Amsterdam, 1968, 433 pp.

- (30) Wilson, I.G., "Universal discontinuities in bedforms produced by the wind", Jour. Sed. Petrol., Vol. 42, 1972b, pp. 667-669.
- (31) Twidale, C.R., "Evolution of sand dunes in the Simpson Desert, Central Australia", Trans. Inst. Brit. Geog., Vol. 56, 1972, pp. 77-106.
- (32) Bagnold, R.A., "Journeys in the Libyan Desert", 1929-1930, Geog. Jour., Vol. 78, 1931, pp. 13-39, 524-533.
- (33) Bagnold R.A., "A further journey in the Libyan Desert", Geog. Jour., Vol. 82, 1933, pp. 103-129, 211-235.
- (34) Cutts, J.A., and Smith, R.S.U., "Eolian deposits and dunes on Mars", Jour. Geophys. Res., Vol. 78, 1973, pp. 4139-4154.
- (35) McCauley, J.F., "Mariner 9 evidence for wind erosion in the equatorial and mid-latitude regions of Mars", Jour. Geophys. Res., Vol. 78, 1973, pp. 4123-4137.
- (36) Fink, D.F., "Search for Viking landing site continued", Aviation Week & Space Technology, Vol. 105, 1976, pp. 20-23.
- (37) Peel, R.F., "The landscape in aridity", Trans. Inst. Brit. Geog., Vol. 38, 1966, pp. 1-23.
- (38) Madigan, C.T., "The Australian sand-ridge deserts", Geog. Rev., Vol. 26, 1936, pp. 205-227.
- (39) Madigan, C.T., "Simpson Desert expedition 1939, scientific reports: No. 6, Geology - the sand formation", Trans. Roy. Soc. S. Australia, Vol. 70, 1946, pp. 45-63.
- (40) Holm, D.A., "Desert geomorphology in the Arabian Peninsula", Science, Vol. 132, 1960, pp. 1369-1379.
- (41) Warren, A., "Observation on dunes and bimodal sands in the Ténéré Desert", Sedimentology, Vol. 19, 1972, pp. 37-44.
- (42) Mainguet, M., Callot, Y. et Guy, M., "Taxonomic classification of dunes in Fachi-Bilma erg, diagnosis of wind direction", Rev. Photo Interprétation, Vol. 74-1 et 74-2, 1974.
- (43) Murray, B.C., "Mars from Mariner 9", Scientific American, Vol. 228, 1973, pp. 49-69.
- (44) Wilson, I.G., "Ergs", Sedimentary Geol., Vol. 10, 1973, pp. 77-106.
- (45) Folk, R.L., "Bimodal supermature sandstone: product of the desert floor", 23rd Int. Geol. Cong., Vol. 8, 1968, pp. 9-32.
- (46) Brooks, C.E.P., and Carruthers, N., "Handbook of statistical Methods in Meteorology", Air Ministry Meteorological Office, M.O. 538, London, 1953, 412 pp.
- (47) Chepil, W.S., "Dynamics of wind erosion, I: Nature of movement of soil by wind", Soil Sci., Vol. 60, 1945, pp. 305-320, 397-411.

- (48) Hsu, S.A., "Computing eolian sand transport from routine weather data", Proc. 14th Conf. Coastal Eng., 1974, pp. 1619-1626.
- (49) Allen, J.R.L., "Physical Processes of Sedimentation", Unwin University books, London, 1970, 248 pp.
- (50) Sharp, R.P., "Kelso Dunes, Mojave Desert, California", Geol. Soc. Am. Bull., Vol. 77, 1966, pp. 1045-1073.
- (51) Fritschen, L.J., and Hinshaw, R., "A Reed Switch anemometer", Jour. Appl. Meteorology, Vol. 11, 1972, pp. 742-744.
- (52) Bradley, E.F., "A small sensitive anemometer system for agricultural meteorology", Agricultural Meteorology, Vol. 6, 1969, pp. 185-193.
- (53) Svasek, J.N., and Terwindt, J.H.J., "Measurements of sand transport by wind on a natural beach", Sedimentology, Vol. 21, 1974, pp. 311-322.
- (54) Raudkivi, A.J., "Study of sediment ripple formation", Proc. ASCE Jour. Hydraulics Div., Vol. 89(HY6), 1963, pp. 15-33.
- (55) Cornish, V., "Waves of sand and snow", T.F. Unwin, London, 1914, 383 pp.
- (56) King, W.J.H., "Study of a dune belt", Geog. Jour., Vol. 51, 1918, pp. 16-33.
- (57) Landsberg, H., "The structure of the wind over a sand-dune", Am. Geophys. Un. Trans., Vol. 23, 1942, pp. 237-239.
- (58) Bagnold, R.A., "The transport of sand by wind", Geog. Jour., Vol. 89, 1937, pp. 409-438.
- (59) Hoyt, J.H., "Air and sand movement to the lee of dunes", Sedimentology, Vol. 7, 1966, pp. 137-143.
- (60) Mason, C.C., and Folk, R.L., "Differentiation of beach, dune and eolian flat environments by six analysis, Mustang Island, Texas", Jour. Sed. Petrol., Vol. 28, 1958, 211-226.
- (61) Shepard, F.P., and Young, R., "Distinguishing between beach and dune sands", Jour. Sed. Petrol., Vol. 31, 1961, pp. 196-214.
- (62) Sharp, R.P., "Wind ripples", Jour. Geol., Vol. 71, 1963, pp. 617-636.
- (63) Erlich, R., "The role of the homogeneous unit in sampling plans for sediments", Jour. Sed. Petrol., Vol. 34, 1964, pp. 437-439.
- (64) Tsoar, H., "Specific sampling of ripples and microfeatures on desert dunes", 9th International Congress of Sedimentology, Nice 75, Vol. 3, 1975, pp. 101-105.
- (65) McBride, E.F., "Mathematical treatment of size distribution data", in R.E. Carver (ed.) Procedures in Sedimentary Petrology, Wiley Interscience N.Y., 1971, pp. 109-127.

- (66) Mabesoone, J.N., "origin and age of the sandstone reefs of Pernambuco (Northeastern Brazil)", Jour. Sed. Petrol., Vol. 34, 1964, pp. 715-726.
- (67) Hails, J.R., "Significance of statistical parameters for distinguishing sedimentary environment in New-South Wales, Australia", Jour. Sed. Petrol., Vol. 37, 1967, pp. 1059-1069.
- (68) Tsoar, H., "Characterization of sand dune environment by their grain-size, mineralogy and surface texture", Geography in Israel, A collection of papers offered to the 23rd International Geographical Congress, U.S.S.R., July-August 1976, Israel National Committee, I.G.U., Jerusalem, 1976, pp. 327-343.
- (69) Nie, N.H., Hull, C.H., Jenkins, J.G., Steinbrenner, K., and Bent, D.H., "Statistical package for the social science", McGraw-Hill, N.Y., 2nd ed., 1975, 675 pp.
- (70) Daune, D.B., "Significance of skewness in recent sediments, Western Pamlico Sound, North Carolina", Jour. Sed. Petrol., Vol. 34, 1964, pp. 864-874.
- (71) Pettijohn, F.J., Potter, P.E., and Siever, R., "Sand and sandstone", Springer-Verlag, Berlin, 1972, 618 pp.
- (72) Kennedy, V.C., and Kouba, D.L., "Fluorescent sand as a tracer of fluvial sediments", U.S. Geol. Sur. Prof. Pap., Vol. 562E, 1970, pp. E1-E13.
- (73) Ingle, J.C., Jr., "The movement of beach sand", Development in Sedimentology, Vol. 5, Elsevier Amsterdam, 1966, 221 pp.
- (74) Yasso, W.E., "Formulation and use of fluorescent tracer coating in sediment transport studies", Sedimentology, Vol. 6, 1966, pp. 287-301.
- (75) Inman, D.L., and Chamberlain, T.K., "tracing beach sand movement with irradiated quartz", Jour. Geophy. Res., Vol. 64, 1959, pp. 41-47.
- (76) Yaalon, D.H., and Laronne, J., "Internal structures in eolianites and paleowinds, Mediterranean Coast, Israel", Jour. Sed. Petrol., Vol. 41, 1971, pp. 1059-1064.
- (77) Bigarella, J.J., "Eolian environments - their characteristics, recognition and importance", In: Recognition of Ancient Sedimentary Environments, ed. by J.K. Rigby and W.K. Hamblin; Soc. Econ. Paleont. Mineralog., Spec. Pub., Vol. 16, 1972, pp. 12-62.
- (78) McKee, E.D., "Structures of dunes at White Sands National Monument, New Mexico (and a comparison with structures of dunes from other selected areas)", Sedimentology, Vol. 7, 1966, pp. 3-69.
- (79) Yasso, W.E., and Hartman, E.M., "Rapid field technique using spray adhesive to obtain peels of unconsolidated sediment", Sedimentology, Vol. 19, 1972, pp. 295-298.



- (80) Gorycki, M.A., "Sheetflood structure: mechanism of beach cusp formation and related phenomena", Jour. Geol., Vol. 81, 1973, pp. 109-117.
- (81) Wilson, I.G., "Desert sandflow basins and a model for the development of ergs", Geog. Jour., Vol. 137, 1971b, pp. 180-199.
- (82) Kerr, R.C., and Nigra, J.O., "Eolian sand control", Am. Assoc. Pet. Geol. Bull., Vol. 36, 1952, pp. 1541-1573.
- (83) Clos-Arceuduc, A., "Essai d'explication des formes dunaires sahariennes", Etudes Des Photo-Interpretation, I.G.N., 1969, 63 pp.
- (84) Clos-Arceuduc, A., "How a group of silks changes direction immediately after being formed", Rev. Photo-Interpretation, Vol. 73-1, 1973.
- (85) Allen, J.R.L., "Reaction, relaxation and lag in natural sedimentary systems: general principles, examples and lessons", Earth-Sci. Rev., Vol. 10, 1974, pp. 263-342.
- (86) Wolman, M.G., and Miller, J.P., "Magnitude and frequency of forces in geomorphic processes", Jour. Geol., Vol. 68, 1960, pp. 54-74.
- (87) Goudie, A., "Statistical laws and dune ridges in Southern Africa", Geog. Jour., Vol. 135, 1969, pp. 404-406.
- (88) Chepil, W.S., and Woodruff, N.P., "The physics of wind erosion and its control", Advances in Agronomy, Vol. 15, 1963, pp. 211-302.
- (89) Woodruff, N.P., Lyles, L., Siddoway, F.H., and Fryrear, D.W., "How to control wind erosion", Agriculture Information Bull., U.S.D.A., Washington D.C., No. 354, 1972, 22 pp.
- (90) Goldsmith, V., "Eolian sedimentation in coastal areas", Virginia Institute of Marine Science, contribution no. 533, 1975, 138 pp.

Appendix 1: Frequency table of wind direction and velocity (percentage) for the period: 1973, 1974.

FREQUENCIES TABLE IN PERCENTAGE NUMBERS

W/SEC DIRECT	0-6	6-8	8-10	10-12	12-14	14-16	>16	TOTAL
0-10	2.1	1.1	0.1	0.1	0.1	0.1	0.1	3.1
10-20	2.1	1.1	0.1	0.1	0.1	0.1	0.1	3.1
20-30	1.1	0.1	0.1	0.1	0.1	0.1	0.1	2.1
30-40	1.1	0.1	0.1	0.1	0.1	0.1	0.1	1.1
40-50	1.1	0.1	0.1	0.1	0.1	0.1	0.1	1.1
50-60	1.1	0.1	0.1	0.1	0.1	0.1	0.1	1.1
60-70	1.1	0.1	0.1	0.1	0.1	0.1	0.1	1.1
70-80	1.1	0.1	0.1	0.1	0.1	0.1	0.1	1.1
80-90	1.1	0.1	0.1	0.1	0.1	0.1	0.1	1.1
90-100	1.1	0.1	0.1	0.1	0.1	0.1	0.1	1.1
100-110	1.1	0.1	0.1	0.1	0.1	0.1	0.1	1.1
110-120	2.1	0.1	0.1	0.1	0.1	0.1	0.1	2.1
120-130	2.1	0.1	0.1	0.1	0.1	0.1	0.1	2.1
130-140	2.1	0.1	0.1	0.1	0.1	0.1	0.1	2.1
140-150	2.1	0.1	0.1	0.1	0.1	0.1	0.1	2.1
150-160	3.1	0.1	0.1	0.1	0.1	0.1	0.1	3.1
160-170	3.1	0.1	0.1	0.1	0.1	0.1	0.1	4.1
170-180	4.1	1.1	0.1	0.1	0.1	0.1	0.1	5.1
180-190	3.1	0.1	0.1	0.1	0.1	0.1	0.1	4.1
190-200	3.1	0.1	1.1	0.1	0.1	0.1	0.1	4.1
200-210	3.1	1.1	0.1	0.1	0.1	0.1	0.1	4.1
210-220	3.1	1.1	0.1	0.1	0.1	0.1	0.1	4.1
220-230	3.1	0.1	0.1	0.1	0.1	0.1	0.1	3.1
230-240	3.1	0.1	0.1	0.1	1.1	0.1	0.1	4.1
240-250	2.1	0.1	0.1	0.1	0.1	0.1	0.1	2.1
250-260	2.1	0.1	0.1	0.1	0.1	0.1	0.1	3.1
260-270	2.1	0.1	0.1	0.1	0.1	0.1	0.1	2.1
270-280	2.1	0.1	0.1	0.1	0.1	0.1	0.1	2.1
280-290	2.1	0.1	0.1	0.1	0.1	0.1	0.1	2.1
290-300	2.1	0.1	0.1	0.1	0.1	0.1	0.1	2.1
300-310	2.1	0.1	0.1	0.1	0.1	0.1	0.1	2.1
310-320	2.1	0.1	0.1	0.1	0.1	0.1	0.1	2.1
320-330	2.1	1.1	0.1	0.1	0.1	0.1	0.1	3.1
330-340	3.1	3.1	1.1	0.1	0.1	0.1	0.1	7.1
340-350	3.1	5.1	2.1	0.1	0.1	0.1	0.1	10.1
350-360	2.1	1.1	1.1	0.1	0.1	0.1	0.1	4.1
TOTAL	74.1	17.1	6.1	1.1	1.1	0.1	0.1	100.1

# Appendix 1 (cont.)

TOTAL CASES = 17520  
MISSING CASES = 2141. IN PERCENTAGE NUMBER = 12.2  
TOTAL VALID CASES = 15379.  
TOTAL CASES OVER 5 M/SEC = 4063. IN PERCENT NUMBER OVER VALID CASES = 26.4  
VECTOR MEAN WIND VELOCITY = 3.6  
VECTOR MEAN WIND DIRECTION = 314.  
CONSTANCY STAGE IN PERCENTAGE = 45.3

## TABLES OF EFFECTIVE WIND EQUIVALENT 6 M/SEC

DEGREE	I	0-10	I	10-20	I	20-30	I	30-40	I	40-50	I	50-60	I	60-70	I	70-80	I	80-90	I	90-100	I	100-110	I	110-120	I
ABSOLUTE	I	457.53	I	231.10	I	57.49	I	9.03	I	5.36	I	3.71	I	29.35	I	15.55	I	11.17	I	15.46	I	0.00	I	3.15	I
PERCENT.	I	4.14	I	2.09	I	.52	I	.08	I	.05	I	.03	I	.27	I	.14	I	.10	I	.14	I	0.00	I	.03	I

DEGREE	I	120-130	I	130-140	I	140-150	I	150-160	I	160-170	I	170-180	I	180-190	I	190-200	I	200-210	I	210-220	I	220-230	I	230-240	I
ABSOLUTE	I	0.00	I	2.65	I	4.24	I	16.08	I	161.75	I	453.05	I	539.16	I	1170.14	I	223.33	I	473.07	I	299.60	I	930.47	I
PERCENT.	I	0.00	I	.02	I	.04	I	.15	I	1.46	I	4.11	I	4.00	I	10.67	I	2.02	I	4.20	I	2.71	I	8.50	I

DEGREE	I	240-250	I	250-260	I	260-270	I	270-280	I	280-290	I	290-300	I	300-310	I	310-320	I	320-330	I	330-340	I	340-350	I	350-360	I
ABSOLUTE	I	162.53	I	663.07	I	69.91	I	197.54	I	133.00	I	155.36	I	86.46	I	277.04	I	443.77	I	1853.67	I	1966.66	I	711.04	I
PERCENT.	I	1.47	I	6.01	I	.63	I	1.70	I	1.20	I	1.41	I	.70	I	2.52	I	4.02	I	9.54	I	17.01	I	6.45	I

TOTAL

ABSOLUTE 11041.78

PERCENT. 100.00

Appendix 2: Frequency table of wind direction and velocity (percentage) for the period: Winter 1972/73; 1973/74.

FREQUENCIES TABLE IN PERCENTAGE NUMBERS

M/SEC DIRECT	0-6	6-8	8-10	10-12	12-14	14-16	>16	TOTAL
0-10	1.1	0.1	0.1	0.1	0.1	0.1	0.1	2.1
10-20	1.1	0.1	0.1	0.1	0.1	0.1	0.1	1.1
20-30	1.1	0.1	0.1	0.1	0.1	0.1	0.1	1.1
30-40	1.1	0.1	0.1	0.1	0.1	0.1	0.1	1.1
40-50	1.1	0.1	0.1	0.1	0.1	0.1	0.1	1.1
50-60	1.1	0.1	0.1	0.1	0.1	0.1	0.1	1.1
60-70	1.1	0.1	0.1	0.1	0.1	0.1	0.1	1.1
70-80	2.1	0.1	0.1	0.1	0.1	0.1	0.1	2.1
80-90	1.1	0.1	0.1	0.1	0.1	0.1	0.1	1.1
90-100	2.1	0.1	0.1	0.1	0.1	0.1	0.1	2.1
100-110	4.1	0.1	0.1	0.1	0.1	0.1	0.1	4.1
110-120	4.1	0.1	0.1	0.1	0.1	0.1	0.1	4.1
120-130	3.1	0.1	0.1	0.1	0.1	0.1	0.1	3.1
130-140	3.1	0.1	0.1	0.1	0.1	0.1	0.1	3.1
140-150	3.1	0.1	0.1	0.1	0.1	0.1	0.1	3.1
150-160	5.1	0.1	0.1	0.1	0.1	0.1	0.1	5.1
160-170	4.1	0.1	1.1	0.1	0.1	0.1	0.1	5.1
170-180	4.1	2.1	1.1	0.1	0.1	0.1	0.1	7.1
180-190	3.1	0.1	1.1	0.1	0.1	0.1	0.1	4.1
190-200	3.1	1.1	1.1	0.1	1.1	0.1	0.1	7.1
200-210	3.1	2.1	0.1	0.1	0.1	0.1	0.1	5.1
210-220	3.1	2.1	0.1	0.1	0.1	0.1	0.1	5.1
220-230	2.1	1.1	0.1	0.1	0.1	0.1	0.1	3.1
230-240	2.1	0.1	0.1	0.1	1.1	0.1	0.1	4.1
240-250	2.1	0.1	0.1	0.1	0.1	0.1	0.1	2.1
250-260	1.1	0.1	1.1	1.1	0.1	0.1	0.1	4.1
260-270	2.1	0.1	0.1	0.1	0.1	0.1	0.1	2.1
270-280	1.1	0.1	0.1	0.1	0.1	0.1	0.1	2.1
280-290	1.1	0.1	0.1	0.1	0.1	0.1	0.1	1.1
290-300	2.1	0.1	0.1	0.1	0.1	0.1	0.1	2.1
300-310	1.1	0.1	0.1	0.1	0.1	0.1	0.1	2.1
310-320	1.1	0.1	0.1	0.1	0.1	0.1	0.1	2.1
320-330	1.1	0.1	0.1	0.1	0.1	0.1	0.1	1.1
330-340	2.1	1.1	0.1	0.1	0.1	0.1	0.1	3.1
340-350	1.1	2.1	0.1	0.1	0.1	0.1	0.1	3.1
350-360	1.1	0.1	0.1	0.1	0.1	0.1	0.1	1.1
TOTAL	74.1	14.1	6.1	2.1	3.1	1.1	0.1	100.1



# Appendix 2 (cont.)

TOTAL CASES = 7560  
MISSING CASES = 1136, IN PERCENTAGE NUMBER = 15.0  
TOTAL VALID CASES = 6424  
TOTAL CASES OVER 6 M/SEC = 1685, IN PERCENT NUMBERS OVER VALID CASES = 26.2  
VECTOR MEAN WIND VELOCITY = 4.9  
VECTOR MEAN WIND DIRECTION = 226  
COSTANCY STAGE IN PERCENTAGE = 56.7

## TABLES OF EFFECTIVE WIND EQUIVALENT 6 M/SEC

DEGREE	I 0-10	I 10-20	I 20-30	I 30-40	I 40-50	I 50-60	I 60-70	I 70-80	I 80-90	I 90-100	I 100-110	I 110-120
ABSOLUTE	I 122.09	I 21.60	I 5.43	I 5.94	I 7.33	I 2.26	I 22.51	I 16.60	I 11.17	I 10.05	I 0.00	I 0.00
PERCENT	I 2.05	I .40	I .09	I .10	I .12	I .04	I .36	I .26	I .19	I .18	I 0.00	I 0.00

DEGREE	I 120-130	I 130-140	I 140-150	I 150-160	I 160-170	I 170-180	I 180-190	I 190-200	I 200-210	I 210-220	I 220-230	I 230-240
ABSOLUTE	I 0.00	I 0.00	I 4.24	I 14.62	I 157.09	I 143.33	I 49.42	I 1269.71	I 265.95	I 455.42	I 246.07	I 883.65
PERCENT	I 0.00	I 0.00	I .07	I .25	I 2.64	I 5.77	I 8.31	I 21.34	I 4.47	I 7.66	I 4.10	I 14.86

DEGREE	I 240-250	I 250-260	I 260-270	I 270-280	I 280-290	I 290-300	I 300-310	I 310-320	I 320-330	I 330-340	I 340-350	I 350-360
ABSOLUTE	I 147.71	I 650.01	I 16.92	I 123.75	I 74.91	I 69.56	I 13.75	I 43.69	I 40.35	I 76.81	I 205.32	I 75.32
PERCENT	I 2.48	I 11.07	I .24	I 2.08	I 1.26	I 1.17	I .23	I 1.41	I .68	I 1.29	I 3.45	I 1.27

TOTAL

ABSOLUTE 5346.57

PERCENT 100.00

Appendix 3: Frequency table of wind direction and velocity (percentage) for the period: Summer 1973, 1974, 1975.

FREQUENCIES TABLE IN PERCENTAGE NUMBERS

M/SEC DIRECTION	0-6	6-8	8-10	10-12	12-14	14-16	>16	TOTAL
0-10	2.1	1.1	0.1	0.1	0.1	0.1	0.1	4.1
10-20	2.1	0.1	0.1	0.1	0.1	0.1	0.1	2.1
20-30	1.1	0.1	0.1	0.1	0.1	0.1	0.1	1.1
30-40	1.1	0.1	0.1	0.1	0.1	0.1	0.1	1.1
40-50	1.1	0.1	0.1	0.1	0.1	0.1	0.1	1.1
50-60	0.1	0.1	0.1	0.1	0.1	0.1	0.1	0.1
60-70	0.1	0.1	0.1	0.1	0.1	0.1	0.1	0.1
70-80	0.1	0.1	0.1	0.1	0.1	0.1	0.1	0.1
80-90	0.1	0.1	0.1	0.1	0.1	0.1	0.1	0.1
90-100	0.1	0.1	0.1	0.1	0.1	0.1	0.1	0.1
100-110	0.1	0.1	0.1	0.1	0.1	0.1	0.1	0.1
110-120	0.1	0.1	0.1	0.1	0.1	0.1	0.1	0.1
120-130	0.1	0.1	0.1	0.1	0.1	0.1	0.1	0.1
130-140	1.1	0.1	0.1	0.1	0.1	0.1	0.1	1.1
140-150	1.1	0.1	0.1	0.1	0.1	0.1	0.1	1.1
150-160	2.1	0.1	0.1	0.1	0.1	0.1	0.1	2.1
160-170	2.1	0.1	0.1	0.1	0.1	0.1	0.1	2.1
170-180	3.1	0.1	0.1	0.1	0.1	0.1	0.1	3.1
180-190	3.1	0.1	0.1	0.1	0.1	0.1	0.1	3.1
190-200	3.1	0.1	0.1	0.1	0.1	0.1	0.1	3.1
200-210	4.1	0.1	0.1	0.1	0.1	0.1	0.1	4.1
210-220	4.1	0.1	0.1	0.1	0.1	0.1	0.1	5.1
220-230	4.1	0.1	0.1	0.1	0.1	0.1	0.1	4.1
230-240	4.1	0.1	0.1	0.1	0.1	0.1	0.1	4.1
240-250	4.1	0.1	0.1	0.1	0.1	0.1	0.1	4.1
250-260	3.1	0.1	0.1	0.1	0.1	0.1	0.1	3.1
260-270	2.1	0.1	0.1	0.1	0.1	0.1	0.1	2.1
270-280	2.1	0.1	0.1	0.1	0.1	0.1	0.1	2.1
280-290	2.1	0.1	0.1	0.1	0.1	0.1	0.1	2.1
290-300	3.1	0.1	0.1	0.1	0.1	0.1	0.1	3.1
300-310	3.1	0.1	0.1	0.1	0.1	0.1	0.1	3.1
310-320	2.1	0.1	0.1	0.1	0.1	0.1	0.1	3.1
320-330	2.1	2.1	1.1	0.1	0.1	0.1	0.1	6.1
330-340	3.1	6.1	1.1	0.1	0.1	0.1	0.1	11.1
340-350	3.1	6.1	3.1	0.1	0.1	0.1	0.1	12.1
350-360	1.1	2.1	1.1	0.1	0.1	0.1	0.1	6.1
TOTAL	74.1	19.1	6.1	0.1	0.1	0.1	0.1	100.1

# Appendix 3 (cont.).

TOTAL CASES = 6192  
MISSING CASES = 753. IN PERCENTAGE NUMBER = 4.1  
TOTAL VALID CASES = 5939.  
TOTAL CASES OVER 6 M/SEC = 1539. IN PERCENT NUMBERS OVER VALID CASES = 25.9  
VECTOR MEAN WIND VELOCITY = 7.9  
VECTOR MEAN WIND DIRECTION = 342.  
COSTANCY STAGE IN PERCENTAGE = 91.8

## TABLES OF EFFECTIVE WIND EQUIVALENT 6 M/SEC

DEGREE	I	0-10	I	10-20	I	20-30	I	30-40	I	40-50	I	50-60	I	60-70	I	70-80	I	80-90	I	90-100	I	100-110	I	110-120	I
ABSOLUTE	I	205.61	I	51.45	I	1.60	I	1.10	I	0.00	I	2.55	I	0.00	I	0.00	I	0.00	I	0.00	I	0.00	I	0.00	I
PERCENT.	I	6.72	I	1.68	I	.05	I	.04	I	0.00	I	.04	I	0.00	I	0.00	I	0.00	I	0.00	I	0.00	I	0.00	I

DEGREE	I	120-130	I	130-140	I	140-150	I	150-160	I	160-170	I	170-180	I	180-190	I	190-200	I	200-210	I	210-220	I	220-230	I	230-240	I
ABSOLUTE	I	0.00	I	0.00	I	0.00	I	0.00	I	0.00	I	0.00	I	0.00	I	1.52	I	9.93	I	29.51	I	34.42	I	2.56	I
PERCENT.	I	0.00	I	0.00	I	0.00	I	0.00	I	0.00	I	0.00	I	0.00	I	.95	I	.32	I	.97	I	.11	I	.68	I

DEGREE	I	240-250	I	250-260	I	260-270	I	270-280	I	280-290	I	290-300	I	300-310	I	310-320	I	320-330	I	330-340	I	340-350	I	350-360	I
ABSOLUTE	I	1.27	I	7.94	I	0.00	I	2.56	I	4.06	I	22.57	I	31.05	I	62.36	I	334.02	I	791.32	I	1104.94	I	346.02	I
PERCENT.	I	.04	I	.26	I	0.00	I	.04	I	.13	I	.74	I	1.02	I	2.04	I	10.92	I	25.64	I	36.14	I	12.63	I

TOTAL

ABSOLUTE 1057.57

PERCENT. 100.00

Appendix 4: Frequency table of wind direction and velocity (percentage) for the period: Fall 1973, 1974.

FREQUENCIES TABLE IN PERCENTAGE NUMBERS

M/SEC DIRECT	I	0-6 I	6-8 I	8-10 I	10-12 I	12-14 I	14-16 I	>16 I	TOTAL I
0-10	I	2. I	1. I	0. I	0. I	0. I	0. I	0. I	4. I
10-20	I	2. I	1. I	0. I	0. I	0. I	0. I	0. I	3. I
20-30	I	2. I	0. I	0. I	0. I	0. I	0. I	0. I	2. I
30-40	I	1. I	0. I	0. I	0. I	0. I	0. I	0. I	1. I
40-50	I	1. I	0. I	0. I	0. I	0. I	0. I	0. I	1. I
50-60	I	1. I	0. I	0. I	0. I	0. I	0. I	0. I	1. I
60-70	I	1. I	0. I	0. I	0. I	0. I	0. I	0. I	1. I
70-80	I	1. I	0. I	0. I	0. I	0. I	0. I	0. I	1. I
80-90	I	1. I	0. I	0. I	0. I	0. I	0. I	0. I	1. I
90-100	I	1. I	0. I	0. I	0. I	0. I	0. I	0. I	1. I
100-110	I	1. I	0. I	0. I	0. I	0. I	0. I	0. I	1. I
110-120	I	2. I	0. I	0. I	0. I	0. I	0. I	0. I	2. I
120-130	I	2. I	0. I	0. I	0. I	0. I	0. I	0. I	2. I
130-140	I	3. I	0. I	0. I	0. I	0. I	0. I	0. I	3. I
140-150	I	3. I	0. I	0. I	0. I	0. I	0. I	0. I	3. I
150-160	I	4. I	0. I	0. I	0. I	0. I	0. I	0. I	4. I
160-170	I	4. I	0. I	0. I	0. I	0. I	0. I	0. I	4. I
170-180	I	4. I	1. I	0. I	0. I	0. I	0. I	0. I	5. I
180-190	I	3. I	0. I	0. I	0. I	0. I	0. I	0. I	4. I
190-200	I	3. I	0. I	0. I	0. I	0. I	0. I	0. I	4. I
200-210	I	3. I	1. I	0. I	0. I	0. I	0. I	0. I	3. I
210-220	I	3. I	1. I	0. I	0. I	0. I	0. I	0. I	4. I
220-230	I	3. I	0. I	0. I	0. I	0. I	0. I	0. I	3. I
230-240	I	4. I	0. I	0. I	0. I	1. I	0. I	0. I	4. I
240-250	I	2. I	0. I	0. I	0. I	0. I	0. I	0. I	2. I
250-260	I	2. I	0. I	0. I	0. I	0. I	0. I	0. I	2. I
260-270	I	1. I	0. I	0. I	0. I	0. I	0. I	0. I	1. I
270-280	I	1. I	0. I	0. I	0. I	0. I	0. I	0. I	2. I
280-290	I	1. I	0. I	0. I	0. I	0. I	0. I	0. I	2. I
290-300	I	2. I	0. I	0. I	0. I	0. I	0. I	0. I	2. I
300-310	I	2. I	0. I	0. I	0. I	0. I	0. I	0. I	2. I
310-320	I	1. I	0. I	0. I	0. I	0. I	0. I	0. I	2. I
320-330	I	2. I	0. I	0. I	0. I	0. I	0. I	0. I	2. I
330-340	I	2. I	1. I	0. I	0. I	0. I	0. I	0. I	5. I
340-350	I	4. I	6. I	1. I	0. I	0. I	0. I	0. I	11. I
350-360	I	2. I	2. I	0. I	0. I	0. I	0. I	0. I	5. I
TOTAL	I	77. I	18. I	1. I	1. I	1. I	0. I	0. I	100. I



# Appendix 4 (cont.)

TOTAL CASES = 3648  
MISSING CASES = 293. IN PERCENTAGE NUMBER = 0.0  
TOTAL VALID CASES = 3355.  
TOTAL CASES OVER 6 M/SEC = 785. IN PERCENT NUMBERS OVER VALID CASES = 23.4  
VECTOR MEAN WIND VELOCITY = 3.9  
VECTOR MEAN WIND DIRECTION = 329.  
COSTANCY STAGE IN PERCENTAGE = 50.5

TABLES OF EFFECTIVE WIND EQUIVALENT 6 M/SEC

DEGREE	I	0-10	I	10-20	I	20-30	I	30-40	I	40-50	I	50-60	I	60-70	I	70-80	I	80-90	I	90-100	I	100-110	I	110-120	I
ABSOLUTE	I	107.55	I	59.01	I	16.79	I	2.98	I	1.52	I	0.00	I	10.25	I	0.00	I	0.00	I	4.10	I	0.00	I	3.15	I
PERCENT	I	6.12	I	3.36	I	1.07	I	.17	I	.09	I	0.00	I	.50	I	0.00	I	0.00	I	.23	I	0.00	I	.16	I

DEGREE	I	120-130	I	130-140	I	140-150	I	150-160	I	160-170	I	170-180	I	180-190	I	190-200	I	200-210	I	210-220	I	220-230	I	230-240	I
ABSOLUTE	I	0.00	I	2.65	I	0.00	I	1.46	I	17.93	I	164.66	I	84.07	I	70.61	I	26.13	I	53.41	I	14.26	I	150.71	I
PERCENT	I	0.00	I	.15	I	0.00	I	.08	I	1.02	I	9.37	I	4.83	I	4.02	I	1.49	I	3.04	I	.93	I	8.50	I

DEGREE	I	240-250	I	250-260	I	260-270	I	270-280	I	280-290	I	290-300	I	300-310	I	310-320	I	320-330	I	330-340	I	340-350	I	350-360	I
ABSOLUTE	I	6.67	I	79.11	I	0.00	I	36.79	I	28.34	I	34.71	I	13.84	I	33.71	I	47.46	I	134.86	I	403.09	I	142.61	I
PERCENT	I	.38	I	4.50	I	0.00	I	2.09	I	1.62	I	1.98	I	.79	I	1.92	I	2.70	I	7.67	I	22.94	I	6.12	I

TOTAL

ABSOLUTE 1757.29

PERCENT. 100.00

Appendix 5: Frequency table of wind direction and velocity (percentage) for the period: Spring 1973, 1974, 1975.

FREQUENCIES TABLE IN PERCENTAGE NUMBERS

M/SEC	I	0-6	I	6-8	I	8-10	I	10-12	I	12-14	I	14-16	I	>16	I	TOTAL	I
DIRECT	I	I	I	I	I	I	I	I	I	I	I	I	I	I	I	I	I
0-10	I	2. I		2. I		1. I		0. I		0. I		0. I		0. I		5. I	
10-20	I	4. I		1. I		0. I		0. I		0. I		0. I		0. I		5. I	
20-30	I	2. I		0. I		0. I		0. I		0. I		0. I		0. I		3. I	
30-40	I	2. I		0. I		0. I		0. I		0. I		0. I		0. I		2. I	
40-50	I	2. I		0. I		0. I		0. I		0. I		0. I		0. I		2. I	
50-60	I	1. I		0. I		0. I		0. I		0. I		0. I		0. I		2. I	
60-70	I	1. I		0. I		0. I		0. I		0. I		0. I		0. I		2. I	
70-80	I	1. I		0. I		0. I		0. I		0. I		0. I		0. I		1. I	
80-90	I	1. I		0. I		0. I		0. I		0. I		0. I		0. I		1. I	
90-100	I	1. I		0. I		0. I		0. I		0. I		0. I		0. I		1. I	
100-110	I	1. I		0. I		0. I		0. I		0. I		0. I		0. I		1. I	
110-120	I	1. I		0. I		0. I		0. I		0. I		0. I		0. I		1. I	
120-130	I	1. I		0. I		0. I		0. I		0. I		0. I		0. I		1. I	
130-140	I	2. I		0. I		0. I		0. I		0. I		0. I		0. I		2. I	
140-150	I	2. I		0. I		0. I		0. I		0. I		0. I		0. I		2. I	
150-160	I	2. I		0. I		0. I		0. I		0. I		0. I		0. I		2. I	
160-170	I	2. I		0. I		0. I		0. I		0. I		0. I		0. I		2. I	
170-180	I	2. I		0. I		0. I		0. I		0. I		0. I		0. I		2. I	
180-190	I	2. I		0. I		0. I		0. I		0. I		0. I		0. I		2. I	
190-200	I	2. I		0. I		0. I		0. I		0. I		0. I		0. I		2. I	
200-210	I	2. I		0. I		0. I		0. I		0. I		0. I		0. I		2. I	
210-220	I	2. I		0. I		0. I		0. I		0. I		0. I		0. I		2. I	
220-230	I	2. I		0. I		0. I		0. I		0. I		0. I		0. I		2. I	
230-240	I	2. I		0. I		0. I		0. I		0. I		0. I		0. I		2. I	
240-250	I	2. I		0. I		0. I		0. I		0. I		0. I		0. I		2. I	
250-260	I	2. I		0. I		0. I		0. I		0. I		0. I		0. I		3. I	
260-270	I	2. I		0. I		0. I		0. I		0. I		0. I		0. I		2. I	
270-280	I	2. I		0. I		0. I		0. I		0. I		0. I		0. I		2. I	
280-290	I	2. I		0. I		0. I		0. I		0. I		0. I		0. I		3. I	
290-300	I	2. I		0. I		0. I		0. I		0. I		0. I		0. I		3. I	
300-310	I	3. I		0. I		0. I		0. I		0. I		0. I		0. I		3. I	
310-320	I	2. I		0. I		0. I		0. I		0. I		0. I		0. I		3. I	
320-330	I	2. I		1. I		0. I		0. I		0. I		0. I		0. I		4. I	
330-340	I	3. I		3. I		1. I		0. I		0. I		0. I		0. I		7. I	
340-350	I	4. I		5. I		3. I		0. I		0. I		0. I		0. I		11. I	
350-360	I	2. I		2. I		1. I		0. I		0. I		0. I		0. I		5. I	
TOTAL	I	72. I		14. I		7. I		1. I		1. I		0. I		0. I		100. I	

# Appendix 5 (cont.)

TOTAL CASES = 6624  
 MISSING CASES = 1091. IN PERCENTAGE NUMBER = 16.5  
 TOTAL VALID CASES = 5533.  
 TOTAL CASES OVER 3 M/SEC = 1529. IN PERCENT NUMBERS OVER VALID CASES = 27.6  
 VECTOR MEAN WIND VELOCITY = 5.7  
 VECTOR MEAN WIND DIRECTION = 337.  
 CONSTANT STAGE IN PERCENTAGE = 72.2

## TABLES OF EFFECTIVE WIND EQUIVALENT 6 M/SEC

DEGREE	0-10	10-20	20-30	30-40	40-50	50-60	60-70	70-80	80-90	90-100	100-110	110-120
ABSOLUTE	333.24	205.63	44.19	7.51	5.41	3.75	11.21	1.66	3.72	10.06	0.00	1.39
PERCENT	6.47	5.23	1.12	.19	.14	.10	.29	.04	.09	.26	0.00	.04

DEGREE	120-130	130-140	140-150	150-160	160-170	170-180	180-190	190-200	200-210	210-220	220-230	230-240
ABSOLUTE	0.00	0.00	2.24	4.77	24.26	45.28	171.03	42.94	23.72	67.14	61.31	67.59
PERCENT	0.00	0.00	.05	.12	.62	1.15	4.35	1.00	.60	1.71	2.07	1.72

DEGREE	240-250	250-260	260-270	270-280	280-290	290-300	300-310	310-320	320-330	330-340	340-350	350-360
ABSOLUTE	51.66	122.68	121.69	140.41	61.62	80.59	96.43	203.47	214.13	427.10	634.56	397.10
PERCENT	1.32	3.12	3.10	3.57	2.08	2.65	2.51	5.17	5.45	10.06	21.22	10.10

TOTAL

ABSOLUTE 3932.52

PERCENT 100.00

Appendix 6: Table of wind velocity (in meters/sec) and direction measured at point no. 18 (Fig. 3.3).

Anemometer No. of measurement	5	4	Wind direction (in degrees)	3	2	Wind direction (in degrees)	1
1	4.3	4.4	300	3.6	2.8	40	6.1
2	3.6	4.0	260	4.0	3.2	50	6.3
3	3.2	3.4	265	3.0	2.5	30	5.4
4	3.7	3.7	250	3.3	2.5	40	5.6
5	3.5	3.9	260	3.3	2.6	310	5.5
6	2.9	3.1	260	2.5	2.5	5	4.7
7	4.8	5.3	250	5.1	3.8	10	6.5
8	3.1	3.1	240	2.5	1.6	15	4.7
Average	3.6	3.9	260	3.4	2.7	17	5.6

Appendix 7: Table of wind velocity (in meters/sec) and direction measured at point no. 5 (Fig. 3.4).

Anemometer No. of measurements	5	Wind direction (in degrees)	4	Wind direction (in degrees)	3	Wind direction (in degrees)	2	1
1	5.5	240	5.1	260	4.1	240	8.5	7.1
2	6.0	290	5.5	280	4.7	235	8.1	7.5
3	4.8	280	5.1	300	4.3	240	8.0	6.0
4	4.9	285	5.7	255	4.9	245	7.6	6.0
5	5.1	290	5.7	295	4.7	250	8.2	7.0
6	5.3	280	6.5	295	4.8	240	8.9	8.5
7	5.9	285	6.1	300	4.8	240	10.8	7.9
Average 1-7	5.4	280	5.7	285	4.6	240	8.6	7.1
8	6.0	310	5.6	285	5.0	250	7.6	7.2
9	4.9	270	5.7	280	5.1	230	8.9	6.0
10	6.2	285	5.9	290	5.4	245	8.7	6.8
11	5.5	300	5.9	270	5.4	240	9.4	7.5
12	6.5	260	6.3	300	5.3	235	8.7	6.5
13	5.5	290	6.6	265	4.9	245	7.5	7.5
14	6.3	310	6.1	310	5.1	240	8.9	7.7
Average 8-14	5.8	290	6.0	285	5.2	240	8.5	7.3
15	5.1	290	5.5	290	5.0	230	6.0	7.0
16	6.3	285	5.3	290	5.1	230	10.9	7.1
17	5.8	320	5.8	295	5.7	240	10.8	8.5
18	6.5	310	5.8	290	4.9	250	5.4	7.1
19	5.9	295	6.4	300	5.6	240	11.5	8.6
20	6.2	280	6.0	295	5.0	240	10.7	8.2
21	6.6	275	6.7	295	5.4	240	9.7	7.5
Average 15-21	6.1	295	5.9	295	5.2	240	9.7	7.7
22	7.0	285	6.8	280	5.6	290	8.5	7.5
23	7.3	280	6.4	295	6.3	250	8.4	8.0
24	7.3	300	6.7	295	6.2	260	10.1	8.1
25	6.1	280	8.5	320	7.3	270	8.6	7.8



Appendix 7 (cont.)

Anemometer No. of measurement	Wind direction (in degrees)	5	Wind direction (in degrees)	4	3	Wind direction (in degrees)	2	1
26	315	5.1	270	7.3	6.9	260	7.4	7.7
27	260	5.1	305	7.1	5.5	250	9.9	8.5
28	300	8.5	275	7.3	6.1	250	9.9	8.0
Average 22-28	290	6.6	290	7.1	6.3	260	9.0	7.9
29	245	5.8	270	6.7	6.1	265	6.1	7.8
30	250	7.3	260	6.4	6.0	250	9.9	7.3
31	305	6.2	275	5.8	4.9	245	10.3	8.5
32	300	7.3	250	6.4	5.6	240	9.4	8.0
33	280	5.5	280	5.7	5.0	235	9.9	8.1
34	275	6.7	270	7.0	6.2	240	11.7	8.4
35	280	5.9	310	5.7	4.7	250	8.8	7.4
Average 29-35	275	6.4	275	6.2	5.5	245	9.4	7.9
36	285	6.2	250	5.6	5.6	250	9.4	7.8
37	270	5.0	290	5.4	5.3	245	6.0	6.8
38	280	6.4	275	6.1	5.4	240	8.9	6.6
39	275	7.4	290	7.0	6.4	250	8.1	8.1
40	280	7.7	290	7.6	6.6	240	9.8	9.9
41	280	7.2	285	6.5	5.9	240	8.7	6.9
42	285	6.7	255	5.5	5.9	245	9.4	7.5
Average 36-42	280	6.7	275	6.2	5.9	245	8.6	7.7
43	270	5.3	250	6.3	6.3	260	7.9	7.7
44	275	7.5	270	6.2	6.7	240	9.8	9.3
45	270	6.2	310	7.6	6.6	250	9.6	8.5
46	280	6.5	300	6.5	5.8	235	8.8	8.6
47	270	5.5	320	6.7	6.0	240	10.4	7.4
48	270	6.6	285	5.6	5.7	235	8.4	8.5
49	290	6.1	300	6.8	6.1	250	10.4	9.1
Average 43-49	275	6.2	290	6.5	6.2	245	9.3	8.4
Average	285	6.2	285	6.2	5.5	245	9.0	7.7

Appendix 8: Table of wind velocity (in meters/sec) and direction measured at point no. 5 (Fig. 3.5).

Anemometer No. of measurement	Wind direction (in degrees)	3	Wind direction (in degrees)	2	Wind direction (in degrees)	1
1	270	4.8	290	5.1	210	6.1
2	280	4.6	295	4.7	210	5.6
3	280	4.5	295	3.5	200	6.6
4	280	3.8	290	3.3	210	6.7
5	285	4.7	290	2.7	205	6.8
6	270	5.0	295	5.5	220	5.2
7	260	4.4	295	4.5	210	5.5
8	280	4.4	290	3.9	230	4.8
9	255	5.3	285	4.5	210	6.0
10	270	4.2	290	5.2	225	5.0
11	260	4.3	285	4.5	220	4.2
12	270	4.8	290	5.5	210	5.6
13	270	3.8	285	3.8	220	4.7
Average	271	4.5	290	4.4	214	5.6

Appendix 9: Table of wind velocity (in meters/sec) and direction measured at point no. 5 (Fig. 3.6).

Anemometer No. of measurement	Wind direction (in degrees)	3	Wind direction (in degrees)	2	Wind direction (in degrees)	1
1	230	2.8	280	3.5	220	4.5
2	235	3.7	290	4.8	210	5.8
3	230	3.7	290	3.5	205	5.9
4	230	2.9	290	2.2	210	6.1
5	230	2.9	295	4.2	205	5.1
6	230	2.8	290	2.7	225	4.5
7	230	2.2	290	2.7	210	3.3
8	240	2.7	270	4.3	210	4.1
9	235	2.2	280	3.0	230	2.6
10	240	3.3	270	3.8	220	4.4
11	240	2.9	280	3.3	225	4.2
12	230	3.0	270	4.2	220	4.2
13	245	3.5	275	3.5	215	6.0
Average	234	3.0	282	3.5	215	4.5

Appendix 11: Table of wind velocity (in meters/sec) and direction measured at point no. 4 (Fig. 3.10).

Anemometer No. of Measurement	6	Wind direction (in degrees)	5	4	Wind direction (in degrees)	3	2	Wind direction (in degrees)	1
1	2.3	290	2.4	1.3	340	0.9	3.0	260	4.0
2	2.6	320	1.9	1.9	300	1.8	4.5	250	4.0
3	3.4	315	2.8	2.4	340	2.1	3.8	260	3.0
Average 1-3	2.8	308	2.4	1.9	327	1.6	3.8	257	3.7
4	3.3	310	2.5	1.2	310	0.9	3.4	247	4.0
5	4.7	320	3.5	1.7	325	1.7	5.6	247	6.5
6	2.5	305	1.8	0.9	310	1.0	3.9	260	3.3
Average 4-6	3.5	312	2.6	1.3	315	1.2	4.3	251	4.6
7	2.5	310	1.8	0.9	340	0.9	3.6	255	3.3
8	2.9	300	3.0	2.1	320	1.7	3.9	255	3.8
9	2.1	310	2.0	0.9	320	0.9	2.5	260	2.6
Average 7-9	2.5	307	2.3	1.3	327	1.2	3.5	257	3.2
10	2.9	315	3.5	2.6	310	1.3	4.4	265	3.8
11	3.0	315	3.2	2.2	310	2.2	3.8	260	3.9
12	3.0	320	4.3	3.8	305	2.4	0.8	258	1.3
Average 10-12	3.0	317	3.7	2.9	308	2.0	3.0	261	3.0
13	2.6	330	2.2	1.4	330	1.6	5.2	260	5.3
14	3.4	300	3.8	2.2	330	1.3	3.7	251	4.1
15	2.6	305	2.3	1.8	310	1.3	3.6	250	2.9
Average 13-15	2.9	312	2.8	1.8	325	1.4	4.2	254	4.1
16	3.2	340	2.1	1.4	325	0.9	2.5	260	3.7
17	2.9	320	2.5	2.0	315	1.8	4.3	270	3.7
18	2.5	300	2.4	1.7	320	1.7	3.0	255	3.0
19	2.4	320	2.3	1.4	330	2.5	2.7	250	2.7
Average 16-19	2.7	320	2.3	1.6	322	1.7	3.1	259	3.3
Average	2.9	312	2.7	1.8	320	1.5	3.6	256	3.6

Appendix 10: Table of wind velocity (in meters/sec) and direction measured at point no. 9 (Fig. 3.7).

Anemometer No.	5	4	Wind direction (in degrees)	3	2	Wind direction (in degrees)	1
No. of measurement							
1	6.2	6.0	240	3.3	3.3	310	4.8
2	5.8	4.6	250	4.7	4.2	300	4.0
3	4.6	4.6	255	4.1	3.3	320	3.6
4	7.9	8.0	260	4.8	4.3	350	5.0
5	5.1	5.2	275	5.1	4.9	295	4.1
6	4.4	4.6	285	3.5	3.7	320	3.0
7	6.0	5.2	295	5.6	4.7	310	4.5
Average	5.7	5.5	266	4.4	4.1	315	4.1

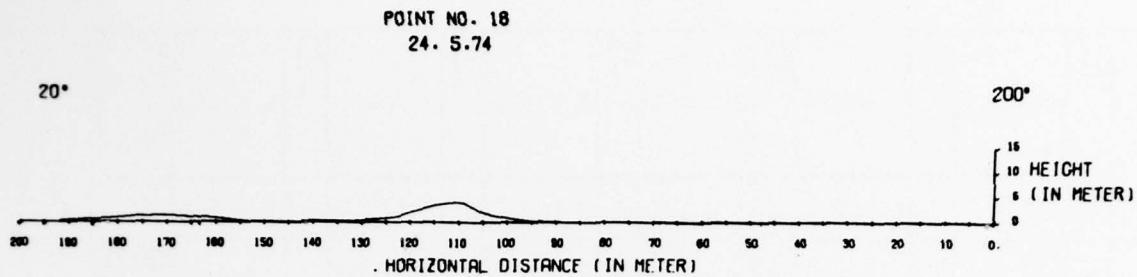
Appendix 12: Table of wind velocity (in meters/sec) and direction measured at point no. 4 (Fig. 3.11).

Anemometer No.	6	5	4	3	2	1
No. of measurement	Wind direction (in degrees)	Wind direction (in degrees)	Wind direction (in degrees)	Wind direction (in degrees)	Wind direction (in degrees)	Wind direction (in degrees)
1	4.5	320	3.3	330	2.7	1.3
2	3.3	310	2.7	305	2.4	1.6
3	4.5	320	3.5	315	3.0	2.5
4	4.9	310	4.2	335	2.7	1.6
Average	4.3	315	3.4	321	2.7	1.7
5	4.8	320	4.2	320	3.9	1.7
6	3.9	315	3.3	300	3.3	3.3
7	4.1	305	3.0	310	3.0	2.5
8	4.4	310	3.4	320	2.2	1.7
Average	4.3	312	3.5	312	3.1	2.3
9	4.2	320	4.0	310	2.7	1.2
10	4.7	320	3.3	310	2.7	2.2
11	5.7	310	4.1	305	2.7	1.9
12	3.7	310	3.0	310	2.5	1.9
Average	4.6	315	3.6	309	2.6	1.8
13	3.0	310	3.2	290	3.2	1.7
14	4.0	315	3.1	330	2.2	0.9
15	3.6	300	2.6	325	2.2	1.9
16	3.7	310	2.7	310	2.2	1.2
Average	3.6	309	2.9	314	2.4	1.4
17	4.4	310	4.0	325	3.1	1.8
18	4.2	300	2.6	310	1.9	1.4
19	4.5	315	3.3	310	1.7	1.9
20	3.8	310	3.0	300	2.0	1.3
Average	4.2	309	3.2	311	2.2	1.6
21	3.3	310	3.0	300	2.5	1.3
22	5.2	315	3.4	310	2.5	0.9
23	3.7	300	2.8	310	2.2	1.8
24	3.7	315	3.4	305	2.2	2.3
Average	4.0	310	3.1	306	2.3	1.6
21-24	4.2	312	3.3	312	2.5	1.7
Average	4.2	312	3.3	312	2.5	1.7

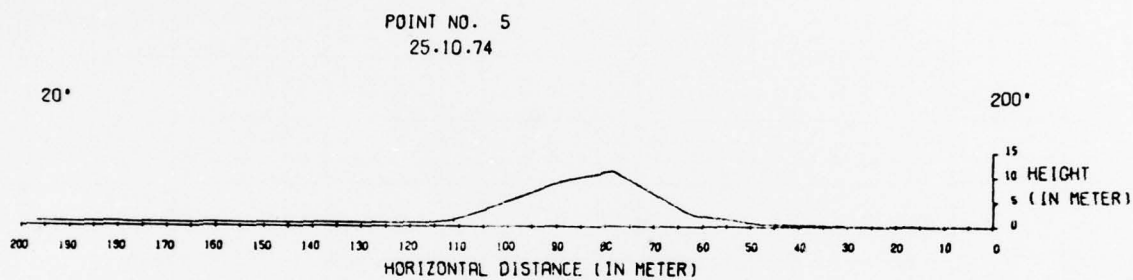
Appendix 13: Table of wind velocity (in meters/sec) and direction measured at point no. 6 (Fig. 3.12).

Anemometer No.	6	5	4	3	2	1
No. of measurement	Wind direction (in degrees)	Wind direction (in degrees)	Wind direction (in degrees)	Wind direction (in degrees)	Wind direction (in degrees)	Wind direction (in degrees)
1	2.8	6.0	340	0.9	2.1	0.6
2	2.3	7.0	335	0.9	1.5	1.6
3	3.0	6.1	335	1.6	0.7	0.6
4	3.3	6.6	240	1.3	1.0	0.4
5	3.3	4.4	350	0.4	0.7	0.7
6	3.2	5.4	340	1.7	0.5	0.9
7	2.8	6.2	340	1.0	1.4	0.9
8	3.0	5.0	320	2.2	0.9	0.7
9	2.7	5.3	340	1.0	0.3	1.3
10	2.8	5.9	340	2.1	0.6	0.2
11	2.3	4.9	345	1.0	0.7	1.7
Average	2.9	5.7	330	1.3	0.9	0.9

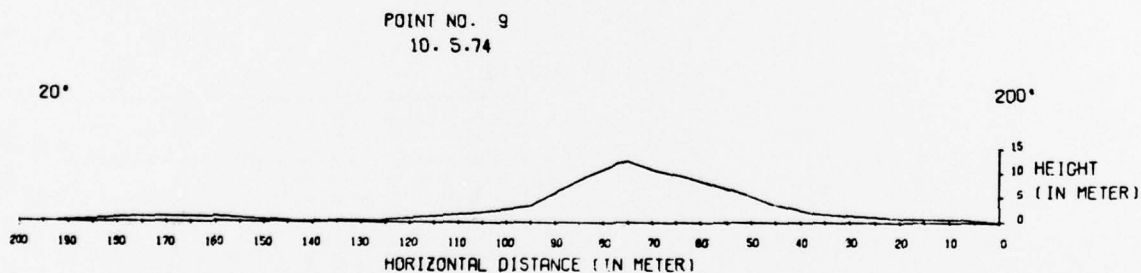
Appendix 14: Cross section of point no. 18 (for Fig. 3.3).



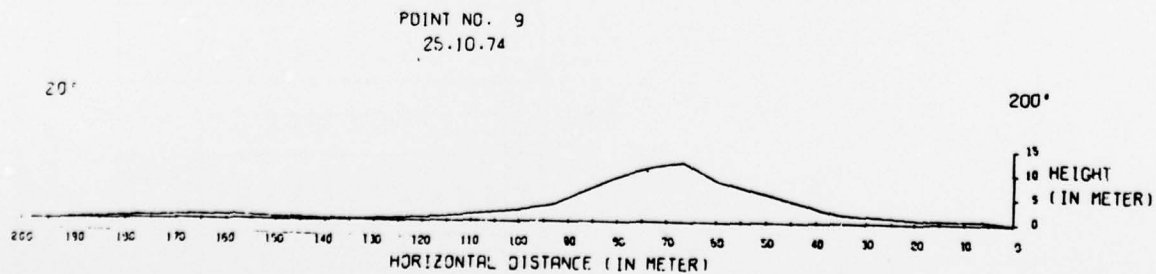
Appendix 15: Cross section of point no. 5 (for Figs. 3.4, 3.5, 3.6).



Appendix 16: Cross section of point no. 9 (for Fig. 3.7).



Appendix 17: Cross section of point no. 9 (for Figs. 3.8, 3.9).





Appendix 18: Results of moment statistics computed for the sand sampled from the ripples trough and crest separately.

No. of sample	No. of point	Location of sampling point on the dune (according to Fig. 4.1)	Location of sample in the ripple (T-crest)	Ripple wave-length (in cm)	$K_g$	$S_k$	$\sigma$	$\bar{x}$
1	1	1	C	40	3.40	1.07	1.00	.32
2	1	1	T	40	1.53	-.09	1.38	1.07
7	1	2	C	10	2.76	.30	.50	2.01
8	1	2	T	10	4.01	.79	.52	2.02
9	1	3	C	15	4.41	.37	.45	1.48
10	1	3	T	15	5.96	.97	.53	1.60
11	1	4	C	15	4.11	.03	.47	1.40
12	1	4	T	15	6.08	.47	.55	1.67
13	1	5	C	15	5.75	.46	.45	1.46
14	1	5	T	15	5.36	.75	.52	1.61
15	3	1	C	15	5.67	.55	.49	1.37
16	3	1	T	15	6.78	-.23	.61	1.62
17	3	2	C	10	6.49	1.24	.38	1.82
18	3	2	T	10	4.45	.54	.44	1.90
19	3	3	C	14	6.19	.97	.37	1.85
20	3	3	T	14	5.62	1.32	.41	1.99
21	3	4	C	13	4.92	.71	.32	1.64
22	3	4	T	13	5.56	1.11	.41	1.75
23	3	5	C	40	3.70	.98	.82	.31
24	3	5	T	40	2.29	-.38	1.15	1.39
25	4	1	C	35	2.93	.74	.91	.41
26	4	1	T	35	4.72	-1.11	.78	1.40
27	4	2	C	20	2.58	-.28	.60	2.16
28	4	2	T	20	2.38	.18	.75	1.92
33	4	3	C	15	3.99	.33	.41	1.86
34	4	3	T	15	4.65	.08	.43	1.89
39	4	4	C	14	5.70	.57	.38	1.75
40	4	4	T	14	5.63	1.06	.40	1.86
41	4	5	C	15	4.51	.62	.49	1.63
42	4	5	T	15	3.57	.55	.48	1.82
43	5	1	C	25	3.90	1.38	1.03	.19
44	5	1	T	25	2.15	.53	1.29	.72
45	5	2	C	10	3.50	.33	.49	2.08
46	5	2	T	10	2.84	-.41	.48	2.35
47	5	3	C	13	5.50	.35	.44	1.74
48	5	3	T	13	5.42	.73	.45	1.83
49	5	4	C	14	5.11	.63	.36	1.75
50	5	4	T	14	6.78	-.27	.56	1.91
51	5	5	C	18	5.80	1.53	.62	1.26
52	5	5	T	18	3.15	.10	.73	1.88

No. of sample	No. of point	Location of sampling point on the dune (according to Fig. 4.1)	Location of sample in the ripple (T-crest)	Ripple wave-length (in cm)	$K_g$	$S_k$	$\sigma$	$\bar{x}$
53	6	1	C	18	3.77	.10	.68	1.49
54	6	1	T	18	4.50	.07	.69	1.66
55	6	2	C	10	3.62	.05	.45	1.82
56	6	2	T	10	3.79	.30	.50	1.84
57	6	3	C	10	5.30	.38	.38	1.76
58	6	3	T	10	5.11	.82	.47	1.86
59	6	4	C	14	7.35	1.43	.63	1.36
60	6	4	T	14	5.35	-.52	.71	1.69
61	6	5	C	12	5.64	.68	.49	1.59
62	6	5	T	12	4.19	.49	.49	1.72
63	7	1	C	50	7.70	1.46	.72	.54
64	7	1	T	50	3.05	-.17	1.07	1.05
65	7	2	C	9	3.80	.74	.36	1.97
66	7	2	T	9	2.76	.46	.41	2.11
67	7	3	C	15	4.80	.79	.35	1.78
68	7	3	T	15	5.82	1.40	.49	2.02
69	7	4	C	8	5.45	.80	.33	1.61
70	7	4	T	8	14.54	-.68	.43	1.65
71	7	5	C	18	5.89	1.46	.66	1.55
72	7	5	T	18	3.23	.34	.80	1.92
73	9	1	C	12	4.68	1.01	.46	1.62
74	9	1	T	12	3.31	.76	.55	1.75
75	9	2	C	12	2.33	.25	.37	2.18
76	9	2	T	12	2.50	.18	.39	2.27
77	9	3	C	11	3.80	.84	.38	1.97
78	9	3	T	11	4.94	1.12	.43	2.05
79	9	4	C	11	10.65	-.60	.43	1.72
80	9	4	T	11	6.69	-.06	.49	1.92
81	9	5	C	12	4.34	.48	.47	1.45
82	9	5	T	12	4.53	.58	.47	1.70
83	11	1	C	13	4.97	.60	.37	1.48
84	11	1	T	13	4.55	.89	.47	1.68
85	11	2	C	11	2.56	.27	.44	2.13
86	11	2	T	11	2.74	.28	.48	2.25
87	11	3	C	13	4.08	.75	.40	1.84
88	11	3	T	13	4.99	.57	.41	1.93
89	11	4	C	12	5.28	.44	.43	1.55
90	11	4	T	12	7.71	-1.02	.72	1.91
91	11	5	C	14	6.13	1.66	.65	1.02
92	11	5	T	14	2.00	.07	1.10	1.34

Appendix 19: Results of moment statistics computed for the sand samples from the ripple trough and its crest together.

No. of sample	No. of point	Location of sampling point on the dune (according to Fig. 4.1)	Ripple wave-length (in cm)	$Kg_{\phi}$	$Sk_{\phi}$	$\sigma_{\phi}$	$\bar{x}_{\phi}$
1+2	1	1	40	2.02	.56	1.23	.63
7+8	1	2	10	3.50	.58	.51	2.02
9+10	1	3	15	5.62	.75	.49	1.53
11+12	1	4	15	5.28	.34	.52	1.50
13+14	1	5	15	5.70	.66	.48	1.52
15+16	3	1	15	6.00	.22	.56	1.48
17+18	3	2	10	5.08	.81	.41	1.87
19+20	3	3	14	6.03	1.14	.39	1.90
21+22	3	4	13	5.86	1.04	.37	1.69
23+24	3	5	40	2.37	.56	1.08	.69
25+26	4	1	35	2.33	.06	.99	.78
27+28	4	2	20	2.42	-.05	.70	2.02
33+34	4	3	15	4.39	.19	.42	1.88
39+40	4	4	14	5.74	.75	.39	1.79
41+42	4	5	15	4.08	.56	.49	1.70
43+44	5	1	25	2.85	.98	1.17	.41
45+46	5	2	10	2.86	.03	.50	2.19
47+48	5	3	13	5.50	.50	.44	1.77
49+50	5	4	14	7.04	.29	.44	1.80
51+52	5	5	18	3.61	.93	.72	1.46
53+54	6	1	18	4.05	.07	.69	1.57
55+56	6	2	10	3.79	.21	.47	1.83

No. of sample	No. of point	Location of sampling point on the dune (according to Fig. 4.1)	Ripple wave-length (in cm)	$Kg_{\phi}$	$Sk_{\phi}$	$\sigma_{\phi}$	$\bar{x}_{\phi}$
57+58	6	3	10	5.50	.71	.43	1.80
59+60	6	4	14	5.29	.56	.68	1.49
61+62	6	5	12	4.97	.59	.49	1.64
63+64	7	1	50	3.84	.52	.94	.76
65+66	7	2	9	3.40	.67	.38	2.01
67+68	7	3	15	6.47	1.35	.44	1.89
69+70	7	4	8	11.96	-.05	.37	1.62
71+72	7	5	18	4.12	.95	.74	1.69
73+74	9	1	12	4.04	.93	.50	1.67
75+76	9	2	12	2.44	.24	.38	2.72
77+78	9	3	11	4.64	1.03	.41	2.01
79+80	9	4	11	8.30	.22	.47	1.81
81+82	9	5	12	4.28	.48	.49	1.56
83+84	11	1	13	5.19	.89	.42	1.56
85+86	11	2	11	2.70	.30	.46	2.18
87+88	11	3	13	4.40	.69	.41	1.87
89+90	11	4	12	7.08	-.19	.59	1.69
91+92	11	5	34	3.13	.71	.88	1.15

Appendix 20: Results of moment statistics computed for sand samples of the three top layers of the ripple.

A - Results of samples of ripple trough and crest separately

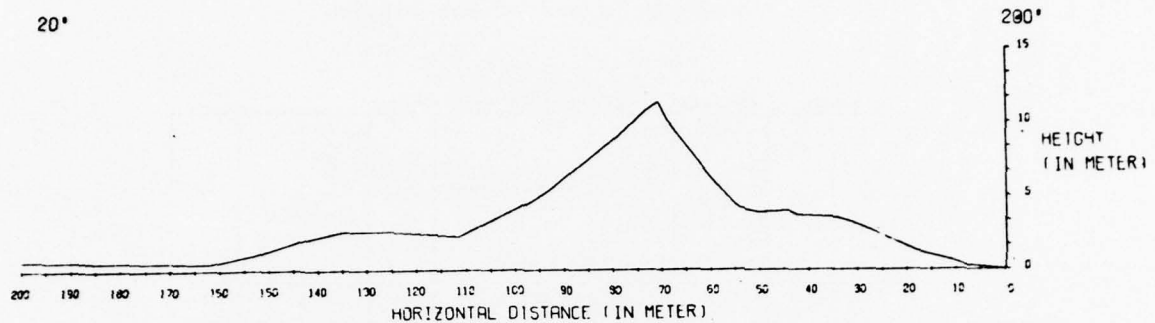
No. of sample	No. of point	Location of sampling point on the dune (according to Fig. 4.1)	Location of sample in the ripple T-trough C-crest	Ripple wave-length (in cm)	Layer	$Kg_{\phi}$	$Sk_{\phi}$	$\sigma_{\phi}$	$\bar{x}_{\phi}$
1	1	1	C	40	1	3.40	1.07	1.00	.32
2	1	1	T	40	1	1.53	-.09	1.38	1.07
3	1	1	C	40	2	2.10	.15	1.14	1.15
4	1	1	T	40	2	5.37	-.94	.76	2.21
5	1	1	C	40	3	2.27	.12	1.14	1.15
6	1	1	T	40	3	5.34	-.61	.73	2.19
27	4	2	C	20	1	2.58	-.28	.60	2.16
28	4	2	T	20	1	2.38	.18	.75	1.92
29	4	2	C	20	2	2.23	.03	.61	1.97
30	4	2	T	20	2	3.37	.79	.61	1.67
31	4	2	C	20	3	2.56	.09	.63	1.99
32	4	2	T	20	3	3.16	.71	.71	1.92
33	4	3	C	15	1	3.99	.33	.41	1.86
34	4	3	T	15	1	4.65	.08	.43	1.89
35	4	3	C	15	2	4.79	.63	.38	1.89
36	4	3	T	15	2	4.23	1.01	.41	1.99
37	4	3	C	15	3	4.99	1.00	.34	1.87
38	4	3	T	15	3	5.88	1.30	.41	2.01

B - Results of samples of ripple trough and crest together

1+2	1	1	C+T	40	1	2.02	.56	1.23	.63
3+4	1	1	C+T	40	2	2.24	-.35	1.13	1.57
5+6	1	1	C+T	40	3	2.47	-.36	1.12	1.56
27+28	4	2	C+T	20	1	2.42	-.05	.70	2.02
29+30	4	2	C+T	20	2	2.39	.30	.62	1.85
31+32	4	2	C+T	20	3	2.92	.45	.67	1.95
33+34	4	3	C+T	15	1	4.39	.19	.42	1.88
35+36	4	3	C+T	15	2	4.62	.82	.40	1.94
37+38	4	3	C+T	15	3	5.88	1.23	.38	1.93

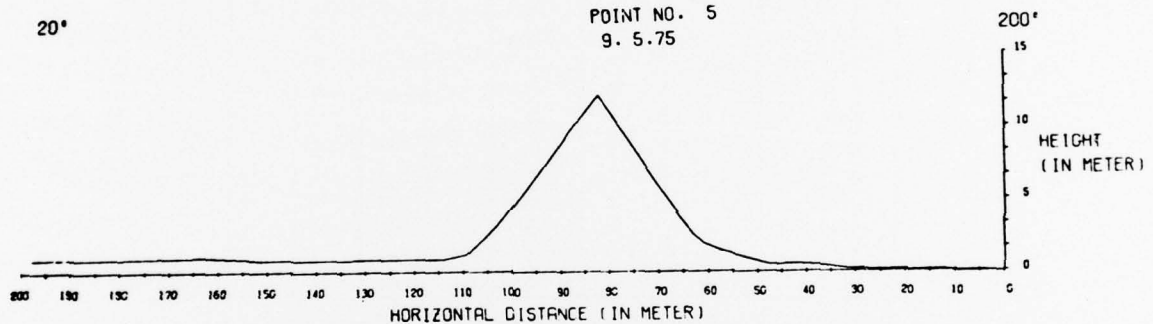
Appendix 21: Cross section of point no. 3 (vertical exaggeration x3).

POINT NO. 3  
11. 5.73



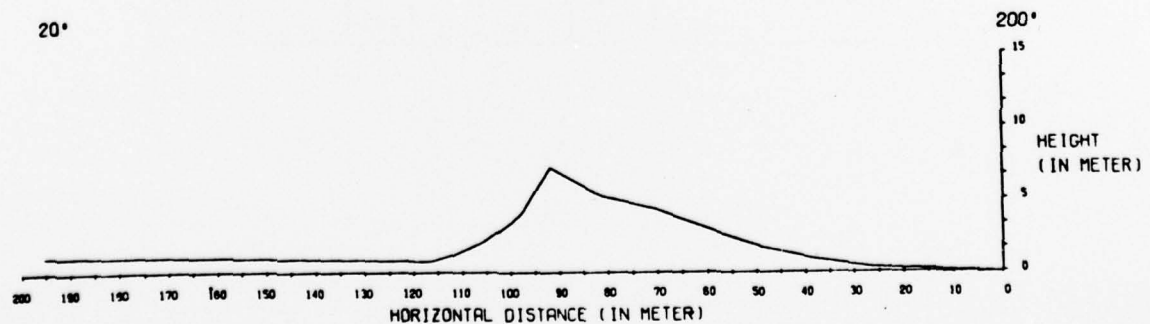
Appendix 22: Cross section of point no. 5 (vertical exaggeration x3).

POINT NO. 5  
9. 5.75



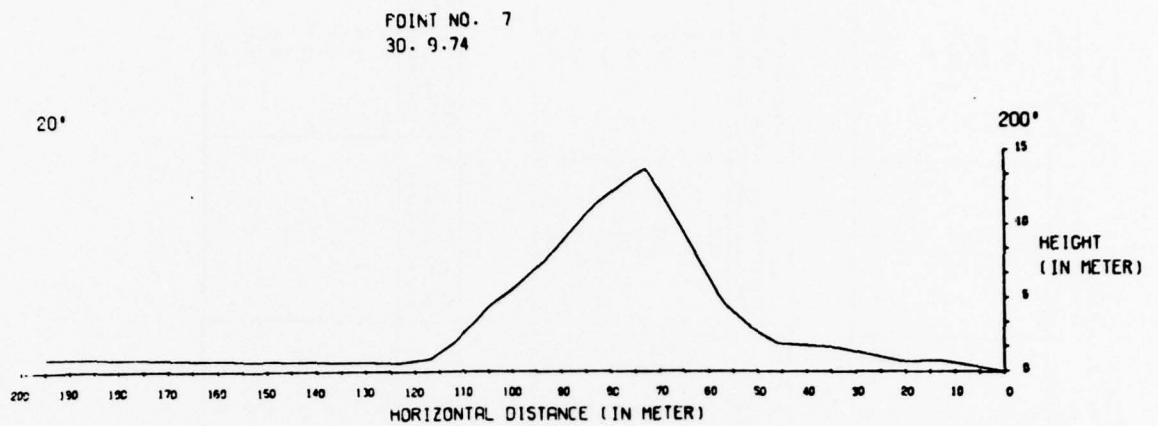
Appendix 23: Cross section of point no. 6 (vertical exaggeration x3).

POINT NO. 6  
27. 4.73

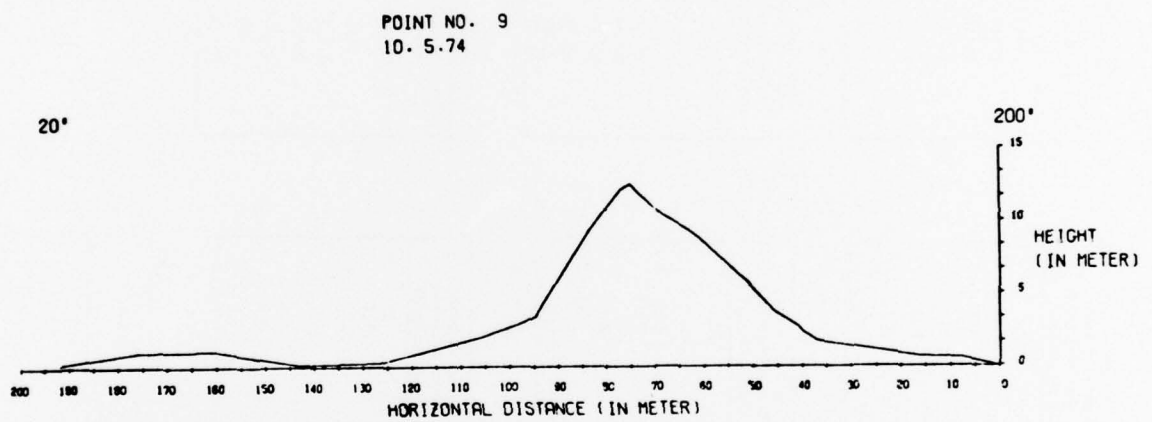




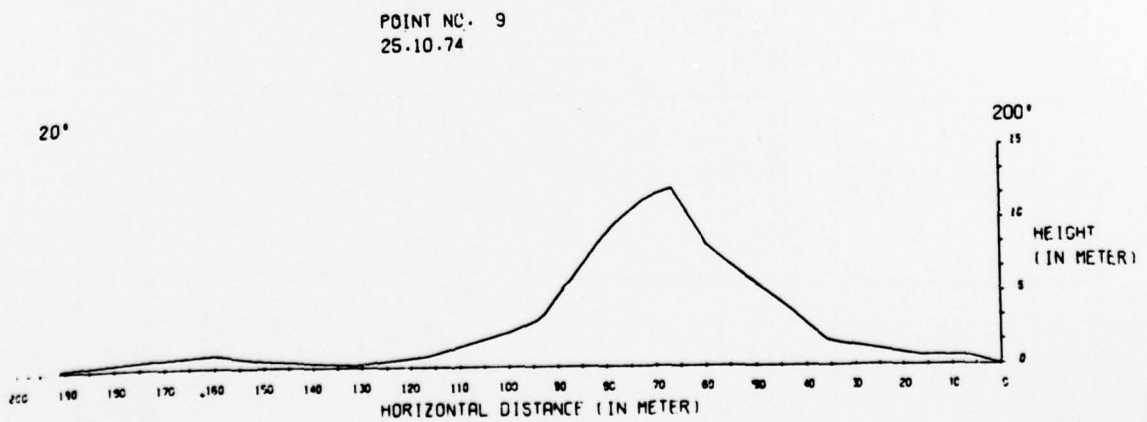
Appendix 24: Cross section of point no. 7 (vertical exaggeration x3).



Appendix 25: Cross section of point no. 9 (vertical exaggeration x3).



Appendix 26: Cross section of point no. 9 (vertical exaggeration x3).



Appendix 27: Frequency tables of distribution of declinations across the dune flanks.

Point no. 1, Nov. 11, 1974.

Declination (in degrees)	Extent of northern flank (in percentage)	Extent of southern flank (in percentage)	Extent of both flanks together (in percentage)
0-5	61.3	37.8	49.5
6-10	38.7	62.2	50.5
11-15	0.0	0.0	0.0
16-20	0.0	0.0	0.0
21-25	0.0	0.0	0.0
26-30	0.0	0.0	0.0
31-35	0.0	0.0	0.0

Point no. 1, June 6, 1975.

Declination (in degrees)	Extent of northern flank (in percentage)	Extent of southern flank (in percentage)	Extent of both flanks together (in percentage)
0-5	58.9	41.8	50.5
6-10	41.1	58.2	49.7
11-15	0.0	0.0	0.0
16-20	0.0	0.0	0.0
21-25	0.0	0.0	0.0
26-30	0.0	0.0	0.0
31-35	0.0	0.0	0.0

Point no. 3, April 27, 1973.

Declination (in degrees)	Extent of northern flank (in percentage)	Extent of southern flank (in percentage)	Extent of both flanks together (in percentage)
0-5	0.0	2.1	1.0
6-10	24.2	6.1	15.1
11-15	57.2	0.0	28.6
16-20	18.6	43.2	30.9
21-25	0.0	48.6	24.3
26-30	0.0	0.0	0.0
31-35	0.0	0.0	0.0

Point no. 3, Sept. 30, 1974.

Declination (in degrees)	Extent of northern flank (in percentage)	Extent of southern flank (in percentage)	Extent of both flanks together (in percentage)
0-5	0.0	0.0	0.0
6-10	18.3	3.8	11.1
11-15	73.8	0.0	36.9
16-20	7.9	0.0	3.9
21-25	0.0	10.6	5.3
26-30	0.0	85.5	42.8
31-35	0.0	0.0	0.0

Point no. 4, March 19, 1973.

Declination (in degrees)	Extent of northern flank (in percentage)	Extent of southern flank (in percentage)	Extent of both flanks together (in percentage)
0-5	0.0	1.8	.9
6-10	10.2	19.1	14.7
11-15	0.0	79.1	39.5
16-20	45.5	0.0	22.7
21-25	0.0	0.0	0.0
26-30	44.3	0.0	22.2
31-35	0.0	0.0	0.0

Point no. 4, May 24, 1974.

Declination (in degrees)	Extent of northern flank (in percentage)	Extent of southern flank (in percentage)	Extent of both flanks together (in percentage)
0-5	0.0	0.0	0.0
6-10	0.0	7.7	3.8
11-15	27.9	0.0	14.0
16-20	72.1	0.0	36.0
21-25	0.0	92.3	46.2
26-30	0.0	0.0	0.0
31-35	0.0	0.0	0.0

Point no. 5, Oct. 25, 1974.

Declination (in degrees)	Extent of northern flank (in percentage)	Extent of southern flank (in percentage)	Extent of both flanks together (in percentage)
0-5	0.0	0.0	0.0
6-10	17.1	6.6	11.9
11-15	6.9	0.0	3.4
16-20	76.0	7.4	41.7
21-25	0.0	0.0	0.0
26-30	0.0	86.0	43.0
31-35	0.0	0.0	0.0

# Appendix 27 (cont.)

Point no. 5, May 9, 1975.

Declination (in degrees)	Extent of northern flank (in percentage)	Extent of southern flank (in percentage)	Extent of both flanks together (in percentage)
0-5	0.0	0.0	0.0
6-10	0.0	4.7	2.4
11-15	0.0	0.0	0.0
16-20	18.1	6.4	12.3
21-25	75.6	10.2	42.9
26-30	6.3	78.6	42.4
31-35	0.0	0.0	0.0

Point no. 7, May 10, 1974.

Declination (in degrees)	Extent of northern flank (in percentage)	Extent of southern flank (in percentage)	Extent of both flanks together (in percentage)
0-5	0.0	0.0	0.0
6-10	1.7	4.4	3.0
11-15	9.6	0.0	4.8
16-20	33.5	32.6	33.1
21-25	25.0	63.1	44.0
26-30	20.3	0.0	10.1
31-35	9.9	0.0	5.0

Point no. 7, May 9, 1975.

Declination (in degrees)	Extent of northern flank (in percentage)	Extent of southern flank (in percentage)	Extent of both flanks together (in percentage)
0-5	.8	0.0	.4
6-10	3.4	0.0	1.7
11-15	12.3	2.5	7.4
16-20	54.7	0.0	27.4
21-25	28.8	22.4	25.6
26-30	0.0	75.1	37.5
31-35	0.0	0.0	0.0

Point no. 9, May 10, 1974.

Declination (in degrees)	Extent of northern flank (in percentage)	Extent of southern flank (in percentage)	Extent of both flanks together (in percentage)
0-5	0.0	0.0	0.0
6-10	0.0	0.0	0.0
11-15	4.1	32.8	18.5
16-20	0.0	67.2	33.6
21-25	31.0	0.0	15.5
26-30	59.9	0.0	30.0
31-35	5.0	0.0	2.5

Point no. 9, Oct. 25, 1974.

Declination (in degrees)	Extent of northern flank (in percentage)	Extent of southern flank (in percentage)	Extent of both flanks together (in percentage)
0-5	0.0	2.7	1.3
6-10	9.1	0.0	4.6
11-15	22.5	52.7	37.6
16-20	13.1	8.9	11.0
21-25	55.3	0.0	27.7
26-30	0.0	28.9	14.5
31-35	0.0	6.8	3.4

Point no. 13, Aug. 12, 1973

Declination (in degrees)	Extent of northern flank (in percentage)	Extent of southern flank (in percentage)	Extent of both flanks together (in percentage)
0-5	0.0	0.0	0.0
6-10	3.0	0.0	1.5
11-15	40.7	4.1	22.4
16-20	56.3	0.0	28.1
21-25	0.0	0.0	0.0
26-30	0.0	95.9	48.0
31-35	0.0	0.0	0.0

Point no. 13, May 10, 1974.

Declination (in degrees)	Extent of northern flank (in percentage)	Extent of southern flank (in percentage)	Extent of both flanks together (in percentage)
0-5	0.0	0.0	0.0
6-10	0.0	0.0	0.0
11-15	23.5	7.8	15.7
16-20	68.7	39.3	54.0
21-25	7.8	40.5	24.1
26-30	0.0	12.4	6.2
31-35	0.0	0.0	0.0